INTERNATIONAL SCHOOL FOR ADVANCED STUDIES

PhD Course in Statistical Physics

Field and Gauge Theories with Ultracold Gauge Potentials and Fields

Thesis submitted for the degree of

Doctor Philosophiae

Supervisors:
Dr. Andrea Trombettoni
Dr. Marcello Dalmonte

Candidate:
João C. Pinto Barros

The music of this awe
Deep silence between the notes
Deafens me with endless love

- Nightwish in Shudder Before the Beautiful, Endless Forms Most Beautiful

Abstract

In the last decade there has been an intense activity aimed at the quantum simulation of interacting many-body systems using cold atoms [1, 2]. The idea of quantum simulations traces back to Feynman [3], who argued that the ideal setting to study quantum systems would be a quantum experimental setup rather then a classical one - the latter one being fundamentally limited due to its hardware classical structure. This is a particularly important problem given the intrinsic complexity of interacting many-body problems, and the difficulties that arise when tackling them with numerical simulations - two paradigmatic examples being the sign(s) problem affecting Monte Carlo simulations of fermionic systems, and the real time dynamics in more than one spatial dimension.

Ultracold atoms offer a very powerful setting for quantum simulations. Atoms can be trapped in tailored optical and magnetic potentials, also controlling their dimensionality. The inter-atomic interactions can be tuned by external knobs, such as Feshbach resonances. This gives a large freedom on model building and, with suitable mappings, they allow the implementation of desired target models. This allowed an impressive exploitation of quantum simulators on the context of condensed matter physics.

The simulation of high-energy physics is an important line of research in this field and it is less direct. In particular it requires the implementation of symmetries like Lorentz and gauge invariance which are not immediately available in a cold atomic setting. Gauge fields are ubiquitous in physics ranging from condensed matter [4–6] and quantum computation [7, 8] to particle physics [9], an archetypical example being Quantum Chromodynamics (QCD) [10,11], the theory of strong nuclear forces. Currently open problems in QCD, providing a long-term goal of cold atomic simulations, include confinement/deconfinement and the structure of color superconducting phases at finite chemical potential [12]. Even though QCD is a very complicated theory (to simulate or study), it is possible to envision a path through implementation of simpler models. Furthermore, it is also expected that interesting physics is found on such "intermediate models" which may deserve attention irrespectively of the QCD study. A very relevant model in this regard is the Schwinger model (Quantum Electrodynamics in 1+1 dimensions) [13]. This theory exhibits features of QCD, such as confinement [14], and is at the very same time amenable to both theoretical studies and simpler experimental schemes. This model was the target of the first experimental realization of a gauge theory with a quantum simulator [15].

The work on this Thesis is, in part, motivated by the study of toy models which put in evidence certain aspects that can be found in QCD. Such toy models provide also intermediate steps in the path towards more complex simulations. The two main aspects of QCD which are addressed here are symmetry-locking and confinement. The other main motivation for this study is to develop a systematic framework, through dimensional mismatch, for theoretical understanding and quantum simulations of long-range theories using gauge theories.

The model used to study symmetry-locking consists of a four-fermion mixture [16]. It has the basic ingredients to exhibit a non-Abelian symmetry-locked phase: the full Hamiltonian has an $SU(2) \times SU(2)$ (global) symmetry which can break to a smaller $SU(2)$ group. Such phase is found in a extensive region of the phase diagram by using a mean-field approach and a strong coupling expansion. A possible realization of such system is provided by an Ytterbium mixture. Even without tuning interactions,

it is shown that such mixture falls inside the the locked-symmetry phase pointing towards a possible realization in current day experiments.

The models with dimensional mismatch investigated here have fermions in a lower dimensionality $d+1$ and gauge fields in higher dimensionality $D+1$. They serve two purposes: establish mappings to non-local theories by integration of fields [17] and the study of confinement [18].

In the particular case of $d=1$ and $D=2$ it is found that some general non-local terms can be obtained on the Lagrangian [17]. This is found in the form of power-law expansions of the Laplacian mediating either kinetic terms (for bosons) or interactions (for fermions). The fact that such expansions are not completely general is not surprising since constraints do exist, preventing unphysical features like breaking of unitarity. The non-local terms obtained are physically acceptable, in this regard, since they are derived from unitary theories. The above mapping is done exactly. In certain cases it is shown that it is possible to construct an effective long-range Hamiltonian in a perturbative expansion. In particular it is shown how this is done for non-relativistic fermions (in $d=1$) and $3+1$ gauge fields. These results are relevant in the context of state of the art experiments which implement models with long-range interactions and where theoretical results are less abundant than for the case of local theories. The above mappings establish a direct relation with local theories which allow theoretical insight onto these systems. Examples of this would consist on the application of Mermin-Wagner-Hohenberg theorem [19, 20] and Lieb-Robinson bounds [21], on the propagation of quantum correlations, to non-local models. In addition they can also provide a path towards implementation of tunable long-range interactions with cold atoms. Furthermore, in terms of quantum simulations, they are in between the full higher dimensional system and the full lower dimensional one. Such property is attractive from the point of view of a gradual increase of complexity for quantum simulations of gauge theories.

Another interesting property of these models is that they allow the study of confinement beyond the simpler case of the Schwinger model. The extra dimensions are enough to attribute dynamics to the gauge field, which are no longer completely fixed by the Gauss law. The phases of the Schwinger model are shown to be robust under variation of the dimension of the gauge fields [18]. Both the screened phase, of the massless case, and the confined phase, of the massive one, are found for gauge fields in $2+1$ and $3+1$ dimensions. Such results are also obtained in the Schwinger- Thirring model. This shows that these phases are very robust and raises interesting questions about the nature of confinement. Robustness under Thirring interactions are relevant because it shows that errors on the experimental implementation will not spoil the phase. Even more interesting is the case of gauge fields in higher dimensions since confinement in the Schwinger model is intuitively atributed to the dimensionality of the gauge fields (creating linear potentials between particles).

This Thesis is organized as follows. In Chapter 1, some essential background regarding quantum simulations of gauge theories is provided. It gives both a brief introduction to cold atomic physics and lattice gauge theories. In Chapter 2, it is presented an overview over proposals of quantum simulators of gauge potentials and gauge fields. At the end of this Chapter, in Section 2.3 it is briefly presented ongoing work on a realization of the Schwinger model that we term *Half Link Schwinger* model. There, it is argued, some of the generators of the gauge symmetry on the lattice can be neglected without comprimising gauge invariance. In Chapter 3, the results regarding the phase diagram of the four-fermion mixture, exhibiting symmetry-locking, is presented. In Chapter 4, the path towards controlling non-local kinetic terms and interactions is provided, after a general introduction to the formalism of dimensional mismatch. At the end the construction of effective Hamiltonians is described. Finally, Chapter 5 concerns the study of confinement and the robustness of it for $1+1$ fermions. The first part regards the Schwinger-Thirring with the presence of a θ-term while, in the second part, models with dimensional mismatch are considered. The thesis ends with conclusions and perspectives of future work based on the results presented here.

Contents

Chapter 1

Introductory material

As our understanding of physical phenomena develops, the problems we have to face become more complex to be treated, as a general trend. From a conceptual point of view it is understandable that this happens. Indeed, on general ground, the new proposed theories have to reproduce in the relevant range of validities the previous theories, the classical limit of quantum mechanics and the non-relativistic limit of relativity being two prototypical examples. It is then clear that the computational complexity have to increase in order to satisfy this logical constraint. As a concrete example, the classical equation of motion, $m\frac{d^2}{dt^2}x(t) = 0$, have its counterpart in quantum mechanics in the Schrödinger equation, that in its time-dependent form for a free paprticle reads $-\frac{\hbar^2}{2m}\frac{\partial^2}{\partial x^2}\psi(x) = E\psi(x)$. Considering also relativistic effects, in the realm of quantum field theory, one has to quantize an infinite number of simple harmonic oscillators: $\frac{\partial^2}{\partial t^2}\phi(k,t) = -\left(k^2+m^2\right)\phi(k,t)$. This "hierarchy" depends on the theoretical formulation one uses and it is not guaranteed that the order of difficulty does not change using other formulations of the different theories. However, it is expected that the computational complexity increases moving from classical to quantum systems: *e.g.*, the Newton equations for N particle in one dimensions requires the solution of $2N$ coupled *ordinary* differential equations, but the corresponding solution of the quantum problem via the Schrödinger equation requires to solve a *partial* differential equation in N variables. It is then no surprise that, using those tools, classical physics will tend to provide us technically simpler problems (when compared to their quantum analogues, for example). In this sense technical difficulties run along conceptual ones, since one may speculate that our "classical mind" develops mathematical tools that fit better the "classical world".

It is then possible that current unsolved problems may become simpler if we uncover a "better" formalism to tackle them. Of course this is not in itself an easy task. A clear example of this kind of principle is illustrated in the famous 1972 paper by Anderson "More is different" [22]. There it is argued that the physics of many particles is more than just the some of its parts and new formalisms, as challenging as uncovering fundamental physics, are necessary to uncover the physics of many particles. Were we to use formalism developed for few particles to uncover many particles physics we would quickly get stuck.

This discussion is valid also for non-analytical approaches. The success of numerics is not only dependent on how the problem is implemented on the computer, but also on how the problem is formulated in the first place and all the previous discussion translates here. One could hope, however, that with an increasing computational power, more and more problems would become approachable in this manner. This is not necessarily the case. Taking the example of statistical mechanics at finite temperature or lattice field theory, one has to sum over configurations in order to compute expectation values. Attempting this kind of sum directly would be in itself a formidable task due to the large volume of the phase space. This is can be circumvented by the so-called Monte Carlo methods [23]. Here an important sampling takes place and only the most important configurations are summed over. Monte

Carlo methods have been very successfully in characterizing different physical systems, however a lot of interesting systems may suffer from sign problems or complex actions [24]. As it will be explained in more detail bellow, these problems introduce large errors on the analysis which require exponentially larger resources on the volume of the system. In certain cases strategies exist that are able to solve these problems, but a large class of systems remain unreachable through numerical simulations. As a paradigmatic example, relevant for the study of QCD, a brief overview of the sign problem and complex actions will be presented in the next Section.

1.1 Feynman and quantum simulators

The idea of quantum simulators goes back to Feynman [3]. In this seminal talk Feynman approaches the problem of simulating quantum physics on a classical computer and how in principle the approach is limited from a fundamental level. If, for example, one can consider a lattice where, in each state, the degree of freedom can take one of n values (for example for a quantum spin labeled by the projection on the z direction is $n = 2$). Then the wave function will have a total of n^V components where V is the number of lattice points (in a cubic lattice in d dimensions $V = N^d$). In other words, the number of components that need to be specified scales exponentially with the volume of the system. These values need then to be constantly updated upon time evolution. In order to plug in some numbers, for $n = 2$ the total number of components is $10^{N^d \log 2} \sim 10^{0.3N^d}$. For a simple 10×10 lattice one has already around 10^{30} components. For any macroscopic material with a number of spins of the order of the Avogadro number, the task is completely hopeless. This contrasts with a classical system. If one consider a total of N classical particles, with some given interactions, the physics is described by a set of $2dN$ differential equations where d is the dimensionality of the system (these are the d position coordinates and the d momenta for example). At each time step one should update the new $2dN$ coordinates which is dramatically different from the number of amplitudes to be updated on the quantum system n^{N^d}. One is then lead to try to explore whether it is possible to approach analytically the problem, or devise an appropriate approximation scheme that allows a new numerical or analytical solution. Of course such kind of approximations exists and are extensively used like mean field approximation or renormalization group methods. At the numerical level the Monte Carlo methods play an important role by doing an importance sampling over configuration space visiting more often the more probable configurations. Even though successful in many physical systems, Monte Carlo methods suffer sometimes of certain sign-problems and complex action problems summarized below. Yet another class of methods, called tensor network methods, have emerged relatively recently [25]. An important feature is that they do not suffer the sign problems and complex actions and therefore can naturally supplement the Monte Carlo methods. They found application on strongly correlated systems [26, 27] and have been applied in the context of lattice gauge theories as well [28–43]. This approach is outside the scope of this thesis. For a pedagogical generic review see for example [44] and for the introduction to the application on lattice gauge theories see [45].

Feynman was hinting to yet another alternative approach not contemplated above, namely that of *quantum simulations*. He argues that even if one tries to use classical probabilities to imitate the quantum probabilities, the approach is doomed to fail. This is related to a series of theorems, generally called Bell's theorem, which states that no physical theory of local hidden variables can reproduce the predictions made by quantum mechanics [46]. One should not then try to imitate nature, which is intrinsically unpredictable, but rather simulate it. And to simulate quantum probabilities there is no way around using quantum mechanics to do so. The idea then is to construct a controllable system which allows a mapping of its degrees of freedom with the degrees of freedom of our system of interest. The system that one is able to control should be tuned in such a way that the transition amplitudes match the transition amplitudes of the original model. Experiments can then be performed on the controlled system and, thanks to the existent mapping between the two systems, one can have access to otherwise inaccessible quantities since the controlled system, a quantum device, "performed" the

difficult computations. This approach goes by the name of quantum simulations and poses short- and long-term goals [47].

Far from expecting that quantum simulations completely replace classical simulations of quantum systems it is expectable instead that both approaches shall work together. They will serve to validate each other results and both will help on model building and making predictions for experiments.

This section shall end with the already well known last sentenced used by Feynman in 1981:

"And I'm not happy with all the analyses that go with just the classical theory, because nature isn't classical, dammit, and if you want to make a simulation of nature, you'd better make it quantum mechanical, and by golly it's a wonderful problem, because it doesn't look so easy."

Richard P. Feynman

1.1.1 Sign problem and complex actions

In Monte Carlo methods one wants, in general, to compute the expectation value of observables by averaging over configurations. In quantum statistical mechanics, the expectation value of an observable $\hat{\mathcal{O}}$ for a given system at a temperature $T = 1/\beta k_B$ is given by:

$$\left\langle \hat{\mathcal{O}} \right\rangle = \frac{1}{Z} \mathrm{Tr} \left(\hat{\mathcal{O}} e^{-\beta \hat{H}} \right) \tag{1.1}$$

where Z is the partition function $Z = \mathrm{Tr} \left(e^{-\beta \hat{H}} \right)$. For a given basis state which are eigenvectors of the observable $\hat{\mathcal{O}}$, denoted here by $|\{S\}\rangle$, the expectation value of the observable can be written as:

$$\left\langle \hat{\mathcal{O}} \right\rangle = \frac{1}{Z} \sum_{\{S\}} \mathcal{O}\left(\{S\}\right) W\left(\{S\}\right) \tag{1.2}$$

where $\mathcal{O}\left(\{S\}\right) = \langle\{S\}| \hat{\mathcal{O}} |\{S\}\rangle$ and $W\left(\{S\}\right) = \langle\{S\}| e^{-\beta \hat{H}} |\{S\}\rangle$. In a Monte Carlo method one generates configurations with a probability $W\left(\{S\}\right)/Z$ and sample over them. One will never visit all the configuration space but the most relevant configurations are generated with higher probability which guarantees the correct sampling of the system. Ideally M independent configurations $\left\{S^{(i)}\right\}$ are generated with $i = 1, \ldots, M$ and the average value of the observable is approximated by:

$$\left\langle \hat{\mathcal{O}} \right\rangle \simeq \frac{1}{M} \sum_{i=1}^{M} \mathcal{O}\left(\left\{ S^{(i)} \right\} \right) \tag{1.3}$$

In the limit of $M \to +\infty$ the equation becomes an equality. The error is estimated assuming that the configurations are completely independent and that follow a Gaussian distribution. The standard deviation reads:

$$\Delta\mathcal{O} = \frac{1}{\sqrt{M}} \sqrt{\langle \mathcal{O}^2 \rangle - \langle \mathcal{O} \rangle^2} \tag{1.4}$$

A possible drawback of this approach is that the sign of the weight $W\left(\{S\}\right)$ is not necessarily positive for the basis choice made. In that case it is no longer possible to interpret $W\left(\{S\}\right)/Z$ as a probability. This minus sign can be factored out and be averaged over (together with the observable) as follows:

$$\left\langle \hat{\mathcal{O}} \right\rangle = \frac{1}{Z} \sum_{\{S\}} \mathcal{O}\left(\{S\}\right) \mathrm{sign} W\left(\{S\}\right) \left| W\left(\{S\}\right) \right| \tag{1.5}$$

where $W\left(\{S\}\right)$ is written as its modulus times its sign: $W\left(\{S\}\right) = \mathrm{sign} W\left(\{S\}\right) \left| W\left(\{S\}\right) \right|$. The same kind of thing must be done for $Z = \sum_{\{S\}} \mathrm{sign} W\left(\{S\}\right) \left| W\left(\{S\}\right) \right|$. The result is then a modified ensemble

which guarantees positive weights allowing the interpretation of $|W(\{S\})|/Z_M$ as probabilities. The partition function is given by $Z_M = \sum_{\{S\}} |W(\{S\})|$ and the subscript M stands for "modified". The expectation value of observable of the original theory are computed from the expectation values of quantities on the modified ensemble:

$$\left\langle \hat{\mathcal{O}} \right\rangle = \frac{\langle \mathcal{O} \mathrm{sign} W \rangle_M}{\langle \mathrm{sign} W \rangle_M} \tag{1.6}$$

In principle one can compute both numerator and denominator using Monte Carlo and, therefore, have access to $\left\langle \hat{\mathcal{O}} \right\rangle$. In practice the situation is not as simple due to the errors associated with these averages. In order to see this one can observe that:

$$\langle \mathrm{sign} W \rangle_M = \frac{1}{Z_M} \sum_{\{S\}} \mathrm{sign} W(\{S\}) |W(\{S\})| = \frac{Z}{Z_M} \sim e^{-V(f-f_M)} \tag{1.7}$$

where f and f_M are respectively the free energy densities of the original system and of the modified one. By construction $Z < Z_M$ and, therefore, the denominator of 1.6 is exponentially small on the volume. The same will happen for the numerator. As a consequence, one has a ratio of small numbers, each one obtained by averaging quantities of order one. Large cancellations are then obtained and it is very difficult to get accurate results for large volumes. This can be made explicit by estimating the error of $\langle \mathrm{sign} W \rangle_M$ (referring to Equation 1.4):

$$\frac{\Delta \mathrm{sign} W}{\langle \mathrm{sign} W \rangle_M} \sim \frac{1}{\sqrt{M}} \sqrt{1 - e^{-2V(f-f_M)}} e^{V(f-f_M)} \to \frac{1}{\sqrt{M}} e^{V(f-f_M)} \tag{1.8}$$

In the first passage Equation 1.7 was used while in the second the "large volume limit" was taken. One concludes that in order to obtain a small error, an exponentially large number of configurations on the volume has to be taken. For large systems this is not only inefficient but also impossible in practice.

The analysis that was made here for the sign can be made as well, with the same conclusions, for the case where the weight is complex (complex action problem) and this complex number is factorized on the average. Sign problems appear, for example, in frustrated magnets and on fermionic systems (due to fermionic commutation relations). Complex actions occur in quantum field theory when the action is complex, for example, due to the presence of θ terms, in the study of real time dynamics or in QCD at finite baryon density. In certain cases sign problems or complex action problems can be overcomed. This is possible, for example, through a change of basis which completely eliminates the sign problem, using a meron-cluster algorithm or with a fermion bag approach. For examples of these approaches see respectively [48], [49] and [50].

1.2 Ultracold atoms and quantum simulations

With the idea of quantum simulations in mind, one can then take a suitable platform and try to implement experimentally a given target system. This may include ultracold atoms, trapped ions, photonic systems and Rydberg atoms. Here a brief introduction to ultracold atomic physics is provided along with its potential for quantum simulations. For detailed description see for example [2, 51–54]

Ultracold atomic gases are very close to the absolute zero. By ultracold typically one means temperatures below 1 μK and it is possible to achieve temperatures as low as 10-10^2 nK in current experiments as, for example, in [55].

Just to name a few examples, ultracold atomic physics find applications in several different fields of physics from condensed matter (like Hubbard models and spin chains) [56–59], artificial gauge potentials [60–63], analogue models with Hawking and Unruh radiation [64–66], to field theory and

high energy physics. The research activity in the latter subjects include the study of the Dirac equation [67, 68], or supersymmetry [69–71] among others. Another interesting possibility is the simulation of nontrivial topologies and extra dimensions, realizable using internal degrees of freedom [72]. Simulation of lattice gauge theories will be discussed in more detail in the following.

The following Subsection starts with a brief description of the structure and relevant parameters of ultracold atoms. In the subsequent Section it is discussed how they can be further trapped, put on lattices and tune their interactions. In the last section it is presented some of the potential of the systems described and physical regimes achieved.

1.2.1 Atomic levels and scattering

Inside an atom the dominating interactions have their origin on the Coulomb force. This gives the well known atomic structure built on a progressive filling of the orbitals. Depending on the valence band, there could be an orbital angular momentum. Furthermore, electrons carry spin and the nucleus may have spin as well. The existence of these magnetic moments generate interactions beyond the Coulomb force which, being weaker, should not be disregarded. This means that there is a further hyperfine structure due to magnetic interactions. For the discussion the case of alkaline atoms is considered, where there is only one valence electron. The hyperfine level is characterized by two quantum numbers, l_F and m_F, resulting from the total angular momentum $\hat{\vec{F}}$ which is the sum of the orbital angular angular momentum of the electron $\hat{L}$, its spin $\hat{S}$ and the nuclear spin $\hat{I}$:

$$\hat{\vec{F}} = \hat{\vec{L}} + \hat{\vec{S}} + \hat{\vec{I}} \tag{1.9}$$

In the case of alkali atoms the orbital angular momentum is zero since the electron is in a s orbital. Then the total angular momentum is just a sum of nuclear and electron spin $\hat{\vec{F}} = \hat{\vec{S}} + \hat{\vec{I}}$. With a spin of $1/2$ for the electron addition of angular momentum yields a total angular momentum l_F which can be either $l_I + 1/2$ or $l_I - 1/2$ (assuming $l_I \neq 0$) where l_I is the total nuclear angular momentum. Without magnetic interactions all the $\{l_F, m_F\}$ states are degenerate. However, by considering a magnetic interaction, $H_{hf} \propto \hat{\vec{S}} \cdot \hat{\vec{I}}$ some degeneracy is lifted. In fact, since $2\hat{S} \cdot \hat{I} = F^2 - S^2 - L^2$, then when $l_F = l_I + 1/2 \Rightarrow 2\hat{S} \cdot \hat{I} = 2l_I$ while when $l_F = l_I - 1/2 \Rightarrow 2\hat{S} \cdot \hat{I} = -l_I - 1$. Therefore each one of these values for l_F corresponds to a different manifold with different eigenvalues which still have degeneracy due to its independence from m_F. This degeneracy can be further lifted in the presence of an external magnetic field $\vec{B}$: $H_B \propto \vec{B} \cdot \hat{\vec{F}}$.

This is a single atom description. The next step consists in understanding the interaction between two atoms. As an initial assumption, it is assumed that the atoms are the same and that they will not change their internal degree of freedom, that is, their initial and final hyperfine levels are the same before and after scattering. The interaction between the atoms is assumed spherically symmetric and short-range. The latter is a reasonable assumption since they are neutral, dilute and at a very low temperature. One can then take the center of mass reference frame and study the equivalent problem of scattering of a particle by a spherically symmetric potential. For a detailed discussion of this problem see, for example, [73]. Here the calculations are briefly reviewed and the discussion is assumed to be in three spatial dimensions. The total Hamiltonian of the system is taken to be $H = H_0 + V$ where H_0 is the usual kinetic term and V is the spherically symmetric potential. Far away from the range of influence of the potential the wave function can be written as:

$$\psi_{\vec{k}}(\vec{r}) = \frac{1}{(2\pi)^{3/2}} \left(e^{i\vec{k}\cdot\vec{r}} + f_{\hat{r}}\left(\vec{k}\right) \frac{e^{ikr}}{r} \right) \tag{1.10}$$

The second term constitutes a deviation from the plane wave and is a correction to the free particle solution. The amplitude $f_{\hat{r}}\left(\vec{k}\right)$ depends on the wave vector $\vec{k}$ and only on the direction of spatial

vector $\vec{r}$. It is formally given by:

$$f_{\hat{r}}\left(\vec{k}\right) = -\frac{4\pi^2 m}{\hbar}\left\langle k\hat{r}\left|T\right|\vec{k}\right\rangle \tag{1.11}$$

where $|k\hat{r}\rangle$ is the plane wave with a momentum magnitude of $k\hbar$ in the direction of $\hat{r}$, $\left|\vec{k}\right\rangle$ is the plane wave solution of the free Hamiltonian and the operator T is defined such that $T\left|\vec{k}\right\rangle = V\left|\psi_{\vec{k}}\right\rangle$[1]. Since $\left|\psi_{\vec{k}}\right\rangle$ enters in the construction of f this is not yet a closed-form solution. The function f can be suitably written as a sum of the so-called partial waves. Since T is a scalar, from the Wigner-Eckart theorem, it is diagonal on the basis $:|lm\rangle$ of the angular momentum operators $\vec{J}^2$ and J_z. Furthermore its diagonal elements only depend on the total energy E and on orbital angular momentum l, but not on the magnetic quantum number m. They are denoted here by $T_l(E)$. This allows a partial wave expansion by performing a change for this basis in Equation 1.11. This results in $f_{\hat{r}}\left(\vec{k}\right) = \sum_l (2l+1) f_l(k) P_l(\cos\theta)$ where $\vec{k}$ is assumed to be taken in the z direction, θ is the angle between $\hat{r}$ and the z axis, and P_l are the Legendre polynomials. The partial-wave amplitude $f_l(k)$ are given by $-\pi T_l(E)/k$. The plane wave, which appear in the first part of 1.10, admits a similar expansion by replacing the partial-wave amplitudes by spherical Bessel functions, j_l, at the point kr: $e^{i\vec{k}\cdot\vec{r}} = \sum_l (2l+1) i^l j_l(kr) P_l(\cos\theta)$. In turn the spherical Bessel functions, in the limit of large distance, can be written as a sum of an incoming and an outgoing spherical waves. Joining all these pieces together results in:

$$\psi_{\vec{k}}(\vec{r}) = \frac{1}{(2\pi)^{3/2}}\sum_l (2l+1)\frac{P_l(\cos\theta)}{2ik}\left(\left(1+2ikf_l(k)\right)\frac{e^{ikr}}{r} - \frac{e^{-i(kr-l\pi)}}{r}\right) \tag{1.12}$$

This expression allows a particularly transparent physical interpretation of the scattering. If the scattering is absent then $V=0$ and consequently $f_l = 0$ for every l. In general the plane wave solution can be seen as a sum of incoming and outgoing waves. All the effects of the scattering are condensed on the prefactor of the outgoing wave, that is, all that the scattering does is to change the coefficient of the outgoing wave. Furthermore, due to conservation of the probability flux, the absolute value of this coefficient must be 1. This means that all that scattering does, at large distances, is to change the phases of the the outgoing waves. These phases are usually written as $1+2ikf_l(k) = e^{2i\delta_l(k)}$.

The scattering description can be further simplified if one considers the limit of low temperature and low energy, which also suits well the cold atomic setting. In this regime k is small and the main contribution comes from $l=0$. Then there is only a single parameter characterizing the scattering between the atoms: the s-wave scattering length which is defined to be

$$a = -\lim_{k\to 0}\frac{1}{k\cot\delta_0(k)} \tag{1.13}$$

Note that this result is independent of the form of the potential given that it is short range. In this regime one can consider the atoms to be hard spheres, without loss of generality, having the scattering length as the single parameter describing the interaction. It is then possible to use the so-called pseudopotentials as shown in [74]

$$U(\vec{r}) = \frac{4\pi\hbar^2 a}{m}\delta(\vec{r})\,\partial_r r \tag{1.14}$$

The term $\partial_r r$ is a regulator. The coefficient of the δ function is such that this potential correctly reproduces a scattering length a. If the wave functions are regular in the limit of r going to zero the regulator can be dropped and the potential is just a delta function with an amplitude regulated by

[1] Formally T obeys the Lippmann-Schwinger equation given by $T = V + V\frac{1}{E-H_0+i\varepsilon}T$ where the small complex part $i\varepsilon$ is present in order to deal with the singularities of the operators.

the scattering length. The case of different atoms, which conserve their hyperfine levels, is completely analogous where $m/2$ on the above expression is replaced by the reduced mass of two atoms m_r.

In a general scenario collisions between (possibly different) atoms in different hyperfine levels can change their internal state. When to alkali atoms scatter, for example, with a total nuclear spin of $l_f^{(1)}$ and $l_f^{(2)}$, they can be found in a total of $4\left(2l_f^{(1)}+1\right)\left(2l_f^{(2)}+1\right)$ states. Analogous to the previous discussion where the hyperfine structure was ignored, one now has the same structure of Equation 1.10 with labels for the internal states (see [75]):

$$\left|\psi_{\vec{k}}\left(\vec{r}\right)\right\rangle = \frac{1}{\left(2\pi\right)^{3/2}}\left(e^{i\vec{k}\cdot\vec{r}}\left|\alpha\beta\right\rangle + \sum_{\alpha',\beta'} f_{\hat{r}}^{\alpha'\beta'\alpha\beta}\left(\vec{k}\right)\frac{e^{ikr}}{r}\left|\alpha'\beta'\right\rangle\right) \tag{1.15}$$

where the two atoms are initially in an hyperfine state $|\alpha\beta\rangle$ and then they can scatter through different channels to states $|\alpha'\beta'\rangle$ which must be summed over. The new f function is given by:

$$f_{\hat{r}}^{\alpha'\beta'\alpha\beta}\left(\vec{k}\right) = -\frac{2\pi^2 m_r}{\hbar}\left\langle k'\hat{r},\alpha'\beta'\left|T\right|\vec{k},\alpha\beta\right\rangle \tag{1.16}$$

While in the previous case the absolute value of the initial and final momenta were the same, meaning $k'=k$, now this is no longer mandatory as change on the hyperfine states may absorb or emit energy according to the equation:

$$k'^2 = k^2 + \frac{2m_r}{\hbar^2}\left(E_\alpha + E_\beta - E_{\alpha'} - E_{\beta'}\right) \tag{1.17}$$

where the above E's are the single particle energies due to their respective internal state. In particular, if the total energy from the internal states are the same, the absolute value of the momentum is the same as well. This also points out that there may be forbidden processes. Namely, if the change of internal states requires an energy superior to the initial kinetic energy (which would mean $k'^2<0$) then this solution should be excluded of the sum in Equation 1.15. With this in mind the rest of the analysis holds and one has a series of pseudopotentials:

$$U_{\alpha'\beta'\alpha\beta}\left(\vec{r}\right) = \frac{2\pi\hbar^2}{m_r}a_{\alpha'\beta'\alpha\beta}\delta\left(\vec{r}\right) \tag{1.18}$$

with a respective scattering length for each process $a_{\alpha'\beta',\alpha\beta}$.

The Dilute Gas Limit: As described above due to their very low temperature (and the fact that atoms are not charged) interaction between ultracold atoms can be well parameterized by contact interactions. In principle one should account for all type of interactions that can occur in this limit: two body, three body and so on. For the case of a dilute gas, which is the one considered here, the probability of having a three (or higher) body collision is very low and only the two body interactions remain relevant. Typically the density of atoms n is found to be in the range 10^{12} cm^{-3} to 10^{15} cm^{-3} which gives an average density $n^{-1/3}$ typically between 0.1 μm to 1 μm [53].

1.2.2 Traps, lattices and interactions

The existence of an external potential trapping the atoms is of fundamental importance in order to achieve the desired low temperatures. They also allow the construction of some desired specific one-body potentials and enable also the possibility to confine the atoms in a lower dimensionality by creating a large potential barrier in the directions that one desires to freeze. Optical dipole traps are grounded on the coupling between the electric dipole of the atom with light, which shall be far-detuned, as described for example in [2, 52, 53, 76]. The key feature is that, even though the atom is neutral, it is still polarizable. In this discussion it is assumed the single particle problem has a metastable state

$|e_0\rangle$ with energy ω_0 and an excited states $|e_i\rangle$ with energy ω_i. The Hamiltonian of the atom can then be written as:

$$H_{\text{atom}} = H_0 \otimes \left(\sum_i \omega_i |e_i\rangle \langle e_i| \right) \tag{1.19}$$

where H_0 corresponds to the translational movement of the atom. The center of mass dynamics is decoupled from the atomic internal states. From now, without loss of generality, the energies can be shifted such that $\omega_0 = 0$. The external laser electric field with a frequency ω takes the form:

$$\vec{E}\left(t, \vec{R}\right) = \vec{E}_0\left(\vec{R}\right) e^{-i\omega t} + \text{c.c.} \tag{1.20}$$

where c.c. stands for "complex conjugate" and the capital letter indicates the center of mass coordinate. This will induce a dipole which will interact with the field but it will not influence it (assuming the field is non-dynamical). The dipole moment of the atomic eigenstates is zero since there is an inversion symmetry, therefore the dipole moment operator will correspond to off-diagonal transitions on the basis of $|e_i\rangle$:

$$\hat{\vec{d}} = \sum_{i \neq j} \vec{d}_{ij} |e_i\rangle \langle e_j| \tag{1.21}$$

where $\vec{d}_{ij}$ are the dipole matrix elements satisfying $\vec{d}_{ij} = \vec{d}^*_{ji}$. The dipole will then interact with the electric field through $\hat{V} = -\vec{E}\left(t, \vec{R}\right) \cdot \hat{\vec{d}}$ coupling center of mass degrees of freedom with the internal states. The dipole created will point in the same direction of the electric field (in a general medium this needs not to be the case). Then, under the assumption that there is a dominant contribution from a single excited state, this extra interacting term can be written as:

$$\hat{V} = -\left(\vec{E}_0\left(\vec{R}\right) \cdot \vec{d}_{10} e^{-i\omega t} + \vec{E}_0\left(\vec{R}\right)^* \cdot \vec{d}_{10} e^{i\omega t}\right) |e_1\rangle \langle e_0| + \text{h.c.} \tag{1.22}$$

Now changing the basis for the rotating framing corresponding to consider $U(t) = e^{-i\omega |e_1\rangle\langle e_1| t}$:

$$\hat{V}' = U(t)^\dagger \hat{V} U(t) = -\left(\vec{E}_0\left(\vec{R}\right) \cdot \vec{d}_{10} + \vec{E}_0\left(\vec{R}\right)^* \cdot \vec{d}_{10} e^{2i\omega t}\right) |e_1\rangle \langle e_0| + \text{h.c.} \tag{1.23}$$

Under the rotating wave approximation, i.e. neglecting the fast rotating terms, one finds $\hat{V}' = \Omega\left(\vec{R}\right)/2 |e_1\rangle \langle e_0| + \text{h.c.}$ where $\Omega\left(\vec{R}\right)/2 \equiv \vec{E}_0\left(\vec{R}\right) \cdot \vec{d}_{10}$. The Hamiltonian transforms under:

$$H' = U(t)^\dagger H U(t) - i U(t)^\dagger \dot{U}(t) \tag{1.24}$$

The unitary transformation acts trivially on the Hamiltonian 1.19. Then the full transformed Hamiltonian reads:

$$H' = H_0 \otimes (\omega_1 - \omega) |e_1\rangle \langle e_1| + \frac{\Omega\left(\vec{R}\right)}{2} |e_1\rangle \langle e_0| + \text{h.c.} \tag{1.25}$$

It is then assumed that the far-detuned condition is fulfilled, that is, $\omega_1 - \omega$ is sufficiently large, so that the probability of transition to the excited state is very low. In this scenario the last term can be treated in second order perturbation theory (first order gives no contribution) and obtain:

$$H'_{eff} = \left(H_0 - \frac{\left|\Omega\left(\vec{R}\right)\right|^2}{4(\omega_1 - \omega)} \right) \otimes |e_0\rangle \langle e_0| + H_0 \otimes (\omega_1 - \omega) |e_1\rangle \langle e_1| \tag{1.26}$$

Now the obtained Hamiltonian, in its internal ground state, feels an effective potential provided by $\left|\Omega\left(\vec{R}\right)\right|^2$. This potential can serve as trapping potential and in particular can generate optical lattices

in which the atoms feel a background lattice. In fact with $\vec{d}_{10}\left(\vec{R}\right) = \alpha(\omega)\vec{E}_0\left(\vec{R}\right)$ being α the polarizability (which can depend on the frequency of the laser), the potential is just proportional to the intensity. Therefore a standing periodic wave of the form $E\left(\vec{R}\right) = E_0\cos(kx)$ generates a periodic potential $\propto \cos^2(kx)$. If two waves are counter-propagating the standing wave will have a period of $\lambda/2$ being λ the wave-length of the waves. By varying the angle at which the two beams interfere large periods of optical lattices can be achieved. The lasers can be combined in several directions in order to create $2D$ and $3D$ lattices as well as considering deep potentials in orthogonal directions in order to confine the atoms in a lower dimensionality [2].

Atoms in optical lattices Here it is assumed that the atoms are loaded on an optical lattice. Therefore, neglecting further one body potentials or interactions, the wave functions $\psi_{n\vec{k}}$ will be just Bloch waves:

$$\psi_{n\vec{k}}(\vec{r}) = e^{i\vec{k}\cdot\vec{r}}u_{n\vec{k}}(\vec{r}) \tag{1.27}$$

where $u_{n\vec{k}}(\vec{r})$ are periodic functions with the period of the lattice. This is just Bloch theorem explained in many textbooks as in [77]. Then the system develops band denoted by n and the wave vector $\vec{k}$ belongs to the Brillouin zone. Alternatively the Bloch wave functions can be written in terms of Wannier functions, denoted here by w_{nr_0}:

$$\psi_{n\vec{k}}(\vec{r}) = \sum_{\vec{r}_0} w_{n\vec{r}_0}(\vec{r})\, e^{i\vec{k}\cdot\vec{r}_0} \tag{1.28}$$

Wannier functions are orthogonal on both indices (n and r_0). The sum is to be performed over the lattice sites. They depend only on the distance $|\vec{r}-\vec{r}_0|$ and are typically localized around $\vec{r}_0$ for the lowest bands (less energetic states). An actual proof of this fact for all bands of a one dimensional system was given in [78]. It is worth noting that this is not not always the case. Each Bloch wave has, as usual, an arbitrary phase that can be chosen freely. In particular for each Bloch wave one can choose a phase that depends on $\vec{k}$: $\psi_{n\vec{k}} \to \psi_{n\vec{k}}e^{i\theta_{\vec{k}}}$. Difference choices of phases, despite a trivial change on the Block waves, have a dramatic impact on the Wannier functions. These phases must be chosen accordingly in order to maximize the localization of the Wannier function. In practice, for deep lattices and in the non-interacting limit, the Wannier functions can be taken to be the eigenstates of the harmonic potential (for which the ground state is a Gaussian), when restricting to the lowest band. This consists on the tight-binding approximation.

In second quantization the operator that annihilates a particle at position $\vec{r}$ of the type α (which can be internal state or different atomic species), $\hat{\psi}_\alpha(\vec{r})$, can be written at the cost of the operators that annihilate a particle in a Wannier state $\hat{a}_{\alpha n\vec{r}_0}$. In a low energy limit, meaning low temperature and small energy interaction when compared with the band gap, one can consider just the lowest band. In that case, writing $\hat{a}_{\alpha 0\vec{r}_0} \equiv \hat{a}_{\alpha\vec{r}_0}$, the operator becomes:

$$\hat{\psi}_\alpha(\vec{r}) = \sum_{\vec{r}_0} w^\alpha_{0\vec{r}_0}(\vec{r})\,\hat{a}_{\alpha\vec{r}_0} \tag{1.29}$$

The Hamiltonian part of one-body terms can be written as $H_{1B} = \sum_i h_{0i}$ where the sum is over identical particles. In term of second quantization this will give rise to a sum $H_{1B} = \sum_{r_0} T^{\alpha\beta}_{\vec{r}\vec{r}'}\hat{a}^\dagger_{\alpha\vec{r}}\hat{a}_{\beta\vec{r}'}$ where the coefficients are given by:

$$T^{\alpha\beta}_{\vec{r}\vec{r}'} = \int d^3R w^\alpha_{0\vec{r}}\left(\vec{R}\right)^* h_0 w^\beta_{0\vec{r}'}\left(\vec{R}\right) \tag{1.30}$$

where the index i was dropped from h_{0i} since it is no longer necessary to indicate in which Hilbert space h_0 is acting on. The typical single-particle terms in cold atomic systems are the kinetic term,

corresponding to single particle hopping, one-body potential, corresponding to a background potential, and Rabi terms corresponding to change of internal states. The later ones can be induced by resonant lasers, promoting the transition between these states. The hopping is explicitly written as:

$$t^{\alpha}_{\vec{r}\vec{r}'} = -\frac{\hbar^2}{2m_\alpha}\int d^3R \nabla w^{\alpha}_{0\vec{r}}\left(\vec{R}\right)^* \nabla w^{\alpha}_{0\vec{r}'}\left(\vec{R}\right) \tag{1.31}$$

where m_α is the mass of the species α. An extra minus sign was introduced, with respect to 1.30, that then is compensated by a minus sign on the Hamiltonian. There is also the two-body part $H_{2B} = \sum_i h^{2B}_{ij}$ which, as described above, correspond to contact interactions. This will give rise, in second quantization, to $H_{2B} = \sum_{r_0} U_{\alpha\beta\gamma\delta}\hat{a}^\dagger_{\alpha\vec{r}}\hat{a}^\dagger_{\beta\vec{r}}\hat{a}_{\delta\vec{r}}\hat{a}_{\gamma\vec{r}}$ with a coefficient given by:

$$U_{\alpha\beta\gamma\delta} = \frac{\pi\hbar^2}{m_r}a_{\alpha\beta\gamma\delta}\int d^3R w^{\alpha}_{0\vec{r}}\left(\vec{R}\right)^* w^{\beta}_{0\vec{r}}\left(\vec{R}\right)^* w^{\gamma}_{0\vec{r}}\left(\vec{R}\right) w^{\delta}_{0\vec{r}}\left(\vec{R}\right) \tag{1.32}$$

In the expression above an atomic species change the internal state from $\delta \to \alpha$ and $\gamma \to \beta$. The reduced mass m_r is calculated with respect to these two species. There is a factor of $1/2$ with respect to the pseudopotential of Equation 1.18 which compensates the double sum (see Hamiltonian below). Putting all this together, in the tight-biding limit, the Hamiltonian is given by:

$$\hat{H} = -\sum_{\langle\vec{r},\vec{r}'\rangle,i} t^{\alpha}_{\vec{r}\vec{r}'}\hat{a}^\dagger_{\alpha\vec{r}}\hat{a}_{\alpha\vec{r}'} + \text{h.c} + \sum_{\vec{r},\alpha,\beta} u^{\alpha\beta}_{\vec{r}}\hat{a}^\dagger_{\vec{r}\alpha}\hat{a}_{\vec{r}\beta} + \sum_{\vec{r},\alpha,\beta,\gamma,\delta} U_{\alpha\beta\gamma\delta}\hat{a}^\dagger_{\alpha\vec{r}}\hat{a}^\dagger_{\beta\vec{r}}\hat{a}_{\delta\vec{r}}\hat{a}_{\gamma\vec{r}} \tag{1.33}$$

The sum over $\langle\vec{r},\vec{r}'\rangle$ is a nearest neighbor sum.. The second term includes possible background potentials and changes of the hyperfine states induced by external lasers.

There is a further ingredient which makes ultracold atoms a very interesting setting for quantum simulations. While the first two terms are allowed a certain degree of manipulation from external lasers, the last one seems not to allow an independent tuning. Of course $U_{\alpha\beta\gamma\delta}$ depends not only on the scattering length but also on the Wannier functions which ultimately depend on the external lasers building the lattice. However these laser dependence does not give a great freedom and only allows a variation that is coupled to a variation in the hopping term. There are however ways in which this term can be tuned separately, e.g. by using Feshbach resonances to change the effective scattering. Therefore also this term enjoys an extra freedom of choice.

Feshbach resonances rely on the existence of a low energy bound state. In the limit in which the energy of this bound state is close to the energy of the scattering state (large atomic separation between scattering particles), a Feshbach resonance can occur. Since the magnetic moments of the atomic and molecule (bound) states are different, this energy difference can be controlled by an external magnetic field. Then, a proper tuning of this difference in energies leads to the so-called Feshbach resonances. The effect can be calculated in second order perturbation theory and can be interpreted as a virtual process in which the particles initially form a bound state and then decay to the scattering state. When the energy of the bound state is below the scattering state this gives rise to an attraction while if the bound state has a greater energy it will give rise to a repulsion. The correction on the s-wave scattering length a_0 (when there is only the open channel) for a given external magnetic field B can be parameterized by the equation (introduced in [79]):

$$a\left(B\right) = a_0\left(1 - \frac{\Delta}{B - B_0}\right) \tag{1.34}$$

where B_0 is the resonant value of the magnetic field for which the energies of the scattering and bound states are the same. The parameter Δ is the resonance width and indicates the value for which the scattering length vanishes (explicitly for $B = B_0 + \Delta$). A similar phenomena of magnetic Feshbach resonances described above are the optical Feshbach resonances. In the later case the two atoms couple to an electronically excited bound state through a laser field. The study of the resonance phenomena was initially carried out by Feshbach [80, 81] and by Fano [82]. Currently the subject can be found in several reviews and books, for example [52, 53, 75, 83].

1.2.3 Quantum simulations with ultracold atoms

The features described in the previous sections makes the ultracold atom setting an interesting platform to explore new physics, as concisely exposed in [1]. In this subsection two examples are given illustrating their potential where successful experimental implementation was achieved. These will be the BCS-BEC transition in the and the Superfluid-Mott transition on the lattice.

For the first case one considers a gas of atomic fermions that have an attractive interaction between them. In such gases there are two relevant length scales. One is the average interatomic distance which is related to the inverse of the Fermi momentum k_F^{-1}. The other is the scattering length that characterizes the interactions between the atoms (it is being considered a single fermionic mixture so that only one scattering length is present). Such mixture can then be characterized by a single dimensionless parameter given by the ratio of these two length. The goal is then to explore the physics of the system as the scattering length (or equivalently the interaction) is varied.

For a weak attractive interaction the scattering length is small and negative. By increasing the attraction the scattering length increases in absolute value but remains negative. At a certain finite value of the interaction the scattering length actually diverges (to $-\infty$). This is associated to the development of a bound state. By continuing to increase the interaction the scattering length jumps to $+\infty$ and starts to decrease becoming smaller and smaller as the interaction becomes more and more attractive (see for example [73]). This behavior is then translated to the parameters $1/k_F a$: it goes to $-\infty$ for weak attraction, the 0 is associated with a a development of a bound state and finally at $+\infty$ one finds the large attractive regime. The first and last limits are well understood:

- Weak attractive regime, $1/k_F a \to -\infty$: Fermions form pairs that are large than the interparticle distance. This is the well know BCS state (due to Bardeen-Cooper-Schrieffer [84]).
- Large attractive regime, $1/k_F a \to +\infty$: Fermions experience such a strong attraction that form bound states (molecules). Two fermions together form a boson, and these bosons are now weakly coupled. Therefore they form a BEC (Bose-Einstein condensate).

In between these values the system passes through several regimes and together they form what is known as the BCS-BEC crossover (see for example [85, 86]). The behavior of the intermediate regime, as a many-body problem, poses a challenge in the theoretical understanding since no small parameter exist to be used in perturbation theory. The fact that these system can be implemented with ultracold atoms allows, not only to gain insight into the physics of these systems, but also to validate other techniques giving an accurate reference to be compared to. As an example, precise measurements of the equation of state in the unitary limit ($1/k_F a \to 0$) [87, 88] were able to validate the diagrammatic Monte Carlo technique [88].

In a completely different setting, now a lattice system loaded with bosons is considered and the resulting model is the Hubbard model. It is a special case of the lattice Hamiltonian of 1.33 where there is only one species. There are two energy scales involved: the hopping parameter t and a density-density same site interaction U (the interaction term takes the form $\sim U n_r \left(n_r - 1\right)$ where n_r is the site number operator on site r). The relevant parameter is given by the ration U/t. Considering the case of repulsive interactions ($U > 0$) one finds the same general structure as before, in which there are two regimes that can be understood in perturbation theory:

- Small repulsion, $U/t \to 0$: Hopping dominates. Bosons are spread through the entire lattice with a macroscopic wave function $\to$ Superfluid state
- Strong repulsion $U/t \to 0$: Interaction dominates. Bosons are localized and there is a fixed number of bosons per site $\to$ Mott insulator state.

There is therefore a quantum phase transition for some critical value of U/t [56, 89, 90]. Again this ratio can be varied experimentally in a cold atomic setting and new regimes can be investigated.

This variation can be done by tuning the interactions (by Feshbach resonances) but also changing the hopping by varying the amplitude of the lattice potential. Both approaches have been used, respectively, in [91] and [56]. The simulator can give insights into the physics of non-perturbative regimes. For example, it is actually possible to achieve single-atom and single-site resolution which can give access to thermal and quantum fluctuation [92]. Insights into hidden order parameters is another interesting application. Typically these are local quantities. However that is not always the case which makes the identification of suitable order parameters much more complicated. An example of this is the identification of a string order in one dimensional gas of bosons [93, 94].

1.3 Gauge theories

A gauge theory is a model which has a gauge symmetry. Such symmetry is a redundancy on the description of the degrees of freedom. In other words, this means that one can have two mathematically distinct solutions of the equations describing the system and nonetheless they describe the same physical situation. The most well known gauge theory is most likely classical electrodynamics. It describes the behavior of the electric field $\vec{E}(t,\vec{x})$ and the magnetic field $\vec{B}(t,\vec{x})$ throughout space in the presence of an electric charge density $\rho(t,\vec{x})$ and the current density $\vec{j}(t,\vec{x})$. The system is governed by the Maxwell equations:

$$\begin{array}{ll} \nabla\cdot\vec{E}(t,\vec{x})=\rho(t,\vec{x}) & \nabla\times\vec{B}(t,\vec{x})-\partial_t\vec{E}(t,\vec{x})=\vec{j}(t,\vec{x}) \\ \nabla\cdot\vec{B}(t,\vec{x})=0 & \nabla\times\vec{E}(t,\vec{x})+\partial_t\vec{B}(t,\vec{x})=0 \end{array} \tag{1.35}$$

In the above equations and in the rest of this Thesis natural units shall be adopted, $\hbar=c=1$, unless for the particular cases in which explicitly ranges for experimental parameters are calculated. The homogeneous equations, which are independent of charges and currents, can be automatically solved by introducing a scalar potential $\phi(t,\vec{x})$ and a vector potential $\vec{A}(t,\vec{x})$:

$$\vec{E}(t,\vec{x})=-\nabla\phi(t,\vec{x})-\partial_t\vec{A}(t,\vec{x}),\quad \vec{B}(t,\vec{x})=\nabla\times\vec{A}(t,\vec{x}) \tag{1.36}$$

Using these two relations the equations of the last row are automatically solved and the ones from the first row can be written in terms of $\phi(t,\vec{x})$ and $\vec{A}(t,\vec{x})$. After a solution is found it can be plugged in again in Equation 1.36 in order to obtain the electric and magnetic fields. However not all different $\phi(t,\vec{x})$ and $\vec{A}(t,\vec{x})$ will give different electric and magnetic fields. In fact if two other fields $\phi(t,\vec{x})'$ and $\vec{A}(t,\vec{x})'$ are related to other solution by:

$$\phi(t,\vec{x})'=\phi(t,\vec{x})+\partial_t\alpha(t,\vec{x}),\quad \vec{A}(t,\vec{x})'=\vec{A}(t,\vec{x})-\nabla\alpha(t,\vec{x}) \tag{1.37}$$

for some function, $\alpha(t,\vec{x})$ then the electric and magnetic fields, given by Equation 1.36, remain unchanged. This means that the solutions $\phi,\vec{A}$ and $\phi',\vec{A}'$ correspond to the same physical situation and therefore they are just redundant descriptions of the same physics. The transformations of Equation 1.37 are called gauge transformations.

The existence of a gauge symmetry does not require that the field is dynamical. Consider a charged quantum particle in a background of a classical electromagnetic field. The Schrodinger equation for this system can be written as the equation in the absence of any field and "correcting" the canonical momentum $\vec{p}\to\vec{p}-e\vec{A}$. In the presence of an electromagnetic field the mechanical momentum, associated with the kinetic energy of the particle and denoted here by $\vec{\pi}$, is no longer the canonical momentum given by $\vec{p}$. The relation between them is $\vec{\pi}=\vec{p}-e\vec{A}$ which is at the core of this substitution. The same happens for the time derivative with the scalar potential $i\partial_t\to i\partial_t-e\phi$. The Schrodinger equation reads then, in the absence of any other interactions:

$$(i\partial_t-e\phi)\,\psi(t,\vec{x})=\left(-i\nabla-e\vec{A}\right)^2\psi(t,\vec{x}) \tag{1.38}$$

Also this equation is invariant under the transformation 1.37 provided that the wave function is transformed by a phase:

$$\psi\left(t,\vec{x}\right)=e^{ie\alpha(t,\vec{x})}\psi\left(t,\vec{x}\right) \tag{1.39}$$

In quantum field theory an illustrative example is provided by QED. The Lagrangian is given by:

$$\mathcal{L}=\bar{\psi}\left(\gamma^{\mu}\left(i\partial_{\mu}-eA_{\mu}\right)-m\right)\psi-\frac{1}{4}F_{\mu\nu}F^{\mu\nu} \tag{1.40}$$

From this point it will always be assumed sum over repeated indices unless otherwise stated. γ^{μ} are the gamma matrices satisfying the Clifford algebra $\{\gamma^{\mu},\gamma^{\nu}\}=2\eta^{\mu\nu}$, $\eta^{\mu\nu}$ is the Minkowski metric $\eta=\mathrm{Diag}\left(1,-1,-1,-1\right)$, ψ the Dirac spinor and $\bar{\psi}=\psi^{\dagger}\gamma^{0}$. The indices μ run from 0 to 3 where 0 corresponds to the time index. The A_{μ} is called gauge field and the last term of the Lagrangian corresponds to their kinetic term where $F_{\mu\nu}=\partial_{\mu}A_{\nu}-\partial_{\nu}A_{\mu}$. Again here there is a local set of transformations that leave this Lagrangian invariant. Explicitly:

$$A_{\mu}\left(x\right)\rightarrow A_{\mu}\left(x\right)-\frac{1}{e}\partial_{\mu}\alpha\left(x\right),\ \psi\left(x\right)\rightarrow e^{i\alpha(x)}\psi\left(x\right) \tag{1.41}$$

This is an example of a $U\left(1\right)$ gauge theory: a gauge transformation is defined, at each point, by phases $\alpha\in[0,2\pi[$ which combine according to the group $U\left(1\right)$. However gauge symmetries can belong to other gauge groups, like $\mathbb{Z}_N$, or also non-Abelian, like $SU\left(N\right)$, for N an integer number. For example, the Kitaev toric code is a $\mathbb{Z}_2$ (Abelian) gauge theory [7] while Quantum Chromodynamics (QCD), the theory that describes strong interactions in particle physics, is a $SU\left(3\right)$ (non-Abelian) gauge theory [95–97]. In the following a brief description of non-Abelian gauge invariance in quantum field theory is provided. For more details see, for example, [10].

As just presented the QED Lagrangian has a local symmetry described by the transformations 1.41. This transformation is said to be local since the phases $\alpha\left(x_{\alpha}\right)$ can depend arbitrarily on the position (provided that their derivative exist). In the absence of the gauge field this symmetry no longer holds. Instead only a very small subset of the transformations survive. These are the global transformations which transform the same way in all space-time points, i.e. for α a constant function. From another point of view, gauge invariance was obtained by replacing the "regular" derivative by a covariant derivative

$$D_{\mu}=\partial_{\mu}+ieA_{\mu} \tag{1.42}$$

When applied to the field, the covariant derivative does not change under a gauge transformation 1.41. By this it is meant that under such transformations $D_{\mu}\psi\left(x_{\alpha}\right)\rightarrow e^{i\alpha(x_{\alpha})}D_{\mu}\psi\left(x_{\alpha}\right)$ and therefore it acts just like the regular derivative for α constant. Note that the covariant derivative can be defined to be:

$$D_{\mu}\psi=\lim_{\varepsilon\rightarrow0}\frac{\psi\left(x_{\mu}+\varepsilon\right)-U\left(x_{\mu}+\varepsilon,x_{\mu}\right)\psi\left(x_{\mu}\right)}{\varepsilon} \tag{1.43}$$

where the the quantity $U\left(x_{\mu}+\varepsilon_{\mu},x_{\mu}\right)$ should have the asymptotic behavior $U\left(x_{\mu}+\varepsilon_{\mu},x_{\mu}\right)=1-ie\varepsilon A_{\mu}\left(x_{\alpha}\right)+\mathcal{O}\left(\varepsilon^{2}\right)$. In general U will be dependent on two points $U\left(x,y\right)$. Assuming that U is a phase and that it conjugates under exchange of variables ($U\left(x,y\right)=U\left(y,x\right)^{*}$) fixes U to be $U\left(y,x\right)=\exp\left(-ie\mathcal{A}\left(y,x\right)\right)$ for some real function $\mathcal{A}\left(y,x\right)$. This function should obey, for $y=x+\varepsilon^{\mu}n_{\mu}$ with ε^{μ} infinitesimal and n_{μ} an unitary vector pointing in an arbitrary direction, $\mathcal{A}\left(y,x\right)=\varepsilon^{\mu}A_{\mu}\left(x\right)$. A choice which satisfies this criteria is

$$\mathcal{A}\left(y,x\right)=\int_{P_{yx}}dz^{\mu}A_{\mu}\left(z\right) \tag{1.44}$$

where P_{yx} is a path connecting the points x and y (for example a straight line). The resulting path dependent object U_P is called Wilson line and transforms, under gauge transformations

$$U_{P}\left(y,x\right)\rightarrow e^{i\alpha(y)}U_{P}\left(y,x\right)e^{-i\alpha(x)} \tag{1.45}$$

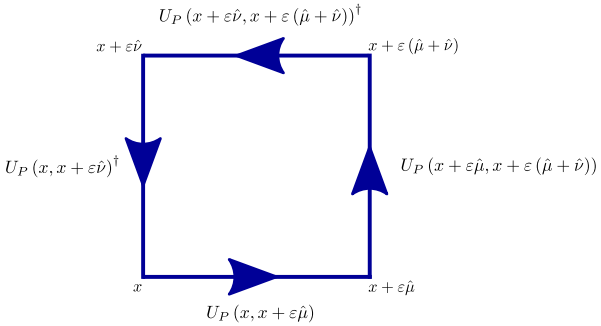

Figure 1.1: In order to find the correct build block for the pure gauge term, one can take a closed path un a form of a square as shown in the figure. By taking a square of size ε and taking the limit of small ε one arrives to Equation 1.46. Note that $U\left(x,y\right)=U\left(y,x\right)^\dagger$.

The Wilson line allows, in particular, to construct easily gauge invariant objects by simply choosing a closed path P. Equivalently one can combine products of different paths to form a closed path. This actually allows the construction of the kinetic term of the gauge field. In fact, $F_{\mu\nu}\left(x\right)$ can be derived from $U_P\left(y,x\right)$ where P is the closed path formed by a square starting at the point x and running counter-clockwise first in the direction μ and then ν, see Figure 1.1. In the infinitesimal limit where the length of the edge of the square is ε one finds:

$$U_\square=1-ie\varepsilon^2F_{\mu\nu} \tag{1.46}$$

Summing up: starting from the Dirac Lagrangian one can construct in a natural way a gauge theory by imposing the existence of a local symmetry. In particular $U_\square$ gives the receipt to obtain a gauge invariant quantity $F_{\mu\nu}$ which has to be contracted with $F^{\mu\nu}$ in order to form a gauge invariant quantity. This approach can be used to construct the Lagrangian for other symmetry groups.

In the case described above the gauge invariance was $U\left(1\right)$ and it corresponded to just a phase. In order to explore other symmetries, an extra index must be inserted (in the paradigmatic example of QCD these are the color indices). In order to simplify the notation, whenever ψ it is used it is meant:

$$\psi\equiv\begin{pmatrix}\psi_1\\ \psi_2\\ \vdots\\ \psi_N\end{pmatrix} \tag{1.47}$$

where each one of the ψ_i corresponds to a (four-component in $3+1$ dimensions) Dirac spinor. Consider then a general symmetry group and a respective set of generators represented by Hermitian $N\times N$ matrices t^a. The goal is to build a Lagrangian which is invariant under the set of local transformations

$$\psi\left(x\right)\rightarrow e^{i\alpha^a\left(x\right)t^a}\psi\left(x\right) \tag{1.48}$$

This transformation mixes the N components of the vector 1.47. The object constructed for the Abelian case, that was identified as the Wilson line 1.45, now has to be a matrix and transforms under:

$$U\left(y,x\right)\rightarrow e^{i\alpha^a\left(x\right)t^a}U\left(y,x\right)e^{-i\alpha^a\left(x\right)t^a} \tag{1.49}$$

which allows the construction of a covariant derivative, like in Equation 1.43. If this transformation is to hold, then the composition rule: $U\left(y,x\right)U\left(x,z\right)=U\left(y,z\right)$ must hold. In order to derive the form

of $U(y,z)$ consider a path between an initial point z and a final point y and consider x infinitesimally close to y. Then the equation can be written as:

$$U(y,y-\varepsilon)\,U(y-\varepsilon,z)=U(y,z)\Leftrightarrow\left(1+\varepsilon^{\mu}\partial_{\mu}U(y.y)\right)\left(U(y,z)-\varepsilon^{\mu}\partial_{\mu}U(y,z)\right)=U(y,z) \tag{1.50}$$

where it was assumed that $U(y,y)=1$ and $U(y,z)^{\dagger}=U(z,y)$. The derivatives act on the first entry (in the expansion of $U(y,y-\varepsilon)$ it is possible to pass the derivative to the first entry by using the conjugation properties of U and of the derivative operator). Then U obeys the equation:

$$igt^{a}A_{\mu}^{a}(y)\,U(y,z)=\partial_{\mu}U(y,z) \tag{1.51}$$

where the derivative of U at the same point in space was written as $\partial_{\mu}U(y,y)=igt^{a}A_{\mu}^{a}(y)$. One has to be careful in solving this equation because U at different points do not commute in general. However this problem is exactly the same that one faces on finding the unitary time evolution operator for a time dependent Hamiltonian (which may not commute at different times). As the solution in that case is the time ordering exponential, the solution here is a path ordering, here denoted by $\mathcal{P}$:

$$U(y,z)=\mathcal{P}\left\{e^{igt^{a}\int_{P}dx^{\mu}A_{\mu}^{a}}\right\} \tag{1.52}$$

Then using the prescription for the covariant derivative of Equation 1.43 one finds:

$$D_{\mu}=\partial_{\mu}-igA_{\mu}^{a}t^{a} \tag{1.53}$$

The kinetic term can also be constructed in a similar way choosing a path corresponding to an infinitesimal square running counter-clockwise in the directions μ and ν (again see Figure 1.1). The result is given by:

$$U_{\square}(x)=1+ig\varepsilon^{2}F_{\mu\nu}^{a}(x)\,t^{a}+\mathcal{O}\left(\varepsilon^{3}\right) \tag{1.54}$$

where $F_{\mu\nu}^{a}$ is calculated by direct computation:

$$F_{\mu\nu}^{a}=\partial_{\mu}A_{\nu}^{a}-\partial_{\nu}A_{\mu}^{a}+gf^{abc}A_{\mu}^{b}A_{\nu}^{c} \tag{1.55}$$

and f^{abc} are the structure constants given by $\left[t^{a},t^{b}\right]=it^{c}f^{abc}$. Note that now $U_{\square}(x)$ is not gauge invariant since it transforms under $U_{\square}(x)\rightarrow e^{i\alpha^{a}(x)t^{a}}U_{\square}(x)\,e^{-i\alpha^{a}(x)t^{a}}$ and there is not a trivial commutation relation between $U_{\square}$ and the exponetials. However it is straightforward to construct a gauge invariant quantity by taking the trace of $U_{\square}(x)$. As the generators t^{a} are traceless one has to go to higher than second order in 1.54. Going though the computation one finds that the fourth order is the lowest non-trivial order giving a gauge invariant quantity $F_{\mu\nu}^{a}F^{a\mu\nu}$. The Lagrangian can be written:

$$\mathcal{L}=\mathcal{L}=\bar{\psi}\left(\gamma^{\mu}D_{\mu}-m\right)\psi-\frac{1}{4}F_{\mu\nu}^{a}F^{a\mu\nu} \tag{1.56}$$

In this equation $\bar{\psi}$ is to be interpreted as line vector with components $\bar{\psi}_{i}$ and γ^{μ} are diagonal on the color indices, i.e. act the same for every color by standard matrix multiplication $\gamma^{\mu}\psi_{i}$.

1.4 A primer on lattice gauge theories

The target of this Section is to do a very brief introduction to lattice gauge theory setting the stage for simulation of theories in which the gauge components of the system are also dynamical. Naive discretization of bosons and fermions plus the doubling problem (occurring for fermions) are introduced. The alternative formulation of lattice gauge theory with quantum links is particularly advantageous for quantum simulations and is introduced at the end of this Section.

1.4.1 Naive discretization of bosons

In this Section the action for the free bosonic field shall be discretized. In Euclidean time the action reads:

$$S[\phi] = \frac{1}{2}\int d^{d+1}x \left((\partial_\mu \phi)^2 + m\phi^2\right) \tag{1.57}$$

For symmetry the kinetic term is written as $-\phi\partial^2\phi$, where $\partial^2 \equiv \sum_\mu \partial_\mu^2$ is the Laplacian in $d+1$ dimensions ($\mu = 0, \ldots, d$), which can be done integrating by parts in the action. Now naive discretization is applied which consists in substituting the derivatives by finite differences, factorized by a lattice spacing a. There are different ways to do this discretization. Here the derivative is discretized as: $\partial_\mu \phi(x) \to (\phi(x + a\hat{\mu}/2) - \phi(x - a\hat{\mu}/2))/a$. This implies that the Laplacian is discretized as: $\partial^2\phi(x) \to (\phi(x + a\hat{\mu}) + \phi(x - a\hat{\mu}) - 2\phi(x))/a^2 \equiv (\phi_{n+\hat{\mu}} + \phi_{n-\hat{\mu}} - 2\phi_n)/a^2$. A general point x of the lattice has components that are multiple integers of the lattice spacing $x = a(n_0, \ldots, n_d) \equiv an$ so a notation was adopted to make this explicit. The integral is also transformed in a discrete sum $\int d^{d+1}x \to a^{d+1}\sum_n$. To avoid unnecessary complications the lattice is considered to have the same extension in all the directions: $n_i = 0, \ldots, N-1$ so the total volume is $V = (aN)^{d+1}$. The discretized action is then written as:

$$S[\phi] = \frac{1}{2}a^{d+1}\sum_n \left(\phi_n(\phi_{n+\hat{\mu}} + \phi_{n-\hat{\mu}} - 2\phi_n)a^{-2} + m\phi_n^2\right) \equiv \frac{1}{2}a^{d+1}\sum_{l,n}\phi_l K_{ln}\phi_n \tag{1.58}$$

where a matrix K was defined having components:

$$K_{ln} = -\frac{\delta_{n,l+\hat{\mu}} + \delta_{n,l-\hat{\mu}} - 2\delta_{nl}}{a^2} + m \tag{1.59}$$

Within path integral quantization expectation values are calculated integrating over configuration (here still in Euclidean time):

$$\langle \mathcal{O}[\phi] \rangle = \frac{1}{Z}\int D\phi \mathcal{O}[\phi] e^{-S[\phi]} \tag{1.60}$$

where $Z = \int D\phi e^{iS[\phi]}$. In this discretized version the measures were abbreviated by: $D\phi = \prod_n d\phi_n$. The next step consists on calculating the two point function and see if the continuum two point function is obtained on the limit $a \to 0$. The action is quadratic on the fields and therefore the integration is carried out explicitly. The propagator reads:

$$\langle \phi_l \phi_n \rangle = \frac{1}{a^{d+1}} K_{ln}^{-1} \tag{1.61}$$

This is most easily computed in momentum space where K is diagonal. Defining

$$K_{pq} = \left(\frac{1}{aN}\right)^{d+1} \sum_{l,n} K_{ln} e^{ia(lp-nq)} \tag{1.62}$$

and substituting directly on 1.59 results in:

$$K_{pq} = \frac{1}{a^{d+1}}\left(-\frac{2}{a^2}\sum_\mu \cos(ap_\mu) + \frac{2}{a^2} + m^2\right)\delta_{pq} \tag{1.63}$$

The two point function in momentum space can be written as:

$$\langle \phi(-p)\phi(p) \rangle = \frac{1}{\frac{4}{a^2}\sum_\mu \sin^2\left(\frac{ap_\mu}{2}\right) + m^2} \tag{1.64}$$

where there was a simple rearrangement of the denominator. Here also $\phi(p) = (a/N)^{(d+1)/2} \sum_n \phi_n e^{-ipn}$ and equivalently $\phi_n = (aN)^{-(d+1)/2} \sum_p \phi_p e^{ipn}$. When the continuum limit is taken, when $a \to 0$, the Brillouin zone where p_μ takes values, $p_\mu \in [-\pi/a, \pi/a[$, covers the entire real line. In that limit the function becomes simply:

$$\langle \phi(-p)\, \phi(p) \rangle_{a\to 0} = \frac{1}{p^2 + m^2} \tag{1.65}$$

where $p^2 \equiv \sum_\mu p_\mu^2$. This is precisely the two point function of the continuum theory and therefore the expected two point function is obtained.

1.4.2 Naive discretization of fermions and doubling problem

The free Dirac fermion action in $d+1$ dimensions in Euclidean time is given by:

$$S\left[\bar{\psi}, \psi\right] = \int d^{d+1}x \bar{\psi} \left(\gamma_\mu \partial_\mu + m\right) \psi \tag{1.66}$$

From this point it will always be assumed sum over repeated indices unless otherwise stated. γ^μ are the gamma matrices satisfying the Clifford algebra $\{\gamma^\mu, \gamma^\nu\} = 2\delta^{\mu\nu}$, $\delta^{\mu\nu}$ the Euclidean metric (δ is the identity matrix in $d+1$ dimensions) and $\bar{\psi} = \psi^\dagger \gamma^0$. The gamma matrices have dimensions $2^{[(d+1)/2]} \times 2^{[(d+1)/2]}$ and the spinor ψ $2^{[(d+1)/2]} \times 1$ where $[x]$ means the integer part of x. The naive discretization follows the same procedure as for the bosonic theories replacing derivatives for finite differences. In order to do this in a symmetric way first the kinetic term is written as:

$$\int d^{d+1}x \bar{\psi}\gamma_\mu \partial_\mu \psi = \frac{1}{2} \int d^{d+1}x \left(\bar{\psi}\gamma_\mu \partial_\mu \psi - \partial_\mu \bar{\psi}\gamma_\mu \psi\right) \tag{1.67}$$

using integration by parts. The discretization is taken explicitly as: $\partial_\mu \psi(x) \to (\psi(x + a\hat{\mu}) - \psi(x))/a \equiv (\psi_{n+\hat{\mu}} - \psi_n)/a$. The discretized action will read:

$$S\left[\bar{\psi}, \psi\right] = a^d \sum_n \left(\frac{1}{2}\bar{\psi}_{n+\hat{\mu}}\gamma_\mu \psi_n - \frac{1}{2}\bar{\psi}_n \gamma_\mu \psi_{n+\hat{\mu}} + am\bar{\psi}_n \psi_n\right) \equiv a^{d+1} \sum_{l,n} \bar{\psi}_l K_{ln} \psi_n \tag{1.68}$$

where the matrix K as components:

$$K_{ln} = \sum_\mu \frac{1}{2a} \gamma^\mu \left(\delta_{l,n+\hat{\mu}} - \delta_{l,n-\hat{\mu}}\right) + \delta_{ln} m \tag{1.69}$$

Within path integral quantization expectation values are calculated integrating over configuration (here still in Euclidean time):

$$\left\langle \mathcal{O}\left[\bar{\psi}, \psi\right] \right\rangle = \frac{1}{Z} \int D\bar{\psi} D\psi \mathcal{O}\left[\bar{\psi}, \psi\right] e^{-S[\bar{\psi}, \psi]} \tag{1.70}$$

where $Z = \int D\bar{\psi} D\psi e^{iS[\bar{\psi}, \psi]}$. Again in this discretized version the measures were abbreviated: $D\psi = \prod_n d\psi_n$ with the analogous formula for $D\bar{\psi}$. The fermionic fields are Grassman variables. The next step consists on calculating the two point function and see if the continuum two point function is obtained on the limit $a \to 0$. The action is quadratic on the fermion fields is still quadratic and therefore the integration is carried out explicitly:

$$\left\langle \bar{\psi}_l \psi_n \right\rangle = \frac{1}{a^{d+1}} K_{ln}^{-1} \tag{1.71}$$

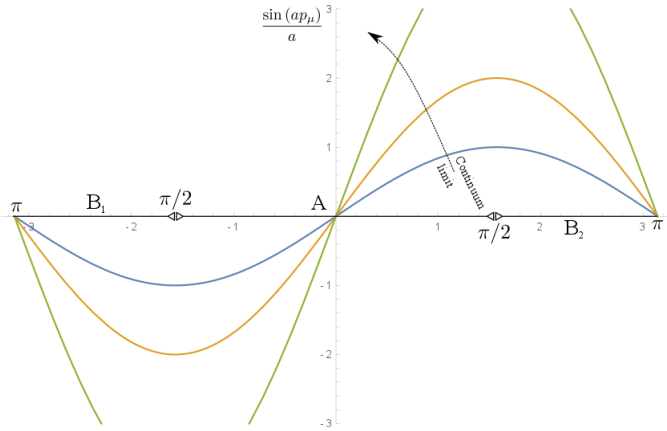

Figure 1.2: Continuum limit of naive fermions. On the vertical axis the value of $k_\mu = \sin(ap_\mu)/a$ which will be the momentum in the continuum limit. The interval $k_\mu \in]-\infty, +\infty[$ is covered twice: for p_μ in the interval indicated by A and again by joining B_1 (negative momentum) and B_2 (positive momentum).

Again by going to momentum space and substituting directly on 1.69 results in:

$$K_{pq} = \frac{1}{a^{d+1}} \left(\frac{i}{a} \sum_\mu \gamma^\mu \sin(ap_\mu) + m \right) \delta_{pq} \tag{1.72}$$

as a result the two point function in momentum space are:

$$\left\langle \bar{\psi}(-p)\, \psi(p) \right\rangle = \frac{1}{\frac{i}{a}\sum_\mu \gamma_\mu \sin(ap_\mu) + m} \tag{1.73}$$

here also $\psi(p) = (a/N)^{(d+1)/2} \sum_n \psi_n e^{-ipn}$ and $\bar{\psi}(p) = (a/N)^{(d+1)/2} \sum_n \bar{\psi}_n e^{-ipn}$.

In order to check the continuum limit here, one has to be more careful than for the bosonic case. For the later case, in Equation 1.64, the $\sin^2(ap_\mu/2)$ was a monotone function on p_μ in all the Brillouin zone. This is not the case for $\sin(ap_\mu)$ as it is schematized on Figure 1.2. In the continuum limit $k_\mu = \lim_{a\to 0} \sin(ap_\mu)/a$ there are two values of p_μ which give the same momentum. This results in an extra quantum label which consists in an extra flavor that was not intended to be there. This is commonly referred as the doubling problem and consists on the fact that naive discretization leads, in the continuum limit, to extra fermionic flavors. For every discretized dimension one has two degrees of freedom to choose from which will correspond to the same momentum. This means that in total, for $d+1$ discretized dimensions, there are 2^{d+1} fermionic flavors instead of just 1.

In order to solve this problem it is useful to refer to the Nielsen-Ninomiya Theorem [98–100]. This theorem states that for a free fermion lattice action that is:

- real
- sufficiently local (smooth fourier transform)
- translation invariant (under lattice translations)
- chiral invariant

suffers from fermion doubling problem. Nielsen-Ninomiya Theorem hints to what kind of things one might think to give up in order to solve the fermion doubling problem. The most natural condition to give up is chiral symmetry. One of such solutions was proposed by Wilson by adding to the action a term that explicitly breaks chiral symmetry. This term is also responsible for giving a large mass to the doublers in the continuum limit. This term is added to the action 1.68 and takes the form $a^{d+1}\sum_{n,\mu}\left(2\bar{\psi}_n\psi_n - \bar{\psi}_{n+\hat{\mu}}\gamma_\mu\psi_n - \bar{\psi}_n\gamma_\mu\psi_{n+\hat{\mu}}\right)/2a$. Explicitly computation shows that the doublers are removed.

Another approach consists on using the so called staggered fermions (also known as Kogut-Susskind fermions). This is however less severe and a $U(1)$ symmetry remains with respect to the Wilson approach. The idea consists use the doublers to build the Dirac spinors. Assuming that $d+1$ is even then the Dirac spinor has $(d+1)/2$ components. Distributing each of the doubler for the components of the spinor one reduces the number of doublers to: $2^{d+1}/2^{(d+1)/2} = 2^{(d+1)/2}$. Naturally this is a drawback of the approach since it does not eliminate completely the fermion doubling problem. The construction of staggered fermions for $1+1$ dimensions are described in detail in the last section using the Hamiltonian approach instead of the path integral. Generalizations for higher dimensions are also presented. A particularity of the $1+1$ Hamiltonian case is that, since time is not discretized, there is an extra factor of $1/2$ reducing the doublers and the doubling problem is completely solved. In other words, when keeping time continuous, the number of doublers is 2^d. Using staggered fermions they are reduced to $2^d/2^{(d+1)/2} = 2^{(d-1)/2}$. If $d=1$ than this is equal to 1 and there are no doublers.

1.4.3 Staggered fermions

In this Section, since is the Hamiltonian approach that will be discussed, real time is taken instead of Euclidean time. First the construction of the Hamiltonian for the case of $1+1$ Dirac fermions is discussed by using the idea of encoding the degrees of freedom of the spinor in different lattice sites. In the end the lattice formulation is generalized to $3+1$ dimensions by recognizing that it is possible to decouple spinor degrees of freedom.

1+1 fermions The Dirac Hamiltonian in continuous space time takes the form:

$$H = \int d^d x \bar{\psi}\left(-i\gamma^i\partial_i + m\right)\psi \tag{1.74}$$

where i takes the values of special indices: $i = 1,\ldots,d$. Now, focusing on the $d=1$ case, given a lattice $n \in \mathbb{Z}$ instead of placing a ψ_n 2×1 spinor in each lattice site, a single fermion c_n is inserted. Then the spinors are represented by:

$$\psi_n = \frac{1}{\sqrt{a_{st}}}\begin{pmatrix} c_{2n} \\ c_{2n+1} \end{pmatrix} \tag{1.75}$$

being a_{st} the lattice spacing. The pre-factor ensures the correct dimensions so that one can work with the usual adimensional operators on the lattice as well as guarantees the correct scaling for the continuum limit $a_{st}\to 0$. A concrete representation of the Clifford algebra is adopted. The two gamma matrices in $1+1$ are taken here to be the Pauli matrices $\gamma^0 = \sigma_z$ and $\gamma^1 = i\sigma_y$. Then one should discretize, with the above recipe, the Hamiltonian . To discretized the Hamiltonian is written as

$$H = \int dx\left(-i\psi^\dagger\sigma^+\partial_1\psi + i\partial_1\psi^\dagger\sigma^-\psi + m\psi^\dagger\sigma_z\psi\right) \tag{1.76}$$

In this expression σ_x was decomposed into $\sigma^\pm = (\sigma_x \pm i\sigma_y)/2$ (and therefore $\sigma_x = \sigma^+ + \sigma^-$) and, on the σ^-, integration by parts was used. This may look as a strange way to write the same theory. The goal is to have, after discretization of the derivatives, a lattice theory without second nearest neighbor hoppings. This will be made clear at the end of the discretization process. Both derivatives

are replaced by $\partial_1\psi \to (\psi_n - \psi_{n-1})/a_{st}$ and $\partial_1\psi^\dagger \to \left(\psi_n^\dagger - \psi_{n-1}^\dagger\right)/a_{st}$. Plugging all this in the Hamiltonian 1.76

$$H = \sum_{n=0}^{N_{st}-1} \left(\psi_n^\dagger \sigma_y \psi_n + i\psi_n^\dagger \sigma^+ \psi_{n-1} - i\psi_{n-1}^\dagger \sigma^- \psi_n + a_{st} m \psi_n^\dagger \sigma_z \psi_n\right) \tag{1.77}$$

and expanding the spinor components:

$$H = \frac{1}{a_{st}} \sum_{n=0}^{N_{st}-1} \left(-ic_{2n}^\dagger c_{2n+1} + ic_{2n+1}^\dagger c_{2n} + ic_{2n}^\dagger c_{2n-1} - ic_{2n-1}^\dagger c_{2n} + a_{st} m c_{2n}^\dagger c_{2n} - a_{st} m c_{2n+1}^\dagger c_{2n+1}\right) \tag{1.78}$$

which can be written as a sum on a lattice with twice as much lattice sites. The number of sites in the new lattice is $N = 2N_{st}$ and the lattice spacing is half the original one $a = a_{st}/2$ (the physical dimension of the system remains the same). Then the resulting lattice Hamiltonian can be written as:

$$H = \sum_{l=0}^{N-1} \left(-\frac{i}{2a} c_l^\dagger c_{l+1} + \text{h.c.} + m\,(-1)^l\, c_l^\dagger c_l\right) \tag{1.79}$$

As mentioned before the lattice discretization would have a different look depending on how one would approach the discretization. For example if instead of $\partial_1\psi \to (\psi_n - \psi_{n-1})/a_{st}$ one uses $\partial_1\psi \to (\psi_{n+1} - \psi_n)/a_{st}$, which is the same in the continuum limit, there would be second nearest neighbor hopping. For the lattice model this is of course different but it should not matter when the continuum limit is take. Particularly in taking the continuum limit naively the corrections are of higher order on the lattice spacing and the differences on the lattice model vanish.

Higher dimensions The discussion above can be generalized to higher dimensionality. Here the case of three spatial dimensions shall be described. Now there are four Dirac component to be distributed on the lattice. In the one dimensional case there were two sublattices, corresponding to even and odd sites, building respectively the upper and lower component of the Dirac spinor. Now there should be four sublattices that will encode the four degrees of freedom. The procedure followed here could also be followed for the later case. The starting point corresponds to a naive discretization of the Hamiltonian 1.74 analogous to the case of one spatial dimension:

$$H = a^d \sum_n \left[\frac{i}{2a}\left(-\bar{\psi}_n \gamma^i \psi_{n+\hat{i}} + \bar{\psi}_{n+\hat{i}} \gamma^i \psi_n\right) + m\bar{\psi}_n \psi_n\right] \tag{1.80}$$

The idea consists on performing a spin diagonalization (effectively diagonalizing the gamma matrices) by a local transformation of the spinors:

$$\psi_n = C_n \varphi_n,\ \psi_n^\dagger = \varphi_n^\dagger C_n^\dagger \tag{1.81}$$

with C_n an unitary transformation. The γ-matrices are replaced by the following matrices:

$$C_n^\dagger \gamma^0 \gamma^i C_{n+\hat{i}} = \Delta_i(n),\ C_n^\dagger \gamma^0 C_n = \Delta_0(n) \tag{1.82}$$

The goal consists on choosing the C matrices in such a way that the Δ's are diagonal. For concreteness it will be considered the case of $d = 3$ and, furthermore, one can fix the chiral representation of the Clifford algebra:

$$\gamma^0 = \begin{pmatrix} 0 & I_2 \\ I_2 & 0 \end{pmatrix},\ \gamma^i = \begin{pmatrix} 0 & \sigma_i \\ -\sigma_i & 0 \end{pmatrix},\ \gamma_5 = \begin{pmatrix} I_2 & 0 \\ 0 & -I_2 \end{pmatrix} \tag{1.83}$$

There are possible choices like, for example:

$$C_n = \Gamma \left(\gamma_5 \gamma^1\right)^{n_1} \left(\gamma_5 \gamma^2\right)^{n_2} \left(\gamma_5 \gamma^3\right)^{n_3} \tag{1.84}$$

where the different n_i are the components of the lattice index n and Γ is defined to be:

$$\Gamma = \frac{1}{\sqrt{2}} \begin{pmatrix} I_2 & -I_2 \\ I_2 & I_2 \end{pmatrix} \tag{1.85}$$

This matrix commutes with the γ^i and diagonalizes γ^0: $\Gamma^\dagger \gamma^0 \Gamma = \gamma_5$. It is useful to observe that the matrices $\gamma_5 \gamma^i$ are Hermitian, unitary and anticommute between each other. One finds:

$$\Delta_i (n) = (-1)^{n_1 + \ldots + n_{i-1}} I_4, \ \Delta_0 (n) = (-1)^{n_1 + n_2 + n_3} \gamma_5 \tag{1.86}$$

What is observed is that, in this transformed variables, each component of the Dirac spinor is decoupled from the other due to the fact that the "new γ-matrices", Δ, are diagonal. One can then keep a single component per site throwing away the rest which are decoupled from the system. For instance, choosing the first component of the spinor and denoting it by $[\psi_n]_1 = c_n / a^{3/2}$ (in general dimensions one has $c_n / a^{d/2}$) yields:

$$H = \sum_{n,i} \left[-\frac{i}{2a} (-1)^{n_1 + \ldots + n_{i-1}} \left(c_n^\dagger c_{n+\hat{i}} - c_{n+\hat{i}}^\dagger c_n \right) + (-1)^{n_1 + n_2 + n_3} m c_n^\dagger c_n \right] \tag{1.87}$$

This generalizes the previous staggered fermions Hamiltonian in 1+1 dimensions. Writing the hopping explicitly for clarity:

$$\begin{aligned} H = \sum_n \Bigg[-\frac{i}{2a} \Big[\left(c_n^\dagger c_{n+\hat{1}} - c_{n+\hat{1}}^\dagger c_n \right) + (-1)^{n_1} \left(c_n^\dagger c_{n+\hat{2}} - c_{n+\hat{2}}^\dagger c_n \right) \\ + (-1)^{n_1 + n_2} \left(c_n^\dagger c_{n+\hat{3}} - c_{n+\hat{3}}^\dagger c_n \right) \Big] + (-1)^{n_1 + n_2 + n_3} m \bar{c}_n c_n \Bigg] \end{aligned} \tag{1.88}$$

The structure of the minus signs in from of each hopping term is not unique. Other choices are possible by alternative solutions to 1.84, for example by considering: $C_n = \Gamma \left(\gamma^1\right)^{n_1} \left(\gamma^2\right)^{n_2} \left(\gamma^3\right)^{n_3}$.

This construction can be carried out to any dimension generalizing to:

$$H = \sum_{n,i} \left[-\frac{i}{2a} (-1)^{n_1 + \ldots + n_{i-1}} \left(c_n^\dagger c_{n+\hat{i}} - c_{n+\hat{i}}^\dagger c_n \right) + (-1)^{n_1 + \ldots + n_d} m c_n^\dagger c_n \right] \tag{1.89}$$

where, naturally, i runs from 1 to d.

1.4.4 Lattice gauge theory

Since the final goal will be to provide an Hamiltonian formulation of a lattice gauge theory, it is useful to start by considering the continuum Hamiltonian formulation for Abelian gauge theory. Consider the Lagrangian of QED 1.40. It is seen that the component A_0 is non-dynamical (there is no term $\partial_0 A_0$) and acts as a Lagrange multiplier enforcing the Gauss' law as a constraint of the system. The equations of motion for this component are simply $\partial \mathcal{L} / \partial A_0 = 0$ resulting in

$$-\partial_i F^{0i} - e \psi^\dagger \psi = 0 \tag{1.90}$$

which is the Gauss law, as announced. The electric field is $E^i = -F^{0i}$ and it is the conjugate momentum of the variable A_i ($E^i = \partial \mathcal{L} / \partial \dot{A}_i$ with the dot denoting time derivative). In order to construct the Hamiltonian the temporal gauge, $A_0 = 0$, shall be adopted. As a consequence the Gauss law 1.90 must be imposed as a constraint of the system. The resulting Hamiltonian density reads:

$$\mathcal{H} = \bar{\psi} \left(-i \gamma^i \left(\partial_i + i e A_i \right) + m \right) \psi + \frac{1}{2} \left(E^i E_i + B^i B_i \right) \tag{1.91}$$

where $B_i = \varepsilon_{ijk}\partial^j A^k$ is the magnetic field. In canonical quantization, since E_i is the canonical conjugate of A_i:

$$[A_i(x), E_j(y)] = i\delta_{ij}\delta^{(d)}(x-y) \tag{1.92}$$

The operator $E_j(y)$ can be represented as $E_j(y) = -i\partial/\partial A_j(y)$. The constraints on the states read:

$$G(x)|\Psi\rangle = 0 \tag{1.93}$$

where $G(x) = \partial_i E^i - e\psi^\dagger\psi$ is the generator of the residual gauge invariance. In fact the gauge fixing used, $A_0 = 0$, does not fix completely the gauge as any gauge transformation 1.41 with α time independent leaves the gauge fixing condition untouched. The residual gauge transformations are therefore time independent phases.

1.4.4.1 $U(1)$ gauge theory in $1+1$ dimensions

Now the goal is to construct a gauge invariant lattice Hamiltonian. The starting point shall be the staggered fermions Hamiltonian of Equation 1.79 in $1+1$ dimensions. The final Hamiltonian should have a local symmetry corresponding to the transformation $c_n \to e^{i\alpha_n}c_n$. As expected the Hamiltonian 1.79 does not have such symmetry. The solution passes by including a a link variable connecting the two fermion operators $c_n^\dagger U_{n,n+1}c_{n+1}$ which under gauge transformations compensates the transformations of the fermions. This amounts to say:

$$\begin{cases} c_n \to e^{i\alpha_n}c_n \\ U_{n,n+1} \to e^{i\alpha_n}U_{n,n+1}e^{-i\alpha_{n+1}} \end{cases} \tag{1.94}$$

Making contact with the continuum theory the link variable can be written as:

$$U_{n,n+1} = \exp\left(ie\int_{an}^{a(n+1)} dx A_1(x)\right) \tag{1.95}$$

which transforms correctly under the gauge transformation. These link variables are then inserted on the kinetic term. Furthermore, one should supply the pure gauge part corresponding to the electric field E_n (which is also a link variable). In fact this is, in spirit exactly, the same approach that was carried out in Section 1.3 to build a gauge theory out of the idea of a local symmetry. The link variable 1.95 is nothing more than the Wilson line constructed in 1.52, specialized for $1+1$ case of $U(1)$ with a straight line path $\mathcal{P}$ between an and $a(n+1)$. In the small lattice spacing limit $U_{n,n+1} = \exp(ieaA_n) \equiv U_n$, where $A_n \equiv A_1(an)$, and with $E_n = -i\partial/\partial A_n$ one finds $[U_n, E_m] = e\delta_{nm}U_n$ [2]. It is then convenient to introduce the variables $L_n = E_n/e$ and the commutation relation becomes:

$$[L_m, U_n] = \delta_{nm}U_n, \ \left[L_m, U_n^\dagger\right] = -\delta_{nm}U_n^\dagger, \tag{1.96}$$

The link variables U_n can also be written in terms of a phase θ_n: $U_n = e^{i\theta_n}$. The variable θ_n is the canonical conjugate of L_n:

$$[\theta_n, L_m] = i\delta_{nm} \tag{1.97}$$

With all these ingredients the Hamiltonian takes the form:

$$H = -\frac{i}{2a}\sum_n \left(c_n^\dagger e^{i\theta_n}c_{n+1} - \text{h.c.}\right) + m\sum_n (-1)^n c_n^\dagger c_n + \frac{ae^2}{2}\sum_n L_n^2 \tag{1.98}$$

[2] The Dirac delta $\delta(x-y) = \delta(na-ma)$ was replaced, in its discretized version, by δ_{nm}/a. That this is the correct discretization can be seen by considering the representation of the Delta function as $\delta(x) = \lim_{a\to 0}\frac{\theta(x-a)\theta(a-x)}{a}$. By considering x a multiple integer of a and removing the limit one obtains the desired discretized version δ_{nm}/a.

Finally it remains to be imposed the Gauss law through the generator for the gauge transformations of Equation 1.94. To identify the generators an infinitesimal transformation is considered where, say, α_n is infinitesimal and all the other α's are set to zero. Then the only variables affected by the gauge transformation are

$$\begin{cases} c_n \to (1 + i\alpha_n)\, c_n \\ c_n^\dagger \to (1 - i\alpha_n)\, c_n^\dagger \\ \theta_n \to \theta_n + \alpha_n \\ \theta_{n-1} \to \theta_{n-1} - \alpha_n \end{cases} \tag{1.99}$$

For a generator G of a transformation with a parameter α, an operator $\mathcal{O}$ is transformed according to $\mathcal{O} \to e^{i\alpha G}\mathcal{O}e^{-i\alpha G}$. For infinitesimal transformations $\mathcal{O} \to \mathcal{O} + i\alpha\,[G, \mathcal{O}]$. Applying this for the present case yields:

$$\begin{cases} [G_n, c_n] = c_n \\ \left[G_n, c_n^\dagger\right] = -c_n^\dagger \\ [G_n, \theta_n] = -i \\ [G_n, \theta_{n-1}] = i \end{cases} \tag{1.100}$$

while it should commute with all the other operators. The solution of these equations takes then the form $G_n = L_n - L_{n-1} - c_n^\dagger c_n + \text{const}$. The constant can be determined by imposing that the bare vacuum, with no electric field, is a physical state. Such state is the ground state of the limit of infinite mass and is characterized by:

$$c_n^\dagger c_n \,|0\rangle = \frac{1 - (-1)^n}{2},\ L_n \,|0\rangle = 0 \tag{1.101}$$

This fixes the generators to be:

$$G_n = L_n - L_{n-1} - c_n^\dagger c_n + \frac{1 - (-1)^n}{2} \tag{1.102}$$

Of course any other constant choice will not alter the symmetry for which G_n is a generator. This choice just allows to impose the Gauss law requiring that the states are annihilated by G_n:

$$G_n \,|\Psi\rangle = 0 \tag{1.103}$$

Bare vacuum, pair creation on the lattice and the Gauss law: The bare vacuum defined in Equation 1.101 has fermions filling the odd number sites while leaving the even number emptied. This is the same ground state for the infinite massive case of the free staggered fermions of the Hamiltonian 1.79. The interpretation of this structure is related to the fact that the spinor degrees of freedom are distributed along the lattice. Occupied odd sites have the interpretation of a filled Dirac see. When a fermion hops from a odd to an even site it creates a hole on the Dirac see while creating a particle above the Dirac sea. This is interpreted as the creation of particle/anti-particle pair where the hole plays the role of an anti-particle. When in the presence of gauge fields, the hop described above must be accompanied by a change on the electric field according to Equations 1.102 and 1.103. Given the bare vacuum and an an odd site n from which lattice fermion hops to the neighboring even site $n+1$, then L_n goes from 0 to 1 according to Equation 1.79. This initial fermion hopping breaks the Gauss law for the sites n and $n+1$ which are both restored by the above change on L_n.

1.4.4.2 $U(1)$ gauge theory in $d+1$ dimensions

The principle applied above translates to higher dimensions. While in the $d = 1$ case the links could be labeled by just one index (the lattice site from which they emanate) for higher dimensions a direction must supplement this label. Therefore they are represented by U_{ni} meaning "link emanating from n in

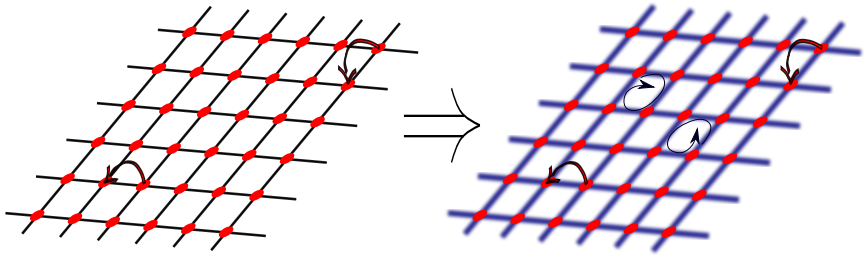

a) No dynamical links b) Dynamical links: Lattice gauge theory

Figure 1.3: Illustration of the construction of a lattice gauge theory by introducing dynamical links. In a) the links are not dynamical and only fermions are present. Their kinetic terms are represented which consist on nearest neighbor hopping. In b) the links become dynamical through plaquette terms (represented by the circular arrows).

the i-th direction. Analogously one has $U_{ni} = e^{i\theta_{ni}}$ and L_{mi}, related to the discretized electric field by $L_{ni} = E_{ni}a^{d-1}/e$, with commutation relations $[\theta_{ni}, L_{mj}] = i\delta_{ij}\delta_{nm}$. The gauge transformations are:

$$\begin{cases} c_n \to e^{i\alpha_n} c_n \\ U_{ni} \to e^{i\alpha_n} U_{ni} e^{-i\alpha_{n+\hat{i}}} \end{cases} \tag{1.104}$$

For U_{ni} again one can use the Wilson line 1.95. Now, for $d > 1$ there is a magnetic field which corresponds to a plaquette term. For an ij plaquette in the point n this means $U_{\square} = U_{ni}U_{n+\hat{i},j}U^{\dagger}_{n+\hat{j},i}U^{\dagger}_{n,j}$ (this is the same situation presented in Figure 1.1 where now, instead of an infinitesimal distance ε, one uses the lattice spacing). This is exactly the same principle that was used in the continuum: using the Wilson line to construct the kinetic term for the gauge fields (see Equation 1.46). Equation 1.46 can also be written as $U_{\square} = e^{-iea^2 F_{\mu\nu}}$. Since here one is dealing only with spatial plaquettes it actually correspond to $U_{\square} = e^{-iea^2 F_{ij}}$. This expression indicates what must be the pre-factor of this terms in the Hamiltonian in order to recover the correct continuum limit:

$$\begin{aligned} H = &- \frac{i}{2a}\sum_{n,i} (-1)^{n_1+\ldots+n_{i-1}} \left(c^{\dagger}_n e^{i\theta_{ni}} c_{n+\hat{i}} - \text{h.c.}\right) + m\sum_n (-1)^{n_1+\ldots+n_d} c^{\dagger}_n c_n \\ &+ \frac{a^{2-d}e^2}{2}\sum_{n,i} L^2_{ni} - \frac{a^{d-4}}{4e^2}\sum_{\square}\left(U_{\square} + U^{\dagger}_{\square}\right) \end{aligned} \tag{1.105}$$

In Figure 1.3 it is illustrated the construction of a lattice gauge theory: degrees of freedom are introduced on the links that become dynamical. This allows the implementation of a local symmetry.

The generators of the gauge symmetry can be built again by imposing that they implement the transformations 1.104. This will lead to $G_n = \sum_i L_{ni} - L_{n-\hat{i},i} - c^{\dagger}_n c_n + \text{const}$ and the constant can be determined again by imposing that the bare vacuum:

$$c^{\dagger}_n c_n |0\rangle = \frac{1-(-1)^{n_1+\ldots+n_d}}{2},\ L_{ni}|0\rangle = 0 \tag{1.106}$$

is a physical state. This condition fixes the generators to be:

$$G_n = \sum_i L_{ni} - L_{n-\hat{i},i} - c^{\dagger}_n c_n + \frac{1-(-1)^{n_1+\ldots+n_d}}{2} \tag{1.107}$$

1.4.4.3 $U(N)$ and $SU(N)$ gauge theories

While for $U(1)$ there was only one generator of the group, here there is a given set $\{t^a\}$ which translates to the generators of the gauge transformation. In order to build the quantum links for the $SU(N)$

symmetry, one can look at the transformation law:

$$U_{ni} \to U_{ni} + i\left(\alpha_n^a t^a U_{ni} - \alpha_{n+\hat{i}}^a U_{ni}\sigma^a\right) \tag{1.108}$$

for a set of small parameters α^a. The goal is to find a set of generators that will fulfill this transformation in the usual way: $U_{ni} \to U_{ni} - i\alpha_n^a \left[G_n^a, U_{ni}\right]$. This implies that the following relations should hold:

$$\left[G_n^a, U_{ni}\right] = -t^a U_{ni}, \ \left[G_n^a, U_{n-\hat{i},i}\right] = U_{n-\hat{i},i}t^a \tag{1.109}$$

This generators obey the same algebra of $\{t^a\}$:

$$\left[G_n^a, G_n^b\right] = i\delta_{nm}f^{abc}G_n^c \tag{1.110}$$

They can be realized by distinguishing a "left" and "right" part of a link, and identifying in each site the right end and left end of the links connected to it:

$$G_n^a = \sum_i \left(R_{n-\hat{i},i}^a + L_{ni}^a\right) \tag{1.111}$$

R_{ni} and L_{ni} are called, respectively, right and left generators where

$$\left[R_{ni}^a, U_{ni}\right] = U_{ni}t^a, \ \left[L_{ni}^a, U_{ni}\right] = -t^a U_{ni} \tag{1.112}$$

with the commutation at different sites and/or directions trivial. Furthermore there are non-trivial relations between them:

$$\left[R_{ni}^a, R_{mi'}^b\right] = i\delta_{mn}\delta_{ii'}f^{abc}R_{ni}^c, \ \left[L_{ni}^a, L_{mi'}^b\right] = i\delta_{mn}\delta_{ii'}f^{abc}L_{ni}^c, \ \left[R_{ni}^a, L_{mi'}^b\right] = 0 \tag{1.113}$$

Including the fermions one should have $\left[G_n^a, \chi_n\right] = t^a\chi_n$ or in terms of components: $\left[G_n^a, \left[\chi_n\right]_i\right] = \left[t^a\right]_{ij}\left[\chi_n\right]_j$. Fermions were denoted by χ to remind that they are vectors now. The generator can then be written as:

$$G_n^a = \sum_i \left(L_{ni}^a + R_{n-\hat{i},i}^a\right) + \chi_n^\dagger t^a \chi_n \tag{1.114}$$

The lattice Hamiltonian for the non-Abelian theory will then be:

$$\begin{aligned} H = -\tfrac{i}{2a}\sum_{n,i}(-1)^{n_1+\ldots+n_{i-1}}\left(\chi_n^\dagger U_{ni}\chi_{n+\hat{i}} - \text{h.c.}\right) + m\sum_n (-1)^{n_1+\ldots+n_d}\chi_n^\dagger\chi_n \\ +\tfrac{a^{2-d}g^2}{2}\sum_{n,i,a}\left(\left(L_{ni}^a\right)^2 + \left(R_{ni}^a\right)^2\right) - \tfrac{a^{d-4}}{4g^2}\sum_{\square}\text{Tr}\left(U_\square + U_\square^\dagger\right) \end{aligned} \tag{1.115}$$

This Hamiltonian has an extra $U(1)$ symmetry. For an operator obeying $\left[E_{mi}, U_{nj}\right] = \delta_{nm}\delta_{ij}U_{nj}$ and commuting with the rest of the the operators. Than the generator: $G_n = -\chi_n^\dagger\chi_n + \sum_i\left(E_{ni} - E_{n-\hat{i},i}\right)$ commutes with the Hamiltonian and with the other generators G_n^a. If one wishes to study the $SU(N)$ theory rather than a $U(N)$, terms breaking this last symmetry should be added like

$$\sum_{n,i}\left(\det U_{ni} + \det U_{ni}^\dagger\right) \tag{1.116}$$

which still preserve the original $SU(N)$ symmetry.

1.4.5 Quantum links formulation

The so called quantum link models constitute a generalization of the formulation above, following Wilson prescription, where the U_n variables are constructed from the gauge field according to 1.95. These kind of models were introduced by Horn in 1981 [101] and were further studied in [102–106]. Particularly, in [104–106], they were studied as an alternative formulation to Wilson's gauge field theories on the lattice.

Recently they proved to be an interest target for the quantum simulation of gauge theories since several proposals rely on them (see reviews on quantum simulations for example [45,107,108] and next Chapter for more details). The fundamental motivation is that the algebra of the links, characterized by Equation 1.96 and all the other commutation relations zero, span an infinite Hilbert space per each link. In the quantum links formulation the Hilbert space is finite and an implementation becomes, theoretically, simpler. This is achieved by giving up the unitarity of the U_{ni} operators.

$U(1)$ **Quantum Links** In a quantum link model each link is associated with a given spin $\vec{S}_{ni} = (S^x_{ni}, S^y_{ni}, S^z_{ni})$ and these spin variables are used to construct the link variables analogous to U_{ni} and L_{ni} necessary to construct the gauge theory. It consists on taking alternative links:

$$L_{+ni} = S^x_{ni} + iS^y_{ni},\ L_{ni} = S^z_{ni} \tag{1.117}$$

With this construction the relation 1.96 is still satisfied. However other commutation relations, which were zero, are not anymore. Namely L_{+ni} and $L^\dagger_{+ni} = L_{-ni}$ no longer commute:

$$[L_{+ni}, L_{-ni}] = 2L_{ni} \tag{1.118}$$

This is just another way of writing the angular momentum algebra. Even though the algebra itself is different, these operators can be equally used to construct a gauge theory without compromising the gauge symmetry. The dimensional of the Hilbert space in each of these links is $2S+1$ with S a positive half integer (corresponding to, in the spin language, to the total spin). One expects that in the limit of large S the Wilson formulation should be recovered. Explicitly one can use the following link variables $U_{ni} \to L_{+ni}/\sqrt{S(S+1)}$. Then again the commutation relations 1.96 still hold and there is a extra non-zero commutation relation corresponding to:

$$\left[U_n, U^\dagger_n\right] = \frac{2}{S(S+1)} L_n \tag{1.119}$$

In the limit of $S \to +\infty$ the right hand side of the above equation goes to zero and the initial algebra is recovered. In the quantum link formulation the Hamiltonian for $U(1)$ gauge theory reads:

$$\begin{aligned} H = &-\tfrac{i}{2a\sqrt{S(S+1)}} \sum_{n,i} (-1)^{n_1+\ldots+n_{i-1}} \left(c^\dagger_n L_{+ni} c_{n+\hat{i}} - \text{h.c.}\right) + m \sum_n (-1)^{n_1+\ldots+n_d} c^\dagger_n c_n \\ &+ \tfrac{a^{2-d}e^2}{2} \sum_{n,i} L^2_{ni} - \tfrac{a^{d-4}}{4e^2 S^2 (S+1)^2} \sum_{\square} \left(L_\square + L^\dagger_\square\right) \end{aligned} \tag{1.120}$$

where the plaquette terms $U_\square$ were replaced by the analogous plaquette terms on the new link variables $L_\square$,

Non-Abelian Quantum Links A non-unitary U_{ni} is built upon $2N^2$ Hermitian operators (referring to real and imaginary part). By other side each L^a and R^a are Hermitian having N^2-1 components plus E which is another Hermitian operators. In total this gives a number of generators that is equal to $2N^2 + 2\left(N^2-1\right) + 1 = (2N)^2 - 1$. These are precisely the number of generators of $SU(2N)$ and therefore the algebra can be realized in an embedding $SU(2N)$ algebra. In fact, this was observed previously for the particular case of $U(1)$ that was realized by an $SU(2)$ algebra.

Giving up unitarity of U_{ni} will allow a representation of the algebra in terms of fermions [106]. These are the so-called "rishon fermions" and are written in terms of the operators $c^l_{n\pm}$. The index n indicates the site, $\pm$ is an extra fermionic label associated with left and right, and i is the color index. Then one can write:

$$\begin{aligned} L^a_{ni} &= \frac{1}{2}\left(c^l_{n+}\right)^\dagger t^a_{lk} c^k_{n+},\ R^a_{ni} = \frac{1}{2}\left(c^l_{n+\hat{i}-}\right)^\dagger t^a_{lk} c^k_{n+\hat{i}-}, \\ E_{ni} &= \frac{1}{2}\left(\left(c^l_{n+\hat{i}-}\right)^\dagger c^l_{n+\hat{i}-} - \left(c^l_{n+}\right)^\dagger c^l_{n+}\right), \\ U^{kl}_{ni} &= c^k_{n+}\left(c^l_{n+\hat{i}-}\right)^\dagger \end{aligned} \tag{1.121}$$

It is worth reinforcing that quantum link models are well suited for quantum simulations due to the finiteness of the links Hilbert space. In the the standard Wilson approach, in path integral formulation, the fields are classical taking a continuum set of values. By use of an extra dimension and a posterior dimensional reduction, the effective continuum limit can be achieved even if one uses quantum link models [104].

Chapter 2

Simulation of gauge potentials & fields

In the previous Chapter two very different types of physical systems were presented. The cold atomic system where atoms are neutral, and a general scenario of gauge theories where charged particles interact with bosonic fields. One might wish to understand if the control allowed by a cold atomic setting can be pushed as far as the simulation of gauge theories. After all they are both local theories. Such implementation is, however, far from straightforward, as remarked above, since neutral particles must behave as charged ones. In order to achieve the desired effect one has to be able to implement an "artificial field" which mimics a real magnetic field on charged particles (or generalizations like non-Abelian fields). It turns out that this is indeed possible.

Here the distinction between "gauge potentials" and "gauge fields" shall be made. The first concerns the existence of static fields, external potentials which enjoy a gauge symmetry. They are responsible by the existence of Landau levels (for example [109–111]) and other generalizations like topological insulators ([112–114]). By other side, the study of many-body properties in the presence of a static magnetic field and a periodic potential is a major area of research. Such systems provide a paradigmatic example of, for instance, exotic energy spectrum with a fractal structure as the Hofstadter butterfly [115]. Furthermore, as in the example of the Hall conductance of electrons in a periodic potential in the presence of a constant magnetic field [116], there is a close connection with topological invariants which further motivates the study of these systems. Implementation of such artificial static potentials is possible and was already realized. For example signatures of the Hofstadter bands, not observed yet in natural crystals, were already found in artificial settings [117–120]. The second case of dynamical gauge fields, with emphasis to their lattice formulation, have direct application not only to particle physics but also in other areas like quantum computation. Experimental implementations are more difficult to achieve with the firs example reached just last year [15]. In the following, an overview over some proposals, for both cases, is done. At the end of this Section an overview over some original material is presented, regarding the possibility of simpler target models for quantum simulation of lattice gauge theories.

2.1 Gauge potentials

The inclusion of an external static magnetic field on the Hamiltonian can be achieved by replacing the momentum components of each particle by $p_i \to p_i - eA_i$ where e is the charge of the particle and A_i the i-th component of the vector potential. On the lattice, instead, this can be approximated by the Peierls substitution, valid in a tight-binding regime and for a slow varying magnetic field, where the

hopping parameter becomes complex. Explicitly:

$$\sum_{\vec{r},j} t_j \hat{a}^\dagger_{\vec{r}+\hat{j}} \hat{a}_{\vec{r}} + \text{h.c.} \rightarrow \sum_{\vec{r},j} t_j \hat{a}^\dagger_{\vec{r}+\hat{j}} e^{i\theta_j(\vec{r})} \hat{a}_{\vec{r}} + \text{h.c.} \tag{2.1}$$

In this notation the sum of $\vec{r}$ is taken over lattice sites and the sum of j is taken over all d directions corresponding to the dimensionality of the system. The angle $\theta_j(\vec{r})$ is just a phase that can depend, on general grounds, on both the direction of the hopping and on the position. This was described in detail in the Introduction in the context of $U(1)$ gauge theories. The key difference is that this phase here is non dynamical, so there is no kinetic term. Effectively corresponds to allow the hopping parameter to be complex. Not all complex hoppings represent different physical scenarios as there is gauge invariance. In what follows three example of techniques to engineer complex phases on the hopping parameters are discussed. Reviews can be found in [121–123].

2.1.1 Adiabatic change of external parameters

The idea of this approach has in its core the tight relation between the Aharonov-Bohm phase [124] and the Berry phase which was a concept introduced by Berry in [125]. The first is the phase acquired by a particle traveling around a closed contour. At the end of the path, when it is back to the initial position, the wave function acquires a new phase which is independent of the details of how the path was done and only depending on the total magnetic flux through the contour. By other side the Berry phase corresponds to the phase acquired when some external parameters of the system are varied on time, "slowly", coming back again to their initial value for a non-degenerate state. In a more precise way, the starting point is an Hamiltonian $H(q^a, \lambda_i)$ where q^a are degrees of freedom and λ_i are a set of external parameters. If this parameters are varied sufficiently slow returning, in the end, to their initial value, and if the state is non degenerate, then the system is back to its initial state. The most it can do is to acquire a phase:

$$|\psi\rangle \underset{\text{adiabatic chage}}{\longrightarrow} e^{i\gamma} |\psi\rangle \tag{2.2}$$

γ can be derived by computing the time evolution operator and subtract the "trivial" phase acquired simply due to time evolution ($e^{-i\int E(t)dt}$ where $E(t)$ is the energy of the state at each time). The result is

$$\gamma = \oint_{\mathcal{C}} \tilde{A}_i(\lambda)\, d\lambda_i \tag{2.3}$$

where $\mathcal{C}$ is the closed path on space of the parameters λ_i and $\tilde{A}_i$ are given by:

$$\tilde{A}_i(\lambda) = i \langle \phi(\lambda)| \frac{\partial}{\partial \lambda_i} |\phi(\lambda)\rangle \tag{2.4}$$

and $|\phi(\lambda)\rangle$ are reference states which have a fixed choice of phases. $\tilde{A}(\lambda)$ is called the Berry connection. Different choices of reference states with some other phase, for example $e^{i\alpha(\lambda)} |\phi(\lambda)\rangle$, would just reproduce a gauge transformation on $\tilde{A}$:

$$\tilde{A} \rightarrow \tilde{A} + \frac{\partial \alpha}{\partial \lambda_i} \tag{2.5}$$

This principle can be applied in multi-level atomic systems in order to reproduce artificial gauge fields in an ultracold atomic setting. As an exemple the computation can be done for a two level atom, where it is shown how this vector potential appears explicitly at the Hamiltonian level. These two levels correspond to two internal states, a ground state $|g\rangle$ and an excited state $|e\rangle$. The center of mass Hamiltonian, assumed diagonal on the internal states, is taken to be just the free particle Hamiltonian. The total Hamiltonian $H = H_0 + U$. By an appropriate choice of a constant shift of all the energies

one can assume that $E_g = -E_e$ where the referred quantities are respectively the energy of the ground state and excited state. Then, in general U can be written as:

$$U = \frac{\Omega}{2}\begin{pmatrix} \cos\theta & e^{i\phi}\sin\theta \\ e^{i\phi}\sin\theta & -\cos\theta \end{pmatrix} \tag{2.6}$$

where θ and ϕ may depend on the position. The frequency Ω characterizes the strength of the coupling between the two states and it is assumed to be position independent. The eigenstates of this operator, that shall be called "dressed states", are given by:

$$|\chi_1\rangle = \begin{pmatrix} \cos\frac{\theta}{2} \\ e^{i\phi}\sin\frac{\theta}{2} \end{pmatrix},\ |\chi_2\rangle = \begin{pmatrix} -e^{-i\phi}\sin\frac{\theta}{2} \\ \cos\frac{\theta}{2} \end{pmatrix} \tag{2.7}$$

with eigenvalues $\pm\hbar\Omega/2$ respectively. It will be assumed that initial internal state is $|\chi_1\rangle$ and that an adiabatic following occurs, so the system remains on it through all times. Then the state of the system can be described by a wave function $|\psi(t,\vec{r})\rangle = \phi(t,\vec{r})\,|\chi_1(\vec{r})\rangle$ where $\phi(t,\vec{r})$ will obey a modified Schrodinger equation due to the dependence of $|\chi_1(\vec{r})\rangle$ on the position. Plugging this into the Schrodinger equation and projecting on $|\chi_1(\vec{r})\rangle$, one finds an effective Hamiltonian governing ϕ:

$$H_{eff} = \frac{\left(p_i - i\langle\chi_1(\vec{r})|\frac{\partial}{\partial x_i}|\chi_1(\vec{r})\rangle\right)^2}{2m} + \frac{\langle\chi_2(\vec{r})|\frac{\partial}{\partial x_i}|\chi_1(\vec{r})\rangle^2}{2m} + \frac{\Omega}{2} \tag{2.8}$$

As expected due to the discussion of the Berry connection in the begining of the Section, a vector potential is found $\tilde{A}_i(\vec{r})$. Furthermore a potential $\tilde{V}(\vec{r})$ is also created which is related to virtual transitions to the other state $|\chi_2(\vec{r})\rangle$. Explicitly these two quantities are given by, in the two level approximation, $\tilde{A}_i(\vec{r}) = \frac{\cos\theta - 1}{2}\frac{\partial\phi}{\partial x_i}$ and $\tilde{V}(\vec{r}) = \frac{(\nabla\theta)^2 + \sin^2\theta(\nabla\phi)^2}{8m}$. Discussion of practical implementation on optical lattices can be found in [121, 126, 127]. First experimental evidence of scalar potentials in quantum optics was found in [128] and the first observation of geometric magnetic fields in cold atomic physics was done in [129]. By considering a set of degenerate or quasi-degenerate dressed states it is possible to achieve non-Abelian gauge potentials as well [121].

2.1.2 Effective Hamiltonian in periodic driven system

In contrast to the approach of the previous Subsection, where the creation of the magnetic field relied on a slow change in time of external parameters, in this case one relies in fast oscillations. The basic principle consists on having two very distinct timescales. A fast oscillating time dependent potential will give rise to an effective time independent Hamiltonian which will present the desired complex hopping term. A general technique was proposed in [130] and consists on considering a time dependent periodic Hamiltonian:

$$H = H_0 + V(t) \tag{2.9}$$

where all the the time dependence is relegated to $V(t)$ which can be decomposed into

$$V(t) = \sum_n \left(V_{n+}e^{in\omega t} + V_{n-}e^{in\omega t}\right) \tag{2.10}$$

where $V_{n\pm}$ are operators. The condition $V_{n+} = V_{n-}^{\dagger}$ guarantees the Hermiticity of the Hamiltonian. The expansion shall rely on the small parameter $\tau = 2\pi/\omega$ which is the period of the Hamiltonian. Applying an unitary transformation $e^{iK(t)}$ generates an effective Hamiltonian given by:

$$H_{eff} = e^{iK(t)}He^{-iK(t)} + i\left(\frac{\partial}{\partial t}e^{iK(t)}\right)e^{-iK(t)} \tag{2.11}$$

The operator $K(t)$ should also be periodic and should be chosen such that the effective Hamiltonian is time independent. Under the time independence of H_{eff} the time evolution operator can be represented as $U(t_i \to t_f) = e^{iK(t_f)} e^{-iH_{eff}(t_f - t_i)} e^{-iK(t_f)}$. One can then show [130] that the effective Hamiltonian can be written in lowest order as:

$$H_{eff} = H_0 + \tau \sum_n \frac{1}{n} [V_{n+}, V_{n-}] + \mathcal{O}(\tau^2) \tag{2.12}$$

This expansion turns out to be very useful in the effective description of ultracold atomic systems though care should be taken, in a case by case scenario, in order to be sure about the convergence of the series.

Lattice Shaking The lattice shaking approach consists on having an external time dependent optical potential that is changing in time in accordance to the previous description. Then a change of basis is performed for a co-moving frame that, along with a time average, will create an effective Hamiltonian with the desired complex hopping. As an example, a brief prescription is presented along the lines of the first realization in a *Rb* Bose-Einstein condensate [131]. The Hamiltonian considered is the usual tight-biding Hamiltonian in 2D with the usual hopping and on-site part H_{os} (by on-site it is intended one body potential and scattering terms that act in single sites). There is an extra time dependent term which corresponds to a time dependent potential:

$$H = -\sum_{\vec{r},j} t_{\vec{r}j} \hat{a}^\dagger_{\vec{r}+\hat{j}} \hat{a}_{\vec{r}} + H_{so} + \sum_{\vec{r}} v_{\vec{r}}(t)\, \hat{a}^\dagger_{\vec{r}} \hat{a}_{\vec{r}} \tag{2.13}$$

The function $v_i(t)$ is a periodic function of time with period T: $v_i(t) = v_i(t+T)$. Now an unitary transformation on the states is performed and plugged in on the Schrodinger equation (new states $|\psi'\rangle$ given by $|\psi(t)\rangle = U(t)|\psi'(t)\rangle$). The Hamiltonian, after this unitary transformation becomes $H'(t) = U(t)^\dagger H U(t) - iU(t)^\dagger \dot{U}(t)$ (where the dot stands for time derivative). The transformation is given by

$$U(t) = e^{-i\int_0^t dt' \sum_{\vec{r}} v_i(t') \hat{a}^\dagger_{\vec{r}} \hat{a}_{\vec{r}}} \tag{2.14}$$

It is straightforward to see that this transformation will cancel the part of H (which will be present also on $U^\dagger H U$) corresponding to $v_i(t)\, \hat{a}^\dagger_{\vec{r}} \hat{a}_{\vec{r}}$. By other side, since this does not commute with the kinetic term, the time dependence will be carried to hopping term. For a rapid set of oscillating function $v_i(t)$ the Hamiltonian can be replaced by an effective one, resulting from time averaging over a period. The new hopping parameters will read:

$$t_{\vec{r}j} \to t_{\vec{r}j} \left\langle e^{i\Delta v_{\vec{r}j}} \right\rangle \tag{2.15}$$

where $\langle\rangle_T$ stands for average over a period: $T^{-1}\int_0^T dt$ and $\Delta v_{\vec{r}j} = v_{\vec{r}}(t) - v_{\vec{r}+\hat{j}}(t) - \left\langle v_{\vec{r}}(t) - v_{\vec{r}+\hat{j}}(t) \right\rangle$.

Laser-assisted hopping In this case the effective dynamics is induced by the coupling of the atoms on the optical lattice with a pair of Raman lasers. A fundamental ingredient consists on introducing an energy offset Δ on neighboring sites. It is enough to consider such scenario along a single direction. Considering a $2D$ lattice:

$$H = -t \sum_{\vec{r},j} \left(\hat{c}^\dagger_{\vec{r}+\hat{j}} \hat{c}_{\vec{r}} + \text{h.c.} \right) + \frac{\Delta}{2} \sum_{\vec{r}} (-1)^x c^\dagger_{\vec{r}} \hat{c}_{\vec{r}} + V(t) \tag{2.16}$$

where $\vec{r} = (x, y)$ runs through the lattice sites. The offset term characterized by Δ can be obtained by tilting the lattice, introducing magnetic gradients or through superlattices. The potential $V(t)$ is the result of the two external lasers that induce an electric field $E_1 \cos\left(\vec{k}_1 \cdot \vec{r}_1 - \omega_1 t\right) + E_2 \cos\left(\vec{k}_2 \cdot \vec{r}_2 - \omega_2 t\right)$.

It is assumed that the frequencies are fine tuned such that they match the offset $\omega_1 - \omega_2 = \Delta$. Neglecting fast moving terms the potential is written as:

$$V(t) = 2E_1E_2\sum_{\vec{r}} e^{i\left(\vec{k}_R\cdot\vec{r}-\Delta t\right)}c^\dagger_{\vec{r}}c_{\vec{r}} + \text{h.c.} \tag{2.17}$$

with $\vec{k}_R = \vec{k}_1 - \vec{k}_2$. Then one can get the effective Hamiltonian in two steps. First performing an unitary transformation $e^{-it\frac{\Delta}{2}\sum_{\vec{r}}(-1)^x c^\dagger_{\vec{r}}\hat{c}_{\vec{r}}}$ will create oscillatory hopping terms (with $e^{\pm i\Delta t}$ in front). Then one applies the previous formalism building an effective Hamiltonian using Equation 2.12:

$$\begin{aligned} H =& -t\sum_{x,y}\left(\hat{c}^\dagger_{x,y}\hat{c}_{x,y+1} + \text{h.c.}\right) \\ &- \frac{2tE_1E_2}{\Delta}\sum_{x\ \text{even},y}\left[\left(e^{i\vec{k}_R\cdot\vec{r}}-1\right)\left(e^{i\vec{k}_R\cdot\vec{r}}\hat{c}^\dagger_{x,y}\hat{c}_{x+1,y} + e^{-i\vec{k}_R\cdot\vec{r}}\hat{c}^\dagger_{x-1,y}\hat{c}_{x,y}\right) + \text{h.c.}\right] + \mathcal{O}\left(\Delta^{-2}\right) \end{aligned} \tag{2.18}$$

It is clear that this generates complex hopping but looking more carefully one finds that the lattice has a staggered flux. With a choice $\vec{k}_R = (\Phi, \Phi)$ (choice also made in the experiment [132]) one can write upon a gauge transformation:

$$\begin{aligned} H =& -t\sum_{x,y}\left(\hat{c}^\dagger_{x,y}\hat{c}_{x,y+1} + \text{h.c.}\right) \\ &- \frac{2tE_1E_2\sin\Phi/2}{\Delta}\sum_{x\ \text{even},y}\left[\left(e^{i\Phi y}\hat{c}^\dagger_{x,y}\hat{c}_{x+1,y} + e^{-i\Phi y}\hat{c}^\dagger_{x-1,y}\hat{c}_{x,y}\right) + \text{h.c.}\right] + \mathcal{O}\left(\Delta^{-2}\right) \end{aligned} \tag{2.19}$$

where it is clear that there is an alternated sequence of $\pm\Phi$ along the x direction. This issue can be addressed by making use of an extra pair of Raman lasers with opposite frequency shifts $\pm\Delta$ as it is shown in [133]. The Chern number of the Hofstadter bands was measured in [134] within this framework. It is worth noting that other kind of one body terms, beyond the staggered term, can be used as it was done in the first quantum simulations of this model with ultracold atoms [135, 136]. In that case a linear potential is used. These kind of approaches can be adapted to more general scenarios including different geometries and multi-component species. The later one, for example, can be achieved by introducing spin dependent potentials as done in [135].

2.2 Gauge fields

In the context of Abelian gauge theories, the goal of simulating gauge fields consists in attributing dynamics to the complex phases on the hopping parameters that were identified in the previous Section. In order to construct such dynamics one should identify degrees of freedom that will play the role of the gauge field. Several proposals have been put forward which map the gauge degrees of freedom into some other controllable variables. The platforms used include ultracold atoms, trapped ions and superconducting qubits. They may be analogue or digital quantum simulators and include Abelian or non-Abelian symmetries [6, 39, 137–161]. A more detailed description of two particular approaches in analogue cold atomic simulators will follow: gauge invariance from energy penalty and from microscopic symmetries. Furthermore the symmetries addressed are either $U(N)$ and $SU(N)$.

There are other symmetries which have been explored, namely $\mathbb{Z}_n$ [39, 150] which, in particular, can provide an alternative route towards $U(1)$ symmetry in the large n limit [39] and can be addressed with similar approaches. Proposal for the realization of $\mathbb{C}P(N-1)$ [162, 163] models have bee put forward in [156, 157]. These models can serve as toy models for QCD and are also relevant in studying the approach to the continuum limit, in the context of D-theories , where the continuum limit is taken

via dimensional reduction [105, 106]. Furthermore other formulations are possible for specific groups [31, 37, 164, 165]. Gauge theories with Higgs fields have also been the target of quantum simulation proposals [166–169].

Other relevant approach is the so-called quantum Zeno dynamics which takes inspiration on the quantum Zeno effect. The later states that a system which is being continuously observed does not evolve on time. Furthermore, if the measurement commutes with a certain part of the Hamiltonian, then it can freeze a certain part of the Hilbert space but still enable dynamics in another subspace [170]. This feature can be used in order to freeze gauge dependent quantities and let the system evolve in the gauge invariant subspace. The Hamiltonian to be implemented has the form $H_{\text{noise}} = H_0 + H_1 + \sqrt{2\kappa}\sum_{x,a} G_x^a$ where H_0 and H_1 are time independent and are, respectively, gauge invariant and gauge variant parts of the Hamiltonian. The operators G_x^a are associated to the constraint one wishes to impose $G_x^a |\psi\rangle = 0$. In the case of gauge theories G_x^a are the generators of gauge transformations. An advantage of this approach, with respect to the energy punishment approach of the next Section, is that only linear terms on the generators must be imposed on the Hamiltonian (energy punishment requires quadratic terms). By other side leakage from the gauge invariant subspace of the Hilbert space happens as a function of time, which does not happen in the energy penalty approach. This approach was developed in [148].

Yet another approach, that was successfully implemented in the first quantum simulator of a gauge theory using trapped ions [15], is the digital quantum simulator [171]. The key idea consists on in dividing the full time evolution operator e^{-iHt} into smaller pieces of sizes $\tau = t/N$ and apply time evolution of smaller parts of the Hamiltonian at a time. Consider for example an Hamiltonian which is a sum of M contributions : $H = \sum_\alpha^M H_\alpha$. Each part H_α can represent, for example, a nearest neighbor spin interaction in which case only two spins are coupled on each H_α. For large enough N one can write:

$$e^{-iHt} = \left(e^{-iH\tau}\right)^N \simeq \left(\prod_{\alpha=1}^{M} e^{-iH_\alpha \tau}\right)^N \tag{2.20}$$

Each time step can now be interpreted as an individual gate. While in the analogue simulation the great difficult lies on building the appropriate gauge invariant Hamiltonian, in digital quantum simulations that is not a problem. The difficulty lies, however, in building an efficient sequence of gates. Beyond the scheme used in the experimental realization [172], proposals towards implementation of lattice gauge theories have been put forward [137, 138, 146, 154, 158, 159]

2.2.1 Gauge invariance from energy punishment

The energy punishment approach is widely used in the field of frustrated quantum magnets. This is however a quite general approach which allows the theoretical construction of models which will exhibit a given symmetry in its low energy sector. This consists on building an Hamiltonian which does not prohibit the symmetry violation to occur but instead punishes it with a large energy. In a more concrete way, suppose one wants to implement a set of symmetries which has as a respective set of generators $\{G_x\}$ commuting with each other $[G_x, G_y] = 0$. Furthermore consider a typical Hamiltonian H_0 which does not respect these symmetries. Then one constructs the following Hamiltonian:

$$H = H_0 + \Gamma \sum_x G_x^2 \tag{2.21}$$

where Γ is a large energy scale, meaning much larger than the energy scales involved in H_0. Since G_x are Hermitian G_x^2 have non-negative eigenvalues. One can choose the lowest eigenvalue to be zero by an appropriate definition of G_x. Then, at low energy ($\ll \Gamma$), the states will respect approximately the condition $G_x |\psi\rangle \simeq 0$. If not, this would give a state automatically in an energy scale $\sim \Gamma$. It is then possible to construct an effective Hamiltonian, valid in low energy, which will respect the symmetries

generated by $\{G_x\}$. Let G be the projector operator on the subspace of the total Hilbert space obeying $G_x |\psi\rangle = 0$ and let $P = 1 - G$. Then the low energy Hamiltonian can be written as:

$$H_{eff} = GH_0G - \frac{1}{\Gamma} GH_0P \frac{1}{\sum_x G_x^2} PH_0G + \mathcal{O}\left(\Gamma^{-2}\right) \tag{2.22}$$

which respect the symmetries. Within this framework an effective Abelian gauge theory can be constructed. In non-Abelian theories the generators of the gauge transformation do not commute and this construction fails. There are, of course, several possible drawbacks even in a theoretical level. For example the Hamiltonian 2.22, even though gauge invariant, may contain terms which one does not intend to implement or miss some particular terms which are present on the target system.

In order to construct a quantum simulator the first task is naturally to map the degrees of freedom of the target theory into the laboratory controlled ones, in this case the atomic variables. The matter fields, which are fermionic, will naturally be described by fermionic atomic species. Regarding gauge fields, the target will be the quantum links formulation discussed on Section 1.4.5. Therefore the goal consists on building the quantum links satisfying the algebra $[L_{mi}, U_{nj}] = \delta_{ij}\delta_{mn}U_n$ and $\left[U_{mi}, U_{nj}^\dagger\right] = \delta_{ij}\delta_{mn}2L_n$. This can be achieved using the Schwinger representation. Given two bosonic species $b^{(\sigma)}$ with $\sigma = 1, 2$ which are associated to each link, one can write

$$U_{mi} = b_{mi}^{(2)\dagger} b_{mi}^{(1)}, \; L_{mi} = \frac{1}{2}\left(b_{mi}^{(2)\dagger} b_{mi}^{(2)} - b_{mi}^{(1)\dagger} b_{mi}^{(1)}\right) \tag{2.23}$$

Each link is loaded with a total of $2S$ bosons where S is an half integer. Then one has the desired representation for the quantum links in terms of atomic variables. Now the variables are identified. One then can then build a d dimensional optical lattice where fermions are allowed to hop among lattice points and in each links there are a total of $2S$ bosons. For $1D$, the target Hamiltonian is of the form:

$$H = -t\sum_n \left(c_n^\dagger U_m c_{n+1} + \text{h.c.}\right) + m\sum_n (-1)^n c_n^\dagger c_n + \frac{g^2}{2}\sum_n L_n^2 \tag{2.24}$$

When comparing to the general structure of 1.115 there are three ingredients missing: the plaquette term, the alternating sign on the mass and the kinetic term which is picking the "real part" of $c_n^\dagger e^{i\theta_{ni}} c_{n+\hat{i}}$ instead of its "imaginary part. The plaquettes are naturally absent in $1D$. The second issue is easily solved by a canonical transformation $c_n \to (-i)^n c_n$. This Hamilton now has structure that can be targeted with the approach described. Making use of the Schwinger representation it has the form:

$$H = -t\sum_n \left(c_n^\dagger b_n^{(\bar{\sigma})\dagger} b_n^{(\sigma)} c_n + \text{h.c.}\right) + m\sum_n (-1)^n c_n^\dagger c_n + \frac{g^2}{8}\sum_n \left(b_n^{(2)\dagger} b_n^{(2)} - b_n^{(1)\dagger} b_n^{(1)}\right)^2 \tag{2.25}$$

The two last terms can be, in principle, implemented directly using a proper tune of the interactions between the bosons and the potential for the fermions. The first term, instead, is a correlated hopping between bosons and fermions which come less easily. Furthermore the terms like $b_n^{(\bar{\sigma})\dagger} b_n^{(\sigma)}$ and $c_n^\dagger c_{n+\hat{i}}$, which are not gauge invariant, must be suppressed. This is solved by the energy punishment approach. In general the non-gauge invariant Hamiltonian with the ingredients described has the form:

$$\begin{aligned} H_0 = &- \sum_{n,i}\left[t_F\left(c_n^\dagger c_{n+1} + \text{h.c.}\right) - t_B\left(b_n^{(2)\dagger} b_n^{(1)} + \text{h.c.}\right)\right] \\ &+ \sum_n \left(v_n^F c_n^\dagger c_n + \sum_\sigma v_n^{B\sigma} b_{ni}^{(\sigma)\dagger} b_{ni}^{(\sigma)}\right) + U\sum_n \left(b_n^{(2)\dagger} b_n^{(2)} - b_n^{(1)\dagger} b_n^{(1)}\right)^2 \end{aligned} \tag{2.26}$$

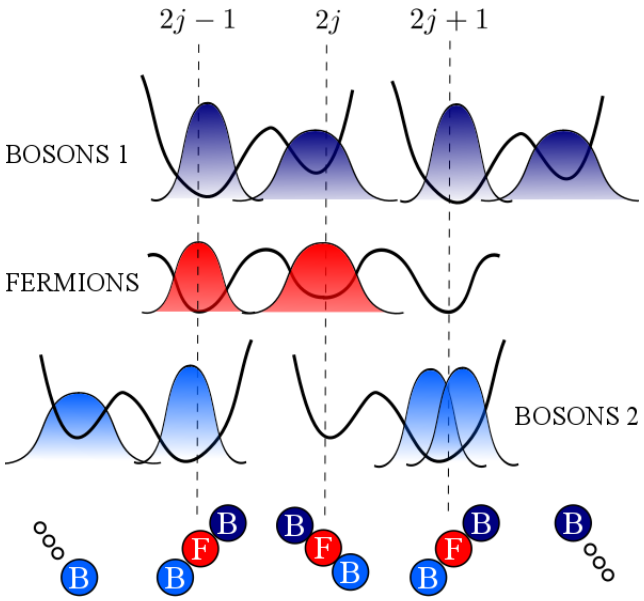

Figure 2.1: Superlattice configurations for the the two boson species and the fermionic one. Bosons of the species 1 at an even site $2j$ can only hop to $2j-1$ while a boson of species 2 has only access to the site $2j+1$. The Figure presents a an example of a gauge invariant state configuration (on these three sites) where $G_x |\psi\rangle = 0$.

Using the generators for the $U(1)$ gauge symmetry in Equation 1.107 one considers the full Hamiltonian:

$$H = H_0 + \Gamma \sum_n \left(L_n - L_{n-1} - c_n^\dagger c_n + \frac{1-(-1)^n}{2} \right)^2 \tag{2.27}$$

It is crucial that one has access to the interactions that are introduced on the last term corresponding to the energy punishment. To see that this is the case it useful to be more specific about the labels σ. One can take, as in [139], the labels $\sigma = 1, 2$ meaning respectively left and right part of the link, which can be thought to coincide with the lattice site. In this way $b_n^{(2)\dagger} b_n^{(1)}$ are just regular hopping terms. Furthermore it is recalled that the total number of bosons associated to each link is conserved. Therefore one can write: $L_n = -S + b_n^{(2)\dagger} b_n^{(2)} = S - b_n^{(1)\dagger} b_n^{(1)}$. This means that terms like L_n^2 and and $L_n L_{n-1}$ can be written as a density-density interaction. Regarding the last case, recall that $b_n^{(1)}$ and $b_{n-1}^{(2)}$ are effectively in the same site, see Figure 2.1. Now Equation 2.22 can be applied. The number of particles in each site is a good quantum number to describe the eigenstates of G_x. The number of particles in the site j are denoted by $n_j^F = c_j^\dagger c_j$, $n_j^1 = b_j^{(1)\dagger} b_j^{(1)}$ and $n_j^2 = b_{j-1}^{(2)\dagger} b_{j-1}^{(2)}$. The subspace of gauge invariant states is then characterized by:

$$n_j^F + n_j^1 + n_j^2 = 2S + \frac{1-(-1)^j}{2} \tag{2.28}$$

In the lowest order only the two last terms of 2.26 survive as any single hopping destroys the above relation. At the next order there are three possible virtual processes that preserve this condition. Up to some linear terms on the particle density operator, they are:

1. Boson-boson hopping: a boson hops to the neighboring, same link, site and another boson hops back. Gives rise to a boson density-density interaction.

2. Fermion-Fermion hopping: a fermion hops to a neighboring site and then hops back. Only possible if neighboring site is unoccupied and gives rise to a nearest neighbor fermion density-density interaction.

3. Boson-Fermion hopping: a fermion hops to a neighboring site and a boson belonging to the link that connects the two sites does the opposite path. Gives rise to a correlated hopping.

The terms coming from 1. should be joined with the last term of 2.26 in order to form the correct kinetic term for the gauge fields. The terms in 2. are somehow unwanted and correspond to a repulsion between neighbor fermions $n_j^F n_{j+1}^F$. Naturally, they do not spoil gauge invariance and their inclusion should not be a problem [139]. Finally the terms originating from 3. give rise to the correlated hopping responsible for the matter-gauge coupling as written on the first term of 2.23. There is another issue which should be addressed. From the beginning it was assumed that the the number of bosons in each link is conserved. In particular this means that bosons are not allowed to pass to a neighboring link. In order to guarantee this condition in an experiment one should introduce an extra bosonic species and this is the reason that bosons in neighboring links were represented with different colors on Figure 2.1. Then one bosonic species is trapped on the even links and the other in the odd links. This will prevent bosonic hopping between links. A numerical study of real dynamics of the the model as well as accuracy of the effective gauge invariance obtained was also done in [139].

Finally, in a possible experimental realization, the first fundamental step is to guarantee that the system is initialized on a gauge invariant state. This can be done by loading the atoms in a deep lattice such that they are in Mott phase. After the system should evolve according to the fine tuned Hamiltonian described above (after lowering the lattice barriers). Finally measures of relevant quantities can be performed.

This principle is valid in higher dimensionality where one has to face the difficulty of generating plaquette terms. This was done for the pure gauge in [173] and [144] by suitably allowing hopping between links. In the first case each link has an infinite dimensional Hilbert space that is represented by a Bose-Einstein condensate. In the second the proposal is simplified by considering a quantum link model.

2.2.2 Gauge invariance from many body interaction symmetries

This approach consists on building a lattice which will have the necessary local gauge invariance arising from microscopic symmetries. Specific proposals may vary significantly even though the same principal is used. For example in [161] the simulation is built upon the global symmetry conserving the total number of excitations and is achieved via a state-dependent hopping. In turn, for example [150,174], are built upon conservation of angular momentum. For concreteness the later approach will be described in more detail below. In the case of [147] $SU(N)$ symmetries of the ground state manifold of alkaline-earth-like atoms are exploited in order to built non-Abelian gauge theories. This approach shall be discussed in Section 2.2.3.

Symmetries only allow certain type of processes to occur and, by exploiting these constraints, one can build a gauge symmetry. This can be done, as said before, considering angular momentum conservation. To this end one can take the Schwinger representation, placing the bosons that will make up the gauge fields at the two boundaries of the links. Because the goal consists, partially, in forbidding gauge dependent terms like simple boson or fermion hopping, the lattice should be spin dependent. In this way a single hopping is forbidden as it does not conserve angular momentum. By other side one should guarantee that correlated spin between bosons and fermions is allowed. This can be achieved by a judicious choice of respective hyperfine angular momentum in each lattice site. For concreteness, consider a single link connecting two sites and a total of two bosonic ($b^{(1)}$,$b^{(2)}$) and two fermionic species (c,d). The site at the left of the link can only be populated by c while the right side by d. Analogously the left end of the link can only be populated by $b^{(1)}$ while the right end can only be populated by $b^{(2)}$. Then the conditions described above for allowed/forbidden hopping

are automatically satisfied if one chooses the hyperfine angular momentum of each atomic species to satisfy:

$$m_F(d) - m_F(c) = m_F\left(b^{(1)}\right) - m_F\left(b^{(2)}\right) \tag{2.29}$$

It is intended that in a spin dependent lattice $m_F(d) \neq m_F(c)$ and $m_F\left(b^{(1)}\right) \neq m_F\left(b^{(2)}\right)$. In other words, what the expression above means is that the difference of angular momentum caused by a fermion hop can be exactly compensated by a bosonic hop in the opposite direction. This leads directly to the correlated hopping desired, which in fact comes from the scattering terms between bosons and fermions (last term of Equation 1.33). The only other allowed scattering term between fermions and bosons correspond to density-density interactions like $c^\dagger c\left(b^{(2)\dagger}b^{(2)} + b^{(1)\dagger}b^{(1)}\right)$. These are just linear terms on the fermionic number operator due to the conservation of the total number of bosons per link. Summing over all lattice sites this gives a simply a constant shift of the energy. The scattering terms between bosons give rise to the gauge kinetic term as before (in $1+1$ dimensions).

Again, for higher dimensionality, there is a non-trivial extra step consisting on building plaquette interactions. If plaquettes are ignored and the model described above is loaded on an higher dimensional lattice the result corresponds to a strong coupling limit where plaquettes can be ignored. Obtaining plaquette terms can be achieved, instead, by the so-called loop method which uses perturbation theory in a similar way that was used in the energy penalty approach. Here gauge invariant building blocks instead are used. There are progressive layers of difficulty:

- no dynamical fermions and unitary links corresponding to regular Kogut-Susskind or equivalently a quantum link model in the limit $S \to +\infty$: $\left[U, U^\dagger\right] = 0$,
- no dynamical fermions and truncated links corresponding to quantum link models: $\left[U, U^\dagger\right] = 2/S(S+1)$,
- dynamical fermions and unitary/truncated links.

The first two points correspond to an effective pure gauge theory and only in the third point one has the matter coupling present. Here the general framework is described indicating the difficulties on passing to each new step. The first aim is to build then the pure gauge theory as an effective theory

$$H_{target} = \frac{g^2}{2}\sum_{n,i} L_{ni}^2 - \frac{1}{4g^2}\sum_{\square}\left(U_\square + U_\square^\dagger\right) \tag{2.30}$$

The description will be specialized for $2+1$ dimensions but the theoretical construction for higher dimensions is analogous. As announced the structure consists on adopting the structure of the energy penalty approach of Equation 2.21 but instead in this case H_0 is already a gauge invariant Hamiltonian. For reasons that will be explained below one should have two fermionic species, say χ and ψ, and build the trivial part of the generalization of the $1+1$ process:

$$H_0 = -t\sum_{n,i}\left(\psi_n^\dagger U_{ni}\psi_{n+\hat{i}} + \chi_n^\dagger U_{ni}\chi_{n+\hat{i}} + \text{h.c.}\right) + \frac{g^2}{2}\sum_{n,i} L_{ni}^2 \tag{2.31}$$

These fermionic species are auxiliary and in the effective model they will be integrated out. There should be no interacting term between them. For building this one should use the ingredients described in the beginning of this Section with an energy penalty that will enforce the following conditions at each site $n = (n_1, n_2)$:

- there is a fermion ψ if both n_1 and n_2 are even
- there is a fermion χ if both n_1 and n_2 are odd
- no fermion otherwise

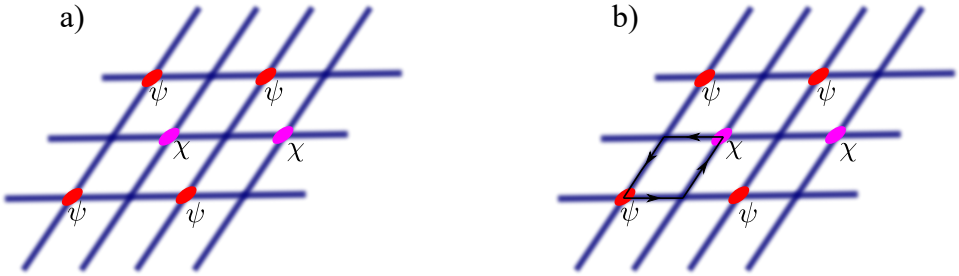

Figure 2.2: In the panel a) it is depicted the positions of the auxiliary fermions that are used to construct the plaquette term using gauge invariant building blocks. One of the species, say ψ, is represented in red and placed on sites with both coordinates even. In turn χ, in pink, is placed on sites with both coordinates. This correspond to the ground-state of 2.32. In the panel b) it is represented a virtual process that gives rise to a plaquette term.

The positions of these fermions is represented on Figure 2.2 a). This kind of constraint can be obtained, for large Γ, with an Hamiltonian of the form:

$$H_{penalty} = -\Gamma \sum_n \left[\frac{\left(1+(-1)^{n_1}\right)\left(1+(-1)^{n_2}\right)}{4} \psi_n^\dagger \psi_n + \frac{\left(1-(-1)^{n_1}\right)\left(1-(-1)^{n_2}\right)}{4} \chi_n^\dagger \chi_n \right] \tag{2.32}$$

The ground state of this Hamiltonian is the one described above points, one can then construct perturbation theory on this system according to 2.22. In order to get the plaquettes one has to go until the fourth order. For each order one has:

1. Only the pure gauge part of 2.31 contributes, no fermionic term occurs.

2. Trivial constant contribution assuming that U_n are unitary. The virtual process giving rise to this contribution is a single link interaction where a fermionic-bosonic correlated hopping occurs back and forth restoring the initial state. There are never fermions on the neighbor lattice site. In turn in the unitary limit there are an infinite number of bosons so the bosonic hopping does not distinguish a hopping "up" on the lattice (U) from a hopping "down" on the lattice $\left(U^\dagger\right)$: $\left[U, U^\dagger\right] = 0$. If the number of bosons is finite the two processes will not be equivalent. One can see, however, that this extra contribution corresponds to a renormalization of the pure gauge term of 2.31 and another term which can be discarded by application of the Gauss law.

3. Trivial constant contribution assuming that U_n are unitary. Virtual contributions evolving links constitute again back and forth hopping plus an a pure gauge term at any stage of the process. The extra contributions coming from considering a finite number of boson per link cannot be disregarded trivially as in the second order for this case.

4. Gives the desired plaquette term plus renormalization of the pure gauge term of 2.31 assuming that U_n are unitary. The last case corresponds to the virtual process where a fermion goes around a plaquette and returns to the initial place. This virtual process is represented on Figure 2.2 b). Naturally, in the non-unitary case, more terms appear.

Up to forth order there are only two non-trivial contributions involving t for the standard infinite dimension. Giving up unitarity of U_{ni} will allow a representation of the algebra in terms of fermions: an electric field term $\sim \frac{\left(g^2\right)^2 t^2}{\Gamma^3} \sum_{n,i} L_{ni}^2$ and plaquette terms $\sim \frac{t^4}{\Gamma^3} \sum_\square \left(U_\square + U_\square^\dagger\right)$ so effectively the plaquette term is a second order (on the parameter t^2/Γ^2).

When one considers a finite number of bosons in the links there are extra contributions appearing which cannot be disregarded. As in the case of the energy penalty, these contributions, even though unwanted, can be tolerated as they are naturally gauge invariant. However one should guarantee that these extra contributions are not more important than the plaquette term which is the target term. That can be achieved if the coupling term is parameterized is g^2 is taken to be small in units of t. By taking $g^2 \sim t^2/\Gamma$ one makes the unwanted terms at third order effectively of the same order as the plaquettes and unwanted terms of the fourth order effectively of higher order than the plaquettes.

Finally one can consider, on top of these ingredients, an extra species of fermions to play the role of matter fields. They will consist, in the initial Hamiltonian, to the usual correlated hopping with the bosons. Furthermore the staggered mass term (of Equation 1.105) should also be introduced. In the unitary case this extra piece commutes with the interacting part of 2.31 and no further contribution is obtained in perturbation theory. In the truncated case there is an extra (gauge invariant) correlated hopping coming at third order. Another different aspect of the introduction of dynamical fermions is that the Gauss law ($\sum_i L_{ni} - L_{n-\hat{\imath},i} = \text{const}$) can no longer be used to trivialize terms. The divergence of the electric field becomes gets a contribution from the charge density of the dynamical fermions. Nonetheless it can still be employed and the extra charge density terms can be compensated on the initial Hamiltonian if proper fine tuning is available experimentally.

In [174] it was proposed a realization of the Schwinger $(1+1)$ model using a mixture of ^{23}Na for the bosons and ^{6}Li for the fermions as well as an extensive study on the influence of the finiteness of the number of bosons per link in that case.

2.2.3 Non-Abelian quantum simulations

Due to the non-commutativity of the generators and complicated structure of interactions demanded by $\left(G_x^a\right)^2$ quantum simulations of non-Abelian theories typically rely on microscopic symmetries [147, 149, 150] (but this is not necessarily the case [148]).

In [147] the symmetry exploited concerns the $SU(N)$ symmetry of alkaline-earth-like atoms on their ground state manifold. Pure gauge terms are not addressed in this proposal. The rishon representation for the algebra of the links is considered. In this representation the correlated hopping is written as $\psi_x^{i\dagger} U_{xy}^{ij} \psi_y^j = \psi_x^{i\dagger} c_{x,+k}^i c_{y,-k}^{j\dagger} \psi_y^j$. The notation is fixed in the following way: the operator U_{xy} indicates the link that connects x and y, k is the direction of the link and $c_{x,+k}$ ($c_{x,-k}$) are associated with the rishon fermions immediately up (down) of the site x in the direction k, see part a) of Figure 2.3. These terms can be suitably written in terms of the "constituent quark" operators $Q_{x,\pm k} = c_{x,\pm k}^{j\dagger} \psi_x^j$. It is interesting to observe that these operators are gauge invariant. The correlated hopping is then written as $Q_{x,+k}^\dagger Q_{y,-\hat{k}}$. The fundamental aspect of the simulation scheme consists on interpreting the constituent quarks as a lattice hopping. In other words, instead of thinking about $\psi_x^{i\dagger} c_{x,+k}^i c_{y,-k}^{j\dagger} \psi_y^j$ as a lattice site (quark) hopping coupled to a rishon hopping, one can interpret it as the conversion of a quark into a rishon coupled with an opposite process in neighboring sites as represented in Figure 2.3 part b) and c). In this way one has only to guarantee that these two hoppings occur at the same time which can be done by imposing that the number of atoms in a rishon is conserved. The number of rishons in the link connecting the two sites x and y is given by $N_{xy} = c_{x,+k}^{i\dagger} c_{x,+k}^i + c_{y,-k}^{i\dagger} c_{y,-k}^i$. The term to be introduced in the Hamiltonian takes the form $\Gamma \sum_{\langle x,y\rangle} \left(N_{xy} - N_0\right)^2$ where Γ should be the largest energy scale of the Hamiltonian and N_0 the total number of rishons per link. Analogously to what was seen above, not only the desired terms appear but also other gauge invariant terms are part of the model at second order in perturbation theory. Those terms are given by $\sum_{x,\pm,k} Q_{x,\pm k}^\dagger Q_{x,\pm k}$. The Hamiltonian to be implemented has the form:

$$H = -t \sum_{x,\pm,k} (-1)^{x_1+\ldots+x_{k-1}} \left(Q_{x,\pm k} + \text{h.c.}\right) + m \sum_{x,\pm,k} (-1)^{x_1+\ldots+x_d} \psi_x^\dagger \psi_y + \Gamma \sum_{\langle x,y\rangle} \left(N_{xy} - N_0\right)^2 \quad (2.33)$$

requiring $\Gamma \gg t$. There are two features of this Hamiltonian which are fundamental to achieve the

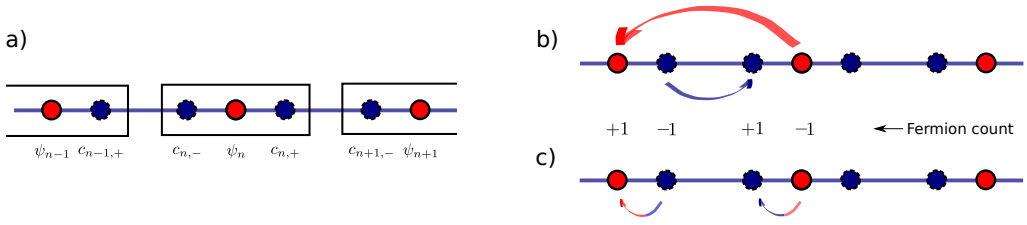

Figure 2.3: Rishon representation in $1D$. a) Rishons building the links are blue (and dashed) and the lattice sites red (and full). Each rishon is indicated with a + or a − depending if it is right or left of the lattice site associated. b) Schematization of the correlated hopping. Looking at the variation of the number of fermions in each site (called in the picture "fermion count"), the process can be interpreted as a simultaneous hopping site/rishon represented in c).

correct implementation:

- The hopping between lattice sites and rishon sites should be the same irrespective of the color index j. All these hopping parameters appear on the Hamiltonian as t.
- The interaction coefficient between any two rishons must be the same. In the Hamiltonian this is a repulsion and the coefficient is given by Γ.

These are feature that can be achieved with alkaline-earth atoms using the nuclear spins degrees of freedom. The hopping will be the same if the atomic species is the same. By other side the scattering the length is almost $SU(2I+1)$ symmetric being I the nuclear spin. This results in an effective interaction which is independent of the magnetic number. As an example one can consider the realization of the $U(2)$ symmetry. This means that in each site there should be two color indices. In a $1D$ setting, atoms will only hop among a triple well centered in the lattice site and connected to the two neighboring rishon sites as represented in Figure 2.3 a). Then one can load each triple well alternatively with $m_I = -3/2, -1/2$ and $m_I = 3/2, 1/2$. Hoppings are realized by adequate choices of laser frequencies and polarizations while the repulsion between the rishon neighbor sites can be controlled by Feshbach resonances. In the case of realizing $SU(N)$ one should add the terms of the Hamiltonian as $\sum_{x,y}\left(\det U_{xy} + \det U_{xy}^{\dagger}\right)$ in accordance with 1.116. This contribution forces the introduction of hopping of two particles on the $SU(2)$ case. This can be realized, in principle, through a Raman process with large detuning that prohibits single particle transition but allows the two particle tuning. For more details on the implementation see [147].

As in the Abelian case, the non-Abelian gauge theory can also conceive an implementation making use of angular momentum conservation [149, 150]. In this case, instead of the rishon representation which writes the link variables in terms of fermionic variables, these proposals represent the links in terms of bosons. Specifically, for $SU(2)$ in the one dimensional case the links are realized by four bosonic species: two on the left (a_1, a_2) and two on the right (b_1, b_2) side of the link. The operators are given by:

$$U = U_L U_R, \quad U_L = \frac{1}{\sqrt{N_L+1}}\begin{pmatrix} a_1^{\dagger} & -a_2 \\ a_2^{\dagger} & a_1 \end{pmatrix}, \; U_R = \frac{1}{\sqrt{N_R+1}}\begin{pmatrix} b_1^{\dagger} & b_2^{\dagger} \\ -b_2 & b_1 \end{pmatrix} \tag{2.34}$$

where N_L and N_R are respectively the total number of bosons on the left and right part of the link. Furthermore one should have $N_L = N_R$. The generators are given by:

$$L_a = -\frac{1}{2}\sum_{i,j} a_i^{\dagger}\left[\sigma_a\right]_{ij} a_j, \; R_a = \frac{1}{2}\sum_{i,j} b_i^{\dagger}\left[\sigma_a\right]_{ij} b_j \tag{2.35}$$

which satisfy, as usual $[L_a, L_b] = i\varepsilon_{abc}L_c$, $[R_a, R_b] = i\varepsilon_{abc}R_c$, $[L_a, U] = -\sigma_a U/2$ and $[R_a, U] = U\sigma_a/2$.

This is enough to realize pure gauge in $1D$ however, as discussed before, there is no interesting dynamics for the pure gauge case since no plaquette terms exist:

$$H_E = \frac{g^2}{2}\sum_{n,a} L_a^2 \tag{2.36}$$

with $\sum_a R_a^2 = \sum_a L_a^2$. For realizing the desired theory with dynamical fermions it is required four bosonic species in each link and two fermionic species (ψ, χ) being one of them auxiliary (χ), integrated out in the end. The fermions are placed in alternating sites on the lattice: $\psi - \chi - \psi - \ldots$. The bosons placed in the link connecting $\psi - \chi$ are denoted by a_i, c_i and on the link connecting $\chi - \psi$ are denoted by b_i, d_i with $i = 1, 2$. Here the links contain all bosonic species plus the auxiliary fermion χ. The effective link, as above, will be built on the bosons a and b. In turn the auxiliary bosons c, d are prepared on a coherent state $c_i |\alpha\rangle = \alpha |\alpha\rangle$ (same for d_i with the same α for all). By suitably choosing the hyperfine levels of each population, as in the Abelian case, one can get a "correlated hopping" through scattering. This hopping is given in such a way that when a χ fermion hops to its neighboring site, it is transformed into ψ at the cost of an analogous transformation between a and c or b and d (depending on which mixture is between them). Explicitly, one should engineer hoppings of the form:

$$\sim \sum_n \left(\psi_n^\dagger W_{L,n}\chi_n + \chi_n^\dagger W_{R,n}\psi_{n+1} + \text{h.c.}\right) \tag{2.37}$$

where

$$W_L = \begin{pmatrix} a_1^\dagger c_1 & -a_2 c_2^\dagger \\ a_2^\dagger c_2 & a_1 c_1^\dagger \end{pmatrix},\ W_R = \begin{pmatrix} b_1^\dagger d_1 & b_2^\dagger d_2 \\ -b_2 d_2^\dagger & b_1 d_1^\dagger \end{pmatrix}, \tag{2.38}$$

Note that the role of the auxiliary bosons is to place a creation/annihilation operator next to the annihilation/creation operator of our target link interaction 2.34. To realize these interactions one should have, for example: $m_F(a_1) + m_F(\psi_1) = m_F(c_1) + m_F(\chi_1)$. More details are found in [149]. Being in a coherent state one can replace approximately $c_i, d_i \to \alpha$ constituting an interaction which has the form:

$$\sim \sum_n \left(\psi_n^\dagger \sqrt{N_{L,n}+1} U_L \chi_n + \chi_n^\dagger \sqrt{N_{R,n}+1} U_R \psi_{n+1} + \text{h.c.}\right) \tag{2.39}$$

What remains to be done is to "glue" the two processes above in order to build the desired $\psi_n^\dagger U_L U_R \psi_{n+1}$ hopping term. This can be done penalizing the occupancy of the χ vertices with a large energy through $\Gamma\sum_n \chi_n^\dagger\chi_n$. Perturbation theory will give, in second order, the desired term. The initial state shall be prepared with all χ sites empty. Other terms in second order perturbation theory include $\psi_n^\dagger\psi_n\left(a_{n,i}^\dagger a_{n,i} + b_{n-1,i}^\dagger b_{n-1,i}\right)$. These should also be included as possible scattering processes on the initial Hamiltonian and by a suitable choice of parameters can cancel each other. The other possible terms $\chi_n^\dagger\chi_n\left(a_{n,i}^\dagger a_{n,i} + b_{n,i}^\dagger b_{n,i}\right)$ are zero on this perturbative regime where χ sites are always unoccupied. One gets effectively the contributions 2.36, 2.39 plus the alternating chemical potential term that should always be added $m\sum_n (-1)^n \psi_n^\dagger\psi_n$. The presence of $\sqrt{N_{L,n}+1}\sqrt{N_{R,n}+1}$ does not spoil gauge invariance and with the appropriate parameters yields qualitatively analogous results [150]. Construction of plaquette terms follow the same principle of the loop method of the Abelian case, having naturally some new particularities due to the nature of the group. Details are found in [150].

2.2.4 Encoding in $1+1$ fermions and the first experimental realization

The case of the Schwinger model, $1+1$ Dirac fermions coupled to a gauge field, is an interesting experimental and theoretical playground. It shares some non-trivial features with QCD like confinement, chiral symmetry breaking and a topological theta vacuum [107]. However, due to its simplicity, it

allows analytical and numerical studies which may become significantly harder in more complicated theories. Furthermore it was the target of the first experimental implementation of a lattice gauge theory [15]. In the context of quantum simulations it may not only provide the entrance door towards more complicated experimental realizations but also a way of benchmarking experimental techniques.

One of the reasons why this model bares an intrinsic simplicity, as mentioned previously, is the fact that the gauge fields are non-dynamical. This is reflected on the absence of plaquette terms in the Hamiltonian formulation. Furthermore the Gauss law fixes the gauge field and can be used to perform the integration of the gauge fields leaving behind a long range interacting model. This shall be addressed next. In the following the lattice Hamiltonian formulation is considered for N lattice sites:

$$H = -it\sum_{n=1}^{N-1}\left[c_n^\dagger U_n c_{n+1} - \text{h.c}\right] + m\sum_{n=1}^{N}(-1)^n c_n^\dagger c_n + \frac{g^2}{2}\sum_{n=1}^{N-1}L_n^2 \tag{2.40}$$

Here the infinite dimensional Hilbert space per link is considered therefore U_n are unitary and the non-trivial commutation relations on the links are given by $[L_m, U_n] = U_n\delta_{mn}$. Equivalently the link can be written as $U_n = e^{i\theta_n}$. The Gauss law imposed is, in accordance with previous discussion, $G_n|\psi\rangle = 0$:

$$G_n = L_n - L_{n-1} - c_n^\dagger c_n + \frac{1}{2}\left(1-(-1)^n\right) \tag{2.41}$$

This model can be formulated in terms of Pauli spin operators [175] and this result will be reproduced here. A Jordan-Wigner transformation [176] is defined by:

$$\begin{cases} c_n = \prod\limits_{l<n}\left(i\sigma_z(l)\right)\sigma^-(n) \\ c_n^\dagger = \prod\limits_{l<n}\left(-i\sigma_z(l)\right)\sigma^+(n) \end{cases} \tag{2.42}$$

where $\sigma_i(n)$ represents the n-th component of the spin in the site l and $\sigma^\pm(n) = \sigma_x(n) \pm i\sigma_y(n)$. In terms of the spins the Gauss law takes the form:

$$G_n = L_n - L_{n-1} - \frac{1}{2}\left(\sigma_z(n) + (-1)^n\right) \tag{2.43}$$

Now, since one will be restricted to work on the physical space for which $G_n|\psi\rangle = 0$, the Gauss law can be used to eliminate almost any trace of link variables. Using periodic boundary conditions: $L_0 = L_N$ one finds:

$$L_n = L_0 + \frac{1}{2}\sum_{l=1}^{n}\left(\sigma_z(l) + (-1)^n\right) \tag{2.44}$$

The value of L_0 is a parameter of the theory and corresponds to a background field. For simplicity it will be taken to zero at the present discussion. By using the above relation on the last term of 2.40, the pure gauge term is exclusively written in terms of the spins:

$$H = t\sum_{n=1}^{N}\left[\sigma^+(n)\,e^{i\theta_n}\sigma^-(n+1) + \text{h.c}\right] + \frac{m}{2}\sum_{n=1}^{N}(-1)^n\sigma_z(n) + \frac{g^2}{8}\sum_{n=1}^{N}\left[\sum_{l=1}^{n}\left(\sigma_z(l) + (-1)^n\right)\right]^2 \tag{2.45}$$

where a trivial constant term was dropped. The remaining gauge field variable θ_n can be eliminated by a residual gauge transformation [177]:

$$\sigma^\pm(n) \to \sigma^\pm(n)\prod_{i<n}e^{\pm i\theta_i} \tag{2.46}$$

Plugging this transformation and expanding the interaction term, the resulting model is a long-range interacting spin model:

$$H = t\sum_{n=1}^{N}\left[\sigma^{+}(n)\,\sigma^{-}(n+1)+\text{h.c}\right]+\sum_{n=1}^{N}\left(\frac{m}{2}(-1)^{n}-\frac{g^{2}}{8}\left(1-(-1)^{n}\right)\right)\sigma_{z}(n)+\frac{g^{2}}{4}\sum_{n=1}^{N-2}\sum_{l=1}^{N-1}(N-l)\,\sigma_{z}(n)\,\sigma_{z}(l) \tag{2.47}$$

This is an attractive formulation since the total of N particles and $N-1$ gauge fields are simulated by just N spins (with exotic long-range interactions). The difficulty was moved towards an efficient way of implementing the long-range asymmetric interaction between spins. This Hamiltonian was implemented as a digital quantum simulator in [15] using trapped ions ($^{40}Ca^{+}$). The system was composed of four qubits. The Schwinger mechanism of pair creation of particle-antiparticle was explored, as well as real time evolution of entanglement in the system. From the Jordan-Wigner transformation $c_n^{\dagger}c_n = (\sigma_z(n)+1)/2$ and from the discussion of the Section 1.4.4.1 a particle on an odd site is effectively interpreted as empty and a hole as an antiparticle (the contrary holds for particles in the even sites). Following this picture the number of particles at the site n is given by $\nu_n = (1-(-1)^n)/2 + (-1)^n c_n^{\dagger}c_n$ and therefore a relevant observable is the particle density $\nu(t) = (2N)^{-1}\sum_n \langle 1+(-1)^n\sigma_z(n)\rangle$. Starting from a bare vacuum ($\nu(0)=0$) it is observed a rapid increase of the particle density followed by a decrease which is due to recombination. Also vacuum persistence $G(t) = \langle 0|\, e^{-iHt}\,|0\rangle$ and entanglement are evaluated. The later is done by reconstructing the density matrix and evaluating the entanglement in one half of the system with the other half through logarithmic negativity. Entanglement is produced through particle creation that get distributed across the two halves. More details on the simulation and experimental results can be found in [15, 172]. Future challenges include the simulation of larger systems as well higher dimensionality and non-Abelian symmetries.

2.3 Half Links Schwinger (HLS) model

This Section concerns ongoing work and provides some ideas concerning an alternative approach for the lattice implementation of gauge theories. The fundamental idea is that one can give up some of the dynamical links of the staggered fermionic lattice gauge models without compromising gauge invariance. In the $1+1$ dimensional case, which will serve as illustrative example in this Section, this principle will lead to consider only half of the dynamical links and therefore will be referred as Hal Links Schwinger (HLS) model.

2.3.1 Local symmetry: Continuum vs Lattice

Staggered fermions were discussed in Section 1.4.3 and the associated gauge theory for $1+1$ dimensions in Section 1.4.4.1. As a quick recapitulation, the components of the spinors are placed on different lattice sites. The spinors are recovered in the continuum limit according to Equation 1.75. In order to get a local symmetry and introduce gauge fields on this model, the links become dynamical according to Equation 1.98 and display a set of local symmetries characterized by 1.94 (or equivalently 1.100). In turn the local symmetries of the Schwinger model, on its continuum version are characterized by 1.41. To facilitate the discussion, the fermion transformations on both formulations are written here as well:

$$\begin{aligned}&\text{Continuum}: \psi(x) \to e^{i\alpha(x)}\psi(x)\\ &\text{Lattice}: c_n \to e^{i\alpha_n}c_n\end{aligned} \tag{2.48}$$

There is an interesting consequence of this construction: an higher symmetry, in a certain way, is being required in the lattice model which is not being required on the continuum. In fact, since even/odd consecutive sites build up different components of the same spinor, on the lattice the symmetry allows

the components of the same spinor (in the perspective of Equation 1.75) to transform with a different phase:

$$\begin{pmatrix} c_{2n} \\ c_{2n+1} \end{pmatrix} \to \begin{pmatrix} e^{i\alpha_{2n}} c_{2n} \\ e^{i\alpha_{2n+1}} c_{2n+1} \end{pmatrix} \tag{2.49}$$

Such general symmetry does not survive the continuum limit. In fact this would mean that the Schwinger model would have a symmetry:

$$\psi(x) \to \begin{pmatrix} e^{i\alpha(x)} & 0 \\ 0 & e^{i\beta(x)} \end{pmatrix} \psi(x) \tag{2.50}$$

for arbitrary function α and β, which is not true and only when $\alpha(x) = \beta(x)$ this is in fact a symmetry. One can investigate what happens to this symmetry in the naive continuum limit. To this end consider the generators of the gauge symmetry in Equation **??** and define the alternative set of generators:

$$G^{\pm}_{2n+1} = G_{2n+1} \pm G_{2n} \tag{2.51}$$

There are now two types of generators $\pm$, but they are only make sense for even sites. This is just an equivalent way of describing the same symmetry but puts in evidence the distinction made above where G^{-}_{2n} is the generator responsible for transformations with different phases in consecutive even/odd sites. Explicitly they read:

$$\begin{aligned} G^{+}_{2n+1} &= L_{2n+1} - L_{2n-1} - c^{\dagger}_{2n} c_{2n} - c^{\dagger}_{2n+1} c_{2n+1} + 1 \\ G^{-}_{2n+1} &= L_{2n+1} + L_{2n-1} - 2L_{2n} + c^{\dagger}_{2n} c_{2n} - c^{\dagger}_{2n+1} c_{2n+1} + 1 \end{aligned} \tag{2.52}$$

By requiring that $G^{\pm}_{2n} |\Psi\rangle = 0$ one sees that G^{+}_{2n} is exactly the Gauss law:

$$G^{+}_{2n} \sim 2a \left(\frac{1}{e} \frac{\partial E}{\partial x} - \psi^{\dagger} \psi \right) \tag{2.53}$$

while the other generator is of higher order on a:

$$G^{-}_{2n} \sim a^2 \left(\frac{1}{e} \frac{\partial^2 E}{\partial x^2} - \frac{1}{a} \psi^{\dagger} \sigma_z \psi \right) \tag{2.54}$$

Since this symmetry does not survive the continuum limit one may choose to give it up all together from the start.

2.3.2 Formulation of the model

As discussed above, giving up this symmetry on the lattice is equivalent to drop the requirement that consecutive even/odd links transform with a different phase. This is then:

$$\begin{cases} c_{2n} \to e^{i\alpha_{2n}} c_{2n} \\ c_{2n+1} \to e^{i\alpha_{2n}} c_{2n+1} \\ U_{2n+1} \to e^{i\alpha_{2n}} U_{2n+1} e^{-i\alpha_{2n+2}} \end{cases} \tag{2.55}$$

where now the link variables U_l are only defined for l odd. The generators of these symmetries are given by G^{+}_{2n} in Equation (2.52). The Hamiltonian will read:

$$H_{\text{HLS}} = -\frac{i}{2a} \sum_n \left(c^{\dagger}_{2n} c_{2n+1} + c^{\dagger}_{2n+1} U_{2n+1} c_{2n+2} - \text{h.c.} \right) + m \sum_n (-1)^n c^{\dagger}_n c_n + \frac{ae^2}{2} \sum_n L^2_{2n+1} \tag{2.56}$$

This Hamilton is represented on Figure 2.32 and it is invariant under the transformations 2.55. As in the usual formulation, one can represent the link variables $U_{2n+1} = e^{i\theta_{2n+1}}$ and can also encode the

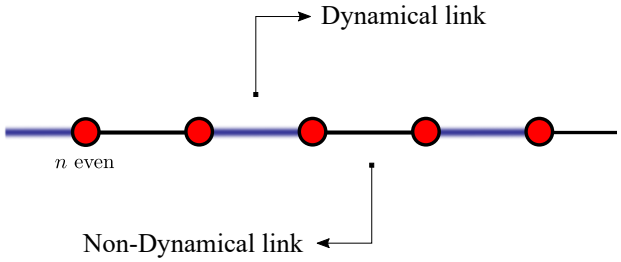

Figure 2.4: Representation of the HLS model where only the links between odd/even sites are dynamical. The pair even/odd is used to build the spinor and does not require a dynamical link.

model in terms of spins, integrating the gauge fields, as done in Section (2.2.4). Using the Jordan-Wigner transformation:

$$G_{2n}^{+} = L_{2n} - L_{2n-2} - \frac{1}{2}\left(\sigma_z\left(2n\right) + \sigma_z\left(2n+1\right)\right) \tag{2.57}$$

Again setting a possible background field to zero, the Gauss law imposes:

$$L_{2n} = \frac{1}{2}\sum_{l=1}^{2n+1}\sigma_z\left(l\right) \tag{2.58}$$

This relation can be used in (2.56) and a residual gauge transformation can be constructed to eliminate the θ's from the Hamiltonian:

$$\begin{aligned}\sigma^{\pm}\left(2n\right) &\rightarrow \sigma^{\pm}\left(2n\right)\prod_{i<n}e^{\pm i\theta_{2i}}\\ \sigma^{\pm}\left(2n+1\right) &\rightarrow \sigma^{\pm}\left(2n+1\right)\prod_{i<n}e^{\pm i\theta_{2i}}\end{aligned} \tag{2.59}$$

The resulting model reads:

$$H = \frac{1}{2a}\sum_{n}\left[\sigma^{+}\left(n\right)\sigma^{-}\left(n+1\right) + \text{h.c}\right] + \frac{m}{2}\sum_{n}\left(-1\right)^{n}\sigma_z\left(n\right) + \frac{ae^2}{8}\sum_{n}\left[\sum_{l=1}^{2n+1}\sigma_z\left(l\right)\right]^2 \tag{2.60}$$

When comparing this to the resulting case of the usual formulation, Equation 2.45, one can make an interesting observation. While in 2.45 all symmetries that involve $\sigma_z\left(l\right) \rightarrow -\sigma_z\left(l\right)$ are forbidden, even for $m = 0$, due to the oscillating term that originates due integration of the gauge fields, here it is not the case. This model exhibits then symmetries that 2.45 does not, like, for example, $\sigma_x\left(l\right), \sigma_y\left(l\right), \sigma_z\left(l\right) \rightarrow \sigma_x\left(l\right), -\sigma_y\left(l\right), -\sigma_z\left(l\right)$.

2.3.3 Experimental implementation and perspectives

The possible advantages of this formulation for experimental implementation are clear: there are less degrees of freedom to be implemented and, in particular less, correlated hopping between bosons and fermions must be constructed. By eliminating the dynamics on every other link, one is then able to implement this model. For example, in the energy punishment approach introduced on Section 2.2.1, one was forced to introduce an extra bosonic species to alternate the occupancy of the links in such a way that no hoping between neighboring links could occur. By eliminating every odd link, this is no longer necessary. It is, however, interesting to observe that there are certain possible implementations which do not find a counterpart on other proposals that are meant to implement the Kogut-Susskind Hamiltonian fully. This can be a fundamental key to achieve more suitable proposals.

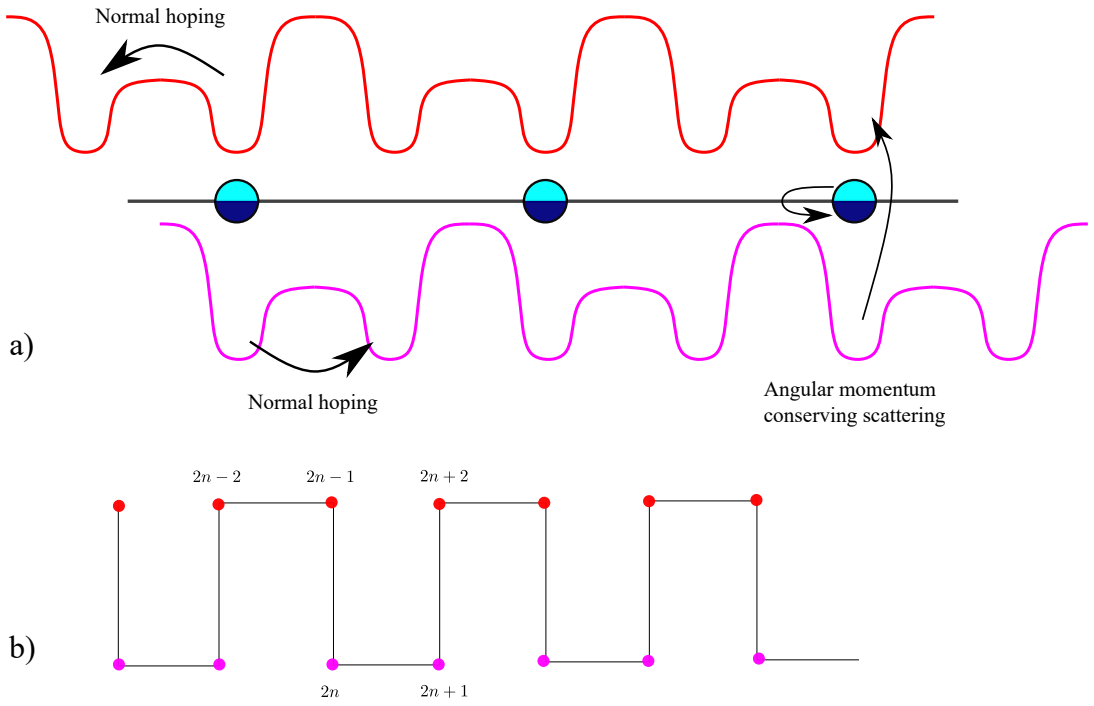

Figure 2.5: Scheme for a possible implementation of the HLS model. In the panel a) the two hyperfine states of the fermions with their respective optical potentials are represented in red and pink. The two bosonic hyperfine states are placed in the same site and are unable to escape. They are represented in two different shades of blue. Independentely of the fermionic state, the fermion will only feel a double well potential and is trapped there. The only way it can leave the trap is to scatter with the bosons changing their hyperfine states only to find itself trapped in another double well. Normal hopping between double wells corresponds to hoping without gauge link while the change in hyperfine state implies the existence of a gauge link. In panel b) it is represented how the lattice sites of the fermions in the different hyperfine states map to the sites of the HLS Hamiltonian.

As an example, consider a fermionic and a bosonic atomic species that can take two possible hyperfine levels. The bosonic mixture is placed on a single site and hoping is forbidden. Each fermionic species is only on a double well, unable to escape. The two double wells of the fermions are aligned in such a way that a fermion, in order to proceed in a given direction, can do so if it changes its hyperfine state. It can do so, in the spirit of angular momentum conservation, by scattering with the bosons. Normal hoping will correspond to even/odd jump on the Hamiltonian 2.56 while the change on the hyperfine state, which is effectively a same site scattering term, corresponds to an odd/even jump. See Figure 2.5.

This formulation puts in evidence a non-trivial consequence: it may be possible to implement a lattice gauge theory without correlated hoping. In fact this general scheme only requires same site scattering and usual hopping. It is worth to note that a hoping $2n \to 2n+1$ is a physical hoping on the experimental scheme but in the lattice gauge theory will serve to construct a same site spinor. In turn, a change in the hyperfine state on the experimental scheme corresponding to $2n-1 \to 2n$, without an actual change of the physical position, will correspond to build a change on the spinor in two different sites.

Chapter 3

Non-Abelian symmetry locking for fermionic mixtures

The results of this Chapter can be also found in [16]. Ultracold multicomponent mixtures, including quantum gases where more atomic species are simultaneously trapped, also opened in a natural way the possibility to study exotic phases and unconventional superfluidity, in accordance with the previous discussion [178]. In this Chapter it shall be addressed the realization of non-Abelian superfluid phases, focusing in particular on the so-called symmetry-locked phases. Such phases are realizable in suitable fermionic mixtures in which the components can be divided in two subsets, and they are induced by a order parameter connecting fermions belonging to the different subsets. The peculiar property of this parameter is that it involves all the possible pairing channels permitted by the symmetry of the system.

The concept of symmetry-locking is a central concept for various areas of high energy physics. It occurs in the presence of a phase (typically superfluid), characterized by a particular non vanishing vacuum expectation value, acting as an order parameter and inducing a spontaneous symmetry breaking pattern. Indeed, because of this expectation value, two independent symmetry groups of the normal phase are mixed in a residual symmetry subgroup.

In the system considered in the present Chapter it is addressed the dynamics of four fermionic components which will be generically divided in two sates conventionally denoted as c and f. In other words, two of the fermionic components will be associated with the label c while the other two with the label f. In this system, a symmetry-locking occurs in the presence of a non-vanishing order parameter between two atoms (one belonging to c and the other to f). The pairing can occur, in principle, between any pair of atomic species. Depending in pairing combinations some symmetry is retained or not.

Symmetry-locking results in a number of peculiar properties, especially when the locked groups are non-Abelian, for instances ordered structures as nets and crystals [179, 180] or vortices and monopoles with semi-integer fluxes, confining non-Abelian modes [181–185]. A remarkable example of this phenomenon appears in the study of nuclear matter under extreme conditions, as in the core of ultra-dense neutron stars [186]. There the locking interests the $SU(3)_c$ (local) color and the $SU(3)_f$ (global) flavor groups. Similarly the chiral symmetry breaking transition involves a locking of global $SU(3)_L$ and right $SU(3)_R$ global flavor symmetries [179, 180].

In [187] a study of symmetry-locked states was presented based on multi-component fermionic mixtures. In there it was proposed the synthesis of a superfluid phase locking two non-Abelian global symmetries has been presented. This state has been denoted as a two-flavor symmetry-locked (TFSL) state. In the analysis presented in [187] it was considered a four component mixture. The setting is described by the four component mixture described above with labels c and f. The system considered

has an attractive interaction between all the components with an Hubbard parameter U, as described in Section 1.2. In the following $U > 0$ will correspond to attractive interactions while $U < 0$ to repulsive. This system hosts very peculiar phenomena significant for high-energy physics as TFSL states, fractional vortices and non-Abelian modes confined on them [187]. Besides the intrinsic interest of such setting, it also represents a first step towards the simulation of phases involving the breaking of gauge symmetries, as in the QCD framework.

Multi-component fermionic mixtures present a natural playground to simulate symmetry-locking. A prominent example is given by multi-components Yb gases, that can be synthesized and controlled at the present time [188]. Yb atoms, as all the earth-alkaline atoms, have the peculiar property that their interactions do not depend on the hyperfine quantum number labeling the states of a certain multiplet. This fact allows the realization of interacting systems, bosonic and fermionic, with non-Abelian $U(N)$ or $SU(N)$ symmetries [189]. This property was already used explicitly to construct a non-Abelian gauge theory in Section 2.2 following [147]. One can make use of this property to realize the mixture described above using a mixture of ^{171}Yb and ^{173}Yb atoms [187]. This will be described here as well. One can populate can attribute the label c to two hyperfine levels of ^{171}Yb and the label f to two hyperfine levels of ^{173}Yb. Each species is selectively populated in two different hyperfine levels and loaded on a cubic optical lattice. For such mixture one has three kinds of interactions (for the following values see [190]):

- ^{171}Yb and ^{173}Yb: Scattering length $a_{171-173}$ is negative and rather large ($a_{171-173} = -578a_0$, with a_0 the Bohr radius). Attractive interaction.
- ^{171}Yb and ^{171}Yb: Scattering length $a_{171-171}$ is negative and small ($a_{171-171} = -3a_0$). Weakly attractive interaction.
- ^{173}Yb and ^{173}Yb: Scattering length $a_{173-173}$ is negative and small ($a_{173-173} = +200a_0$). Repulsive interaction.

In the case discussed above, an attractive interaction between the ^{171}Yb and ^{173}Yb atoms favors the symmetry-locked phase, while a too strong attraction or repulsion between the populated hyperfine levels of ^{171}Yb or of ^{173}Yb may spoil it. Therefore a natural question is to what extent the TFSL phase can remain stable. This question fits into the more general problem of determining the phase diagram and the actual extension of the TFSL phase as the interactions between the atoms of the considered four-component mixture are varied. This question shall be addressed on the following Sections by determining the phase diagram of a the four component mixture with attractive inter-pair interaction. By this it is meant that it will be assumed that interactions between atoms c and f will be attractive while interactions between atoms within c or within f can be attractive or repulsive. It will be observed, in particular, that the interactions described above fall within a region of a symmetry-locked phase. This results is particularly relevant in the light of the known difficulty to tune interactions between earth alkaline atoms, as the Yb, without destructing their $U(N)$ invariance and avoiding important losses of atoms or warming of the experimental set-ups.

3.1 Four fermion mixture model

According to the scenario described above, a four species fermionic mixture involving atoms in two different pairs of states (possibly pairs of hyperfine levels) is considered. For convenience these four degrees of freedom will be labeled as $\sigma \in \{r, g, u, d\}$ and they will be grouped like$\{r, g\}$ and $\{u, d\}$. The first pair will be associated to the label c and the second to the label f. In other words, when one speaks about an atom c (f) it means that it belongs to the pair $\{r, g\}$ ($\{u, d\}$).

Even if the mechanism that is going to described is independent of the space where the atoms are embedded, in the following the mixture will be considered to be loaded in a cubic optical lattice. A

discussion of possible advantages of this choice will be presented in Section 3.4. The system is described by an Hubbard-like Hamiltonian $H = H_{kin} + H_{int}$

$$H = -t \sum_{\langle i,j\rangle,\sigma} c^{\dagger}_{i\sigma} c_{j\sigma} - \sum_{i,\sigma\sigma\prime} U_{\sigma\sigma'} n_{i\sigma} n_{i\sigma'} \tag{3.1}$$

In the above equation and in the following it is considered that $U_{\sigma\sigma'} > 0$ corresponds to an attractive interaction while $U_{\sigma\sigma'} < 0$ describes a repulsive interactions. The matrix $U_{\sigma\sigma'}$ is symmetric with vanishing diagonal elements (because of the Fermi statistics).

As advanced before the situation of interest in the context of symmetry-locking is the one where the interactions between the multiplets c and f does not depend on the specific levels chosen in each pair. The system in Equation (3.1) is therefore characterized by three interaction parameters labeled as $U_{rg} \equiv U_c$, $U_{ud} \equiv U_f$ and $U_{ru} = U_{rd} = U_{gu} = U_{gd} \equiv U_{cf}$. In the following it will referred to interactions associated with U_c and U_f as "intra-pair" interactions and to the ones associated with U_{cf} as "inter-pair" interactions.Due to the sign convention, a TFSL phase is expected to be found for U_{cf} positive (attractive) and large enough. Once the hoppings and the occupation numbers of the species are set equal in each multiplet, the system in the normal (Fermi liquid) state has a group symmetry $\mathcal{G} = U(2)_c \times U(2)_f$ corresponding to independent rotations on the c and f degrees of freedom respectively. More in detail, these transformations act as:

$$\begin{pmatrix} c'_1 \\ c'_2 \end{pmatrix} = \mathcal{U}_c \begin{pmatrix} c_1 \\ c_2 \end{pmatrix}, \quad \begin{pmatrix} f'_1 \\ f'_2 \end{pmatrix} = \mathcal{U}_f \begin{pmatrix} f_1 \\ f_2 \end{pmatrix} \tag{3.2}$$

where $\mathcal{U}_c = e^{i\vec{\theta}_c \cdot \vec{\sigma}}$, $\vec{\sigma}$ are the Pauli matrices and $\vec{\theta}_c$ a vector parameterizing the rotation and corresponding to free parameters. The same goes for $\mathcal{U}_f = e^{i\vec{\theta}_f \cdot \vec{\sigma}}$. These transformations are independent and one has:

$$\mathcal{U}_c H \mathcal{U}_c^{-1} = H, \quad \mathcal{U}_f H \mathcal{U}_f^{-1} = H \tag{3.3}$$

By other side, as it was shown in [187], when superfluidity is induced, $\mathcal{G}$ may undergo in general a spontaneous symmetry breaking into a smaller subgroup $\mathcal{H}$. In particular, when superfluidity occurs between the c and the f atoms, the following spontaneous symmetry breaking (SSB) pattern takes place:

$$U(2)_c \times U(2)_f \to U(2)_{c+f}. \tag{3.4}$$

This means that the superfluid phase has a residual non-Abelian invariance group $\mathcal{H} = U(2)_{c+f}$ composed by a subset of the group of elements $(\mathcal{U}_c, \mathcal{U}_f) = (\mathcal{U}_c, \mathcal{U}_c) = (\mathcal{U}_f, \mathcal{U}_f)$, where $\mathcal{U}_c$ and $\mathcal{U}_f$ belong to $U(2)_c$ and $U(2)_f$ respectively. Notably $\mathcal{H} = U(2)_{c+f}$ involves at the same time c and f transformations, originally independent.

The SSB at the basis of the symmetry-locking is explicit in the fact that the superfluid is described by a gap matrix $\mathbf{\Delta}_{cf}$ transforming under G as $\mathcal{U}_c \mathbf{\Delta}_{cf} \mathcal{U}_f^{-1}$, and left invariant by the subgroup of transformations $H = U(2)_{c+f}$. This mechanism is called symmetry-locking(see e.g. [186]).

The mentioned relevance and generality of the symmetry-locking phenomenon, as well as the intrinsic interest for non-Abelian superfluid phases (as for instance for some models of high-temperature superconductivity), motivate an effort to realize the model in Equation (3.1) in current ultracold atoms experiments.

3.2 Mean field energy and consistency equations

In this Section it shall be investigated the emergence of of superfluid states, considering all possible pairings in the system described by Equation. (3.1), investigating more in general the superfluid BCS

phases that can arise in it. The discussion here will be based a mean field approximation. Strong-coupling results in Section 3.3.

In mean field approximation the energy $\mathcal{F}$ at zero temperature can be written as:

$$\mathcal{F} = \frac{1}{2}\sum_{\vec{k}} \hat{\psi}^{\dagger}_{\vec{k}} F_{\vec{k}} \hat{\psi}_{\vec{k}} + F_c, \tag{3.5}$$

where $\hat{\psi}^{\dagger}_{\vec{k}} = \left(c_{kr} \dots c_{kd}, -c^{\dagger}_{-kr} \dots - c^{\dagger}_{-kd}\right)$, and $F_{\vec{k}}$ is the 8×8 matrix:

$$F_{\vec{k}} = \begin{pmatrix} \xi_{\vec{k},\{\sigma\}} & 2\Delta_{\sigma\sigma'} \\ 2\Delta^{*}_{\sigma\sigma'} & -\xi_{\vec{k}.\{\sigma\}} \end{pmatrix}, \tag{3.6}$$

In this equation the labels on $\Delta_{\sigma\sigma'}$ run through their four possible values: $\sigma \in \{r, g, u, d\}$, therefore $\Delta_{\sigma\sigma'}$ represents a 4×4 matrix. The factor 2 in front of $\Delta_{\sigma\sigma'}$ is due to the double sum in Equation (3.1). Moreover

$$\xi_{\vec{k}\sigma} = \mathrm{Diag}\left(\varepsilon_{\vec{k}} - \tilde{\mu}_{\sigma}\right),$$

where

$$\varepsilon_{\vec{k}} = -2t \sum_{l=1}^{3} \mathrm{cos} k_{\hat{l}}$$

and

$$\tilde{\mu}_{\sigma} = \mu_{\sigma} + \nu_{\sigma} U_{\sigma} + 2\nu_{\bar{\sigma}} U_{cf} \tag{3.7}$$

are the chemical potentials shifted by the Hartree terms. In Equation (3.7) ν_{σ} denote the fillings of each component σ and $\bar{\sigma}$ denotes "opposite" degree of freedom, meaning that if σ is a c index then $\bar{\sigma}$ is an f and vice-versa. It is implicitly assumed that, at most, one is considering two different fillings: $\nu_r = \nu_g \equiv \nu_c$ and $\nu_u = \nu_d \equiv \nu_f$. This is in the origin of the factor 2 in from of $\nu_{\bar{\sigma}} U_{cf}$ in Equation (3.7):it accounts for the two possible labels belonging to the opposite degree of freedom. The constant F_c in Equation (3.5) has the form:

$$F_c = \frac{1}{2}\sum_{\vec{k},\sigma} \xi_{\vec{k}\sigma} + V \sum_{\sigma \neq \sigma'} U^{-1}_{\sigma\sigma'} |\Delta_{\sigma\sigma'}|^2 \tag{3.8}$$

V being the number of the lattice sites, $\left\langle c^{\dagger}_{k\sigma} c_{k\sigma'} \right\rangle = \delta_{\sigma\sigma'} n_{\sigma}$ and $\Delta_{\sigma\sigma'} \equiv -V^{-1} U_{\sigma\sigma'} \sum_{\vec{k}} \langle c_{k\sigma} c_{-k\sigma'} \rangle$, assumed real. Moreover $\mu_r = \mu_g \equiv \mu_c$ and $\mu_u = \mu_d \equiv \mu_f$ which holds since it is assumed that each pair $\{r, g\}$ and $\{u, d\}$ have the same fillings, ν_c and ν_f, the same intra-pair interactions, U_c and U_f, and the same inter-pair interactions U_{cf}.

The problem to describe superfluid phases of the Hamiltonian in Equation (3.1) is then reduced, at the mean field level, to the diagonalization of $F_{\vec{k}}$ and to the subsequent determination of of $\Delta_{\sigma\sigma'}$ and $\tilde{\mu}_{\sigma}$ by the solution of self-consistent equations. In a general case the self-consistent equations will have more than one solution and the energy of each one should be computed in order to determine the ground state.

The general situation can be approached numerically finding the matrix $P_{\vec{k}}$ that as the column vectors the eigenvectors of $F_{\vec{k}}$

The diagonalization of the matrices may not be easy analytically but can be accessed numerically. This way a matrix P_k can be found such that $P^{\dagger}_k F_{\vec{k}} P_k$ is diagonal $D = \mathrm{Diag}\left(\lambda_a\right)_{a=1,\dots,8}$. The eight eigenvalues obtained are, of course, an artifice of writing $\hat{\psi}_{\vec{k}}$ with both creation and annihilation operators and do not constitute extra modes. One can get rid of them observing that, for $\tau = I_{4d} \otimes \sigma_x = \tau^{-1}$, the relation $\tau^{-1} F_{\vec{k}} \tau = -F_{\vec{k}}$ holds if $\Delta_{\alpha\beta}$ are real. In this way if v is an eigenvectors of

$\mathcal{F}_k$ with eigenvalue λ, one can get $F_{\vec{k}}\tau v = -\tau F_{\vec{k}} v = -\lambda\tau v$ and as a result τv is also an eigenvectors of $F_{\vec{k}}$ with symmetric eigenvalue $-\lambda$. Once found the eigenvectors of $P_{\vec{k}}$, the transformed operators are:

$$\Psi_{\vec{k}} = P^{\dagger}_{\vec{k}}\psi_{\vec{k}} = \begin{pmatrix} \gamma_{\alpha\vec{k}} \\ \gamma^{\dagger}_{\alpha\vec{k}} \end{pmatrix} \tag{3.9}$$

This allows to $\hat{\psi}^{\dagger}_{\vec{k}}F_{\vec{k}}\hat{\psi}_{\vec{k}} = \Psi^{\dagger}_{\vec{k}}D_{\vec{k}}\Psi_{\vec{k}}$ and putting them to normal order will give an Hamiltonian bounded from below and an extra term to the constant term of the free energy $F_c \to F_c - \frac{1}{2}\sum_{\vec{k},\sigma}\lambda^{(+)}_{\vec{k}\sigma}$, where $\lambda^{(+)}_{\vec{k},\alpha}$ denote the four positive eigenvalues of $F_{\vec{k}}$. The ground-state energy is found to be

$$F_c = \frac{1}{2}\sum_{\vec{k}}\left(\sum_{\sigma}\xi_{\vec{k}\sigma} - \sum_{\alpha}\lambda^{(+)}_{\vec{k}\alpha}\right) + V\sum_{\sigma\sigma'}U^{-1}_{\sigma\sigma'}\left|\Delta_{\sigma\sigma'}\right|^2. \tag{3.10}$$

The self-consistent equations for $\Delta_{\sigma,\sigma'}$ and the shifted chemical potentials $\tilde{\mu}_\sigma$ can be now obtained from the conditions:

$$\begin{cases} \frac{\partial F_c}{\partial \Delta_{\sigma\sigma'}} = 0 \\ \\ \frac{\partial (F_c + \tilde{\mu}_\sigma n_\sigma)}{\partial \tilde{\mu}_\sigma} = 0 \end{cases} \tag{3.11}$$

Several solutions of the Equations (3.11) are possible in general. In general one should check what is the correct phase for every point $\big(U_c, U_f, U_{cf}\big)/t$ that minimizes the energy. There are three types of solutions:

- Normal: no superfluid pairing exist between any degree of freedom. That means $\Delta_{\alpha\beta} = 0$ for any pair (α, β).
- non-TFSL (NTFSL): intra-pair pairings occur but no inter-pairing takes place: $|\Delta_{c_1c_2}|^2 + |\Delta_{f_1f_2}|^2 \neq 0$ and $\mathbf{\Delta}_{cf} = 0$. In this case the two non-trivial Bogoliubov energies entering (Equation (3.10)) read $\lambda^{(+,c)}_{\vec{k}\alpha} = \sqrt{\xi^2_{\vec{k}} + |\Delta_{c_1c_2}|^2}$ and $\lambda^{(+,f)}_{\vec{k}\alpha} = \sqrt{\xi^2_{\vec{k}} + |\Delta_{f_1f_2}|^2}$.
- TFSL: inter-pair pairings occur but no intra-pair takes place: $|\Delta_{c_1c_2}|^2 + |\Delta_{f_1f_2}|^2 = 0$ and $\mathbf{\Delta}_{cf} \neq 0$. In this case the two non-trivial Bogoliubov energies entering (Equation (3.10)) read $\lambda^{(+)}_{\vec{k}\alpha} = \sqrt{\xi^2_{\vec{k}} + |\Delta_{cf}|^2}$ with $\Delta_{cf} = \frac{1}{2}\,\mathrm{Tr}\mathbf{\Delta}_{cf}$, being $\mathbf{\Delta}_{cf}$ the matrix of the inter-pair pairings.

The normal state solution is always possible. By solving numerically Equations (3.11) one can see that whenever in the presence of an attraction term between the species ($U_{cf} > 0$) a solution with non-zero pairing $\Delta_{\sigma\sigma'}$ also exists. Furthermore, it is found that it exists always a solution with less energy than the normal state. This result assures the presence of a superfluid state, also in presence of intra-pair repulsion. Of course this is a mean field result, expected not to be correct for large intra-pair repulsion: a strong-coupling analysis of such case is presented in Section 3.3.

The obtained superfluid BCS solutions are always of the TFSL or NTFSL types, in other words no solution with both $|\Delta_{c_1c_2}|^2 + |\Delta_{f_1f_2}|^2 \neq 0$ and $\mathbf{\Delta}_{cf} \neq 0$ occurs. It is also observed that setting $n_c = n_f$ for all the three mentioned types of solutions, the shifted chemical potential $\tilde{\mu}_c$ and $\tilde{\mu}_f$ turn out equal, in spite of the intra-pair interactions U_c and U_f, being different in general. In particular, they depend only on n_c and n_f themselves. This means that, at least at the mean field level, these interactions do not determine any effective unbalance between the c and f species. This fact is expected to remain, at least approximately, true in the presence of a trapping potential, since this potential acts, in local density approximation, as a space-dependent correction to the chemical potentials $\mu_{c,f}$ at the center of the trap [75], not to the shifted potentials $\tilde{\mu}_{c,f}$. This appears particularly relevant since it is known

(see [75] and references therein) that generally an unbalance in the normal state can spoil the possible emergence of superfluid states, or at least to modify the critical interaction strength and the critical temperature.

For the case $n_c = n_f \equiv n$, it is true that $\xi_{\vec{k},\sigma} \equiv \xi_{\vec{k}}$ and it is possible to recast the self-consistency Equations (3.11) in a BCS-like form:

$$1 = \frac{U_{c,f}}{V}\sum_{\vec{k}} \frac{1}{\sqrt{\xi_{\vec{k}}^2 + 4\left|\Delta_{c,f}\right|^2}}, \quad \Delta_{cf} = 0, \qquad \text{NTSFL} \tag{3.12}$$

or

$$1 = \frac{U_{cf}}{V}\sum_{\vec{k}} \frac{1}{\sqrt{\xi_{\vec{k}}^2 + 4\left|\Delta_{cf}\right|^2}}, \quad \Delta_{c,f} = 0, \qquad \text{TSFL} \tag{3.13}$$

and

$$n_\theta = \frac{1}{V}\sum_{\vec{k}} \left(1 - \frac{\xi_{\vec{k}}}{\sqrt{\xi_{\vec{k}}^2 + 4\left|\Delta_{\alpha}\right|^2}}\right). \tag{3.14}$$

For sake of brevity, in the last equation Δ_α is meant to include both Δ_{cf} and Δ_c, Δ_f, corresponding to both the cases TFSL and NTFSL. Notice that Equations (3.12)-(3.14) reproduce exactly the standard BCS self-consistency equations, as one should expect: indeed the different numerical factors in Equations (3.12)-(3.14) are due to the different definitions for U_c, U_f, U_{cf} and for the corresponding gap parameters used here.

3.3 The phase diagram

The phase diagram of the Hamiltonian 3.1 as a function of the external parameters t, U_c U_f and U_{cf} is then investigated by solving Equations (3.10)-(3.11). Concretely, the results for the solutions of Equation. (3.11) are presented here for a cubic lattice having 20^3 sites (checking that the phase diagram is not affected by finite size effects), and compare the energies of the obtained solutions to determine the mean field phase diagram. The limitations of the mean field findings are postponed for later in the text.

3.3.1 Attractive U_c, U_f

The results presented in the panel a) of Figure 3.1 refer to the the half-filling case ($n_\sigma = \frac{1}{2}$, corresponding to $n_c = n_f \equiv n = 1$) and different values of the ratio U_{cf}/t and U_c/t, U_f/t. In this case one always find $\tilde{\mu}_\sigma = 0$, as required by particle-hole symmetry (see e.g. [191]).

For each fixed value of $U_{cf}/t > 0$ (attractive regime) a colored curve is drawn, separating the TFSL phase inside of it from the NTFSL phase outside. As the value of U_{cf}/t is increased, higher values of attractive intra-pair couplings U_c/t, U_f/t are required to break the TFSL phase in favor of the NTFSL one. At variance the normal state is never favored over both the superfluid states, even when one of or both the intra-pair interactions are repulsive and not small in comparison with the attractive ones. In this case the mean field approach is expected not to be reliable and, asdiscussed in the next Section, antiferromagnetic states can be favoured. instead

In the panel b) of Figure 3.1 where the curves of the panel a) are rescaled by their values of U_{cf}/t: in this way they all meet in the point $U_c = U_f = U_{cf}$. For this point of the parameter space, all the different Hamiltonians have a $U(4)$ symmetry and the two phases TFSL and NTFSL can be mapped onto each other. This signals a transition point between the two phases, in agreement with [187].

The black point in the second panel of Figure 3.1 represents the case of the mixture composed by ^{171}Yb and ^{173}Yb, where natural interactions between these isotopes are also assumed. This mixture,

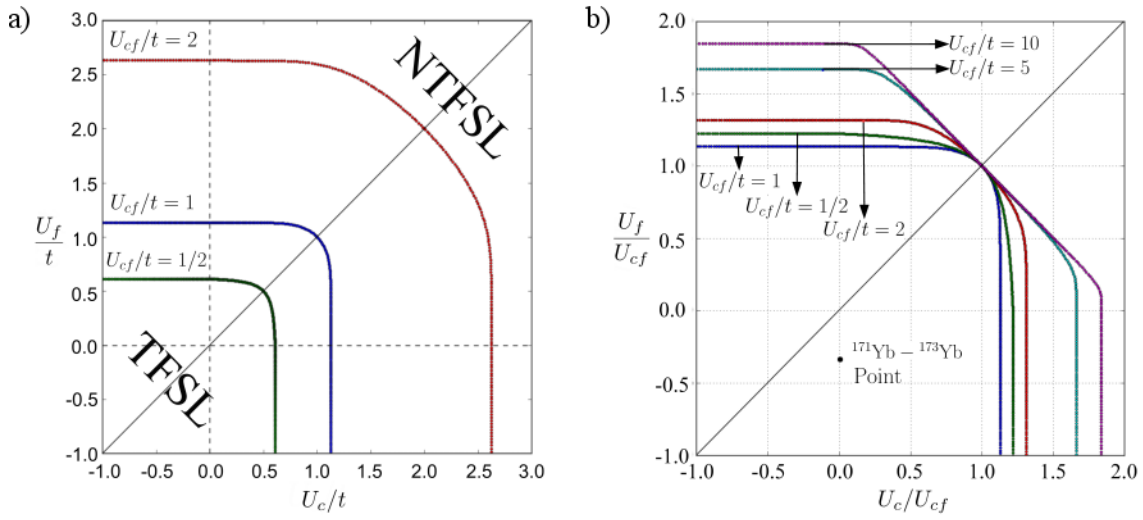

Figure 3.1: a) Phase diagram at half filling for $U_{cf}/t = \{1/2, 1, 2\}$. Inside the curves (at smaller values of U_σ) the TFSL phase occurs, while outside one has the NTFSL phase. As U_{cf}/t increases, the zone of the TFSL phase becomes larger. b) Phase diagram in units of U_{cf} at half filling. The point $U_c = U_f = U_{cf}$ is a transition point between the phases TFSL and NTFSL, irrespectively of the value for t. It is also depicted the point representing the natural interactions of the mixture ^{171}Yb-^{173}Yb [192]. The corresponding estimates for this point are performed in Sec. 3.4.

mentioned in the introduction , will be discussed in detail in Section 3.4. For now it is only observed that the point lies well inside the TFSL zone.

The phase diagram shown in Figure 3.1 b) is not a consequence of the hypothesis of balanced mixture. Indeed in Figure 3.2 a) the same phase diagram is plotted for different fillings (but still equal for the four σ species), finding qualitative agreements with small quantitative differences.

Similarly, in Figure 3.2 b) the case where the pairs c and f have fillings differing by ten percent is reported. Again it is clear that the imbalance in the populations does not produce significative differences on the results. An imbalance in the number of particles is generally known able to spoil the appearance of superfluid states [75]. In the present case the reliability of the results is guaranteed by the absence of other non-trivial solutions for the Equations (3.11) (see for comparison, e.g., [193]) and by the direct comparison between the energies of the normal states and the one of the BCS-like superfluid solutions.

3.3.2 Repulsive U_c, U_f

When U_c, U_f assume negative values, meaning a repulsive intra-pair interactions appear in the Hamiltonian of Equation (3.1), the formation of intra-pair pairs start to become suppressed. However the normal state is never favored in the mean field approximation as shown in Figures 3.1-3.2.

If it is reasonable that for small intra-pair repulsion the TFSL is favored, for large enough values of U_c/t, U_f/t and U_c/U_{cf}, U_f/U_{cf} this superfluid phase is expected to eventually disappear, replaced by insulator phases with a magnetic-like order. The latter regime is qualitatively described in the strong coupling limit U_c/t, U_f/t by spin Hamiltonians, similarly to the Heisenberg model for a two species repulsive mixtures at half filling (see, e.g., [191]).

In the strong-coupling limit two cases are explicitly considered here:

1. Both intra-species interaction large: $|U_c|/t, |U_f|/t \gg 1$,

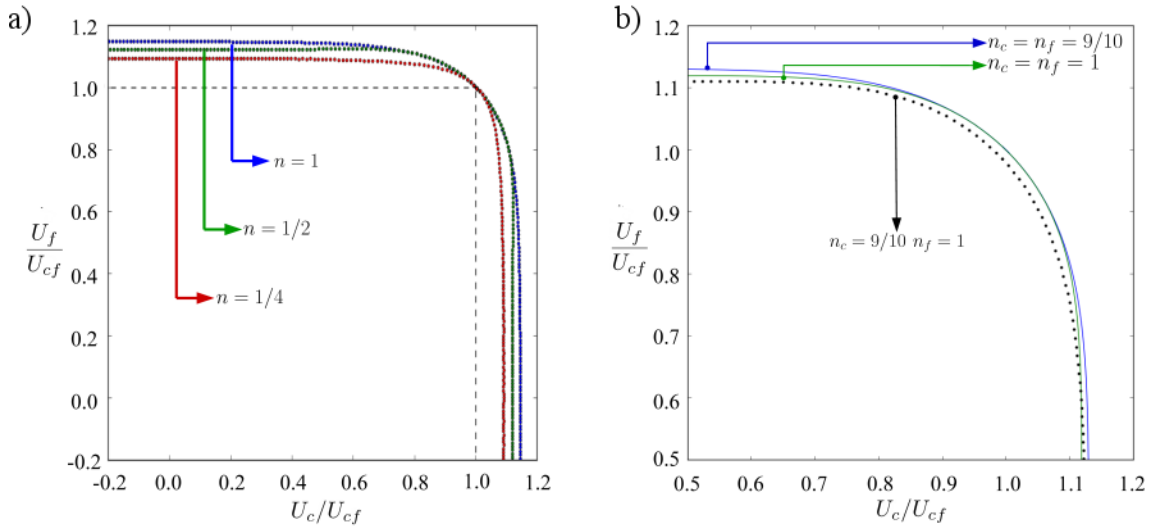

Figure 3.2: a) Phase diagrams for $U_{cf}/t = 1$ and for different fillings: $n = 1$ (blue), $n = 1/2$ (green) and $n = 1/4$ (red). They appear qualitatively very similar indicating that the filling does not play a fundamental role. b) Phase diagram in the presence of a small unbalance between the populations $n_f - n_c = 0.1$ and $U_{cf} = t$. The result is qualitatively very similar to the balanced cases (see also Figures 3.1).

2. One intra-species interaction large and other small: $|U_c|/t \ll 1$ and $|U_f|/t \gg 1$. The converse case of U_c large and U_f small is completely analogous due tot he symmetry of the Hamiltonian ((3.1)).

Notice that in both cases the further condition $|U_c/U_{cf}|, |U_f/U_{cf}| \gg 1$ is implicitly assumed. In the first case the strong coupling Hamiltonian reads (details of the derivation are in the Appendix 3.A):

$$H^{cf}_{eff} = \frac{t^2}{4}\sum_{\langle i,j\rangle}\left(\frac{1}{|U_c|}\vec{C}_i\cdot\vec{C}_j + \frac{1}{|U_f|}\vec{F}_i\cdot\vec{F}_j\right) - E^{cf}_{GS} \tag{3.15}$$

where $\vec{C}$ and $\vec{F}$ are effective spin variables for c and f respectively defined by $\vec{C}_i = \sum_{\alpha,\beta\in\{r,g\}} c^\dagger_{i\sigma}\vec{\tau}_{\sigma\sigma'}c_{i\sigma'}$ and $\vec{F}_i = \sum_{\alpha,\beta\in\{u,d\}} c^\dagger_{i\sigma}\vec{\tau}_{\sigma\sigma'}c_{i\sigma'}$ ($\vec{\tau}$ denoting the Pauli matrices). The constant E^{cf}_{GS} is the ground-state energy and is given by:

$$E^{cf}_{GS} = -NU_{cf} - \frac{zNt^2}{4}\left(\frac{1}{|U_c|} + \frac{1}{|U_f|}\right) \tag{3.16}$$

where $N = 2V$ is the total number of atoms of each pair. The Hamiltonian in Equations (3.15) corresponds to two decoupled Heisenberg models. The case 2. is of interest for the Yb discussed in the next Section, in the perspective of a possible experimental realization for the TFSL mechanism. Here the ground-state energy is found in the limit $U_c/t \to 0$ (see details in Appendix 3.B):

$$E^c_{GS} = 2E^{NS}_{GS} + \Delta E = 2E^{NS}_{GS} - N\left(\frac{U_c}{4} + \frac{z\,t^2}{4\,|U_f|}\right), \tag{3.17}$$

where E^{NS}_{GS} is the energy of a single c component in the normal state. Indeed the energy in Equation (3.17) is proper of a system of free fermions c on a antiferromagnetic background describing the

dynamics of the f fermions. The f fermions will be described by a spin Hamiltonian similar to Equation (3.15).

The regions of the phase diagram where both the TFSL and NTFSL superfluid phases occur can be bounded comparing their ground-state energies with the energies of the antiferromagnetic phases in Equations (3.16) and (3.17).

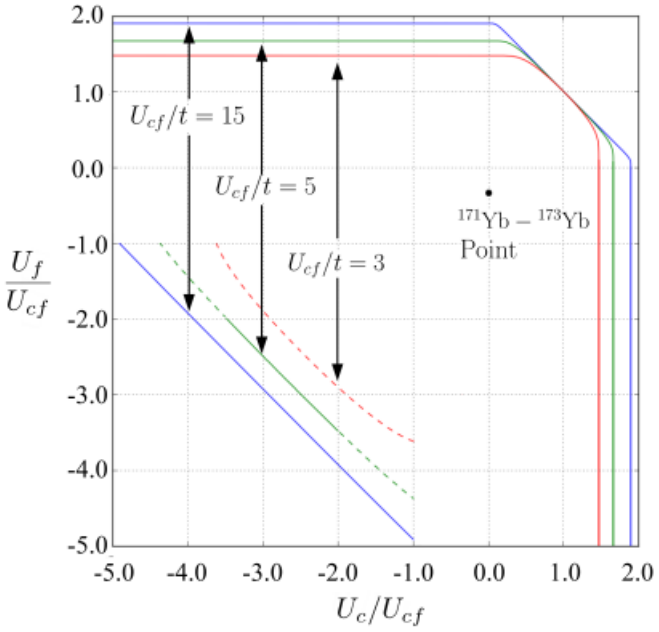

Figure 3.3: Phase diagram, containing the natural point for the Ytterbium mixture, for the cases $U_{cf} = 3t$ (red), $U_{cf} = 5t$ (green) and $U_{cf} = 15t$ (blue). The oblique lines bounding the superfluid phases are obtained by the strong coupling approach leading to Equations. (3.16) and (3.17). The transition from solid lines to dashed lines signals where this approach is not reliable any longer because it does not hold that $|U_c/t|, |U_f/t| \gg 1$.

Postponing the details for the case 2. to the Section 3.4, here the results of this calculation for the case 1. are presented in Figure 3.3. There the oblique lines represent a set of points where, according to the energy criterium mentioned above, the insulator states become favorable over the superfluid phases. Notice that increasing the optical potential depth V_0 results in a increase of the area of the TFSL phase, compared with the insulator one.

The calculation leading to Equations. (3.16) and (3.17) are perturbative in t/U_σ, therefore the comparison between the energies in the same equations and the ones for the superfluid states is reliable only while $t/U_\sigma \ll 1$. For this reason a dashed line, instead of a solid one, is drawn in Figure 3.3 where the condition $|t/U_\sigma| > 10^{-1}$ (a threshold conventionally chosen) starts to hold. For the dashed line, therefore, the strong-coupling approach is no longer expected to be fully reliable. From the Figure one can see that for $U_{cf}/t = 3$ the transition line can never be located pertubatively, while for $U_{cf}/t = 15$ the converse is true. As an intermediate example $U_{cf}/t = 5$ exhibits both a zone where perturbation theory can be assumed valid and other ones where it cannot.

3.4 Experimental feasibility and limits

As briefly discussed in the beginning of the Chapter, a possible experimental realization of the system described above involves a mixture of ^{171}Yb and ^{173}Yb. The first isotope has a 1/2 hyperfine multiplet while the second one has 5/2 hyperfine degeneracy. For the latter atomic species only two levels could be selectively populated. The mixture obtained in this way exhibits natural interactions characterized as follows: using conventionally the label c for the hyperfine levels of ^{171}Yb and the label f for the ones of ^{173}Yb, the scattering lengths are $a_c = -3a_0$, $a_f = 200a_0$ and $a_{cf} = -578a_0$, where a_0 is the Bohr radius (see e.g. [190,192]). As in all the earth-alkaline atoms, the tunability of these interactions is very difficult using the magnetic Feshbach resonance, because of the negligible magnetic moment of such atoms. Moreover, in the recent literature this problem revealed challenging also using alternative techniques, due to important atomic losses and without spoiling their characteristic $U(N)$ invariance (N denoting here the number of hyperfine levels of the considered atomic species). For details on this subject see [194] and references therein. This problem can prevent the realization of certain phases and the exploration of the full phase diagram. For the purposes of realization of a symmetry-locked phase the relevant question is then if without tuning the interaction the TFSL superfluid phase is realized or not.

For the considered earth-alkaline mixture loaded on a cubic lattice, the hopping parameters, in principle different, are given by:

$$t^{\alpha}_{\vec{r}\,\vec{r}'} = -\int d^3\vec{r}\frac{\hbar^2}{2m_\alpha}\left(\nabla\phi_{\alpha\vec{r}'}\left(\vec{r}\right)\cdot\nabla\phi_{\alpha\vec{r}''}\left(\vec{r}\right) + \phi_{\alpha\vec{r}'}\left(\vec{r}\right)V_{\text{ext}}\left(\vec{r}\right)\phi_{\alpha\vec{r}''}\left(\vec{r}\right)\right) \tag{3.18}$$

The expressions for the interaction parameters U_c, U_f , U_{cf} in the form of $U_{\alpha\beta}$ for $\alpha \neq \beta \in \{r, g, u, d\}$ are, for the conventions used in this Chapter:

$$U_{\alpha\beta} = -\frac{\pi\hbar^2 a_{\alpha\beta}}{m_{\alpha\beta}}\int d^d\vec{r}\phi_{\alpha\vec{r}'}\left(\vec{r}\right)^2\phi_{\alpha\vec{r}'}\left(\vec{r}\right)^2 \tag{3.19}$$

In Equations (3.18) and (3.19), $\phi_{\{\alpha,\beta\}\vec{r}'}\left(\vec{r}\right)$ are the Wannier functions describing the localization on a given lattice site $\vec{r}'$ (these labels are suppressed in the following for sake of brevity), $\vec{r}$ is the distance from a chosen site, and $m_{\alpha\beta} = \frac{m_\alpha m_\beta}{m_\alpha + m_\beta}$. A simple variational estimate for the Wannier functions, which results in an estimate for the parameters in Equations 3.18 and 3.19, is discussed in Appendix 3.C.

The tight binding regime for the Yb is achieved for an amplitude of the opical lattice potential $V_0 \gtrsim 2 - 3E_{R_c}$ where $E_{Rc} = \hbar^2 k_0^2/2m$ is the recoil energy, k_0 is the wave vector of the laser producing the optical lattice and m is chosen conventionally to be the mass of the ^{171}Yb isotope. The amplitude V_0 is considered up to $\approx 15E_{R_c}$, where the tunneling coefficients are very small and tunneling dynamics effectively suppressed. Assuming this interval for the ratio V_0/E_{R_c} and Equations (3.18) and (3.19) with their optimized Wannier wave functions, the regions on the diagram U_c/U_{cf}, U_f/U_{cf} associated with the considered Yb mixture with natural interactions can be calculated.

In Figure 3.4 it is reported on the left panel the hopping coefficients for different rescaled depths $\tilde{V}_0 = V_0/E_{Rc}$. I is seen in the left panel that, contemplating the small difference in mass between the two isotopes, it always holds $\Delta t/t \lesssim 10^{-1}$ so that the previous assumption $t_c = t_f \equiv t$ (however not strictly required for the TFSL mechanism) is reasonable. On the right panel of the same figure it is presented the variation of $U_{\alpha,\beta}/t$, again as functions of $\tilde{V}_0 = V_0/E_{Rc}$. In the same way, the region in the diagram $U_{c,f}/U_{cf}$ associated with the Yb mixture can be also calculated. More details on the calculation are given in Appendix 3.C.

If one writes the intra-pair interactions in the form $U_{c,f}/U_{cf}$, it is observed that the dependence on the amplitude V_0 effectively drops out such that only the relative value of U_{cf}/t changes significantly and the obtained region resembles a single point. This is the reason why one can speak about just a "natural point" in the diagrams of Figures 3.1 and 3.3. This point is given approximately by the

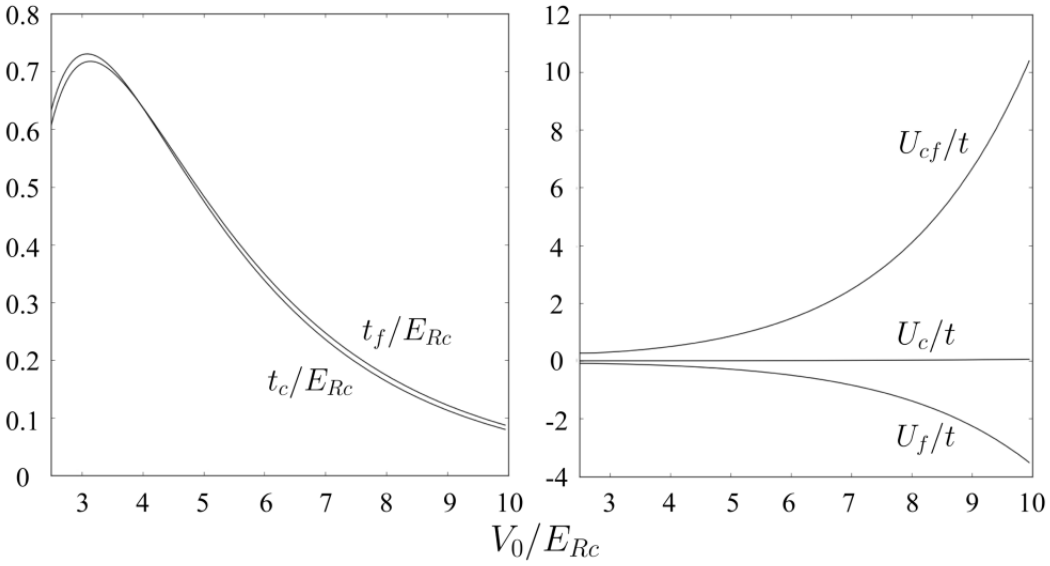

Figure 3.4: Parameters of the Hamiltonian in Equation (3.1) as a function of the depth of the optical lattice potential $\tilde{V}_0 = V_0/E_{Rc}$. Left panel: hopping parameters t_c/E_{Rc} and t_f/E_{Rc}. Right panel: rescaled interaction parameters $U_{c,f}/t_c$ and U_{cf}/t_c.

coordinates $U_c/U_{cf} \approx 0.01$ and $U_f/U_{cf} \approx -0.34$, also very close to the point estimated using the approximation $U_\alpha/U_{cf} \simeq a_\alpha/a_{cf}$ valid in the continuous space limit.

Importantly the natural point falls well inside the TFSL regime, see Figures 3.1 and 3.3. In particular, along the line $U_c/t = 0$ (case b in Section 3.3), where the point almost lies, an estimate for the appearance of the antiferromagnetic regime can be done comparing the energies in Equations (3.8) and (3.17). As a result, the transition is located by the strong coupling approach at the values $U_c/U_{cf} = -3.97$ for $U_{cf}/t = 3$, $U_c/U_{cf} \approx -4.9$ for $U_{cf}/t = 5$ and $U_c/U_{cf} \approx -5.6$ for $U_{cf}/t = 15$, in all the three cases far from the natural point of the Yb (recall its location to be $U_f/U_{cf} \approx -0.34$). In this way, these findings indicate that the TFSL phase can be observed in the zero temperature limit in experiments with Yb mixtures, assuming natural interactions and realistic values for the depth of the lattice potential.

Despite of the zero-temperature results reported, the TFSL phase could be still unreachable in the presence of a critical temperature (at fixed interactions), required for its emergence, smaller than the ones currently realizable in the experiments. This point is particular important in the light of the mentioned difficulty to tune the interactions in earth-alkaline atoms. In the following the critical temperature shall be estimated for the Yb mixture, proceeding as for the two-component attractive Hubbard model in [195], where the results are given as function of the total bandwidth. The relevant case here corresponds to isotropic hoppings t ($t_\perp = t_\parallel = t$ in the notation of [195]) and to the half filling case. Moreover $\tilde{\mu}_c = \tilde{\mu}_f$, as found in Section 3.2.

For the cubic lattice considered the total bandwidth is $D = 12t$. Considering, for instance, $V_0 = 5E_{Rc}$, one obtains $2U_{cf} \approx 0.3D$, which results in $T_c K_B/D \approx 0.05$. Using these values and considering a lattice spacing of $a = 0.5\,\mu m$, the critical temperature turns out $T_c \approx 15$ nK. In terms of the Fermi temperature this amounts to obtain $T_c/T_F \approx 0.1$. This value is reasonably close to the ones achievable in current experiments [55], suggesting that the critical temperature assuming the natural interaction is reachable with current-day experiments and the TFSL phase could be achieved.

The lattice ratio $T_c/T_F \approx 0.1$ can be compared with the typical one for experiments in the con-

tinuous space, finding that apparently on the lattice T_c/T_F is sensibly larger. Indeed a very simple estimate can be done using the results [196] for a two-component mixture (as it is effectively the TFSL phase). Considering a number of loaded atoms $N \approx 10^4$ and a system size $\ell \sim 10\mu m$, one obtains T_c/T_F smaller than 0.01. This value is far from the presently achievable ones, differently from the lattice case. Summing up, the present analysis suggests that, for the task to synthesize a TFSL phase in Yb mixtures, the use of a (cubic) lattice can be advantageous.

3.5 Conclusions

In this Chapter it is addressed the possibility to realize unconventional non-Abelian superfluid states using multicomponent fermionic mixture. This is done by investigating the emergence of a non-Abelian two-flavor locking (TFSL) superfluid phase in ultracold Fermi mixtures with four components and unequal interactions. It is shown that such states could be studied in current day experiments with ^{171}Yb-^{173}Yb mixtures. This problem can be addressed using mean field and strong coupling analysis. The phase diagram was explored for such mixture loaded in a cubic lattice, finding for which ranges of the interactions and of the lattice width the system exhibits a TFSL phase.

These ranges are found to have an extended overlap with the ones realizable in current experiments. In particular, as detailed above, the proposed set-up and phase are found to be realistic and realizable using a mixture of ^{171}Yb and ^{173}Yb. The phase diagram has been studied and the point associated to the natural (not tuned) interactions between these atomic species determined. It was shown to be within the TFSL phase. The fact that no tuning is necessary is central for a possible experiment aiming to realize the TFSL phase, especially due to the known difficulty to tune interactions in earth-alkaline atomic gases without spoiling their peculiar $U(N)$ invariance. The critical temperature required for the appearance of the TFSL superfluid has been found comparable with the ones currently achievable.

Finally, it is also crucial to note that the relative large intra-pair repulsion do not destroy the superfluid states. A different scenario is expected to take place when non-local repulsive interactions are present, whose effects can be considered an interesting subject of future work.

Appendix Chapter 3

3.A c and f strongly coupled limit

In this Appendix the details concerning the perturbative calculation for the strongly coupled limit in the presence of repulsive intra-pair interactions are presented. This process leads to Equation (3.15) in the main text. It is assumed that the system is at half filling.

The described physical situation corresponds to consider the Hamiltonian $H_0 + H_1$ where

$$H_0 = 2\sum_i \left(|U_c| n_{ir} n_{ig} + |U_f| n_{iu} n_{id}\right) - 2|U_{cf}| \sum_{i,c,f} n_{ic} n_{if}, \tag{3.20}$$

$$H_1 = -t \sum_{\langle i,j\rangle,\sigma} c^\dagger_{i\sigma} c_{j\sigma}, \tag{3.21}$$

and perform perturbation theory in the parameters $\varepsilon_c, \varepsilon_f \ll 1$ with $\epsilon_c = t/|U_c|, \epsilon_f = t/|U_f|$. It is assumed $\epsilon_c = \epsilon_f = \epsilon$. The ground-states of H_0, with energies $E = -2V|U_{cf}| = -N|U_{cf}|$, are the states where no single site is doubly occupied by intra-pairing atoms, provided that $|U_{c,f}| > 3/2|U_{cf}|$. Let $\hat{G}$ be the projector on this space and $\hat{P} = 1 - \hat{G}$.

The lowest order correction to E comes at the second order, from the virtual process consisting in the interchange of location of two particles at nearest-neighbor distance. The calculation simplifies noting that $\hat{P} H_1 = H_1$ and that $H_1 |\phi\rangle$ is an eigenvector of H_0 for $|\phi\rangle$with ϕ being one of its (degenerate) ground-states. The related second order effective Hamiltonian then is found to be

$$H_{eff} = \frac{t^2}{4} \sum_{\langle i,j\rangle} \left(\frac{1}{|U_c|} \vec{C}_i \cdot \vec{C}_j + \frac{1}{|U_f|} \vec{F}_i \cdot \vec{F}_j \right) - \frac{zNt^2}{8} \left(\frac{1}{|U_c|} + \frac{1}{|U_f|} \right) \tag{3.22}$$

where $\vec{C}$ and $\vec{F}$ are effective spin variables for c and f respectively defined by $\vec{C}_i = \sum_{\alpha,\beta\in\{r,g\}} c^\dagger_{i\sigma} \vec{\tau}_{\sigma\sigma'} c_{i\sigma'}$ and $\vec{F}_i = \sum_{\alpha,\beta\in\{u,d\}} c^\dagger_{i\sigma} \vec{\tau}_{\sigma\sigma'} c_{i\sigma'}$ ($\vec{\tau}$ denoting the Pauli matrices) as already presented in the main text. The corresponding ground-state energy correction is $\Delta E = -\frac{zNt^2}{4} \left(\frac{1}{|U_c|} + \frac{1}{|U_f|} \right)$, being z the adjacency number for every site. In this way the ground-state energy at the second order perturbation theory in $\frac{t}{U_{c,f}}$ becomes

$$E = -N|U_{cf}| - \frac{zNt^2}{4} \left(\frac{1}{|U_c|} + \frac{1}{|U_f|} \right). \tag{3.23}$$

This formula is Equation (3.16) of the main text.

3.B Strongly coupled f and weakly coupled c

In this case the system is described by the Hamiltonian $H_0 + H_1 + H_2$ where:

$$\begin{aligned} H_0 &= 2|U_f|\sum_i \hat{n}_{iu}\hat{n}_{id} - 2|U_{cf}|\sum_{i,c,f}\hat{n}_{ic}\hat{n}_{if} - t\sum_{\langle i,j\rangle,c} c^\dagger_{ic}c_{jc} \\ H_1 &= -t\sum_{\langle i,j\rangle,f} c^\dagger_{if}c_{jf} \\ H_2 &= -2U_c\sum_i n_{ir}n_{ig} \end{aligned} \tag{3.24}$$

The perturbative parameters are $\epsilon_1 = \frac{t}{|U_f|}$ and $\epsilon_2 = \frac{|U_c|}{t}$. The ground-state of H_0 can be derived in this limit assuming a basis of localized f degrees of freedom. Using such a basis, one can get an effective Hamiltonian for the c degrees of freedom corresponding to non-interacting fermions in a one body potential, which in turn depending on the f configuration.

If $|U_f| \gg t$ and $|U_f| \gg |U_{cf}|$, the dynamics is dominated by the localization of the f atoms and therefore the ground-state does not host any doubly occupied site. In that case, in the ground state of H_0, a single f particle is in each site. Therefore the one-body potential felt by the c particles is site independent: $-2\,|U_{cf}|\,\hat{n}_{ic}$. The effect of this potential is to induce a shift on the chemical potential $\delta\mu_c = -2|U_{cf}|$. Up to the first order of perturbation, the ground-state energy then results on $E_{0c} = 2\sum_{\vec{k}:\varepsilon_{\vec{k}}<0}\varepsilon_{\vec{k}}$. Instead the first order in ϵ_1 vanishes because it is related with forbidden double occupancies of sites by particles of the same species. At the second order in ϵ_1 and ϵ_2, an effective Hamiltonian can be derived:

$$\hat{H}_{eff} = \hat{G}\left[\epsilon_1^2\hat{H}_1\frac{1}{\left(E_0-\hat{H}_0\right)}\hat{P}\hat{H}_1 + \epsilon_1\epsilon_2\left(\hat{H}_1\frac{1}{\left(E_0-\hat{H}_0\right)}\hat{P}\hat{H}_2 + \text{h.c.}\right) + \epsilon_2^2\hat{H}_2\frac{1}{\left(E_0-\hat{H}_0\right)}\hat{P}\hat{H}_2\right]\hat{G} \tag{3.25}$$

with $\hat{G}$ and $\hat{P} = 1 - \hat{G}$ defines as in Appendix (3.A). The term $\propto \epsilon_1\epsilon_2$ vanishes for the same reason for which the linear term in ϵ_1 does. The remaining effective terms are then proportional to ε_2, ϵ_1^2 and ϵ_2^2. These terms commute with each other, so one can focus on them individually. After some algebra one can write the energy correction up to the second order for the ground-state energy:

$$\Delta E = N\left(-\frac{U_c}{4} - \frac{zt^2}{4}\,|U_f| - \frac{U_c^2}{t}\tilde{E}^{(2)}\right) \tag{3.26}$$

where $\tilde{E}^{(2)}$ is a dimensionless positive quantity:

$$\tilde{E}^{(2)} = -\frac{1}{V^3}\sum_{\substack{\vec{k}_1,\vec{k}_2\in\mathbb{F}_S\\ \vec{q}_1,\vec{q}_2\in\mathbb{F}_S}}\frac{\delta_{\vec{k}_1+\vec{k}_2,\vec{q}_1+\vec{q}_2}}{\varepsilon_{\vec{k}_1}+\varepsilon_{\vec{k}_2}-\varepsilon_{\vec{q}_1}-\varepsilon_{\vec{q}_2}} \tag{3.27}$$

with $\mathbb{F}_S$ labeling the set of points of the Fermi sea and $\tilde{\varepsilon_k} = \varepsilon_k/2t$. Equation (3.26) is used to arrive to Equation (3.17) of the main text, where $U_c = 0$ and the calculation of $\tilde{E}^{(2)}$ is not required.

3.C Determination of the model parameters

In the present Appendix the parameters of Hamiltonian 3 are estimated by a variational approach. This is obtained from the expressions

$$\begin{aligned} t_{ij\alpha} &= -\int d^3\vec{r}\left(\tfrac{\hbar^2}{2m_\alpha}\nabla\phi_{i\alpha}\left(\vec{r}\right)\cdot\nabla\phi_{j\alpha}\left(\vec{r}\right)+\phi_{i\alpha}\left(\vec{r}\right)V_{\text{ext}}\left(\vec{r}\right)\phi_{j\alpha}\left(\vec{r}\right)\right) \\ U_{\alpha\beta} &= -\tfrac{\pi\hbar^2 a_{\alpha\beta}}{m_{\alpha\beta}}\int d^3\vec{r}\left|\phi_\alpha\left(\vec{r}\right)\right|^2\left|\phi_\beta\left(\vec{r}\right)\right|^2 \end{aligned} \tag{3.28}$$

where $V_{\text{ext}}\left(\vec{r}\right)=V_0\sum_{j=1}^{3}\sin^2\left(k_0 r_i\right)$ is the external potential creating the lattice ($k_0=\frac{2\pi}{a}$, a being the lattice spacing), $a_{\alpha\beta}$ correspond to the scattering lengths between the α and β species, and $m_{\alpha\beta}$ are their reduced masses. Moreover the $\phi_\alpha\left(\vec{r}\right)$ refer to the Wannier functions centered on the lattice sites. A simple estimate of these functions can be obtained by variational approach. In particular we consider the following ansatz:

$$\phi_\alpha\left(\vec{r}\right)=C_\alpha e^{-\frac{|\vec{r}|^2}{2\sigma_\alpha^2}}, \tag{3.29}$$

where $C_\alpha=\left(\sqrt{\pi}\sigma_\alpha\right)^{-3/2}$. The values of the coefficients σ_α are fixed by minimizing the energy per lattice site. This energy can be found as the expectation value of the Hamiltonian (**??**) acting on the multi-particles fermionic state $\Psi_\alpha(\vec{r}_1,\ldots,\vec{r}_V)$ (V being the number of lattice sites, at half filling equal to the number of c or f atoms) constructed by the Wannier functions. In the mean field approximation it reads:

$$\varepsilon=\int\prod_{i=1}^{V}d^3\vec{r}_i\left(\sum_\alpha\frac{\hbar^2}{2m_\alpha}\left|\nabla\Psi_\alpha\right|^2+V_{ext}\left|\Psi_\alpha\right|^2+\sum_{\beta>\alpha}\frac{2\pi\hbar^2 a_{\alpha\beta}}{m_{\alpha\beta}}\left|\Psi_\alpha\right|^2\left|\Psi_\beta\right|^2\right) \tag{3.30}$$

Using the (approximate) orthogonality of the Wannier functions at different lattice sites one obtains:

$$\varepsilon=\int d^3\vec{r}\sum_{\vec{r}',\alpha}\left(n_\alpha\frac{\hbar^2}{2m_\alpha}\left|\nabla\phi_{\alpha\vec{r}'}\right|^2+n_\alpha V_{ext}\left|\phi_{\alpha\vec{r}'}\right|^2+\sum_{\beta>\alpha}n_\alpha n_\beta\frac{g_{\alpha\beta}}{2}\left|\phi_{\alpha\vec{r}'}\right|^2\left|\phi_{\beta\vec{r}'}\right|^2\right) \tag{3.31}$$

$n_{\{\alpha,\beta\}}$ being the average number of particles of $\{\alpha,\beta\}$ per site and $g_{\alpha\beta}=\frac{4\pi\hbar^2 a_{\alpha\beta}}{m_{\alpha\beta}}$. Moreover the Wannier functions, centered on the lattice sites labeled by $\vec{r}'$, depend on the space vector $\vec{r}$ spanning all the lattice. Using the ansatz in Equation (3.29) one finds

$$\varepsilon/N=\sum_\alpha\left[n_\alpha\frac{\hbar^2}{2m_\alpha}\frac{3}{2\sigma_\alpha^2}+n_\alpha\frac{3V_0}{2}\left(1-e^{-k_0^2\sigma_\alpha^2}\right)+\sum_{\beta>\alpha}n_\alpha n_\beta\frac{g_{\alpha\beta}}{2\pi^{3/2}\left(\sigma_\alpha^2+\sigma_\beta^2\right)^{3/2}}\right] \tag{3.32}$$

Imposing $\frac{\partial\varepsilon}{\partial\sigma_\mu}=0$ and expressing the parameters in Equation (3.32) as adimensional quantities $\tilde{\sigma}_\mu=k_0\sigma_\mu$, $\tilde{V}_\alpha=\frac{V_0}{E_R^\alpha}$ and $\tilde{a}_{\alpha\beta}=k_0 a_{\alpha\beta}$, with $E_R^\alpha=\frac{\hbar^2k_0^2}{2m_\alpha}$, the result is a set of coupled equations:

$$\frac{1}{\tilde{\sigma}_\mu^3}-\tilde{V}_\mu\tilde{\sigma}_\mu e^{-\tilde{\sigma}_\mu^2}+4\sum_{\beta\neq\mu}n_\beta\left(1+\frac{m_\mu}{m_\beta}\right)\frac{\tilde{a}_{\mu\beta}\tilde{\sigma}_\mu}{\sqrt{\pi}\left(\tilde{\sigma}_\mu^2+\tilde{\sigma}_\beta^2\right)^{5/2}}=0. \tag{3.33}$$

Solving this set in $\{\sigma_\alpha\}$, the Hubbard coefficients are finally obtained by substituting the solutions on:

$$\begin{aligned} t_\alpha &= -\left[\tfrac{\hbar^2}{2m_\alpha}\tfrac{1}{4\sigma_\alpha^2}\left(6-\left(\tfrac{a}{\sigma_\alpha}\right)^2\right)+\tfrac{V_0}{2}\left(3-e^{-k_0^2\sigma_\alpha^2}\right)\right]e^{-\frac{a^2}{4\sigma_\alpha^2}}, \\ U_{\alpha\beta} &= -\tfrac{\hbar^2 a_{\alpha\beta}}{\sqrt{\pi}m_{\alpha\beta}}\tfrac{1}{\left(\sigma_\alpha^2+\sigma_\beta^2\right)^{3/2}}. \end{aligned} \tag{3.34}$$

For the case of the Yb mixture the interactions are the same for the species r, g and u, d, resulting in two equations (for $\tilde{\sigma_c}$ and $\tilde{\sigma_f}$):

$$\begin{cases} \frac{1}{\tilde{\sigma}_c^3} - \tilde{V}_c \tilde{\sigma}_c e^{-\tilde{\sigma}_c^2} + \frac{n_c \tilde{a}_{cc}}{\sqrt{2\pi}\tilde{\sigma}_c^4} + \left(1 + \frac{m_c}{m_f}\right) \frac{4 n_f \tilde{a}_{cf} \tilde{\sigma}_c}{\sqrt{\pi}\left(\tilde{\sigma}_c^2 + \tilde{\sigma}_f^2\right)^{5/2}} = 0 \\ \\ \frac{1}{\tilde{\sigma}_f^3} - \tilde{V}_f \tilde{\sigma}_f e^{-\tilde{\sigma}_f^2} + \frac{n_f \tilde{a}_{ff}}{\sqrt{2\pi}\tilde{\sigma}_f^4} + \left(1 + \frac{m_f}{m_c}\right) \frac{4 n_c \tilde{a}_{cf} \tilde{\sigma}_f}{\sqrt{\pi}\left(\tilde{\sigma}_c^2 + \tilde{\sigma}_f^2\right)^{5/2}} = 0. \end{cases} \tag{3.35}$$

The solutions are presented in Figure 3.4 of the main text for the symmetric case $n_c = n_f \equiv n = 1$.

Chapter 4

Long range models from local gauge theories

This Chapter is based on a recent work presented in [17]. The models described up to now, as targets of quantum simulations, are formulated in terms of local fields and interactions. This seems to be a key property of fundamental theories of Nature. Non-local theories, relevant to many physical problems, are expected to provide an effective description, in a certain limit, of a fundamental theory which is in fact local. Examples of this are the Coulomb force between electrons that provide an effective description of Quantum Electrodynamics [197] or the Newton gravity which is an effective description of General Relativity [198], both in a non-relativistic limit. In particular, in this limit, the speed of light is well approximated by infinite and therefore interactions seem to propagate instantaneously. Thanks to advances on control and manipulation of AMO systems kike trapped ions, Rydberg atoms, quantum gases and polar molecules [199–202], implementation of a series of long-range (LR) models was made possible [203–214]. Recent highlights in this directions include the physical realization of Ising and XY quantum spin chains with tunable LR interactions with ions in a Penning trap [203], neutral atoms in a cavity [211, 213, 214], trapped ions [208–210], and Rydberg atoms [204]. Typically, the LR interactions achieved, decay algebraically with the distance r. The precise exponent can be experimentally tuned [208–210]. In fact precisely the possibility of controlling LR interactions was the key feature on the experimental implementation of the Schwinger model [15] (as discussed on Section 2.2.4).

By other side also theoretical development as advanced on the properties of quantum LR systems [215–237]. As examples in [151, 238–244] it was studied the effect of non-local interactions on the dynamics of excitations and on [245–249] the equilibrium properties and phase diagram.

The above mention LR interactions, on the form of power-laws, are typically written as:

$$V(r) \propto \frac{1}{r^{d+\sigma}} \tag{4.1}$$

where r is the distance between the particles or spins, d is the physical space dimension, and σ is the decay exponent. One can distinguish two main regimes:

- $\sigma < 0$: interaction decays slowly with the distance. Internal energy of the system typically diverges in the thermodynamic limit calling for a redefinition of the interaction strength [250].
- $\sigma > 0$: interaction decays quickly with the distance. The system is additive and thermodynamics is well defined.

Furthermore, if σ is large enough, the system turns to be effectively short range (SR). Accordingly a critical value σ^* can be defined such that for $\sigma > \sigma^*$ the critical behavior of the model becomes

the same as its SR counterpart. In the opposite direction, if the interaction remains significant over large distances, the system is well described by mean field. This occurs for $2\sigma \leq d$. In the region bounded by these two regimes, $d/2 < \sigma \leq \sigma^*$, LR interactions are relevant and the determination of the value of σ^* is a subject of continued theoretical research [245–249]. Another way of looking at this is thinking of the variation of σ as a variation on the effective dimensionality. Note that varying σ only affects the interaction term 4.1 while varying the dimensionality affects other parts of the Hamiltonian, namely, the kinetic term. In light of this, at least effectively, there should be for each σ an effective dimensionality d_{eff} that makes the LR system equivalent to a SR living in d_{eff}. Such scenario allows the application of well established results for local many-body systems, such as the Mermin-Wagner-Hohenberg theorem [19, 20] and Lieb-Robinson bounds [21] on the propagation of quantum correlations, to non-local models. This picture is mostly intuitive and it constitutes a challenge to be casted into a rigorous theoretical formalism. One of the main reasons for this is the complexity of such mapping directly at the operator (i.e., Hamiltonian) level.

In this Section a new approach is proposed to the problem. The general framework consists on casting a LR interacting system in d dimensions, through an exact mapping, in a local theory were the initial degrees of freedom remain in "lower" dimension d but are now coupled locally to gauge fields in "higher" dimension $D > d$. The fact that the particles that are interacting initially through a LR interaction remain there, in the local theory, facilitates the mapping while the extra dimensions where the gauge fields live can mediate different types of interactions effectively providing a knob to tune the inter-particle potential. Since the initial theory is fully local in D spatial dimensions, the mapping allows one to exploit the full predictive power of general results for local field theories to the non-local one in D dimensions. Other motivation is the possibility to create tunable interactions with cold atoms, and in particular $1/r$ interactions [251]. Despite the fact that, for trapped ions, interactions of Ising-type can be made to decay algebraically with the distance r with an adjustable exponent (usually in the range $\lesssim 3$), so far no experiments have been performed for a Bose or Fermi gas with an effective $1/r$ interaction also in lower dimension. The extra dimension can provide a path towards new proposals in this direction. Finally, this kind of formalism may be useful in the context of quantum simulations of gauge theories. First, dimensional mismatch models provide an intermediate step between increasingly more difficult gauge theories. For example, it is reasonable to expect that the implementation of $1+1$ fermions coupled to $2+1$ gauge fields will be easier than implementing of full QED in $2+1$ dimensions, but still more challenging than the Schwinger model or pure gauge in $2+1$. Finally the fact that the fermions are in lower dimensionality still allow non-perturbative analytical computations, which can serve as benchmark to experimental implementations, as it will be shown on Chapter 5. Due to the reduced degrees of freedom, also numerical computations will be less expensive when compared to the full gauge theory in higher dimensionality.

In Section 4.2, as an example, the case of $d = 1$ (for fermions/spins in lower dimensionality) is discussed and it is shown how the Coulomb interaction is mapped to the $U(1)$ Abelian gauge theory within the formalism. The approach consists on taking the Lagrangian formalism which will be the preferred paradigm until Section 4.4 where canonical quantization is discussed.

The paper is organized as follows: In Section 4.1 the general formalism is established. This corresponds to the construction of the effective fermionic theory in the lower dimensionality $(d+1)$ and its respective relation with the gauge theory, in the same dimension, with a modified gauge kinetic term. In Section 4.2 the special case $D = 2$ and $d = 1$ is considered, where, in particular, bosonization is used. It is also contemplated the possibility of having several fermionic flavors and gauge fields in such a way that, integrating all of the gauge fields and bosonizing all the fermionic flavors it is possible to construct a general bosonic kinetic term, on the Lagrangian. of the form $\phi f\left(-\partial_\mu^2\right)\phi$. Here ϕ is the bosonic field and f is a function which can be seen as an expansion in half-integer exponents (in powers of α with $2\alpha \in \mathbb{Z}$). When f is the identity function one has the standard kinetic term for a bosonic field. There is freedom on engineering the coefficients of these expansions by modifying the coupling of the initial theory. By following the same process, bosonizing all fermionic flavors but one, it is also possible to construct a similar kind of interaction between fermions $j_\mu V\left(-\partial_\nu^2\right) j_\mu$ again

with V admitting a series expansion on integer and half-integer powers of the Laplacian and j_μ (the fermionic current). In Section 4.3 an overview on how these kind of models can naturally fit in the class of proposals of experimental realization of quantum simulations of gauge theories available on the literature is provided. Section 4.4 deals with canonical quantization and respective construction of Hamiltonians for the models obtained by dimensional reduction. In particular it is illustrated how to obtain non-relativistic fermions interacting via an $1/r$ potential. In Section 4.5 an outlook of the applicability of this formalism and further directions is provided.In Appendices more technical points of the calculations are treated more explicitly.

4.1 Dimensional reduction

The situation where gauge fields are in higher dimension mediating interactions between particles confined in a lower dimensionality is directly related to graphene experiments [252]. In that case the system is two-dimensional, but the electromagnetic field acting on it is not confined to the plane, living instead in three dimensions. Setting the notation, the electrons are confined in a $2D$ (i.e., $2+1$) plane while interacting with the electromagnetic field that lives in the full $3D$ space (i.e., $3+1$). The formalism of Pseudo QED was introduced in [253] and provides a way, keeping the dynamics of the gauge fields, to deal with the problem in hand. The kinetic part of the fermions confined on the plane $(x, y, z = 0)$propagate accordingly with the usual kinetic term of the two-dimensional space. In turn the electromagnetic kinetic term is the usual one for three-dimensional space. The two fields are then coupled through the standard minimal coupling with the additional requirement that no fermionic current exists or flows outside $z = 0$. In standard QED, where fermions visit the full $3 + 1$ space, the 4-current of the fermions has the form $j_4^\mu = \bar{\psi}\gamma_\mu\psi$. These fermions are then coupled to the gauge fields through a term $\sim A_\mu j_4^\mu$. Here, however, this coupling cannot be taken directly. Due to the dimensional mismatch, the components of the current of the $2 + 1$ fermions (j_3^α) runs through $\alpha = 0, \ldots, 2$ while the components of the gauge field take values $\mu = 0, \ldots, 3$. This is overcome by dealing with 4-current j_4^μ and imposing that there are no fermion current nor any flow towards the extra dimension:

$$j_4^\mu(\tau, x, y) = \begin{cases} j_3^\mu(\tau, x, y)\,\delta(z) & \text{if } \mu = 0, 1, 2 \\ 0 & \text{otherwise} \end{cases} \tag{4.2}$$

where $j_3^\alpha = \bar{\psi}\gamma_\alpha\psi$ is the 3-current of the fermions in $2 + 1$ dimensions. By integrating out the gauge field and applying the above condition (4.2) the resulting Lagrangian consists on an effective $2 + 1$ dimensional Lagrangian containing a LR interaction [253–259]. This LR term is fundamentally different from the LR interaction obtained when the fermions are not confined in lower dimensionality $(2 + 1)$ and is at the basis of several peculiar properties of Pseudo QED, such as the dynamical generation of a mass term [256, 258]. The dynamical chiral symmetry breaking in reduced QED theories was studied as well in [260], and the procedure of dimensional reduction was applied to the edge modes of two-dimensional topological insulators [261].

In the following this scenario shall be approached in a general scenario for general $U(1)$ gauge fields live in $D + 1$ dimensions and fermions in $d + 1$ with $D \geq d$. In Figure a schematic representation of the example of $D = 2$ and $d = 1$ is presented. The case $D = d$ is the trivial in the sense that it corresponds to QEDd. It is however useful to keep in mind that the known results for this case should be recovered whenever $D = d$ is taken. The line of thought described above can be inverted and shall be adopted later in the chapter. Instead of determining which long range interaction is obtained from a given gauge field one can:

1. Determine what is the gauge field living in higher dimensions giving rise to a target LR interaction (which can be implemented via the dimensional mismatch)

2. Explore what kind of LR interactions can be realized.

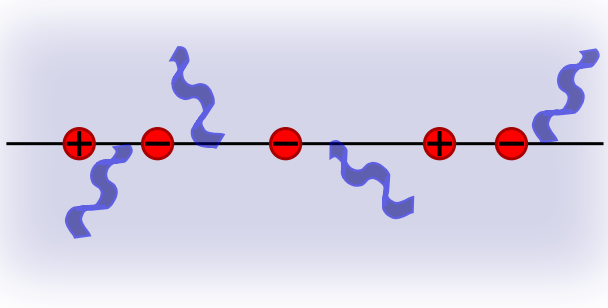

Figure 4.1: Schematic representation of a dimensional mismatch situation where the fermions live in $1+1$ dimensions while the gauge fields in $2+1$. Fermions are confined on the line but photons can explore the full plane.

In light of the previous discussion, the general scenario that one may consider is given by:

- N_f fermionic flavors $\{\psi_a\}_{a=0,\ldots,N_f}$ living in $d+1$ dimensions
- N_g gauge fields $\left\{A_\mu^b\right\}_{b=0,\ldots,N_g}$ each one living in D_b+1 dimensions (where $D_b \geq d, \forall b$)
- Both fields (minimally) coupled through a coupling parameter e_{ab} (generalized electric charge)

The case of $d=1$, $D_b=2, \forall b$ allows a certain degrees of control over both interactions and dispersion relations as it will be discussed in 4.2.

Dimensional reduction: single gauge field Taking the ingredients described above, for a single gauge field, one has a matter Lagrangian living in $d+1$ dimensions $\mathcal{L}_M^{d+1}$, a gauge kinetic term leaving in $D+1$ dimensions $\frac{1}{4}F_{\mu\nu}^2$ and a coupling between the theories $j_{D+1}^\mu A_\mu$ where j_{D+1}^μ will be confined to $d+1$ dimensions. Furthermore a gauge fixing term, $\mathcal{L}_{GF}$. In Euclidean time the fill Lagrangian is given by:

$$\mathcal{L} = \mathcal{L}_M^{d+1} - ie j_{D+1}^\mu A_\mu + \frac{1}{4}F_{\mu\nu}^2 + \mathcal{L}_{GF}. \tag{4.3}$$

The term $\mathcal{L}_{GF}$ will correspond to the Faddeev-Popov Lagrangian [262] given by $\mathcal{L}_{GF} = \frac{1}{2\xi}\left(\partial_\mu A_\mu\right)^2$, where different choices of ξ correspond to different gauges. Here the Feynman gauge where $\xi = 1$, resulting in a propagator $G_{\mu\nu} = \frac{1}{-\partial^2}\delta_{\mu\nu}$. The $D+1$-current should respect the condition:

$$j_{D+1}^\mu\left(x^\alpha\right) = \begin{cases} j_{d+1}^\mu\left(x_0,\ldots,x_d\right)\delta\left(x_{d+1}\right)\ldots\delta\left(x_D\right) & \text{if } \mu = 0,\ldots,d \\ 0 & \text{otherwise} \end{cases} \tag{4.4}$$

In order to formulate the theory exclusively in lower dimensionality $d+1$ one can integrate the gauge fields in the path integral:

$$Z = \int D\bar{\psi}D\psi e^{-\int \mathcal{L}_M^{d+1} d^{d+1}x} \int DA e^{-\int\left[-ie j_{D+1}^\mu A_\mu + \frac{1}{4}F_{\mu\nu}^2 + \mathcal{L}_{GF}\right] d^{D+1}z} \tag{4.5}$$

By completing the square and performing the Gaussian integrals the result will be fermion-fermion current of the form:

$$\mathcal{L}_{int} = \frac{e^2}{2}\int j_D^\mu\left(z\right)\left[\frac{1}{-\partial^2}\right]_{zz'} j_D^\mu\left(z'\right) d^{D+1}z' \tag{4.6}$$

Here ∂^2 is the Laplacian in $D+1$ dimensions and $\left[1/\partial^2\right]_{zz'}$ are the matrix elements at space-time points z, z' of its inverse. This constitutes a long range potential that will be denoted by $G_D\left(z-z'\right)$ exhibiting explicitly the dependence on the dimension where the gauge fields lived [1]. Explicitly it is given by:

$$G_D\left(z-z'\right)=\int\frac{d^{D+1}k}{\left(2\pi\right)^{D+1}}\frac{e^{ik\cdot\left(z-z'\right)}}{k^2} \tag{4.7}$$

The nature of these interactions is encoded in the higher dimension $D+1$ and it is not dependent on the dimensionality where the fermions live, which did not enter yet, as made explicit by the expression above. The resulting interacting part of the Lagrangian is ten written as:

$$\mathcal{L}_{int}=\frac{e^2}{2}\int d^{d+1}x' j_d^{\mu}\left(x\right)G_D\left(z\right)|_{\substack{\left(z_0,\ldots z_d\right)=\left(x_0-x_0',\ldots x_d-x_d'\right)\\ z_{d+1},\cdots z_{D+1}=0}}\ j_d^{\mu}\left(x'\right) \tag{4.8}$$

As an alternative, this term can be written in operator form as well. This consists in taking the Laplacian in $D+1$ dimensions $\partial^2_{(D+1)}=\sum_{\mu=0}^{D+1}\partial_\mu^2$ (before denoted simply by $\partial^2_{(D+1)}$) and integrate out the extra dimensions keeping the Laplacian for the lower dimensions $d+1$, that remain not integrated $\partial^2_{(d+1)}=\sum_{\mu=0}^{d+1}\partial_\mu^2$. Precisely

$$\hat{G}_{D\rightarrow d}\equiv G_{D\rightarrow d}\left(-\partial^2_{(d+1)}\right)=\int\frac{d^{D-d}k}{\left(2\pi\right)^{D-d}}\frac{1}{-\partial_0^2-\ldots-\partial_{d+1}^2+k_1^2+\ldots+k_{D-d}^2}. \tag{4.9}$$

The interacting Lagrangian 4.8 can be equally written as:

$$\mathcal{L}_{int}=\frac{e^2}{2}j_d^{\mu}\hat{G}_{D\rightarrow d}j_d^{\mu} \tag{4.10}$$

The two forms of presenting the non-local term emphasize two different aspects. When writing, as in the first case, the interaction in terms of a space-time function $G_D\left(z\right)$, it is emphasized that the current-current interaction does not depend on the lower dimension and only on the upper dimension where the gauge field propagates. In turn, when writing, as above,e in terms of a modified dispersion relation, the formal structure of the function $G_{D\rightarrow d}\left(X\right)$, which will have as argument the Laplacian, only depends on how many dimensions are integrated out. Of course the two approaches are equivalent. In fact, while the function $G_{D\rightarrow d}\left(X\right)$ only depends on the difference between the dimensions, the operator $\hat{G}_{D\rightarrow d}\equiv G_{D\rightarrow d}\left(-\partial^2_{(d+1)}\right)$, obtained by taking as argument the lower dimensional Laplacian, does not. From now the Laplacian without label is assumed to be the one on lower dimensionality: $\partial^2\equiv\partial^2_{(d+1)}$. The interplay of the two equivalent ways of looking at the theory are equally useful. The later, which is the operator form, becomes useful if one wishes to restore the minimal coupling to a gauge field, now entirely in lower dimensionality. Explicit expressions for both for $G_D\left(z\right)$ and $\hat{G}_{D\rightarrow d}$ are given for the most relevant cases where $D=1,2,3$ and $D-d=0,1,2$ in Appendix 4.C.

The goal now is to transfer the non-local interaction into the the kinetic part of a modified gauge fields living in $d+1$ dimensions. This consists in identifying a theory of the form:

$$\mathcal{L}_d=\mathcal{L}_M^{d+1}-iej_{d+1}^{\mu}A_{\mu}+\frac{1}{4}F_{\mu\nu}\hat{M}_{D\rightarrow d}F_{\mu\nu} \tag{4.11}$$

which will reproduce the interaction term 4.6 (or equivalently 4.8) when integrated as in 4.5. It is worth emphasizing that this Lagrangian is fundamentally different from 4.3. Apart from the gauge

[1] Integrating degrees of freedom and obtaining LR terms (and possible multi-body interactions) is ubiquitous in renormalization group treatments of models, where typically one takes a model and integrate over a sub-class of the original degrees of freedom (see, for example, [263]). The difference with the models considered here is that one performs a dimensional reduction after making the integration of gauge degrees of freedom.

fixing term that shall be discussed next, the key difference is the fact that here both fields, matter and gauge A_μ, are in the same dimensionality, contrary to 4.3. The fact that 4.11 produces effectively the same theory is encoded in the modified kinetic term for the gauge fields $F_{\mu\nu}\hat{M}_{D\to d}F_{\mu\nu}$. The operator $\hat{M}_{D\to d}$ is to be fixed such that this condition is fulfilled. Furthermore, this modified theory is also gauge invariant. For $\mathcal{L}_M^{d+1}$ the Dirac Lagrangian and ψ the fermionic field the gauge transformations are given by $A_\mu \to A_\mu + \frac{1}{e}\partial_\mu\alpha$ and $\psi \to \psi e^{-i\alpha}$. In order to perform the integration of the gauge fields, a gauge fixing must take place. This can be done with the usual gauge fixing term $\mathcal{L}_{GF} = \frac{1}{2\xi}\left(\partial_\mu A_\mu\right)^2$ but it is not the most useful choice. The fundamental reason is that $F_{\mu\nu}\hat{M}_{D\to d}F_{\mu\nu}$ is non-local and such $\mathcal{L}_{GF}$ is purely local. For example, in the Feynman gauge $\xi = 1$, the propagator for the gauge fields becomes diagonal $G_{\mu\nu} = \left[-\partial^2\right]^{-1}\delta_{\mu\nu}$ for usual QED. If a similar diagonal propagator is to be obtained, then $\mathcal{L}_{GF}$ must be non-local as well. For more details see Appendix 4.A. The bottom line is that analogous choice can be made such that the modified propagator is diagonal and takes the form $G_{\mu\nu} = \left[-\partial^2\hat{M}_{D\to d}^{-1}\right]^{-1}\delta_{\mu\nu}$. By comparing with 4.10 it is clear that the relation

$$\hat{M}_{D\to d} = \left(-\partial^2\hat{G}_{D\to d}\right)^{-1} \tag{4.12}$$

should hold establishing the relation between the theory with dimensional mismatch and the gauge theory in lower dimensions. This analysis holds for any $\mathcal{L}_M^{d+1}$ provided that has a linear coupling to the gauge fields as in $j_{d+1}^\mu A_\mu$. This is not the case, for example, for non-relativistic which may involve a other considerations. In a certain limit this analysis is also valid for the non-relativistic case and it shall be discussed in more detail in Section 4.4.

4.2 Exploring dispersion relations from $2 \to 1$ dimensional reduction

In this Section the case to be considered corresponds to a single spatial relation for the lower dimension and two spatial dimensions for the higher dimension. This consists on taking $d = 1$ and $D = 2$. This is the simplest case where dimensional reduction takes place. There are two main reasons to consider this:

- For the fermions in lower dimensionality there is the possibility of using bosonization which considerably simplifies the treatment.
- When dealing with LR interactions the dimensionality is not crucial. At least not as much as in presence of SR interactions since varying the type and the range of the LR interactions one is effectively changing the dimensionality of the system. For example, in the $1D$ LR Ising model, changing σ from 0 to 1 (see Equation 4.1) one is effectively changing the dimensionality from 4 (which is the upper critical dimension of the SR Ising model) to 1. Therefore controlling the LR interactions one is (at least, in the renormalization group sense) controlling the dimensionality of the system. Furthermore, due to the form of the operator $\hat{G}_{2\to1}$ and the possibility of mapping the resulting theory through bosonization (only available when $d = 1$), the class of LR models that can be addressed is larger once extra flavors are introduced and integrate, as will be shown next.

The simplest case is the case of one flavor and a single gauge field. Before moving to the specific case of $2 \to 1$ the treatment is kept general for $D \to 1$. In this The matter Lagrangian kept general in the previous section is taken to be the Thirring Lagrangian (proposed by Thirring [264] see also, for example, [265]). It corresponds to Dirac fermions with a current-current local interaction:

$$\mathcal{L} = -\bar{\psi}\left(\gamma_\mu \partial_\mu + ie\gamma_\mu A_\mu\right)\psi + \frac{g}{2}\left(\bar{\psi}\gamma_\mu\psi\right)^2 + \frac{1}{4}F_{\mu\nu}\hat{M}_{D\to 1}F_{\mu\nu} \tag{4.13}$$

Here the goal is to bosonize the Lagrangian. The massless Thirring model can be mapped to the free boson [266] (see also [14, 265]) so, if the gauge field was absent one finds the bosonized Lagrangian:

$$\mathcal{L}_{\text{bos}} = \frac{1}{2}\left(1 + \frac{g}{\pi}\right)(\partial_\mu\phi)^2 \tag{4.14}$$

Here this Lagrangian will be obtained as a particular case when the matter-gauge coupling, e, is set to zero. By performing an Hubbard-Stratonovich transformation to replace the four fermion coupling by introducing a vector field B_μ, which is taken here to be such that

$$\frac{g}{2}\left(\bar{\psi}\gamma_\mu\psi\right)^2 \to -ieB_\mu\left(\bar{\psi}\gamma_\mu\psi\right) + \frac{e^2}{2g}B_\mu^2 \tag{4.15}$$

When the square is completed on the right hand side one gets: $\frac{e^2}{2g}\left(B_\mu - i\frac{g}{e}\bar{\psi}\gamma_\mu\psi\right)^2 + \frac{g}{2}\left(\bar{\psi}\gamma_\mu\psi\right)^2$ and the integration of B_μ produces just an overall multiplicative factor that can be dropped. The matter-gauge coupling was introduced for convenience. Upon the integration of the gauge field it only enters in this multiplicative constant and therefore there is freedom on choosing this parameter. This specific choice allows the Lagrangian to be written as:

$$\mathcal{L} = -\bar{\psi}\left(\gamma_\mu\partial_\mu + ie\gamma_\mu\left(A_\mu + B_\mu\right)\right)\psi + \frac{e^2}{2g}B_\mu^2 + \frac{1}{4}F_{\mu\nu}\hat{M}_{D\to 1}F_{\mu\nu} \tag{4.16}$$

Given this structure it useful to replace the field B_μ by another field $C_\mu = A_\mu + B_\mu$ condensing the interaction of the fermions with a single field. Then C_μ and A_μ become interacting:

$$\mathcal{L} = -\bar{\psi}\left(\gamma_\mu\partial_\mu + ie\gamma_\mu C_\mu\right)\psi + \frac{e^2}{2g}\left(C_\mu - A_\mu\right)^2 + \frac{1}{4}F_{\mu\nu}\hat{M}_{D\to 1}F_{\mu\nu} \tag{4.17}$$

Because one is working effectivelly in $d = 1$, the fields A_μ,C_μ have only two components which can be parameterized by two scalar fields corresponding to:

$$A_\mu = \partial_\mu\chi - i\varepsilon_{\mu\nu}\partial_\nu\varphi, \quad C_\mu = \partial_\mu\chi' - i\varepsilon_{\mu\nu}\partial_\nu\varphi' \tag{4.18}$$

where $\varepsilon_{\mu\nu}$ is the totally anti-symmetric tensor with $\varepsilon_{01} = 1$. One of the χ fields can be eliminated by a gauge transformation. Within this parameterizations gauge transformations take the form: $\chi \to \chi + \frac{1}{e}\partial_\mu\alpha$, $\chi' \to \chi' + \frac{1}{e}\partial_\mu\alpha$ and $\psi \to \psi e^{-i\alpha}$ and α ca be chosen to eliminate χ'. The Lagrangian takes then the form:

$$\mathcal{L} = -\bar{\psi}\left(\gamma_\mu\partial_\mu + e\gamma_\mu\varepsilon_{\mu\nu}\partial_\nu\varphi'\right)\psi + \frac{e^2}{2g}\left((\partial_\mu\chi)^2 - (\partial_\mu\varphi)^2 - (\partial_\mu\varphi')^2 + 2\partial_\mu\varphi'\partial_\mu\varphi\right) - \frac{1}{2}\left(\partial^2\varphi\right)\hat{M}_{D\to 1}\left(\partial^2\varphi\right) \tag{4.19}$$

The field χ is decoupled from the rest of the fields and, since the final goal it is to integrate the keep only the fermionic degrees of freedom, it can be dropped. The fermions are only coupled to φ'. Upon performing a change of variables corresponding to a chiral transformation $\psi = e^{ie\varphi'\gamma_5}\psi'$ where $\gamma_S = i\gamma_0\gamma_1$ (Euclidean γ matrices), the extra term that comes due to the derivative: $\bar{\psi}'\left(ie\gamma_\mu\partial_\mu\varphi\gamma_S\right)\psi' = -e\varepsilon_{\mu\nu}\bar{\psi}'\gamma_\nu\partial_\mu\varphi\psi'$[2] cancels the coupling to φ'. In this process it should be recalled that the chiral anomaly has to be taken into account. Its origin consists on the fact that the path integral measure, $D\bar{\psi}D\psi$, does not transform trivially under this change of variables. This gives an extra term (see for

[2]It was used that, for Euclidean gamma matrices, $\gamma_\mu\gamma_S = i\varepsilon_{\mu\nu}\gamma_\nu$ which can be seen by direct computation and using $\{\gamma_\mu, \gamma_\nu\} = 0$.

example [265] or [14]) $-\frac{e^2}{2\pi}\left(\partial_\mu\varphi'\right)^2$. With this ψ' appears in the Lagrangian as a free massless Dirac field and can be bosonized and described in terms of a free scalar ϕ'

$$\mathcal{L}_{\text{bos}} = \frac{1}{2}\left(\partial_\mu\phi'\right)^2 - \frac{e^2}{2}\left(\frac{1}{\pi}+\frac{1}{g}\right)\left(\partial_\mu\varphi'\right)^2 - \frac{e^2}{2g}\left(\left(\partial_\mu\varphi\right)^2 - 2\partial_\mu\varphi'\partial_\mu\varphi\right) - \frac{1}{2}\left(\partial^2\varphi\right)\hat{M}_{D\to 1}\left(\partial^2\varphi\right) \quad (4.20)$$

The chiral transformation was useful in order to identify the correct way to bosonize the Lagrangian. Now one can restore the bosonized field ϕ of the initial fermionic field. From bosonization formulas [14] the transformation $\psi' = e^{-ie\varphi'\gamma_s}\psi$ is equivalent to $\phi' = \phi - \frac{e}{\sqrt{\pi}}\varphi'$. Plugging this transformation on $\mathcal{L}_{\text{bos}}$ will give

$$\mathcal{L}_{\text{bos}} = \frac{1}{2}\left(\partial_\mu\phi\right)^2 - \frac{e^2}{2g}\left(\partial_\mu\varphi'\right)^2 - \frac{e}{\sqrt{\pi}}\partial_\mu\varphi'\partial_\mu\phi - \frac{e^2}{2g}\left(\left(\partial_\mu\varphi\right)^2 - 2\partial_\mu\varphi'\partial_\mu\varphi\right) - \frac{1}{2}\left(\partial^2\varphi\right)\hat{M}_{D\to 1}\left(\partial^2\varphi\right) \quad (4.21)$$

and integrating φ' out:

$$\mathcal{L}_{\text{bos}} = \frac{1}{2}\left(1+\frac{g}{\pi}\right)\left(\partial_\mu\phi\right)^2 - \frac{e}{\sqrt{\pi}}\partial_\mu\phi\partial_\mu\varphi - \frac{1}{2}\left(\partial^2\varphi\right)\hat{M}_{D\to 1}\left(\partial^2\varphi\right) \quad (4.22)$$

The fact that this theory is related to a dimensional mismatch theory was completely irrelevant, as the kinetic term of the field φ was just an spectator. Furthermore all the dependence on the parameter g is condensed on the ϑ kinetic term, just like standard bosonization of the Thirring model. A more detailed discussion of this in the context of the Schwinger-Thirring model will be given in Chapter 5. Finally, integrating the remaining φ field leads to:

$$\mathcal{L}_{\text{bos}} = \frac{1}{2}\left(1+\frac{g}{\pi}\right)\left(\partial_\mu\phi\right)^2 + \frac{e}{2\pi}\phi\hat{M}^{-1}_{D\to 1}\phi \quad (4.23)$$

In order to help visualization (mainly when more gauge fields and matter fields are considered) a schematic diagrammatic representation is introduced. In Figure 4.2, different fields of the theory are represented and connected, if they are coupled to each other, by straight lines. Straight lines connecting fermionic flavors (including self coupling) correspond to current-current interaction, lines connecting fermions to vector fields represent the standard minimal coupling and, finally, bosons are connected by as many straight lines as there are derivatives present in their coupling. In the case of the vector fields, as many bars as the original dimension where the field lived originally, are placed on top of the field. This means that if the kinetic term is $F_{\mu\nu}\hat{M}_{D\to 1}F_{\mu\nu}$ there will be D bars on top of the respective vector field. The diagrams do not specify the actual value of the coupling since their main purpose is visualization of the structure of the theory. The initial and final theories (4.13) and (4.22) are plotted in Figure 4.2. In Appendix 4.B the diagrammatic representation is also used to depict the intermediate mappings that allow the passage from the initial to the final theory. This is done systematically for all the theories represented in the main text.

The Lagrangian 4.23 has no interaction terms and corresponds solely to a quadratic Lagrangian with an exhotic kinetic term. In fact, for the familiar case of the Schwinger model, that in this language corresponds to $g = 0$ and $\hat{M}_{1\to 1} = 1$, the gauge fields give rise to a bosonic mass. In the following Section the goal consists in trying to develop more general dispersion relation between bosons since, in the case just described, there is effectivelly only one parameter to play with which determines the relative strength between the usual Laplacian ∂^2 and the extra term $\hat{M}^{-1}_{D\to 1}$.

4.2.1 Controlling the kinetic term of bosonic theories

The Lagrangians 4.13 and 4.22 can be easily generalized to arbitrary number of flavors N_f. This is done by introducing a flavor index $\psi \to \psi_a$, $g \to g_a$ and consequently $\phi \to \phi_a$ where ϕ_a is the bosonic field resulting from bosonizing ψ_a. One can also allow a different matter-gauge coupling for the

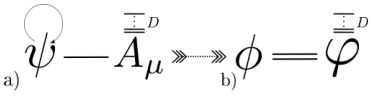

Figure 4.2: Schematic representation of the initial and final theory corresponding to a Pseudo Schwinger-Thirring model with the gauge field living original in $D+1$ dimensions. The initial theory, Equation (4.13), is represented in a) having a self interacting fermion (through a current-current interaction) coupled minimally to a gauge field which originates from an higher dimensional theory (represented by multiple lines on top of A_μ). In b) the resulting theory after bosonization is represented where the fermionic degrees of freedom are encoded on ϕ and the gauge fields in φ.

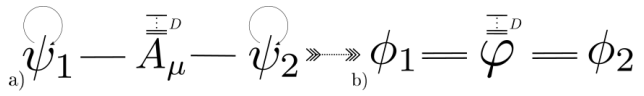

Figure 4.3: Schematic representation of the Pseudo Schwinger-Thirring model with two flavors and the gauge field living originalyl in $D+1$ dimensions. The initial theory, Equation 4.13, is represented in a), while in b) it is represented 4.24, resulting after bosonization.

different flavors $e \to e_a$ and different Thirring couplings $g \to g_a$. The bosonization procedure follows an analogue path: introduce N_f auxiliary fields B^a_μ and define a set of new variables $C^a_\mu = A_\mu + B^a_\mu$. All the rest is analogous to what was described before. Interactions between different flavors are obtained once the gauge field is integrated out:

$$\mathcal{L} = \frac{1}{2}\left(1+\frac{g_a}{\pi}\right)(\partial_\mu\phi_a)^2 + \frac{e_a e_b}{2\pi}\phi_a \hat{M}^{-1}_{D\to 1}\phi_b \tag{4.24}$$

where the sum over flavors is implicit. In Figure 4.3 the case of two flavors is represented diagramatically. The Lagrangian is still quadratic but has couplings between different bosons. These couplings can be used to manipulate the dispersion relation of one (or more) bosonic fields. This is well illustrated by the two flavors case where $a, b = 1, 2$ in 4.23. Integration of ϕ_2 results in:

$$\mathcal{L} = \frac{1}{2}\phi_1\left[\left(1+\frac{g_1}{\pi}\right)(-\partial^2) + \frac{e_1^2}{\pi}\hat{M}^{-1}_{D\to 1} - \frac{e_1^2 e_2^2}{\pi^2}\hat{M}^{-1}_{D\to 1}\frac{1}{\left(1+\frac{g_2}{\pi}\right)(-\partial^2)+\frac{e_2^2}{\pi}\hat{M}^{-1}_{D\to 1}}\hat{M}^{-1}_{2\to 1}\right]\phi_1 \tag{4.25}$$

Now explicit expression for $D = 2$ (therefore $\hat{M}^{-1}_{2\to 1}$) will be used . From Equation 4.9 one can see that $\hat{G}_{2\to 1} = \left[2\sqrt{-\partial^2}\right]^{-1}$ and so $\hat{M}^{-1}_{2\to 1} = \sqrt{-\partial^2}/2$ from Eq. 4.12. For large distances (small momentum) this is the dominant term of the denominator since it is linear on $|k|$. The relevant scales for the validity of this limit can be controlled via g_2 and e_2. Expanding the denominator on a power series one gets

$$\frac{1}{\left(1+\frac{g_2}{\pi}\right)(-\partial^2)+\frac{e_2^2}{\pi}\hat{M}^{-1}_{2\to 1}} = \frac{\pi}{e_2^2}\hat{M}_{2\to 1}\sum_n\left[-\left(1+\frac{g_2}{\pi}\right)\frac{2\pi}{e_2^2}\sqrt{-\partial^2}\right]^n \tag{4.26}$$

By substituting back into the Lagrangian a power series expansion in $\sqrt{-\partial^2}$ is obtained. The result is an infinite sum of integer and half integer powers of the Laplacian:

$$\mathcal{L} = -\frac{1}{2}\phi\left[\sum_{n=1}\sigma_{n/2}\left(-\partial^2\right)^{\frac{n}{2}}\right]\phi, \tag{4.27}$$

where the label of ϕ_1 was dropped. The first terms of these expansion are $\sigma_{1/2} = 0$, $\sigma_1 = 1 + \frac{g_1}{\pi} +$

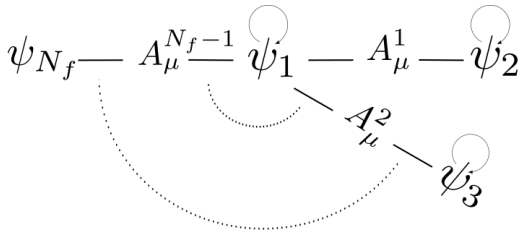

Figure 4.4: Diagrammatic representation of the scheme used with N_f flavors and $N_f - 1$ gauge fields leaving in $2+1$ dimensions. After bosonization and integration of all gauge fields and all but one fermionic field (ψ_1), one can obtain a Lagrangian consisting of an expansion in integers and half integer powers of $-\partial^2$ with some control over the coefficients.

$\frac{e_1^2}{e_2^2}\left(1+\frac{g_2}{\pi}\right)$ and for higher terms

$$\sigma_{n/2} = -\frac{e_1^2}{\pi}\left[-\left(1+\frac{g_2}{\pi}\right)\frac{2\pi}{e_2^2}\right]^n,\ n>1 \tag{4.28}$$

.

There are now a series of infinite coefficients which allow some tunability through four parameters: e_1, e_2, g_1 and g_2. There are two main constrains on controlling this expansion. Evidently the four parameters can control at most four of the infinite number $\sigma_{n/2}$ (note however that if the expansion is controlled likely only a finite number of coefficients need to be controlled). By other side the sign of each $\sigma_{n/2}$ is fixed. For n even the coefficient is even (except for $n=2$) and for n odd it is positive coefficients. There is a direct way to go around the first constraint. The freedom of choice of the absolute value of the coefficients are increased by adding third fermionic flavor ψ_3 with a Thirring interaction and a new gauge field A_μ^2 which is only coupled to flavors 1 and 3. Following the same procedure of bosonization and integration of the degrees of freedom for the third flavor, as was done for the second flavor, one gets a similar expression with new coefficients $\sigma_{n/2}^{\text{new}} \equiv \sigma_{n/2}^{(12)} + \sigma_{n/2}^{(13)}$. In superscript it was denoted between from which kind of interactions the coefficient was obtained. In this way $\sigma_{n/2}^{(12)}$ corresponds to the coefficients determined previously by putting in evidence that it was the result from an interaction between flavors 1 and 2 (mediated by a gauge field). Analogously the new contribution is denoted by the indices (13). The procedure can be followed with an arbitrary number of flavors obtaining an effective coefficient of the form

$$\sigma_{n/2} = \sum_{i=2}^{N_f} \sigma_{n/2}^{(1i)} \tag{4.29}$$

where $\sigma_{n/2}^{(1i)} = -\frac{e_1^2}{\pi}\left[-\left(1+\frac{g_i}{\pi}\right)\frac{2\pi}{e_i^2}\right]^n$ for $n \geq 2$. The coefficient $\sigma_{1/2}$ is always zero. By considering more and more number of flavors obeying this structure, one is able to control the coefficients $\sigma_{n/2}$ to an arbitrary order with some constraints. The general structure of such theories with N_f flavors is illustrated in Figure 4.4.

4.2.2 Controlling interaction term of fermionic theories

The integration of the gauge fields naturally leads to non local interactions in the fermionic action. In order to obtain the half integer powers expansion in 4.27 it was crucial to integrate fermionic degrees of freedom as well overcoming the paradigmatic extra quadratic term of the form $\frac{e^2}{2\pi}\phi\hat{M}_{D\to 1}^{-1}\phi$. In this Section the same principle is applied but since the goal is to deal with fermionic theories, all but one

degrees of freedom are integrated. Therefore all but one fermionic degree of freedom are bosonized. In order to avoid unnecessary complications the Thirring terms are disregarded, but they pose no extra difficulty as it was shown in the previous section. Considering two flavors ψ and ψ' and bosonizing the last one leads to:

$$\mathcal{L} = -\bar{\psi}\gamma_\mu\partial_\mu\psi + ej_\mu\varepsilon_{\mu\nu}\partial_\nu\varphi - \frac{e'}{\sqrt{\pi}}\phi'\left(-\partial^2\right)\varphi + \frac{1}{2}\left(\partial_\mu\phi'\right)^2 - \frac{1}{2}\varphi\left(-\partial^2\right)\hat{M}_{D\to1}\left(-\partial^2\right)\varphi. \tag{4.30}$$

Integrating the degrees of freedom of ψ' (in the form of ϕ') results in:

$$\mathcal{L} = -\bar{\psi}\gamma_\mu\partial_\mu\psi + ej_\mu\varepsilon_{\mu\nu}\partial_\nu\varphi - \frac{e_a^2}{2\pi}\varphi\left(-\partial^2\right)\varphi - \frac{1}{2}\varphi\left(-\partial^2\right)\hat{M}_{2\to1}\left(-\partial^2\right)\varphi. \tag{4.31}$$

The final form of the LR fermionic theory is obtained by integrating out the gauge field. After having bosonized and integrated ψ' it is useful to re-introduce $A_\mu = -i\varepsilon_{\mu\nu}\partial_\nu\varphi$. The resulting effective theory is given by:

$$\mathcal{L} = -\bar{\psi}\gamma_\mu\partial_\mu\psi + \frac{1}{2}e^2 j_\mu \frac{1}{\frac{e'^2}{\pi} + \hat{M}_{2\to1}\left(-\partial^2\right)} j_\mu. \tag{4.32}$$

As for the bosonic case, now an expansion for large distances is taken. The denominator is of the form $1 + \left(2\pi/e'^2\right)\sqrt{-\partial^2}$ so, for large distances, it is no longer the square root that is dominant but the constant term instead. The expansion will take up the form $j_\mu\left(-\partial^2\right)^{\frac{n}{2}} j_\mu$. As previously argued there is a certain freedom of choice on the coefficients of this expansion. This is again achieved by considering more gauge fields, as in Figure 4.4, where Thirring terms can be included or not. The final result has the form:

$$\mathcal{L} = -\bar{\psi}\gamma_\mu\partial_\mu\psi + \frac{1}{2}e^2 j_\mu\left[\sum_{n=1}\lambda_{n/2}\left(-\partial^2\right)^{\frac{n}{2}}\right] j_\mu \tag{4.33}$$

with the coefficients λ given by

$$\lambda_{n/2} = \sum_{i=2}^{N_f}\frac{\pi}{e_i^2}\left(-\frac{2\pi}{e_i^2}\right)^n \tag{4.34}$$

assuming $g_a = 0$ for every flavor (absence of the Thirring term).

4.3 Overview over experimental implementations

In Chapter 2 the simulation of dynamical gauge fields was addressed and they contemplated dimensionalities from 1 to 3. In general, either pure gauge theories are contemplated (no fermions) or they theories where fermions and gauge have matching dimensions. The extension to include a possible mismatch is straightforward. In fact all the relevant terms are already present in Hamiltonian for the existing proposals. All that is needed is to suppress fermion hoppings in the relevant direction(s). A representation of the lattice version constituting the target theory for $d = 1$ and $D = 2$ is provided on Figure

To make the discussion more concrete two examples are taken: one where the energy punishment approach (particularly [139]) and other where microscopic symmetries (particularly [150]) are used to generate the gauge symmetry. Both approaches were discussed in Section 2.2. In this context reducing the dimension that are spanned by the fermions consists on replacing the periodic lattice potential by a confining one in the dimensions to be fixed. Such change poses no threats to the implementation of gauge symmetries.

More in detail, in the first scheme, gauge invariance is achieved by an energy punishment on states that violate gauge symmetry. The relevant terms, arising on perturbation theory, are correlated hoppings of bosons and fermions, corresponding to matter-gauge coupling, and pure bosonic terms,

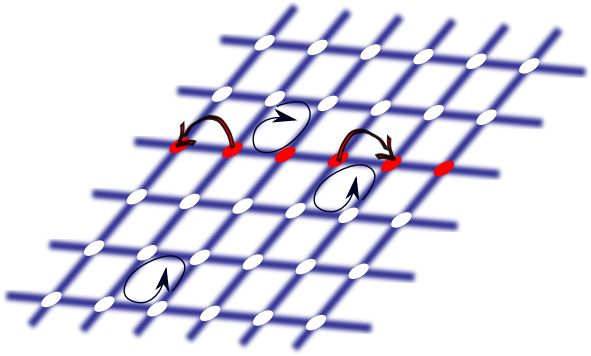

Figure 4.5: Pictorial representation of the target lattice theory for experimental implementation exhibiting dimensional mismatch. The fermions can only hop along the sites of a single line, here represented in red. The links are dynamical across the full plane having, in particular, plaquette terms as well, being coupled with the fermions on the line.

corresponding to the pure gauge contribution for the Hamiltonian. If there are no fermions in a given part of the system no correlated hopping would be obtained but the pure gauge terms would still be present.

In the second case the gauge symmetry arises from internal symmetries of the system (and plaquette terms in perturbation theory of gauge invariant quantities). The principle, however, is exactly the same. Due to conservation of total hyperfine angular momentum only certain scattering processes are selected. Again the absence of fermions will retain only the processes corresponding exactly to the kind of theories explored here. Furthermore, the absence of fermions in certain dimensions, reduces unwanted terms involving fermions on those same dimensions, that even though gauge invariant, are not a target of the implementation (like for example nearest neighbor density-density fermionic interaction). Finally, another technique which is applicable to both schemes is to render fermionic tunneling off-resonant in the transverse directions.

4.4 Long-range effective Hamiltonians

Deriving Hamiltonians from the effective theories described in the previous sections is, in general, highly non-trivial. The reason for this lies on the non-locality in time of the Lagrangian. Due to the presence of arbitrarily high powers of time derivatives, as it is clear from Equations 4.27 and 4.27, the Euler-Lagrange equations are modified. The Hamiltonian formulation of such theories can be achieved within the Ostrogradsky's construction [267], where an extra momentum variable arises from each extra time derivative. The canonical quantization of theories with non-local kinetic terms, like Pseudo QED, was addressed in [268–270].

Here, however, the goal is to perform canonical quantization of fermionic theories having non-locality in the interaction term. It has been shown that, under certain circumstances, and in a perturbative setting, it is possible to use the free equations of motion in order to eliminate the non-locality in time [271, 272]. Specifically, such procedure is possible when the non-local terms are governed by a small coupling parameter. A fundamental observation that allows such perturbative expansion is that there exists a field transformation that is equivalent to the application of the free equations of motion (and consistently disregarding higher orders of the coupling). In practice one can use equations of motion to replace time derivatives by spatial ones. The fact that the non-locality is obtained from the integration of degrees of freedom of a renormalizable theory plays a fundamental role [271]. If a theory is initially well defined, as it is assumed for a given local theory that is taken at the stating point of the

process, the same should be true for the effective theory resulting from integration of certain degrees of freedom. In that case any apparent unphysical effect, like breaking of unitarity, should eventually cancel in the computation of physical observables. In light of this if, in a perturbative setting, there are no unphysical effects at first order due to non-locality, one expects that such unphysical effects will also cancel out at higher orders and perturbative expansion is well defined. Consequently, systematically disregarding the higher powers of the coupling parameter should be consistent and the approximation well defined if the truncated theory is also well defined. This procedure is followed here in first order perturbation theory.

In previous Sections the imaginary (Euclidean) time formulation was suiting emphasizing the connection to statistical mechanics. In this Section, in order to construct a quantum Hamiltonian, real time is adopted.

The discussion will contemplate non-relativistic fermions. The case of Dirac fermions raises different kind of questions not to be addressed here. In particular, for the case of massless Dirac fermions, the free equations of motion imply $\Box\psi = 0$ (being $\Box$ the D'Alembertian $\Box = \eta^{\mu\nu}\partial_\mu\partial_\nu$). By other side the non-local interaction will take the form $\left(\bar{\psi}\gamma_\mu\psi\right)\mathcal{O}\left(\Box\right)\left(\bar{\psi}\gamma_\mu\psi\right)$. By applying the equations of motion, at first order on the coupling, a term of $\mathcal{O}\left(0\right)$ will arise. As it can be seen from 4.6 this may lead to divergences at this order. Therefore, and according to the previous discussion, perturbation theory is not well defined for this case. If gauge and matter have different propagation velocities – a case not considered here – the approach will work but again, at a critical point, the divergence reappears [273]. The inclusion of other fermionic flavors and gauge fields may cure this problem (see Equation 4.32). Here the discussion will be kept for the case of a single fermionic flavor and gauge field. It is then useful to consider non-relativistic fermions where this problem is absent and, furthermore, in the limit of large mass, the infinite sum of temporal derivatives can be truncated. In the following the process is illustrated by computing the Hamiltonian for the lowest order.

The Lagrangian for non-relativistic fermion coupled to a gauge field is then given by:

$$\mathcal{L} = \psi^\dagger\left(i\partial_0 - eA_0 + \frac{\hbar^2}{2m}\left(\partial_i + ieA_i\right)^2 + \mu\right)\psi - \frac{1}{4}F_{\mu\nu}F^{\mu\nu} \tag{4.35}$$

As referred before, non-relativistic fermions do not have exactly the structure contemplated in previous sections. In Equation 4.35 there is an extra interacting term proportional to $e^2A_i^2\psi^\dagger\psi$. This term would give rise to higher order terms on the coupling constant and, since our treatment is perturbative on e, those will be discarded. With this approximation the Lagrangian reduces to the familiar form considered before (Equation 4.3). The current is given by $j_0 = \psi^\dagger\psi$ and $j_i = i\frac{\hbar^2}{2m}\partial_i\psi^\dagger\psi$. The procedure of variable substitution can be done by considering the current-current interaction in position space:

$$\mathcal{L}_{int} \propto j^\mu\left(t,x\right)\mathcal{O}\left(t-t',x-x'\right)j_\mu\left(t',x'\right).$$

A Taylor series expansion is performed on the second current in order to write those current terms evaluated at the time t (and not t'):

$$j_\mu\left(t',x'\right) = \sum_{n=0}^{\infty}\frac{\left(t'-t\right)^n}{n!}\partial_0^n j_\mu\left(t,x'\right).$$

Now the equations of motion can be employed to replace time derivatives. In particular from $\left(i\partial_0 + \left(\hbar^2/2m\right)\partial_1^2 - \mu\right)\psi = 0$ one can make the replacement (up to e^2 order):

$$\partial_0^n j_0 \to \sum_{l=0}^{n}\left(\begin{array}{c} n \\ l \end{array}\right)\left(-i\frac{\hbar^2}{2m}\nabla^2 + i\mu\right)^l\psi^\dagger\left(i\frac{\hbar^2}{2m}\nabla^2 - i\mu\right)^{2n-l}\psi \tag{4.36}$$

with analogous expressions for the other components of the current j_μ. With this substitution the interaction becomes local in time and non-local on space coupling fields at x and x' by the function:

$$\int dt'\mathcal{O}\left(t-t',x-x'\right)\left(t-t'\right)^n \tag{4.37}$$

In other words the theory becomes local in time at the cost of having (generally complicated and non-local) spatial interactions. It is observed that, in general, since $\mathcal{O}(t,x)$ is an even function on time, the terms with n odd will give zero. Now this will be specialized for the particular case of $D=3$. In this notation $\mathcal{O}(t-t',x-x')$ are the matrix elements of the operator $G_{3\to 1}\left(-\partial^2\right)$, in its real time form, presented in Appendix 4.C. Furthermore, for illustrative purposes, the Hamiltonian density is computed for zero chemical potential and large mass limit. Each power of the Laplacian ∇^2 in 4.36 will give rise to a prefactor $\left(\hbar^2/2m\right)$ and therefore, at lowest order in the large mass limit, all terms but $n=0$ can be disregarded. Furthermore, as j_i is proportional to $\left(\hbar^2/2m\right)$, also these terms are of higher order so they are dropped. The only interaction left is:

$$\mathcal{L}_{int}=-\frac{e^2}{2}j_0(t,x)\left[\int dt'\mathcal{O}(t-t',x-x')\right]j_0(t,x') \tag{4.38}$$

For the case of gauge fields in 3 dimensions the effective interaction $\int dt'\mathcal{O}(t-t',x-x')$ is:

$$\begin{aligned}&-\frac{e^2}{8\pi}\int\frac{d^2q}{(2\pi)^2}dt'\log\left(1+\frac{\Lambda^2}{q_1^2-q_0^2}\right)e^{-i\left(t-t'\right)q_0+\left(x-x'\right)q_1}\\&=-\frac{e^2}{8\pi\left|x-x'\right|}\left(1-e^{-\left|x-x'\right|\Lambda}\right)\end{aligned} \tag{4.39}$$

In the limit of large cut-off Λ the effective Lagrangian becomes:

$$\mathcal{L}=\psi^\dagger(t,x)\left(i\partial_0+\frac{\hbar^2}{2m}\partial_1^2\right)\psi(t,x)-\frac{e^2}{8\pi}\int dx'\psi^\dagger(t,x)\psi(t,x)\frac{1}{\left|x-x'\right|}\psi^\dagger(t,x')\psi(t,x') \tag{4.40}$$

This generates an effective Hamiltonian of fermions interacting with a repulsive $1/x$ potential which is the Coulomb potential expected on this limit. Namely the limit of large massive non-relativistic fermions weakly coupled to a three-dimensional gauge field is given by:

$$H=\int dx\left[-\frac{\hbar^2}{2m}\psi^\dagger(t,x)\partial_1^2\psi(t,x)+\frac{e^2}{8\pi}\int dx'\psi^\dagger(t,x)\psi(t,x)\frac{1}{\left|x-x'\right|}\psi^\dagger(t,x')\psi(t,x')\right] \tag{4.41}$$

The inclusion of the next leading order on the mass will give rise to two new kind of terms: one given by the other current component $j_1(t,x)\,j_1(t,x')/\left|x-x'\right|$ and the other being a density-density interaction coming from Equation 4.37 with $n=2$. The later will scale as the inverse square of the cut-off and therefore, in the large cut-off limit, it can be dropped.The other term coming from j_1 interactions can be interpreted, in lattice language, as a correlated hopping between two fermions at a distance $|x-x'|$ and corresponds to a magnetic term. This also allows a better understanding of the initial approximation: for large masses the particles are slow enough that in lowest order the interaction is simply a density-density interaction.

4.5 Outlook

The models with dimensional mismatch have four more straightforward applications:

1. Direct application to physical systems where the dimensional mismatch is a fundamental property (like, for example, graphene).

2. Exploration of results of local theories on non-local models: on providing a consistent map between local and non-local theories an interplay between them may serve the application of both theoretical results (providing immediate access to insights on the dynamics of the latter) and numerical techniques.

3. Realization of LR interacting models: in certain settings, like in cold atomic systems, local interactions are readily available but LR interactions not. The extra dimension allows extra freedom on obtaining LR interactions from local terms. Furthermore it is possible as well, in theory, to go beyond the tunable power law exponent achieved in other settings like trapped ions.

4. Providing intermediate step towards quantum simulations of gauge theories: exclusion of fermions from an higher dimension naturally allows simpler implementations than the case of fermions exploiting all dimensionality but an harder target than the pure gauge system. This is true both at a theoretical and an experimental level.

The point one has been explored in the literature [256, 257, 259, 261]. Regarding the second and third point, it was possible to obtain an expansion on half integer powers of the Laplacian $-\partial^2$ (both on bosonic quadratic terms and fermionic interactions) by suitably introducing several fermionic flavors and gauge fields. The coefficients of these expansions display some freedom of choice by changing the parameters of the initial local theory. They are, however, still bounded by certain conditions. An interesting question is what kind of non-locality can be obtained by a local theory as the ones considered here. In fact, completely general expansions on the Laplacian are likely non achievable from this mechanism, since it is expected that they would break break unitarity. In fact it was showed in [254] that the only unitary theories with the pure gauge term modified to be $\sim F_{\mu\nu}\frac{1}{-(\partial^2)^\alpha}F_{\mu\nu}$ in $2+1$ dimensions are for $\alpha = 0$ and $\alpha = 1/2$. By choosing a different α one could obtain a different expansion from 4.33, but this would violate unitary while 4.33 does not. It would be of particular interest to investigate if the conditions obtained on the coefficients σ are a consequence of the mechanism considered (i.e., a local theory in $d+1$ dimensions with minimal coupling between matter and gauge fields) and/or if they constitute a physical condition provided by unitarity.

Regarding particularly the second point, these results can be applicable to a series of long-range interacting problems, where a mapping to a local higher dimensional field theory would allow the application of generic results for local field theories. This includes the characterization of topological order (for example towards the extension of the 10-fold classification to LR hopping free fermion theories [227]), the spreading of quantum information, and the study of localization mechanisms in the presence of LR hopping in one-dimensional systems [274]. From a different perspective, this approach can potentially be applicable to fracton models, as the latter, in some specific cases, can be understood as physical systems where gauge and matter degrees of freedom effectively live in different dimensionality [275].

For the third point, this procedure showed a way of implementing directly a $1/r$ potential on one dimensional fermions (and also other interactions by changing the dimensionality of the gauge fields). While such hypothetical implementation would be very complicated from the experimental point of view (as discussed in previous sections, the implementation of dynamical gauge fields in 3 dimensions is highly non-trivial) the approach discussed suggests that gauge invariance does not play a fundamental role. In fact, after the gauge was fixed the kinetic term of the gauge field has some resemblance with the kinetic term of the scalar boson. The fundamental role seems to be played by the Laplacian in $D+1$ dimensions: $\partial^2_{(D+1)}$. It is tempting then to replace the gauge field by a simple scalar (still in higher dimensions) with a kinetic term $(\partial_\mu\phi)^2/2$ and coupled to the fermions by $j_\mu\phi$. Such coupling is manifestly not Lorentz invariant however that is something that is not important if the goal is to implement the theory in a cold atomic system, for example. In order to understand the consequences of such theory and an hypothetical experimental implementation further investigation is necessary. It seems however a much more realizable theory from the experimental point of view. Above all, no gauge invariance need to be implemented. Within this philosophy, other type of interactions beyond $1/r$ and density-density s may be equally achievable from this method in the near future.

Finally, regarding the fourth point, in general existing proposals admit a straightforward generalization for the realization of artificial gauge theories with dimensional mismatch. Not only that is the case bu they also suppress unwanted terms competing with other desired ones like plaquette interactions.

Beyond the apparent simpler theoretical formulation and experimental implementation of dynamical gauge fields interacting with matter, it provides an interesting toy model to benchmark numerical and (future) experimental results. As it will be shown in the next Chapter the extension of the gauge fields, of the Schwinger model, to higher dimensions still retains some of the simplicity characterized by one dimensional fermions. As a consequence analytical non-perturbative calculations can also be performed providing a comparison platform in a setting more complicated than the Schwinger model where, in particular, the gauge fields do not even have true dynamics.

This procedure can be further generalized by considering additional couplings to Higgs fields, interaction between gauge fields or other gauge symmetries besides $U(1)$. The integration of bosonic or general gauge fields may also enlarge the space of LR models obtained after the dimensional reduction. Finally, it would be interesting to investigate if one can obtain fermionic interaction expansions like 4.33 in higher dimensions.

Appendix Chapter 4

4.A Non-local gauge fixing

The Faddeev-Popov method [262] (see also [10]) isolates the spurious degrees of freedom by introducing in the path integral

$$1 = \int D\alpha \delta \left(G \left(A^{\alpha} \right) \right) \frac{\delta G \left(A^{\alpha} \right)}{\delta \alpha} \tag{4.42}$$

where $A^{\alpha} = A_{\mu} + \frac{1}{e}\partial_{\mu}\alpha$ for the interest case discussed in the main text of $U(1)$ gauge fields. The gauge fixing that was used in the first integration of the model, having dimensional mismatch (see 4.3), corresponds to take $G\left(A^{\alpha}\right) = \partial_{\mu}A_{\mu} - \omega$ and proceed with an integration over ω weighted by $e^{-\omega^2/2\xi}$. Different choices of ξ contemplate different gauge choices. The convenience of the Feynman gauge, $\xi = 1$, lies in the fact that the off-diagonal terms of the propagator cancel.

When a theory with the modified kinetic term with $\hat{M} \neq 1$ (see Equation 4.11), the cancellation of the off-diagonal terms require a gauge fixing depending on $\hat{M}$. By formally choosing $G\left(A^{\alpha}\right) = \left(M^{-1}\right)^{1/2}\partial_{\mu}A_{\mu} - \omega$ and integrating over ω with the Gaussian weighting function the gauge quadratic term becomes:

$$\frac{1}{2}A_{\mu}\left(-\partial^2\delta_{\mu\nu} + \left(1 - \frac{1}{\xi}\right)\partial_{\mu}\partial_{\nu}\right)A_{\nu} \tag{4.43}$$

from which the propagator can be derived:

$$G_{\mu\nu} = \left[\frac{1}{-\partial^2}\delta_{\mu\nu} + \left(1 - \frac{1}{\xi}\right)\frac{\partial^{\mu}\partial^{\nu}}{\left(-\partial^2\right)^2}\right]\hat{M}^{-1}_{D\to d} \tag{4.44}$$

Alternatively one can consider the same gauge fixing function as before, $G\left(A^{\alpha}\right) = \partial_{\mu}A_{\mu} - \omega$, changing the weighting factor to $e^{-\omega\hat{M}^{-1}\omega/2\xi}$. Both of the approaches are related by a simple variable transformation. In the main text the choice $\xi = 1$ is consistently taken.

4.B General procedure and diagrammatics

In this Appendix the general bosonization procedure used on these theories, with $d = 1$ and $D = 2$, accompanied by diagrammatic illustrations is presented. Even though the diagrams do not replace the calculations they become useful to understand the structure of the procedure. The general strategy consists on four steps:

1. Eliminate quartic fermion interaction terms by an Hubbard-Stratonovich transformation. The adopted notation, here is B^{ab}_{μ} for the fictitious field or B^{a}_{μ} in the case $a = b$. The cases $a \neq b$ contemplates possible current-current interactions between different fermionic flavors. It is worth noting that for that case, having coupling between different flavors, a decoupling can be achieved by replacing the fermionic interacting term between flavors a and b as follows:

$g_{ab} j^a_\mu j^b_\mu \to -ieB^{ab}_\mu \left(j^a_\mu + j^b_\mu\right) + \frac{e^2}{2g_{ab}} \left(B^{ab}_\mu\right)^2$. The scale e can be chosen arbitrarily according to convenience as discussed in the main text. The integration of B^{ab}_μ generates not only the correct coupling between different flavors but also self flavor couplings. For this reason it is necessary, in general, to introduce another field B^a_μ in order to compensate this, even when self flavor coupling is absent in the original fermionic Lagrangian.

Diagrammatically: Eliminate any line connecting fermionic flavors (possibly self coupled) and substitute by a vector field connecting the two flavors a and b. In case of self coupling there is only a line connecting the vector field to the fermion.

2. This point is divided in 3 main parts:

   (a) Take the vector fields and parameterize them by two bosonic fields: $A^{\bar{a}}_\mu = \partial_\mu \chi_{\bar{a}} - i\varepsilon_{\mu\nu}\partial_\nu \varphi_{\bar{a}}$ and $B^{ab}_\mu = \partial_\mu \chi'_{ab} - i\varepsilon_{\mu\nu}\partial_\nu \varphi'_{ab}$. Note that the indices without bars run through the different flavors and with bars through the gauge fields: $a, b \in \{1, ..., N_f\}$ and $\bar{a} \in \{1, ..., N_g\}$.

   (b) Do a chiral transformation eliminating the remaining couplings between fermions and bosons. This is given by $\psi_a = e^{-i\sum_{\bar{b}} e_{a\bar{b}}(\chi_{\bar{b}} + \gamma_S \varphi_{\bar{b}}) - ie\sum_b (\chi_{ab} + \gamma_S \varphi_{ab})} \psi'_a$[3]. Here $\gamma_s = i\gamma_0\gamma_1$. Due to the chiral anomaly the Lagrangian acquires some extra terms in the form of $\mathcal{L} \to \mathcal{L} - \frac{1}{2\pi}\sum_a \left(\sum_{\bar{b}} e_{a\bar{b}}\partial_\mu \varphi_{\bar{b}} + \sum_b e\partial_\mu \varphi_{ab}\right)^2$.

   (c) Map the free fermionic theory to the free boson theory $\psi'_a \to \phi'_a$. Then the bosonic field is transformed back in order to correspond to the bosonized field of ψ: $\phi'_a = \phi_a - \frac{1}{\sqrt{\pi}}\sum_a \left(\sum_{\bar{b}} e_{a\bar{b}}\partial_\mu \varphi_{\bar{b}} + \sum_b e\partial_\mu \varphi_{ab}\right)^2$. This transformation cancels the term originated by the chiral anomaly. It also creates a coupling between the bosonic fields ϕ_a and the degrees of freedom associated with the vector fields. As in the case of Section 4.2.2 one can retain, without bosonizing, the desired fermionic flavors.

   Diagrammatically: Replace fermionic variables ψ_a by bosonic flavors ϕ_a, and the vector field variables by a respective bosonic field. All coupling lines become double, signaling that all interactions have the form $\partial_\mu \phi \partial_\mu \varphi$.D

3. Integrate the desired fields.

   Diagrammatically: Each bosonic variable has the standard kinetic term, with exception to the one with bars on top (that originates from the original gauge field in higher dimensions). When one field is integrated out it is erased from the diagram and it establishes couplings between fields that where connected to it in the previous diagram. Furthermore, it changes the kinetic term of all the fields that were linked to it. Care is needed at this point since if the integrated field is one that originates from a fictitious vector field, it just renormalizes the original kinetic term. For example in Equation 4.22 the integration of the fictitious field just renormalized the pre-factor of the kinetic term $1 \to 1 + g/\pi$.

This process is illustrated for the two specific cases used in the calculations of the main text. An extra explicative example is considered contemplating a current-current coupling between fermions. This serves to illustrate how the diagrams can be used to quickly get the structure of the theory without performing any calculation.

[3]To be more precise the transformations generated proportional to γ_S in the exponent are chiral transformations while the phases (proportional to the identity) are gauge transformations.

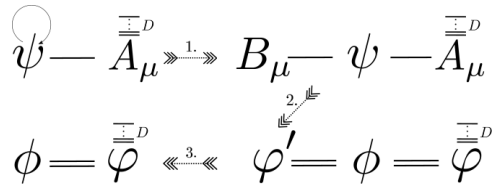

Figure 4.6: Schematic integration of fields from 4.13 to 4.22 (see as well Figure 4.2).

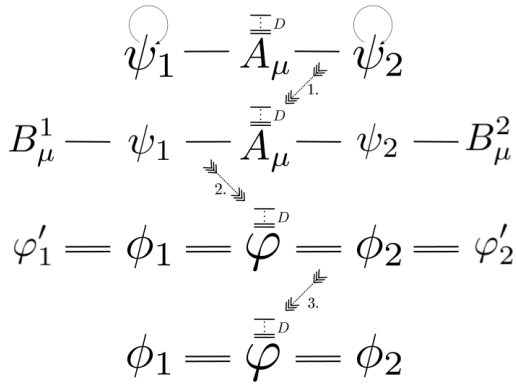

Figure 4.7: Schematic integration of fields in the presence of a gauge field originating from $2+1$ dimensions interacting with two fermionic flavors.

4.B.1 One flavor, gauge field originating from $2+1$

This process is plotted in Figure 4.6. The numbers on top of the arrows indicate the steps described above. In the final diagram, where there is only ϕ and φ, one can read immediately that the theory has the structure:

$$\mathcal{L} = \frac{\lambda_1}{2}\left(\partial_\mu \phi\right)^2 + \lambda_2 \partial_\mu \phi \partial_\mu \varphi - \frac{1}{2}\partial^2 \varphi \hat{M}_{D\to 1} \partial^2 \varphi. \tag{4.45}$$

The actual values of λ_1 and λ_2 are not obtained from the diagrams and one has to do the actual computation obtaining, as in Section 4.2, $\lambda_1 = 1 + g/\pi$ and $\lambda_2 = -e/\sqrt{\pi}$, which is Equation 4.22 of the main text.

4.B.2 Two flavors, gauge field originating from $2+1$

In Figure 4.7 the detailed process of integration of Figure 4.3 concerning Section 4.2.1 of the main text is presented.

4.B.3 Two flavors, coupled to each other, gauge field originating from $2+1$

The diagrammatic process of considering an initial current-current coupling between the fermions is presented in Figure 4.8.

The resulting theory will have the form:

$$\mathcal{L} = \frac{\lambda_1}{2}\left(\partial_\mu \phi_1\right)^2 + \frac{\lambda_2}{2}\left(\partial_\mu \phi_2\right)^2 - \frac{1}{2}\partial^2 \varphi \hat{M}_{D\to 1} \partial^2 \varphi + \lambda_{12} \partial_\mu \phi_1 \partial_\mu \phi_2 + \lambda_1^\varphi \partial_\mu \phi_1 \partial_\mu \varphi + \lambda_2^\varphi \partial_\mu \phi_2 \partial_\mu \varphi. \tag{4.46}$$

This new interaction, concerning the inclusion of a current-current interaction between different fermionic flavors, will not change the general expansions 4.27 or 4.33, but instead will give an extra freedom on choosing the coefficients.

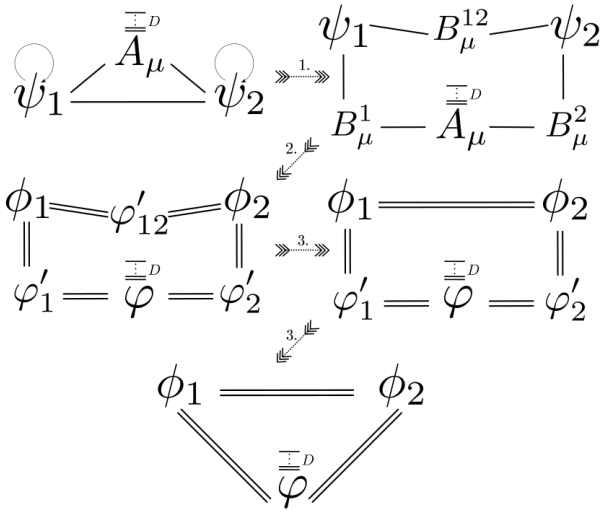

Figure 4.8: Schematic integration of fields in the presence of a gauge field originating from $2+1$ dimensions interacting with two fermionic flavors which are self coupled and coupled to each other.

4.C Non-local quantities for D ranging from 1 to 3

The explicit computation for the function 4.7 can be made explicitly for the most relevant cases ($D = 1, 2, 3$). Changing to hyperspherical coordinates, the integrals can be reduced to:

$$G_D(z) = \frac{\vartheta_{D+1}}{(2\pi)^{D+1}} \int_0^{+\infty} dk \int_0^{\alpha_D} d\theta \sin(\theta)^{D-1} k^{D-2} e^{ik|z|\cos\theta} \tag{4.47}$$

where $\alpha_D = \pi$ for $D = 2, 3$ and $\alpha_1 = 2\pi$ for $D = 1$. For the case of $D = 1$ an IR cut-off q_0 is introduced. The results specialized for each case are given by:

- $D = 1$:
$$G_1(z) = -\frac{1}{2\pi}\left(\gamma + \frac{1}{2}\log(q_0|z|)\right)$$
(γ is the Euler's constant and q_0 the IR cut-off);
- $D = 2$:
$$G_2(z) = \frac{1}{4\pi|z|};$$
- $D = 3$:
$$G_3(z) = \frac{1}{4\pi|z|^2}.$$

Analogously one can compute the functional form of the various operators originated from dimensional integration 4.9. As explained on the main text, the functional form only depends on the dimensionality difference $D-d$ while the Laplacian should be the one of the lower dimensionality $d+1$. Here the cases of $D-d=2$ (having in mind $D=3$ and $d=1$) and $D-d=1$ (corresponding to $D=2$ and $d=1$ or $D=3$ and $d=2$) are computed. For comparison the trivial case $D-d=0$ is also presented. The case of $D-d=1$ corresponds to Pseudo QED which is already reported in literature [253]. For $D-d=2$ the integral is divergent and an UV cut-off Λ is introduced. This cut-off is with respect to the extra dimensions that are being integrated out. In this way this system can be considered, physically, as a continuous system in $d+1$ dimensions with a finite lattice spacing in the remaining two:

- $D - d = 2$:
$$G_{D\to d}\left(-\partial^2\right) = \frac{1}{4\pi}\log\left(\frac{\Lambda^2 - \partial^2}{-\partial^2}\right)$$
(where Λ is the UV cut-off);
- $D - d = 1$:
$$G_{D\to d}\left(-\partial^2\right) = \frac{1}{2}\frac{1}{\sqrt{-\partial^2}};$$
- $D = d$:
$$G_{D\to d}\left(-\partial^2\right) = \frac{1}{-\partial^2}$$
(trivial case where no extra dimensions are integrated). D

Chapter 5

Robustness of confinement for $1+1$ fermions

The case of $d = 1$, which played an important role in the previous Chapter, gives a certain structure that allows more detailed investigation of properties of these models, like confinement [18]. The study of confinement properties in gauge theories is a long-lasting subject of research, with applications in a variety of physical systems ranging from effective gauge theories emerging in strongly correlated systems [276] to Quantum Chromodynamics (QCD) [277]. In the later only bound states of colorless composite quarks are observed (being it mesons: quart anti-quark pair or baryons: three quark bound states). Historically, an important role in the understanding of confinement was played by solvable theories in $1+1$ dimensions, and a paradigmatic example was provided by the Schwinger model [13]. As discussed before, it corresponds to QED in $1+1$ dimensions and it is a well studied field theory [14,265], where relativistic fermions are coupled to a $U(1)$ gauge field. Exhibiting confinement of fermions, chiral symmetry breaking and a topological theta vacuum [107], it can be seen as a toy model for QCD [14].

The Schwinger model and its multi-flavor generalization can be mapped, by bosonization [278], to massive sine-Gordon models. The mass of the sine-Gordon model is proportional to the fermion charge, but the frequency β fixed to $\sqrt{4\pi}$ [279, 280] (and [281] and references therein). The case of massless Schwinger model, which are mapped to massive bosons, was just a particular case of the previous section. On the other side, if the charge is vanishes and an interaction term between fermions is introduced, then the result is a massless sine-Gordon model with variable frequency [266]. This is the Thirring model [264]: in the massless limit its correlation functions are known [282, 283]. In the massive case it is solvable by Bethe ansatz [284].

The purpose of this Chapter is to explore the confinement properties of $1+1$ Dirac fermions in the presence of a $U(1)$ gauge symmetry. More concretely one aims to investigate the robustness of the this phase and the role played by the dimensionality of the fermions. First the problem is addressed regarding interactions, namely, Thirring interactions. This question becomes particularly relevant in the context of quantum simulations of gauge theories. In the naive continuum limit of the staggered lattice formulation of the Schwinger model, the Thirring term can be represented as a nearest neighbor density-density interaction. First, such terms may not be completely suppressed in the implementation of the model. Furthermore they are directly obtained as a by product of existing proposals [139] as it was discussed in Section 2.2.1. In this context, the robustness of the phase under such perturbations become relevant. There is a further interesting ingredient, the so-called topological θ-term, that can be added to the model. This corresponds to the introduction of a background electrical field that was mentioned and set to zero on Section 2.2.4. For this case it is known that deconfinement is possible for $\theta = \pm\pi$, while the system retains the confining character for any other angle in between [280]. This raises the question of the influence of the Thirring term for non-zero background fields and the

robustness of these phases in particular. In order to properly address the role of the dimensionality of the fermions on confinement, the cases where the gauge fields are defined in $D = 2, 3$ dimensions are studied as well. This question is especially relevant since the confinement property of the Schwinger model could be intuitively explained by the fact that, classically, the energy between two point particles grows linearly with the distance (for a gauge field in $1 + 1$ dimensions). When naively applied, this argument would lead to conclude that there should deconfinement when the gauge fields are not subjected to stay in one dimension. This is directly put into test by placing the the gauge fields in higher dimensions ($2+1$ and $3+1$) while the fermions remain in $1+1$. Such question can be addressed with the formalism of Pseudo-QED, and similar models, that were addressed in the previous Chapter.

An usual way to whether there is confinement or not is to compute the string tension σ between two charges. This quantity is defined as follows. Let T be the energy associated with the introduction of two external charges on the system at a distance L. By external charges it is meant that they have no dynamic and are fixed on their given position. In general this energy reads, for large distances:

$$T = \sigma L + \dots \tag{5.1}$$

where the dots indicate subleading terms. The coefficient σ, determining the factor of proportionality between energy and distance of external particles, is the string tension. When $\sigma > 0$ the system exhibits confinement. When $\sigma < 0$ there is a deconfined phase. When σ goes to zero and $|T|$ is not diverging (which is possible, for example, through a logarithm) the ratio will $\mathrm{T}_{with}/T_{\mathrm{without}}$ will be considered. By T_{with} (T_{without}) it is considered the energy with (without) the presence of fermionic fields. In other words, T_{without} is computed in the pure gauge scenario. If this ratio is vanishing, there is a screened phase. In the other cases one cannot conclude about confinement, deconfinement or screening just by looking at the energy T and should look at the behavior (and poles) of correlation functions [265].

This way of characterizing confinement properties covers the cases that are going to be considered in this Chapter. It is well known that the massless Schwinger model is in the screened phase, while the massive is in the confined one [14]. It will be shown that, for massless fermions, the screening phase survives when the four-point local interaction term is turned on (Schwinger-Thirring model). The confined phase remains present as well when a small mass is introduced. In both cases (massless and massive) the string tension does not depend on the Thirring interaction coefficient g, provided that $g > -\pi$ and the same propagates when considering a non-zero θ-term. When the gauge fields are allowed to live in higher dimensions ($2 + 1$ or $3 + 1$), giving rise to the Pseudo-Schwinger-Thirring model, the massless (massive) model remains screened/confined. In particular, it will be shown that, in leading order on the mass, the string tension for gauge fields in $1 + 1$ and $2 + 1$ dimensions is the same.

This Chapter is mainly divided into two main parts: in the first Section 5.1 the confinement properties of the Schwinger-Thirring model is addressed while in Section 5.2 the case of dimensional mismatch is analyzed.

5.1 Schwinger-Thirring model on the lattice and the continuum

This Section starts by analyzing how, in the naive continuum limit, the nearest neighbor density-density interaction scales to the Thirring term. The Kogut-Susskind Hamiltonian in one dimension, corresponding to Equation 1.98, with such interaction term takes the form:

$$H = -\frac{i}{2a}\sum_n \left(c_n^\dagger e^{i\theta_n} c_{n+1} - \text{h.c.}\right) + m\sum_n (-1)^n c_n^\dagger c_n + \frac{ae^2}{2}\sum_n (L_n - L_0)^2 + \frac{g}{a}\sum_n n_x n_{x+1} \tag{5.2}$$

where the background field was inserted explicitly through L_0 and it is related to θ by $L_0 = \theta/2\pi$. The prefactor of the last term can be seen by taking the naive continuum limit. Terms of the form $\psi\partial\psi$ in the extra interaction are of higher order on a and do not appear in the continuum limit.

5.1.1 Robustness under Thirring interactions

As announced, the problem of confinement in this generalized model can be addressed through bosonization. The general procedure adopted here follows closely [285] and can also be seen as a particular case of Chapter 4 with an extra ingredient corresponding to the θ-term. The continuum Lagrangian in Euclidean time is given by [14]:

$$\mathcal{L} = -\bar{\psi}\left(\not{\partial} + ie\not{A} + m\right)\psi + \frac{g}{2}\left(\bar{\psi}\gamma_\mu\psi\right)^2 + \frac{1}{4}F_{\mu\nu}^2 + i\frac{e\theta}{4\pi}\varepsilon_{\mu\nu}F^{\mu\nu} \tag{5.3}$$

As mentioned above, when $g = 0$ this model is known to exhibit (partial) deconfinement for $\theta = \pm\pi$. In turn when $e = 0$ the resulting theory corresponds to the Thirring model which can be mapped perturbatively to a Sine-Gordon model. Such theory makes sense only for $g > -\pi$. In the following it is shown that both statements remain valid when both parameters are finite. In particular the Thirring term does not play any role on confined/deconfined phases of the model.

The quartic fermionic interaction can be recasted in a fictitious field through an Hubbard-Stratonovich transformation as in Chapter 4. This amounts to make the replacement in the Lagrangian $\frac{g}{2}\left(\bar{\psi}\gamma_\mu\psi\right)^2 \to -ieB_\mu J_\mu + \frac{e^2}{2g}B_\mu^2$. A similar redefinition of the vector fields takes place as well where, through a change of variable, A_μ is replaced by $C_\mu = A_\mu + B_\mu$[1]. This results in a Lagrangian of the form:

$$\mathcal{L} = -\bar{\psi}\left(\not{\partial} + ie\not{C} + m\right)\psi + \frac{1}{4}F_{\mu\nu}^{(c)2} + \frac{1}{4}F_{\mu\nu}^{(b)2} - \frac{1}{2}F_{\mu\nu}^{(b)}F_{\mu\nu}^{(c)} + i\frac{e\theta}{4\pi}\varepsilon_{\mu\nu}\left(F_{\mu\nu}^{(c)} - F_{\mu\nu}^{(b)}\right) + \frac{e^2}{2g}B_\mu^2 \tag{5.4}$$

where the indices c, b indicate the respectively if it is the field strength of C or B fields. A gauge transformation acts on the fields ψ and C_μ. In turn the B_μ field does not transform under gauge transformation. Summing up the procedure done before which applies here as well: gauge freedom enables one to pick the Lorentz gauge where $\partial^\mu C_\mu = 0$ and therefore parameterize the field as $C_\mu = -i\varepsilon_{\mu\nu}\partial^\nu\varphi$. There is no gauge freedom to play in what regards B_μ so it must be parameterized with a gradient part too: $B_\mu = \partial_\mu\chi' - i\varepsilon_{\mu\nu}\partial_\nu\varphi'$. It turns out that the field χ' decouples from the rest of the fields and therefore can be left out for this analysis. This is true irrespectively of the gauge used for C_μ. Then one performs a chiral transformation $\psi = e^{ie\varphi\gamma_5}\psi'$ that will cancel the coupling to C_μ. There is now another ingredient that is the finite mass of the fermion fields. This massive term is mapped to $-m\left(\bar{\psi}\psi\cos 2e\varphi + i\bar{\psi}\gamma_5\psi\sin 2e\varphi\right)$ [14, 265]. The Lagrangian on ψ' is decoupled form the rest of the system and can be mapped to to bosonic action $\frac{1}{2}\left(\partial_\mu\phi'\right)^2 - \mu\cos\left(\sqrt{4\pi}\phi' + 2\varphi\right)$ where $\mu = me\exp(\gamma)/\left(2\pi^{3/2}\right)$. Translating the ϑ' through $\phi' = \phi - \frac{e}{\sqrt{\pi}}\varphi$ the full Lagrangian is then quadratic on φ and φ' and it can be integrated out. The full Lagrangian after this procedure (but before integration) is given by:

$$\begin{aligned}\mathcal{L} =& \frac{1}{2}\left(\partial_\mu\phi\right)^2 - \frac{e}{\sqrt{\pi}}\partial_\mu\phi\partial_\mu\varphi - \mu\cos\left(\sqrt{4\pi}\phi\right) - \frac{1}{2}\left(\partial^2\varphi\right)^2 - \frac{1}{2}\left(\partial^2\varphi'\right)^2 + \partial^2\varphi'\partial^2\varphi \\ &+ \frac{e\theta}{2\pi}\left(\partial^2\varphi - \partial^2\varphi'\right) - \frac{e^2}{2g}\left(\partial_\mu\varphi'\right)^2\end{aligned} \tag{5.5}$$

As announced the χ' is decoupled and we drop it. The θ-term of φ is recasted in the cosine by transforming $\phi \to \phi + \theta/\sqrt{4\pi}$ (there is still a θ-term in the field φ') . The integration over φ brings a

[1] In Chapter 4 the field that was chosen to be replaced by C_μ was B_μ while here it was A_μ. Both choices are equivalent for the purpose of bosonizing and integrating out vector fields.

term of the form $-\frac{1}{2}\left(\frac{e}{\sqrt{\pi}}\vartheta+\partial^2\varphi'\right)^2$. The fact that the coupling between φ and φ' had just a 1 in front, makes the terms $\left(\partial^2\varphi'\right)^2$ cancel out. This cancellation is fundamental for the simplicity of the final result. Were the coupling between the bosonic fields be a little different and this would not happen. This is due to the fact that one of the gauge fields is actually a fictitious field derived from a Thirring interaction which, in the end. The next step consists on integrating the field φ'. For it we also have a θ term with the opposite sign which induces a new transformation on $\phi\to\phi-\theta/\sqrt{4\pi}$ opposite to the one made above. However at this point the ϕ field acquired a mass, so as expected the dependence on θ is not erased but instead is explicit in the term $\frac{e^2}{2\pi}\left(\vartheta-\theta/\sqrt{4\pi}\right)^2$. This transformation is useful to perform the integration on φ' which appears in the form $\frac{e^2}{2g}\left(\partial_\mu\varphi'\right)^2-\frac{e}{\sqrt{\pi}}\partial_\mu\vartheta\partial_\mu\varphi'$. Its integration brings the Thirring contribution to the bosonic action $\frac{g}{2\pi}\left(\partial_\mu\vartheta\right)^2$. Finally, the usual mass term is re-stored by the transformation $\vartheta\to\vartheta+\theta/\sqrt{4\pi}$ and the Lagrangian reads:

$$\mathcal{L}=\frac{1}{2}\left(1+\frac{g}{\pi}\right)\left(\partial_\mu\vartheta\right)^2+\frac{e^2}{2\pi}\vartheta^2-\mu\cos\left(\sqrt{4\pi}\vartheta+\theta\right) \tag{5.6}$$

which corresponds precisely to all the ingredients of both the Thirring and Schwinger added together. In other words no mixing between the g and e couplings occur. It is worth noting that the above Lagrangian corresponds exactly to the Lagrangian obtained from 5.3 if the mapping obtained from bosonization of the free massless Dirac fermion is applied and the gauge fields integrated out. Specifically this amounts to replace the pure fermionic action by the respective Sine-Gordon model and replace the current by $\bar{\psi}\gamma_\mu\psi=\frac{1}{\sqrt{\pi}}\varepsilon_{\mu\nu}\partial_\nu\vartheta$ both on the coupling to A_μ and in the Thirring term contribution. After translating the bosonic field ϑ by $\theta/\sqrt{4\pi}$ and integrating the gauge field the Lagrangian 5.6 is obtained. The more intricate procedure described above guarantees that the procedure is correct and one is not abusing of the mapping of the free Dirac fermion.

It follows from the bosonized Lagrangian that, as in the Thirring model, only for $g>-\pi$ one can make sense of this model. The existence of a threshold for a minimum of g is expected from the lattice theory. For $g\to-\infty$ the dominant term on the Hamiltonian is a nearest neighbor strong repulsion which will induce a phase separation in the system. For that limit the field theory, or, in other words, the continuum limit, cannot be taken. Regarding the screening and confinement of the model, the simplest case corresponds to the massless theory where $\mu=0$. The propagator for the the bosonic theory is given by

$$\Delta_\vartheta\left(p\right)=\frac{1}{\left(1+\frac{g}{\pi}\right)p^2+\frac{e^2}{\pi}} \tag{5.7}$$

This result can be used to compute the two point function, for instance, of the the scalar $\bar{\psi}\psi$ and pseudoscalar $\bar{\psi}\gamma_S\psi$. This calculation is performed bellow as well as a perturbative calculation of the string tension for the massive case.

5.1.1.1 Particle spectrum for the massless case

As in the case of the Schwinger model [265] the divergences of the correlation functions $\bar{\psi}\psi$ and $\bar{\psi}\gamma_S\psi$ are of the form $\left(1+\frac{g}{\pi}\right)p^2=-n^2e^2/\pi$ for $n=1$ and no charged fermions appear. The case $n=1$ is the only simple pole and comes from the pseudoscalar two point function.

The connection between the four fermion functions and the propagator can be made along the lines described in [265] with the presence of the Thirring term. From the bosonization procedure that was followed $\bar{\psi}'\psi'\propto\cos\left(\sqrt{4\pi}\phi'\right)$ and $\bar{\psi}'\gamma_S\psi'\propto i\sin\left(\sqrt{4\pi}\phi'\right)$ where the ψ' and ϕ' are the fermionic and bosonic intermediate fields used in the calculation. In terms of initial fermionic and final bosonic variables the relation is given by $\bar{\psi}\psi\cos 2e\varphi-i\bar{\psi}\gamma_S\psi\sin 2e\varphi\propto\cos\left(\sqrt{4\pi}\vartheta-2e\varphi\right)$ and $\bar{\psi}\gamma_S\psi\cos 2e\varphi-i\bar{\psi}\psi\sin 2e\varphi\propto i\sin\left(\sqrt{4\pi}\vartheta-2e\varphi\right)$. From this one can reconstruct $\bar{\psi}\psi\propto\cos\left(\sqrt{4\pi}\vartheta\right)$ and $\bar{\psi}\gamma_S\psi\propto$

$\sin\left(\sqrt{4\pi}\vartheta\right)$. Therrefore the relations between the initial fermionic and final bosonic fields is the same as for the free theory which means:

$$\begin{aligned}\left\langle\bar{\psi}\left(x\right)\psi\left(x\right)\bar{\psi}\left(0\right)\psi\left(0\right)\right\rangle &= \left\langle\bar{\psi}\psi\right\rangle\cosh\left(4\pi\Delta\left(x\right)\right)\\ \left\langle\bar{\psi}\left(x\right)\gamma_s\psi\left(x\right)\bar{\psi}\left(0\right)\gamma_s\psi\left(0\right)\right\rangle &= \left\langle\bar{\psi}\gamma_s\psi\right\rangle\sinh\left(4\pi\Delta\left(x\right)\right)\end{aligned} \tag{5.8}$$

the singularities can be computed by expanding the cosh and the sinh in power series and analyze the singularities term by term.Consider the term of order n which corresponds to cosh if even or sinh if odd. The Fourier transform of 5.7 is plugged in, exponentiated and then new Fourier transformed is taken, corresponding to compute the Fourier transform of 5.8 in terms of the momentum p. The result is given by:

$$\int\frac{d^2q_1}{\left(2\pi\right)^2}\cdots\frac{d^2q_n}{\left(2\pi\right)^2}\frac{1}{\left(1+\frac{g}{\pi}\right)q_1^2+\frac{e^2}{\pi}}\cdots\frac{1}{\left(1+\frac{g}{\pi}\right)q_n^2+\frac{e^2}{\pi}}\delta\left(p-p_1-\ldots-p_n\right) \tag{5.9}$$

The integration of one of the variables, say p_n, can be performed using the Dirac delta. After the $n-1$ integrations of the zeroth component of p_i can be carried out putting them on-shell. This results in:

$$\int\frac{d\left(q_1\right)_1}{2\pi\sqrt{2E_1}}\cdots\frac{d\left(q_{n-1}\right)_{n-1}}{2\pi\sqrt{2E_{n-1}}}\frac{1}{\left(1+\frac{g}{\pi}\right)\left(p-q_1-\ldots-q_{n-1}\right)^2+\frac{e^2}{\pi}}\Bigg|_{q_{i=1,\ldots,n-1}\text{on-shell}} \tag{5.10}$$

The abbreviation $E_i=\sqrt{-q_i^2-m^2}$ was used. Let $Q=q_1+\ldots+q_{n-1}$and consider the denominator of the form $\lambda\left(p-Q\right)^2+m^2$. The momenta part can be written as $\left(p-Q\right)^2\rightarrow p_0^2-2p_0Q_0+Q^2$ where it was used implicitly that one can eliminate the dependence on the spacial component of p by a suitable translation of the spatial variable of integration. The poles obey then $\sqrt{\lambda}p_0=\sqrt{\lambda}Q_0+\sqrt{Q_1^2-m^2}$. Because the particles q_i are on-shell, the maximum value of the total for momenta is $\lambda Q^2=-\left(n-1\right)^2m^2$ corresponding to the situation where all the $n-1$ particles are at rest in a given frame and therefore $Q_1=0$. For this case one finds a pole at $\lambda p_0^2=-n^2m^2$. By increasing the total momentum of Q one finds a branch cut along the axis starting precisely at $-n^2m^2$ which correspond to multiparticle states. This is true for any $n>1$. For the special case $n=1$ one has an isolated pole at $\lambda p_0^2=-m^2$ and therefore the theory does not contain further states.

5.1.1.2 String tension for the perturbative massive case

The massive case is addressed pertubatively. The same kind of process followed above to derive the bosonic Lagrangian can be repeated, now for a system with the presence of two external charges. As the external charges are placed at a finite distance L, terms with an external current of the form $J_0^{\text{ext}}=\delta\left(x-L/2\right)-\delta\left(x+L/2\right)$ and $J_1^{\text{ext}}=0$ should be added to the Lagrangian. The Thirring term will produce no extra contribution for the string tension as $\left(J_\mu^{\text{ext}}\right)^2$ contains no element involving the two different charges together (its purely local) and, therefore, will give an L independent contribution for the final energy. The effect of the external charge enters only in the coupling with external fields $-iQJ_\mu^{\text{ext}}A_\mu$ being Q the absolute value of the external charges placed on the system. After the variable transformation this coupling is transformed into $-iQJ_\mu^{\text{ext}}\left(C_\mu-B_\mu\right)$. As in [279] the effect of the external charges is easily seen if one writes $J_\mu^{\text{ext}}=\varepsilon_{\mu\nu}\partial_\nu K$. This term takes then the form $QK\left(\partial^2\varphi-\partial^2\varphi'\right)$. The function K is mostly constant being 1 for $|x|<L$ and 0 for $|x|>L$. The function is plotted on Figure 5.1. This extra term has the form of the θ term with the difference that K is actually space dependent so when one does transformations $\vartheta\rightarrow\vartheta-\sqrt{\pi}QD/e$ there is a kinetic term contributinat the points $|x|=L$. Again such contribution is independent of L and it is unimportant to compute the string tension. Since one is dealing with non-locality, this conditions is not always

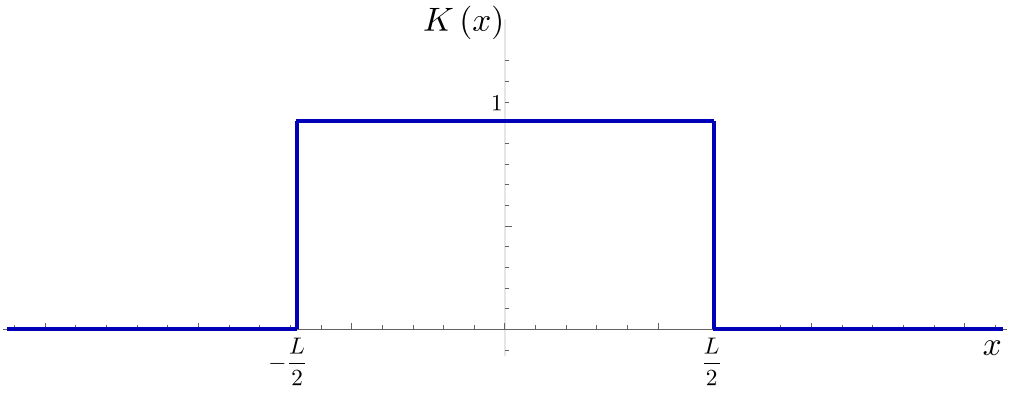

Figure 5.1: Representation of the function $K(x)$. Contributions to the energy involving derivatives on $K(x)$ only contribute near the points $x = \pm L/2$ and will not depend on L.

assured and shall be dealt with care for higher dimensions. Since when $K = 0$ the contribution for the energy from both systems is the same, the difference of energy corresponds to take simply $K = 1$ and multiply the energy density by L.

In lowest order in perturbation theory in the mass, the energy corresponds simply to the expectation value of the cosine term which yields:

$$\sigma = -\mu \left(\cos\left(\theta - \frac{2\pi Q}{e} \right) - \cos(\theta) \right). \tag{5.11}$$

This is the known result for the Schwinger model. Furthermore only for $\theta = \pm\pi$ the partial deconfining is found as in [280]. If the external charge Q is a multiple integer of e the string tension is actually zero which means it can be totally screened. For any $\theta \neq \pm\pi$ there are allays values of Q which encounter a finite positive string tension signaling confinement. In turn for $\theta = \pm\pi$ no external charge produces a positive string tension.

5.1.2 Order of magnitude of the lattice parameters

The goal of this section is to provide an estimate of the values of the different parameters in a possible implementation. To this end the particular proposal [139] discussed in Section 2.2.1 is taken. This model makes use of one species of fermions and two species of bosons and builds the quantum links using the Schwinger representation. Summing up, for completeness: fermions are hopping between all lattice sites, odd links are associated with one species of bosons and even links with other. Each boson is only allowed to hop between its designated link. This situation was illustrated in Figure 2.1.

The cold atomic parameters are t_α (hopping parameters) and h_α (one body potentials). The index $\alpha \in \{F, 1, 2\}$ labeling the fermions or one of the two boson species. To establish the map of parameters between these parameters and the lattice Hamiltonian 5.2 one should re-store the $\hbar$ and c in the Hamiltonian which corresponds to add $\hbar c$ to all terms except the mass term which gets a c^2. The parameters of the Hamiltonian are ${a_s}^2$, the electric charge e and the Thirring term g. The kinetic term is characterized by $t_B t_F/U$, the pure bosonic term by t_B^2/U and the nearest neighbor density-density term by t_F^2/U. The virtual processes that give rise to these terms in perturbation theory are

[2]This not the lattice spacing of the cold atomic lattice but rather the discretization parameter of the continuum model. For this reason a label s was added to avoid confusion. By suitably varying the cold atomic parameters one can probe different lattice spacing of the discretized field theory a_s.

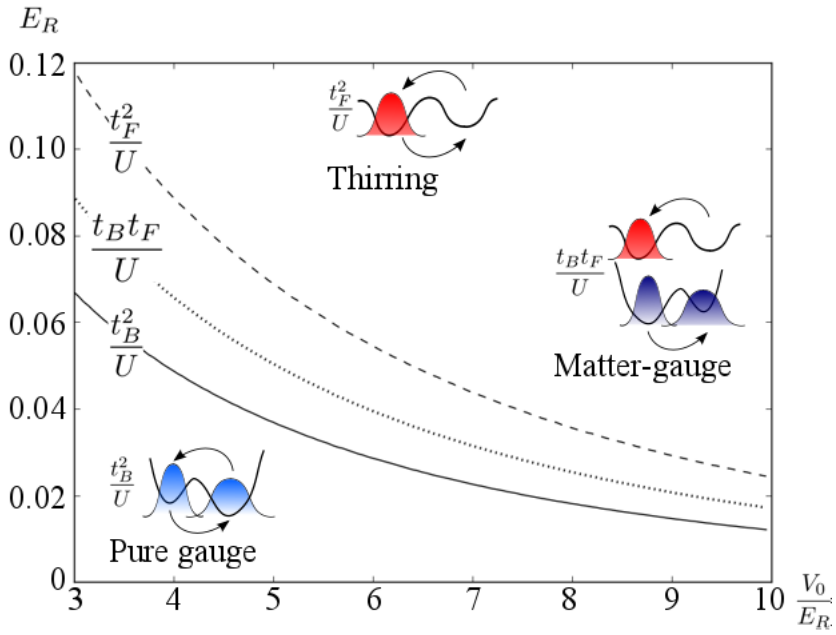

Figure 5.2: Value of different Hamiltonian parameters as the amplitude V_0 of the external potential is varied. The energies are measured in units of $E_R = \hbar^2 a^{-2}/2m$. These parameters correspond to the Thirring, matter-gauge coupling and the pure gauge terms and are illustrated through the virtual process in perturbation theory from where they originate.

depicted in Figure 5.2 along with their estimated value. More details following. The connection with the parameters of the Hamiltonian 5.2 is given by $2g = -t_F/t_B$, $e^2 a_s^2 = t_B/2t_F$ which means that not all lattice parameters can be varied independently.

One difficulty for this implementation concerns the requirement that the interaction between the different atomic species respect $U_{11} = U_{22} = U$ and $2U_{12} = 2U_{1F} = 2U_{2F} = U$ where $U_{\alpha\beta}$ is the on-site interaction parameter between species α and β. The problem may be even more difficult to solve since the proposal requires that the bosons sit in asymmetric minima. This asymmetry will create a different structure to the wave function which ultimately lead to a interaction that is site dependent $U_{\alpha\beta}^{+/-}$ where the relative and absolute minima are represented, respectively, by the labels $+/-$. By other side the existence of two different parameters $U^{+/-}$, which are minima dependent, is not crucial. Effective gauge invariance is obtained in perturbation theory for U large so as long as both $U^{+/-}$ remain larger than the other parameters since it is this condition which sets $G_x |\psi\rangle = 0$. Since the goal of this section is to provide an estimate of the order of magnitude of the parameters that one may have access to, this complication is circumvented by disregarding the asymmetry, which can be made small. More details about this point can be found in Appendix 5.A.

Even without the complication of the asymmetric minima, one still has to match the different interactions between atomic species. Again, the system is robust under small enough deviations from the matching condition above. Possible deviations can be casted in $UG_x^2 \to UG_x^2 + U\sum \Delta U_{\alpha\beta} n_x^\alpha n_x^\beta$ where $\Delta U_{\alpha\beta}$ is the deviation of the interaction between species α and β to the desired value. The fundamental requirement to obtain a gauge invariant theory is still valid as long as $\Delta U_{\alpha\beta}/U \ll 1$.

For this calculation a mixture of ^{52}Cr of spin ± 2 will be used. This particular choice is related to the fact, as explained below, that their scattering lengths generate approximately the required interaction strength between the bosons of the proposal. Other atomic species may require further tuning but, as long as the order of magnitude is the same, the range of achievable parameters should

be retained. The scattering length between pairs with total angular momentum equal to zero is $a_{b0} \simeq 30 - 50$ and for pairs with total angular momentum equal to four is $a_{b4} \simeq 58 \pm 6$ both in units of the Bohr radius a_0 [286]. If one considers a reference value $a_{b0} = 30a_0$ and $a_{b4} = 60a_0$, this will generate the required relations between U_{11}, U_{22} and U_{12}. For the fermionic species it is assumed that a tuning of the interaction is possible in such a way that the remaining conditions are obeyed. For this present calculation it is assumed also that $a_{1F} = a_{2F} = 60a_0$. This does not solve the requirement $2U_{1F} = 2U_{2F} = U$ as $a_{12} = 60a_0$ solves $2U_{12} = U$ due to the presence of bosonic-bosonic interactions which have no fermionic-fermionic counterpart (see the difference between the two equations in 5.54). However, as long as S is not very large it is not expected that the effect is significative. In here the calculations will be done for $S = 1$ and this assumption proves to be enough. In order to increase S one should be careful in adjusting a_{1F} and a_{2F} accordingly.

The Wannier functions are assumed Gaussian with a standard deviation σ_α^i which depend also in the direction i and are fixed variationally by minimizing the Gross-Pitaevskii energy. The system is effectively one dimensional but the wave functions spreads in the two other spatial dimensions. This will influence the value obtained for the parameter $U_{\alpha\beta}$ since smaller spreadings lead to stronger interactions. The standard deviation with respect to the two perpendicular directions is kept at a fixed value $\sigma_\perp$, assumed here to be the same for all the species (fermions and bosons). The potential felt by the particles is characterized by an amplitude $V_{0\alpha}$, which controls the height of the barrier, the off-set $V_{0\alpha}\Delta_\alpha$, which controls the difference of energy between minima, and a lattice spacing a.

In order to get a sense of the parameters it is assumed $S = 1$, $V_{0F} = V_{0B} = V_0$ and $\Delta_F = \Delta_B = \Delta$. For the atomic lattice spacing one considers $a \sim 1/2\mu m$. As detailed in Appendix 5.A, in order to remain in the perturbative regime for the range of potentials $V_{0\alpha} \sim (3-10)\, E_R$ where the reference energy E_R is given by $E_R = \hbar^2 a^{-2}/2m$, it is chosen $\sigma_\perp = 0.2a$ and $\Delta = 10^{-3}$. This guarantees that t_α/U remains $\lesssim 10^{-1}$ and, therefore, perturbative. Other choices are possible but this is enough for an illustrative calculation. For this values one finds that the relation $2U_{1F} = 2U_{2F} = U$ is obeyed within an error of 2% in this interval. By other side this allows to vary, in theory, the ratio t_F/t_B from 1 (close to $V_0 \simeq 10E_R$) to several orders of magnitude higher as t_B approaches zero (occurring for $V_0 \simeq 3.5E_R$). Within this scenario it is always true that $t_F \geq t_B$ due to the higher number of bosons on the system. This can be easily understood considering the $S = 1$ case in which, in average, there is a boson per well. In more detail, consider a double well where each well is labeled by A and B. In an "average configuration" there is one fermion and a boson on A and only a boson on B. If the fermion hops from A to B, the final configuration will host the same energy as the initial configuration. In turn if the boson on B jumps to A the final configuration has an higher energy due to the fact that all the atoms repeal each other. This will result in a smaller hopping for the bosons which is screened out as the amplitude V_0 is increased and starts to dominate the hopping process. Therefore the range of parameters one has access correspond to $-g \geq 1/2$ and $e^2 a_s^2 \leq 1/2$ bounded by the condition $-1/4g = e^2 a_s^2$. The typical energy of the processes of the effective cold atomic system is of the order $t_\alpha t_\beta/U,\ V\Delta \sim 10^{-3} E_R$.

The three terms $t_\alpha t_\beta/U$ remain close to each other satisfying the hierarchy $t_F^2/U \gtrsim t_F t_B/U \gtrsim t_B^2/U$ as it is clear from the previous discussion and from Figure 5.2. The magnitude of the mass parameter is less constrained and can be changed through Δ.

5.2 Screening and confinement with gauge fields in $D+1$ dimensions

As mentioned before, naively one would expect to find deconfinement at least for $D = 3$. There one would expect to find features of normal QED with the particularity of "electrons" being restricted to one spatial dimension. In this Section it is shown that the situation is more subtle. The general formalism of the previous Chapter (4) will be applied. The starting point is the Lagrangian 4.11 for

the case $d = 1$ and Dirac fermions:

$$\mathcal{L} = -\bar{\psi}\gamma_\mu\partial_\mu\psi - iej^\mu_{D+1}A_\mu + \frac{1}{4}F^2_{\mu\nu} + \mathcal{L}_{GF}. \tag{5.12}$$

The calculation of the effect of external charges on the system can be done as for the Schwinger-Thirring case. This amounts to the introduce of an extra contribution $-iQA_\mu j^\mu_{\text{ext}}$ where Q is the absolute value of the two opposite external charges. This external current can be written in the form $j^\mu{}_{\text{ext}} = \varepsilon_{\mu\nu}\partial_\nu K$ and can be eliminated via chiral transformation. The variable change correspond to $\psi = e^{iQK\varphi\gamma_5}\psi'$ where, again, one should have into account the existence of the chiral anomaly. The resulting bosonic theory is given by:

$$\mathcal{L} = \frac{1}{2}\phi\left(-\partial^2 + \frac{e^2}{\pi}M^{-1}_{D\to 1}\right)\phi - \mu\cos\left(\sqrt{4\pi}\phi\right) + \frac{eQ}{\sqrt{\pi}}\phi M^{-1}_{D\to 1}K + \frac{Q^2}{2}KM^{-1}_{D\to 1}K \tag{5.13}$$

When comparing to 4.23 there are three differences:

- There is no Thirring coupling ($g = 0$): it was set to zero as it was shown not to play a role.
- There is an extra interacting term: It corresponds to $\mu\cos\left(\sqrt{4\pi}\phi\right)$ and includes the possibility of massive fermions. In the previous Chapter only massless fermions were addressed (for which $\mu = 0$)
- There is an extra term linear on the field an other that is field independent: It corresponds to $\frac{eQ}{\sqrt{\pi}}\phi M^{-1}K + \frac{Q^2}{2}KM^{-1}K$ and is due to the effect of the external charges. Setting the value of the external charges to zero, $Q = 0$, eliminates these terms.

With a field transformation $\phi' = \phi + \frac{eQ}{\sqrt{\pi}}KM^{-1}_{D\to 1}\frac{1}{-\partial^2+\frac{e^2}{\pi}M^{-1}}$, the coupling between K and the Bosonic field is translated to the cosine. Since the lower dimension is always $d = 1$ and there is no risk of ambiguity, from now on, $M_{D\to 1}$ will be simply denoted by M_D. The resulting Lagrangian reads:

$$\mathcal{L} = \frac{1}{2}\phi^2\left(-\partial^2 + \frac{e^2}{\pi}M^{-1}_D\right)\phi - \mu\cos\left(\sqrt{4\pi}\phi + Q\alpha_D\right) + Q^2\mathcal{K}_D \tag{5.14}$$

where M_D and α_D can be seen as operators acting on the field and K_D is a simple space-time function. With some algebra one can write

$$\alpha_D = 2eF_DK, \quad \mathcal{K}_D = \frac{1}{2}\partial_\mu KF_D\partial_\mu K, \quad F_D = \frac{G_D}{1+\frac{e^2}{\pi}G_D} \tag{5.15}$$

The unperturbed theory, i.e. the theory with no external charges, can be easily recovered by setting $Q = 0$.

Despite the non-locality, the above Lagrangian is still translational invariant in time (in space as well if $Q = 0$). Time translation invariance gives rise to the conservation of energy. The total energy can be computed through the energy-momentum tensor. This will be, in general, a very complicated object. Nonetheless it still allows the computation of difference of energies since the more complicated terms cancel out (for the massive case one should go to first order in perturbation theory as well). In Appendix 5.B the construction of the energy-momentum tensor for theories with higher derivatives is reviewed. The energy is given by the integral in space of T^{00} component of the energy-momentum tensor (Equation 5.61). When quantized the fields are promoted to operators and T^{00} is taken in normal order (denoted by : :). The total energy is then given by $E = \left\langle \int dx : T^{00}(x) : \right\rangle$. The difference of energy as a result of introducing external charges can be written as:

$$\Delta E = \left\langle \int dx : T^{00}_Q(x) - T^{00}_{Q=0}(x) : \right\rangle \tag{5.16}$$

where $T^{00}_Q(x)$ denotes the energy-momentum tensor due to the introduction of external charges according to 5.14. First the massless case is analyzed followed by the small mass limit.

5.2.1 Massless fermions

For this case $\mu = 0$ and it is much simpler to analyze since the effect of external charges is isolated on the term $Q^2\mathcal{K}_D$, completely decoupled from the fields (Equation 5.14). As mentioned before the energy-momentum tensor will be a complicated object (both in absence or presence of external charge). However both $T^{00}_Q(x)$ have a very similar structure $T^{00}_{Q=0}(x)$. The only difference is an additional space-time function which is independent of the fields. In other words, the first term of the tensor in 5.61 is unaffected by the external charges while the second, which is basically the Lagrangian, suffers just from a "translation" of the Lagrangian with no operator content (Q^2K_D in 5.14). Therefore, for the massless case, one obtains $\Delta E_{m=0} = Q^2 \int dx \mathcal{K}_D(t=0,x)$. In $\mathcal{K}_D$ of Equation 5.15, each $\partial_\mu K$ encodes two Dirac deltas corresponding to two different external charges as described above. Therefore, in this expression, there are included interactions between the charges, corresponding to pick the Dirac deltas at different points, and "self-interactions", corresponding to pick the same Dirac delta in both K's. The later ones are independent of L and therefore do not account for actual interaction between different charges. As a result they are neglected in what follows. By performing the implicit integrals on the definition of $\mathcal{K}_D$, making use of the Dirac deltas and the fact that $\partial_\mu K$ is independent of time, the energy can be written as:

$$\Delta E_{m=0} = Q^2 \int \frac{dk_1}{2\pi} F_D(k_0 = 0, k_1) \exp(ik_1 L) \tag{5.17}$$

where $F_D(k_0, k_1)$ are the fourier components of F_D. In order to determine the effect of external charges for each case, one now should specify F_D and perform the integrals for all the cases $D = 1, 2, 3$.

5.2.1.1 Massless $D = 1$

This case corresponds to have $\hat{G}_1 = 1/-\partial^2$ and $F_1(0,k) = 1/\left(e^2/\pi + k^2\right)$. The integral results in:

$$\Delta E_{m=0} = \frac{\sqrt{\pi}Q^2}{4e} \exp\left(-\frac{eL}{\sqrt{\pi}}\right) \tag{5.18}$$

If this calculation was to be reproduced without the presence of the fermion field (or turning off the coupling $e = 0$), the resulting energy would be a linear growth with the distance. Here one has an exponential decay instead, resulting on pair production which screens the charges. This shows explicitly the charge screening known for the massless Schwinger model.

5.2.1.2 Massless $D = 2$

The function F_2 is given by $F_2(0,k) = 1/\left(e^2/\pi + 2|k|\right)$. Again the integral can be made explicitly:

$$\Delta E_{D=2} = \frac{Q^2}{2\pi}\left[\frac{\pi}{2}\sin\left(\frac{e^2L}{2\pi}\right) - \cos\left(\frac{e^2L}{2\pi}\right)\mathrm{Ci}\left(\frac{e^2L}{2\pi}\right) - \sin\left(\frac{e^2L}{2\pi}\right)\mathrm{Si}\left(\frac{e^2L}{2\pi}\right)\right] \tag{5.19}$$

The functions Ci (cosine integral) and Si (sine integral) are respectively given by $\mathrm{Ci} = -\int_{-x}^{+\infty} dt \cos t/t$ and $\mathrm{Si} = \int_0^x dt \sin t/t$. In the limit of $L \to \infty$ the cosine integral goes to zero and the sine integral converges to $\pi/2$. As a result also here the energy goes to zero as the distance increases despite the pure gauge theory exhibiting a logarithm increase of the energy with the distance.

5.2.1.3 Massless $D = 3$

For the three dimensional case, as was explained in Chapter 4, one introduces an UV cut-off Λ in order to regularize the integral over the extra dimensions (where the gauge field lives). The resulting function

F will be dependent on this cut-off: $F(0,k) = \log\left(1+(\Lambda/k)^2\right) / \left(4\pi + \frac{e^2}{\pi}\log\left(1+(\Lambda/k)^2\right)\right)$. Now the integral requires more care. Within a change of variables it can be written as:

$$\frac{Q^2}{4\pi L}\tilde{\Lambda}\int_0^{+\infty}\frac{dq}{2\pi}\frac{\log\left(1+q^{-2}\right)}{1+(e^2/4\pi)\log\left(1+q^{-2}\right)}\cos\tilde{\Lambda}q \tag{5.20}$$

All distance dependence is now isolated in the prefactor $1/L$. The remaining was absorbed into the cut-off $\tilde{\Lambda} = L\Lambda$. In this expression the screening due to pair creation is evident: if one sets $e = 0$ the integral gives simply $\tilde{\Lambda}^{-1}$ (in the large cut-off limit) and all that will remain is the expected Coulomb energy: $Q^2/4\pi L$. When e acquires a finite value one couples the gauge fields to the fermion fields and pair production starts. This is made explicit in the integral since it adds an extra positive term in the denominator (which will lower the absolute value of the integrand). It will now be proven that, for any finite charge e, total screening occurs and actually $\Delta E_{D=3} = 0$ in the large cut-off limit. The integral can be broken into smaller pieces: $\int_0^{+\infty} = \sum_n \int_{2\pi n/\Lambda}^{2\pi(n+1)/\Lambda}$. Let the non-oscillatory part be denoted by $f(q) = \log\left(1+q^{-2}\right) / \left(1+\left(e^2/4\pi\right)\log\left(1+q^{-2}\right)\right)$. Since this function is well behaved for every point except $q = 0$ almost all of these integrals vanish in the large cut-off limit. This can be seen by integrating by parts which brings powers of $\tilde{\Lambda}$ to the denominator. At lowest order, if the functions f has finite derivatives, it goes like $\tilde{\Lambda}^{-3}$. The only part that remains is the case $n = 0$ which can be majorized by using the fact that f is strictly decreasing in the interval of integration:

$$\tilde{\Lambda}\int_0^{2\pi/\tilde{\Lambda}}\frac{dq}{2\pi}f(q)\cos\tilde{\Lambda}q \leq 2\left(\frac{4\pi}{e^2} - f\left(\frac{2\pi}{\tilde{\Lambda}}\right)\right) \tag{5.21}$$

To build the inequality, the value of the function f is replaced by its maximum on the interval $(4\pi/e^2)$ whenever the cosine is positive and by its minimum whenever the cosine is negative. Since the function is continuous one can make $f\left(2\pi/\tilde{\Lambda}\right)$ as close as desired to $4\pi/e^2$ by increasing $\tilde{\Lambda}$ and, therefore, the bound goes to zero. Since the integral is strictly positive, this proves that the energy goes to zero. One can finally write:

$$\Delta E_{D=3} = \begin{cases} \frac{Q^2}{4\pi L} & e = 0 \\ 0 & e \neq 0 \end{cases} \tag{5.22}$$

As the coupling between the gauge fields and the fermions is turned on, the fermionic fields react to the presence of external charges initiating pair production. Remarkably they are able to screen completely the external charges. This shows, in particular, that when the gauge field is in $3+1$ dimensions the fermions become more effective at screening external charges than at $2+1$ or even $1+1$. For the later case the energy decreases exponentially with the distance while here it is zero for any distance.

5.2.2 Massive case

The massive case is naturally more complicated since this is now an interacting theory. Without external charges this interaction is still local and all the non-locality is on the kinetic term. When the external charges are introduced the non-locality is carried over to the interaction through α_D. This means that the insertion of external charges will modify both terms of 5.61. This situation is now addressed in more detail starting with the system with no external charges. In first order perturbation theory on the mass of the fermionic theory, the ground-state will have the structure: $|\Omega_0\rangle = |0\rangle + \mu\,|1\rangle$. The state $|0\rangle$ is the vacuum of the massless theory which is a theory that, however non-local, is still quadratic. The normal ordering is taken with respect to this state. When going to the system with

external charges, even though the quadratic term is modified, the change is of order μ so the ground state of such theory will be, in lowest order in perturbation theory, given by $|\Omega_Q\rangle = |0\rangle + \mu\,|1'\rangle$ where $|0\rangle$ is the same vacuum state of the massless theory and the correction in first order was modified $|1'\rangle$ due to the presence of external charges. The normal ordering is then taken with respect to the same state in both theories. The effect on the energy-momentum tensor 5.61 is now analyzed. With no external charges one has

$$T^{00}_{Q=0} = T_0 - \mu \cos\left(\sqrt{4\pi}\phi\right) \tag{5.23}$$

where all the all the terms independent of μ were condensed on T_0 . In the presence of external charges this is modified to

$$T^{00}_{Q} = T_0 + \mu\tilde{T}_0 - \mu \cos\left(\sqrt{4\pi}\phi + Q\alpha_D\right) + Q^2 K_D \tag{5.24}$$

where $\mu\tilde{T}_0$ is the order μ term obtained from the first part of 5.61. Explicitly one can write:

$$\tilde{T}_0 = \sum_{n=0}^{+\infty}\sum_{i=0}^{n} (-1)^i\, \partial_{\mu_1}\ldots\partial_{\mu_i} \frac{\partial \cos\left(\sqrt{4\pi}\phi + Q\alpha_D\right)}{\partial\left(\partial_0\partial_{\mu_1}\ldots\partial_{\mu_n}\phi\right)} \partial_{\mu_{i+1}}\ldots\partial_{\mu_n}\partial^0\phi \tag{5.25}$$

The presence of this term is due to the fact that the non-locality was carried over to the interacting part, proportional to μ, by the presence of external charges. As a result one has in first order perturbation theory:

$$\Delta E_m = \Delta E_{m=0} + \mu\,\langle 0| \int dx : \left(\tilde{T}_0 + \cos\left(\sqrt{4\pi}\phi\right) - \cos\left(\sqrt{4\pi}\phi + Q\alpha_D\right)\right) : |0\rangle \tag{5.26}$$

Due to the normal ordering, the only term surviving the Taylor expansion of the first cosine is 1. All the others average to zero in the ground state. The same kind of argument holds for $\cos\left(\sqrt{4\pi}\phi + Q\alpha_D\right)$ where only $\cos\left(Q\alpha_D\right)$ survives. Finally note that $\tilde{T}_0$ has always at least one ϕ as it is clear from 5.25 and therefore it averages to zero in the ground state when subjected to normal ordering. The result is then:

$$\Delta E_m = \Delta E_{m=0} + \mu \int_{-\infty}^{+\infty} dx\,(1 - \cos\left(Q\alpha_D\right)) \tag{5.27}$$

From the above expression one expects to find a finite string tension when $Q\alpha_D$ is "mostly" non-multiple of 2π between $-L/2$ and $L/2$ and "mostly" multiple of 2π outside this interval. This, as it will be shown explicitly below, is what happens for the derived α_D in all the different dimensions. From the definition of α_D (5.15) and following the same path used for $\mathcal{K}_D$ when deriving 5.17 one can write::

$$\alpha_D\left(0,x\right) = 8e \int_0^{+\infty} \frac{dk}{2\pi} \frac{F_D\left(k_0=0,k\right)\sin\left(kL/2\right)\cos\left(kx\right)}{k} \tag{5.28}$$

Again, as in the massless case, one has to go through the different dimensions in order to compute the increment to the energy due to the addition of external charges. From this point on, it shall be simply denoted $\alpha_D\left(x\right) \equiv \alpha_D\left(0,x\right)$.

5.2.2.1 Massive $D = 1$

This corresponds to the Schwinger model. The outcome for this case is well known and serves as an illustrative example for the method followed here. Equation 5.28 becomes:

$$\alpha_1\left(x\right) = 8e \int_0^{+\infty} \frac{dk}{2\pi} \frac{\sin\left(kL/2\right)\cos\left(kx\right)}{k\left(k^2 + \frac{e^2}{\pi}\right)} \tag{5.29}$$

The integral can be calculated explicitly giving:

$$\begin{aligned}\alpha_1(x) = \tfrac{\pi}{e}\Big[&\operatorname{sign}(L-2x)\left(1-\cosh\left(\tfrac{e}{2\sqrt{\pi}}(L-2x)\right)+\sinh\left(\tfrac{e}{2\sqrt{\pi}}|L-2x|\right)\right)\\ &+\operatorname{sign}(L+2x)\left(1-\cosh\left(\tfrac{e}{2\sqrt{\pi}}(L+2x)\right)+\sinh\left(\tfrac{e}{2\sqrt{\pi}}|L+2x|\right)\right)\Big]\end{aligned} \tag{5.30}$$

It turns out that, in order to compute the string tension, it is enough to understand the behavior in the limits $|x| \ll L/2$ and $|x| \gg L/2$, as it will be shown bellow. By inspecting directly the function one finds:

$$\alpha_1(x) = \begin{cases} \frac{2\pi}{e} & \text{if } |x| \ll L/2 \\ 0 & \text{if } |x| \gg L/2 \end{cases} \tag{5.31}$$

This is enough to compute the string tension from Equation 5.27 even without computing the remaining complicated integral exactly. The integral in broken in three parts (where it is used the fact that the integrand is symmetric over $x \to -x$): $\int_0^{+\infty} = \int_0^{L/2-x_0} + 2\int_{L/2-x_0}^{L/2+x_0} + 2\int_{L/2+x_0}^{+\infty}$. The value of x_0 is fixed such that guarantees the condition $\exp\left(-\frac{e}{\sqrt{\pi}}(L/2-x_0)\right) \ll 1$. Within this limit one can compute the first and the third integral using the asymptotic expressions of equations 5.31 obtaining:

$$\Delta E_m = \Delta E_{m=0} + \left(1-\cos\left(\frac{2\pi Q}{e}\right)\right)(L-2x_0) + \int_{L/2-x_0}^{L/2+x_0} dx\,(1-\cos(Q\alpha_1(x))) \tag{5.32}$$

One can see that it grows linearly on L. Note that because x_0 can be chosen independent of L, for large enough L, that term actually does not grow with L. In particular the remaining integral just reflects the contribution in the vicinity of the charges which does not depend on their distance (if the distance is large enough). Furthermore, the remaining integral is bounded by values independent of L. Explicitly, substituting the cosine by -1 one has an upper bound of $4x_0$ and substituting the cosine by 1 one has a lower bound of 0. It is therefore clear that the linear behavior in L is exclusive of the first term and one can finally write:

$$\Delta E_m = \Delta E_{m=0} + \mu\left(1-\cos\left(\frac{2\pi Q}{e}\right)\right)L + \dots \tag{5.33}$$

where the dots indicate some bounded dependence on L. By this it is meant that it depends on L but is bounded by values which do not. The string tension reads explicitly:

$$\sigma_1 = \mu\left(1-\cos\left(\frac{2\pi Q}{e}\right)\right) \tag{5.34}$$

This is a well known result [279] which was obtained here by a careful analysis of the energy. The same procedure shall followed for higher dimensions.

5.2.2.2 Massive $D = 2$

For this case one has:

$$\alpha_2(x) = 4e\int_0^{+\infty}\frac{dk}{2\pi}\frac{\sin(kL/2)\cos(kL)}{k\left(k+\frac{e^2}{2\pi}\right)} \tag{5.35}$$

which again can be computed explicitly. For conciseness the abbreviation $X^{\pm} = L \pm 2x$ is adopted. For $x \in [-L/2, L/2]$ one has:

$$\begin{aligned}\alpha_2(x) =& \frac{2}{e}\left(\pi - \frac{\pi}{2}\cos\left(\frac{e^2X^-}{4\pi}\right) - \frac{\pi}{2}\cos\left(\frac{e^2X^+}{4\pi}\right) - \mathrm{Ci}\left(\frac{e^2X^+}{4\pi}\right)\sin\left(\frac{e^2X^+}{4\pi}\right)\right.\\ &\left. -\mathrm{Ci}\left(\frac{e^2X^-}{4\pi}\right)\sin\left(\frac{e^2X^-}{4\pi}\right) + \mathrm{Si}\left(\frac{e^2X^+}{4\pi}\right)\cos\left(\frac{e^2X^+}{4\pi}\right) + \mathrm{Si}\left(\frac{e^2X^-}{4\pi}\right)\cos\left(\frac{e^2X^-}{4\pi}\right)\right)\end{aligned} \tag{5.36}$$

and when $|x| > L/2$:

$$\begin{aligned}\alpha_2(x) =& \frac{1}{e}\left(\pi\cos\left(\frac{e^2X^-}{4\pi}\right) - \pi\cos\left(\frac{e^2X^+}{4\pi}\right) + \pi\sin\left(\frac{e^2x}{2\pi}\right)\right.\\ &\left. -2\mathrm{Ci}\left(\frac{e^2X^+}{4\pi}\right)\sin\left(\frac{e^2X^+}{4\pi}\right) + 2\mathrm{Si}\left(\frac{e^2X^-}{4\pi}\right)\cos\left(\frac{e^2X^-}{4\pi}\right) + 2\mathrm{Si}\left(\frac{e^2X^+}{4\pi}\right)\cos\left(\frac{e^2X^+}{4\pi}\right)\right)\end{aligned} \tag{5.37}$$

Now the same procedure of the $D = 1$ case is followed, studying the limits of $|x| \ll L/2$ and $|x| \gg L/2$. The result obtained is actually the same here. For $|x| \ll L/2$ this is seen by noting that inside the cosine and sine integral one can replace $X^{\pm}$ by L and take the large L limit. In this way the cosine integral is replaced by zero and the sine integral by $\pi/2$. For the$|x| \gg L/2$, $X^{\pm}$ are replaced by $\pm 2x$ inside the cosine and sine integrals and the larger argument is taken again (note also that $\mathrm{Si}(-y) = -\mathrm{Si}(y)$). Then one finds the same kind of result of 5.31 and all that was said about the $1+1$ case translates directly for $2+1$. In particular the string tension is the same at this order in perturbation theory on the mass:

$$\sigma_2 = \mu\left(1 - \cos\left(\frac{2\pi Q}{e}\right)\right) = \sigma_1 \tag{5.38}$$

Even though confinement in itself may not be a surprise for the case where the gauge fields live in $2+1$ dimensions, it is interesting to note that the the resulting string tension, at this order in perturbation theory on the mass, is independent of the gauge fields being present in $1+1$ or $2+1$ dimensions.

5.2.2.3 Massive $D = 3$

Finally the case where the gauge fields live on $3+1$ dimensions is considered. Equation 5.28 for α_3 reads:

$$\alpha_3(x) = \frac{2e}{\pi}\int_0^{+\infty}\frac{dk}{2\pi}\frac{\log\left(\frac{\Lambda^2+k^2}{k^2}\right)\sin(kL/2)\cos(kx)}{k\left(1 + \frac{e^2}{4\pi^2}\log\left(\frac{\Lambda^2+k^2}{k^2}\right)\right)} \tag{5.39}$$

This integral is more complicated than the one obtained for $D = 1, 2$. However it is possible to follow the similar kind of analysis that was done in the massless case of $D = 3$. In the numerator one can write $2\sin(kL/2)\cos(kx) = \sin(k(L/2+x)) + \sin(k(L/2-x))$, breaking the integral in two contributions. Then perform a substitution $q = k/\Lambda$ and reabsorb again a factor on the cut-off: $\tilde{\Lambda} = \Lambda|L/2 \pm x|$choosing $\pm$ depending on the argument of the sine in the piece considered. Note that, as one is interested in the limit where x is far away from $L/2$, this re-scaling is well defined and sending $\tilde{\Lambda} \to +\infty$ still makes sense. The integral will read:

$$\alpha_3(x) = (\mathrm{sign}(L/2+x) + \mathrm{sign}(L/2-x))\frac{e}{\pi}\int_0^{+\infty}\frac{dq}{2\pi}\frac{\log\left(1+q^{-2}\right)\sin\left(\tilde{\Lambda}q\right)}{q\left(1 + \frac{e^2}{4\pi^2}\log\left(1+q^{-2}\right)\right)} \tag{5.40}$$

Each of these "sign" terms comes respectively from $\sin\left(k\left(L/2+x\right)\right)$ and $\sin\left(k\left(L/2-x\right)\right)$. One immediately sees that if the signs of $L/2\pm x$ are different, as they are in $|x|\gg L/2$, α_3 is zero. For the other case of $|x|\ll L/2$ the integral bears similarities to 5.20 and part of the approach can be translated. Namely one can divide the integral in small pieces $\int_0^{+\infty}=\sum_n\int_{2\pi n/\tilde{\Lambda}}^{2\pi(n+1)/\tilde{\Lambda}}$ and observe that most of them converge to zero as the limit of large cut-off is taken due to the rapid oscillation of the sine (or cosine for the case 5.20). Then the only remaining part is:

$$\alpha_3\left(x\right)=\frac{2e}{\pi}\int_0^{2\pi/\tilde{\Lambda}}\frac{dq}{2\pi}\frac{\log\left(1+q^{-2}\right)\sin\left(\tilde{\Lambda}q\right)}{q\left(1+\frac{e^2}{4\pi^2}\log\left(1+q^{-2}\right)\right)},\ |x|<L/2 \tag{5.41}$$

In 5.20 this last piece was also zero as long as e was finite. Now this is no longer true due to the $1/q$ factor which picks a large contribution near $q=0$. To see this explicitly one takes the leading order of $\log\left(1+q^{-2}\right)/\left(1+\frac{e^2}{4\pi^2}\log\left(1+q^{-2}\right)\right)$ for small q which is simply $\frac{4\pi^2}{e^2}$ (assuming that the charge e is finite). Then the result comes independent of the cut-off $\tilde{\Lambda}$:

$$\alpha_3\left(x\right)=\frac{4}{e}\int_0^{2\pi/\tilde{\Lambda}}dq\frac{\sin\left(\tilde{\Lambda}q\right)}{q}=\frac{4\mathrm{Si}\left(2\pi\right)}{e},\ |x|<L/2 \tag{5.42}$$

Summing up these results:

$$\alpha_3\left(x\right)=\begin{cases}\frac{4\mathrm{Si}(2\pi)}{e} & \text{if } |x|<L/2\\ 0 & \text{if } |x|>L/2\end{cases} \tag{5.43}$$

which again corresponds to the expected behavior for a confined phase. The string tension is given by:

$$\sigma_3=\mu\left(1-\cos\left(\frac{4\mathrm{Si}\left(2\pi\right)Q}{e}\right)\right) \tag{5.44}$$

which is finite in general. It is interesting to note that even though $\sigma_1=\sigma_2$ they are still different from σ_3 at this order. Furthermore, in the two previous cases, if the external charge Q was a multiple integer of e the string tension would vanish. Here it is no longer the case. The string tension remains finite when Q is a multiple integer of e. The factor of 2π is replaced by $4\mathrm{Si}\left(2\pi\right)\simeq 5.67<2\pi$.

5.3 Conclusions

It was observed on this Chapter that the screened and confined phases of the Schwinger model are much more robust than one might guess. In the case of the Schwinger-Thirring model with a topological θ-term one sees that the general results obtained when the models are taken separately still hold. Namely that the theory only makes sense when the Thirring coupling is $g>-\pi$ (as in the Thirring model) and most importantly that the system only deconfined for $\theta=\pm\pi$ (as in the Schwinger model). Through an Hubbard-Stratonovich transformation one observes that this model can be regarded as a fermionic field interacting with a massless gauge field which in turn interacts with a "massive gauge field". It is possible that general interactions of this form may break confinement. However the kind of terms obtained from a Thirring interaction are very particular and drive cancellations which would not appear under a general coupling between the gauge fields. The Thirring parameter does not allow to vary interaction between the bosonic fields but only the mass of one of them. This results show that with respect to confinement a possible nearest neighbor density-density interaction plays no role and therefore the phase is stable. This result can be intuitivelly understood by the fact that that the Thirring interaction is purely local and it is not able to fight the dominant interaction driven by the

gauge. It is important to remark that the external charges introduced coupled to the gauge field but a coupled to the dynamical fermions was excluded. In a more general scenario, as it was considered external charges with a charge Q, which in fact corresponds to the coupling with the gauge fields, one can also attribute to this external charges a coupling to fermions, say g_{ext}. This would correspond to consider an extra contribution for the Lagrangian of the form $g_{\text{ext}} j_\mu J^{\text{ext}}_\mu$. This can change the picture of confinement and is a subject of future research.

Also under the assumption of higher dimensionality for the gauge fields, while the fermions remain in $1+1$ dimensions, shows robustness. In the massless case, as for the Schwinger model, there is a strong screening when static charges are introduced on the system. In the Schwinger case the linear growth of the energy with the distance, in the pure gauge theory, is replaced by an exponential decay. In the case of a $2+1$ dimensional gauge field the logarithm is replaced by oscillatory functions (which goes to zero as power laws). Finally in $3+1$ the $1/L$ decay is replaced by zero: external charges are completely screened. When a small mass is considered a linear growth of the energy with the distance is observed and therefore a finite string tension is obtained for the gauge fields living in $1+1$, $2+1$ or $3+1$ dimensions. Furthermore, at this order in perturbation theory, the string tension is the same for the first two cases and smaller for the later one: $\sigma_1 = \sigma_2 > \sigma_3$. This result is non intuitive since the confinement in the Schwinger model is usually attributed to the fact that the Gauss law in $1+1$ dimensions impose a constant electric field (rather than $1/r^2$ of the $3+1$ system). These results suggest that this feature is not necessary to obtain confinement and instead it is the dimensionality of the space-time available for the fermion fields that is dictating confinement in this case. In order to test better this hypothesis it would be interesting to study how far can one extend the space-time allowed for the fermion fields before leaving the confined phase (for gauge fields in 3+1 dimensions for example). Since it is known that when the fermion fields span the full $3+1$ dimensions the theory is deconfining (corresponding to regular QED), this picture should break down at some point. Furthermore, with the advent of quantum simulation of gauge theories, one can hope that an experiment with tunable fermion dimensionality could probe directly interesting phenomena like such transition. These calculations also suggest that these models can provide interesting analytical predictions to be confronted with numerics and experiments.

Appendix Chapter 5

5.A Details on parameter estimates

Here further details are provided on how to obtain an estimate of the parameters of the model. This can be done referring to the Wannier functions of the atomic species, their scattering lengths and the lattice potential through the relations (according to the discussion of Section 1.2):

$$t^{\alpha}_{\vec{r}'\vec{r}''} = -\int d^d\vec{r}\frac{\hbar^2}{2m_\alpha}\nabla\phi_{\alpha\vec{r}'}\left(\vec{r}\right)\cdot\nabla\phi_{\alpha\vec{r}''}\left(\vec{r}\right)+\phi_{\alpha\vec{r}'}\left(\vec{r}\right)V_{\text{ext}}\left(\vec{r}\right)\phi_{\alpha\vec{r}''}\left(\vec{r}\right) \tag{5.45}$$

$$U_{\alpha\beta} = g_{\alpha\beta}\int d^d\vec{r}\phi_{\alpha\vec{r}'}\left(\vec{r}\right)^2\phi_{\alpha\vec{r}'}\left(\vec{r}\right)^2 \tag{5.46}$$

where $t^{\alpha}_{\vec{r}'\vec{r}''}$ are the hopping parameter of species α between $\vec{r}'$ and $\vec{r}''$ and $U_{\alpha\beta}$ the interaction between species α and β and is assumed site independent (no dependence on $\vec{r}'$). Furthermore $g_{\alpha\beta} = \frac{2\pi\hbar^2 a_{\alpha\beta}}{m_{\alpha\beta}}$ where $a_{\alpha\beta}$ is the scattering length between species α and β and $m_{\alpha\beta}$ the reduced masses. In the following it is assumed that the Wannier functions ϕ's to be Gaussians: $\phi_{\alpha\vec{r}''}\left(\vec{r}\right) = C_\alpha\prod_{j=1}^{3}e^{-\left(r_j-r_j'\right)^2/2\sigma^2_{\alpha j}}$ (which is the ground state of the harmonic potential). They are characterized by the $\sigma_{\alpha j}$ which here admit the possibility of being anisotropic and are fixed by requiring energy minimization. For the present case the structure of the function in the dimensions y and z is fixed through a parameter $\sigma_{\perp\alpha}$ while the value of the longitudinal component, which will be called simply σ_α, can be fixed variationally. The relevant potential required can be written as:

$$V\left(x\right) = V_0\left[\sin\left(kx\right)^2+\lambda\sin\left(2kx+\alpha\right)^2\right]. \tag{5.47}$$

To perform the estimates it is easier to work with a potential of the polynomial form. Such potential can be constructed by expanding the expression above in powers of kx . In here such expansion is constructed by hand so one works directly with the relevant parameters like the offset between he minima Δ and the lattice spacing a, instead of parameters like k and α. To design a quartic polynomial potential that has two minima, one at $x = -a/2$ and other at $x = a/2$, and an offset Δ, it is required that the first derivative is of the form $\left(V_0/a^2\right)\left(2x/a+1\right)\left(x-x_0\right)\left(2x/a-1\right)$ where x_0 corresponds to the position of the maxima between the two minima. By integrating one obtains the form of the potential and an extra parameter c as a constant of integration. This parameter is fixed by requiring that the absolute minima, that is chosen arbitrarily to be the one at $x = -a/2$, corresponds to zero energy. Furthermore x_0 can be written in terms of Δ: $x_0 = 3\Delta a/2$. The potential that is considered for, say, the boson species 1 is then:

$$V_{B1}\left(x\right) = V_{B0}\left[\frac{x^4}{a^4}-\frac{2x^3}{a^3}\Delta_B-\frac{x^2}{2a^2}+\frac{3x}{2a}\Delta_B+\frac{\Delta_B}{2}+\frac{1}{16}\right]. \tag{5.48}$$

while for the boson species 2 is $V_{B2}(x) = V_{B1}(-x)$. For the fermions the potential has the same structure. It is worth to note, however, that the fact that the bosons only feel a double well potential is required by the proposal. In contrast the fermions cannot be confined in a double well. For this reason the polynomial double well potential approximation for the fermions is not as good as an approximation as it is for the bosons. Nonetheless, as one is interested on the strong coupling regime of the model this constitutes a reasonable approximation for the estimate of the parameters.

$$V_F(x) = V_{F0}\left[\frac{x^4}{a^4} - \frac{2x^3}{a^3}\Delta_f - \frac{x^2}{2a^2} + \frac{3x}{2a}\Delta_f + \frac{\Delta_f}{2} + \frac{1}{16}\right]. \tag{5.49}$$

The parameters $V_{B/F0}$ control the height of the barrier between the minima. Using this potential the parameters will read:

$$t_\alpha^{\vec{r}'\,\vec{r}''} = \frac{\hbar^2 a^{-2}}{2m_\alpha}\left(\frac{1}{4}\left(\frac{a}{\sigma_\alpha}\right)^4 - \frac{1}{2}\left(\frac{a}{\sigma_\alpha}\right)^2\right)e^{-\frac{\sigma_\alpha^2}{4\sigma^2}} - \frac{V_{0\alpha}}{4}\left(3\left(\frac{\sigma_\alpha}{a}\right)^4 - \left(\frac{\sigma_\alpha}{a}\right)^2 + 2\Delta_\alpha + \frac{1}{4}\right)e^{-\frac{\sigma_\alpha^2}{4\sigma^2}} \tag{5.50}$$

$$U_{\alpha\beta} = \frac{g_{\alpha\beta}}{2\pi^{3/2}}\frac{1}{\sigma_\perp^2}\frac{1}{\sqrt{\sigma_\alpha^2+\sigma_\beta^2}} \tag{5.51}$$

For this proposal it is required that $U = U_{11} = U_{22}$ and $U_{12} = U_{1F} = U_{2F} = 2U$. The fine-tuning of this condition is not absolutely crucial as discussed in the main text. With the parameters $\sigma_\perp$ and σ fixed, one has to rely on the on the control of the scattering length in order to fulfill this condition. Within this variational approach, one computes the average energy per site and requires that σ minimizes it. The problem of the different shape of the minima, also referred in the main text, can be addressed precisely as follows. The total energy is given by:

$$\varepsilon = \int d^3\vec{r}\sum_{\vec{r}',\alpha} n_\alpha \frac{\hbar^2}{2m_\alpha}\left|\nabla\phi_{\alpha\vec{r}'}\right|^2 + n_\alpha V_{ext}\left|\phi_{\alpha\vec{r}'}\right|^2 + \sum_{\beta>\alpha} n_\alpha n_\beta \frac{g_{\alpha\beta}}{2}\left|\phi_{\alpha\vec{r}'}\right|^2\left|\phi_{\beta\vec{r}'}\right|^2 \tag{5.52}$$

The total energy in a site is different depending on which minima one is talking about due to the term $V_{ext}\left|\phi_{\alpha\vec{r}'}\right|^2$. Denoting the minima at $x = \pm a/2$ as $\pm$ the result is:

$$\begin{aligned}\varepsilon/N =& \sum_\alpha n_\alpha \frac{\hbar^2 a^{-2}}{2m_\alpha}\frac{1}{2}\left(\frac{a}{\sigma_\alpha}\right)^2 + \sum_\alpha n_\alpha \frac{3V_0}{4}\left(\left(\frac{\sigma_\alpha}{a}\right)^4 + 2\frac{1\mp 3\Delta_\alpha}{3}\left(\frac{\sigma_\alpha}{a}\right)^2\right) \\ &+ \sum_{\alpha,\beta>\alpha} n_\alpha n_\beta \frac{g_{\alpha\beta}}{4\pi^{3/2}\sigma_\perp^2\sqrt{\sigma_\alpha^2+\sigma_\beta^2}}\end{aligned} \tag{5.53}$$

Where it was already included that the approximation that the spreading in the perpendicular directions are the same for all species and characterized by $\sigma_\perp$. Assuming that all masses are the same the only parameters that depend from species to species are the densities n_α,the offsets Δ_α and the amplitudes $V_{0\alpha}$. The asymmetry of the minima is present whenever $\Delta_\alpha \neq 0$. Therefore the problem of the asymmetry of the different Wannier function on different minima is not present as long as one disregard the Δ's in this calculation, which is the route taken here The estimate should not vary very much on this parameter, and, furthermore, this parameters should not be too large (taken $\sim 10^{-3}$ in the main text). The densities for fermions are $n_F = 1$ while for the other two species of bosons $n_{1,2} = S$. With this one has a total of two parameters to fix, a σ_B and σ_F giving two coupled equations: $\partial\varepsilon/\partial\sigma_F = 0$ and $\partial\varepsilon/\partial\sigma_B = 0$. The reference energy is denoted by $E_R = \hbar^2 a^{-2}/2m$ with an assumed equal mass for all the species m and the dimensionless parameters: $\tilde{V}_{0\alpha} = V_{0\alpha}/E_R$, $\tilde{\sigma}_\alpha = \sigma_\alpha/a$ and the scattering lengths $\tilde{a}_{\alpha\beta} = a_{\alpha\beta}/a$. Regarding the scattering lengths one is working on the assumption that: $a_{1F} = a_{2F} = a_{12} \equiv 2a_{\text{scatt}}$ and $a_{11} = a_{22} = a_{\text{scatt}}$ The dimensionless quantity is then $\tilde{a}_{\text{scatt}} = a_{\text{scatt}}/a$. The two equations are then:

$$\begin{cases} \tilde{\sigma}_F^{-3} - 3\tilde{V}_{0F}\tilde{\sigma}_F\left(\tilde{\sigma}_F^2 + \frac{1}{3}\right) + \frac{4S(\tilde{a}_{1F}+\tilde{a}_{2F})\sigma_F}{\sqrt{\pi}\tilde{\sigma}_\perp^2\left(\sigma_F^2+\sigma_B^2\right)^{3/2}} = 0 \\ \\ \tilde{\sigma}_B^{-3} - 3\tilde{V}_{0B}\tilde{\sigma}_B\left(\tilde{\sigma}_B^2 + \frac{1}{3}\right) + \frac{4S}{\sqrt{\pi}\tilde{\sigma}_\perp^2}\left[\frac{(\tilde{a}_{1F}+\tilde{a}_{2F})\sigma_B}{\left(\sigma_F^2+\sigma_B^2\right)^{3/2}} + \frac{(\tilde{a}_{11}+\tilde{a}_{22}+\tilde{a}_{12})S}{\sqrt{2}\sigma_B^2}\right] = 0 \end{cases} \tag{5.54}$$

Due to the presence of the last term on the last equation the assumption $a_{1F} = a_{2F} = 2a_{\text{scatt}}$ does not solve the requirement of the Hamiltonian parameters of the proposal. For S small, however, the result is approximately valid so these values are taken as reference for the scattering between bosons and fermions.

The first check concerns the inspection of what values of the parameters validate the perturbative approximation. This amounts to guarantee that t_α/U and $V_{0\alpha}\Delta_\alpha$ remain perturbative (in here it is considered that they should be ~ 0.1 or smaller). For illustrative purposes one fixes $S = 1$, $V_{0F} = V_{0B} = V_0$ and $\Delta_F = \Delta_B = \Delta$. The dispersion of the wave function to the extra dimensions should not be very large in order to enhance the interactions. Direct analysis of the above equations yield that, in order to guarantee that the perturbative regime is valid throughout the interval $\tilde{V}_0 \sim 3 - 10$, then one should have $\tilde{\sigma}_\perp \sim 0.2$ and $\Delta \lesssim 10^{-3}$. If one takes $\tilde{\sigma}_\perp$ to be two or three times higher than this, larger potential amplitudes are required. Alternatively, larger scattering lengths can also be used to compensate. By other side there is some freedom on choosing the values of Δ in order to remain in the perturbative regime. However this choice should respect the fact that the two minima should still be present at $x = \pm a/2$ which is translated into $|\Delta| < 1/3$. Finally the analogous of the mass parameter of the target model will scale as $V_0\Delta$ and the choice was taken such that the energy scale of this term matches the order of magnitude of the other terms on the Hamiltonian $t_\alpha t_\beta/U \sim V_0\Delta$, which proves to be $\Delta \lesssim 10^{-3}$ as referred in the main text.

5.B Equations of motion and energy-momentum tensor for theories with higher derivatives

Here the problem of classical field theory with higher derivatives is addressed. The well know Euler Lagrange equation are derived by extremization of the action. The inclusion of higher derivatives on the Lagrangian lead to a reformulation of the equations. In fact by calculating explicitly $\delta S = 0$, integrating by parts whenever necessary one obtains:

$$\sum_{n=0}^{N} (-1)^n \, \partial_{\mu_1} \ldots \partial_{\mu_n} \frac{\partial \mathcal{L}}{\partial \left(\partial_{\mu_1} \ldots \partial_{\mu_n} \phi\right)} = 0 \tag{5.55}$$

where N is the highest number of derivatives appearing on a term of the Lagrangian. For $N = 1$ the usual Euler-Lagrange equations are recovered. Consider now a general translation $x^\mu \to x^\mu + \varepsilon^\mu$. The total change of the Lagrangian is

$$\delta\mathcal{L} = \frac{\delta\mathcal{L}}{\delta\left(\partial_{\mu_1} \ldots \partial_{\mu_n}\phi\right)} \delta\left(\partial_{\mu_1} \ldots \partial_{\mu_n}\phi\right). \tag{5.56}$$

which results in

$$\delta\mathcal{L} = \frac{\partial\mathcal{L}}{\partial\left(\partial_{\mu_1} \ldots \partial_{\mu_n}\phi\right)} \partial_\nu \partial_{\mu_1} \ldots \partial_{\mu_n}\phi\varepsilon^\nu. \tag{5.57}$$

The derivatives that are acting on ϕ can be written as acting on $\frac{\partial\mathcal{L}}{\partial\left(\partial_{\mu_1}\ldots\partial_{\mu_n}\phi\right)}$ with a minus sign plus a total derivative term. Explicitly this is:

$$\begin{aligned}\frac{\partial\mathcal{L}}{\partial\left(\partial_{\mu_1}\ldots\partial_{\mu_n}\phi\right)}\partial_\nu\partial_{\mu_1}\ldots\partial_{\mu_n}\phi =&\partial_{\mu_1}\left(\frac{\partial\mathcal{L}}{\partial\left(\partial_{\mu_1}\ldots\partial_{\mu_n}\phi\right)}\partial_{\mu_2}\ldots\partial_{\mu_n}\partial_\nu\phi\right)\\ &-\partial_{\mu_1}\frac{\partial\mathcal{L}}{\partial\left(\partial_{\mu_1}\ldots\partial_{\mu_n}\phi\right)}\partial_{\mu_2}\ldots\partial_{\mu_n}\partial_\nu\phi\end{aligned} \tag{5.58}$$

By continuing this process with every ∂_{μ_i} acting on ϕ one obtains:

$$\begin{aligned}&\tfrac{\partial\mathcal{L}}{\partial\left(\partial_{\mu_1}\ldots\partial_{\mu_n}\phi\right)}\partial_\nu\partial_{\mu_1}\ldots\partial_{\mu_n}\phi\\ &=\sum_{i=1}^{n}(-1)^{i-1}\,\partial_{\mu_i}\left(\partial_{\mu_1}\ldots\partial_{\mu_{i-1}}\tfrac{\partial\mathcal{L}}{\partial\left(\partial_{\mu_1}\ldots\partial_{\mu_n}\phi\right)}\partial_{\mu_{i+1}}\ldots\partial_{\mu_n}\partial_\nu\phi\right)+(-1)^n\,\partial_{\mu_1}\ldots\partial_{\mu_n}\tfrac{\partial\mathcal{L}}{\partial\left(\partial_{\mu_1}\ldots\partial_{\mu_n}\phi\right)}\partial_\nu\phi\end{aligned} \tag{5.59}$$

The special case of $n=0$ just gives $\frac{\partial\mathcal{L}}{\partial\phi}\partial_\nu\phi$. Summing over all n, the sum of the last terms of the above equation is identified with the equations of of motion 5.55 and therefore they are put to zero. What remains is the sum of total derivatives. This is equated to the variation of the Lagrangian which is given by: $\delta\mathcal{L}=\varepsilon^\nu\partial_\nu\mathcal{L}$. By rearranging the dummy variables one obtains:

$$\sum_{n=1}^{N}\sum_{i=1}^{n}(-1)^{i-1}\,\partial_{\mu_1}\left(\partial_{\mu_2}\ldots\partial_{\mu_i}\frac{\partial\mathcal{L}}{\partial\left(\partial_{\mu_1}\ldots\partial_{\mu_n}\phi\right)}\partial_{\mu_{i+1}}\ldots\partial_{\mu_n}\partial_\nu\phi\right)\varepsilon^\nu-\partial_{\mu_1}\mathcal{L}\delta^{\mu_1}_\nu\varepsilon^\nu=0 \tag{5.60}$$

This allows the identification of the energy-momentum tensor. This is just the conserved current that follows from Noether's theorem for the special case of space-time translations.

$$T^{\mu\nu}=\sum_{n=0}^{N}\sum_{i=0}^{n}(-1)^{i}\,\partial_{\mu_1}\ldots\partial_{\mu_i}\frac{\partial\mathcal{L}}{\partial\left(\partial_\mu\partial_{\mu_1}\ldots\partial_{\mu_n}\phi\right)}\partial_{\mu_{i+1}}\ldots\partial_{\mu_n}\partial^\nu\phi-\mathcal{L}\eta^{\mu\nu} \tag{5.61}$$

Conclusions

Due to the complexity of certain physical problems, in particular of strongly correlated many-body systems, quantum simulations have been the subject of intense research in the last two decades. The obtained progress and developments in this research field are of particularly importance in view of the fact that classical computation is fundamentally limited in solving certain quantum mechanical problems.

One of the holy grails of quantum simulations is Quantum Chromodynamics (QCD) and at this stage can only be a long-time goal. Regarding lattice QCD simulations, there are, for example, fundamental limitations in the Monte Carlo method for finite baryon density due to complex actions problems. Before being able to deal with such a complicated problem one should try first to build simpler examples containing fundamental pieces of a more complex implementation and that, in many cases, are capable of reproduce qualitatively the results expected for QCD. In this regard, the Schwinger model is a paradigmatic example of this principle: it has a simple gauge group ($U(1)$), a simple structure (it is a $1+1$ model which simplifies considerably gauge dynamics for example) and still exhibits QCD-like phenomena like fermion confinement and chiral symmetry breaking. Despite that, the implementation of a lattice version of it is still a great challenge for current experiments with the first implementation made just last year for a small system size. The situation will hopefully improve in the future with both theoretical and experimental developments. From a theoretical point of view it is fundamental to have suitable formulations of the theory that are adequate to experimental implementation. Quantum link models are an example of such situation where the infinite Hilbert space per lattice link is replaced by a finite one.

In this spirit, in Section 2.3 it is proposed that half of the gauge symmetries typically required for the implementation of the Schwinger model could be dropped without affecting the results of the quantum simulation. In fact, with some careful analysis, one sees that half of the number of generators, i.e. half of the symmetries, typically required in a lattice version of the model will disappear in the naive continuum limit. The statement goes beyond the simple naive quantum limit argument. In fact, the Schwinger model in the continuum limit does not have these extra symmetries therefore, if the usual Kogut-Susskind Hamiltonian adopted for the Schwinger model is to reproduce the continuum results in the limit of small lattice spacing, these symmetries *must* disappear. Other versions of this statement are expected to be found for other group symmetries and in higher dimensionality. In this regard it is not only useful, resource wise, to drop this symmetry. In fact, in the spirit of universality, it is desirable that the theory is regularized having the symmetries, and only those symmetries, that one wishes to find in the continuum model. Introducing more symmetries than desired may bias the system towards a slower convergence to the desired continuum limit, or worst, prevent it from reaching the desired theory on this limit. These are general remarks. A careful analysis must be done case-by-case as it is also known, in the spirit of improved actions, that adding terms that go to zero in the continuum limit may help remove lattice artifacts. This subject is currently under investigation. It is shown, however, that such alternative formulations can provide new solutions to quantum simulations that are not just a result of taking previous proposals and eliminate the dynamics of half of the links. Such scenario may considerably help their experimental realization.

In Chapters 3-5 it was considered several aspects of the simulations of field and gauge theories,

in particular with phenomena ispired by QCD. In Chapter 3 it was studied a simple model having common features with color-flavor locking, which is a remarkable phenomenon in QCD. This is an area that Monte Carlo simulations cannot reach due to severe sign problems. The phase expected to find in this limit is the so called Color-Flavor-Locking (CFL) phase, where the $SU(3)$ color symmetry and the $SU(3)$ flavor symmetries get locked together in a smaller symmetry group. Having in mind an ultracold atom setting capable of capturing the essence of the symmetry-locking mechanism, a model of a four fermion mixture was considered. In this model, the locking of symmetries is between two $SU(2)$ symmetries. Furthermore, they are global symmetries, while in QCD only the flavor symmetry is global. Nonetheless the fundamental principle of symmetry locking is present. In fact, by exploring the phase diagram of the model, it is found a vast region of the parameter space where the ground state corresponds to a locked phase, to which is refered to as Two Flavors Symmetry Locked (TFSL) phase. In this phase the system is characterized by an order parameter that breaks partially the total $SU(2) \times SU(2)$ symmetry to a single $SU(2)$ but which is composed by a suitable combination of the two initially independent symmetries. While alkaline-earth atoms are ideal to simulate this kind of systems due to the fact that their interactions do not depend on the hyperfine quantum number, the difficulty to tune interactions in earth-alkaline atomic gases without spoiling their peculiar $U(N)$ invariance is well known. Notably it is found that, taking the example of an Ytterbium mixture of ^{171}Yb and ^{173}Yb, such system naturally exhibits interactions that fall into the TFSL phase. Since the critical temperature for the appearance of this phase is of the same order of the temperatures studied in current-day experiments, the TSFL phase as a consequence is expected to be achievable in realistic ultracold setups.

As argued above, the path towards QCD and other complicated theories, is envisioned in a step-by-step basis, where one is able to, in each step, add further ingredients that ultimately would lead to the final goal. This would not exclude the certainty of finding interesting physics in between and, in particular, phenomena that are characteristic of only these "intermediate" steps. Theories with dimensional mismatch, which find applications in systems like graphene, can potentially be part of this path. In these kind of theories described in Chapter 4 the gauge fields live in an higher dimension $(D+1)$ than the fermion fields $(d+1)$. A natural step, after implementing the Schwinger model, would consist on keeping the fermions in $d=1$ but let the gauge fields be present in $D=2$. This is a non-trivial step as one needs to implement plaquette term for the dynamics of gauge fields. However the matter-gauge correlated hopping is restricted to one dimension and experimental implementations are expected to be simpler than Quantum Electrodynamics (QED) in $2+1$ dimensions. Irrespective of that, these models naturally provide a playground where effective non-local theories can be constructed by integration of the gauge fields. Using bosonization and several gauge fields in higher dimensionality one can construct, with some generality, different fermionic interaction terms on the Lagrangian, as well as bosonic kinetic terms. Such mappings provide a consistent way of establishing a relation between local theories and non-local ones, with particularly emphasis on long-range (LR) interactions. These mappings can be useful by providing insights into the physics of certain LR interacting systems by using well established results of local field theories like Lieb-Robinson bounds. Such formalism is difficult to establish at the Hamiltonian level but are easier to be carried out at the Lagrangian level. It is shown that, under certain condition, an Hamiltonian can be reconstructed from the effective Lagrangian giving a comprehensive path between an initial a) Hamiltonian - b) Lagrangian - c) Effective Lagrangian - d) Effective Hamiltonian. In a) one has some local Hamiltonian describing a theory that is then formulated in term of a path integral in b). By integrating some degrees of freedom one obtains a non-local effective Lagrangian c) which, under certain circumstances, admit a canonical quantization building an effective Hamiltonian d). Not only this mapping is interesting from the point of view of using results of local theories, but can also serve the implementation of LR interacting theories. In settings, like in ultracold atomic system, local interactions are naturally available while LR ones are not. In this way, this also provides a path towards implementation of tunable LR interactions between fermions or spin systems. From this point of view gauge invariance does not seem like a crucial ingredient of these proposals and one can envision future schemes, much more experimentally

feasible since no gauge symmetry is required, that still could implement the desired LR interactions (like $1/r$ Coulomb interaction).

The study of properties of dimensional mismatch with a gauge symmetry has then clear applications. If by one side analytical and numerical results are important for comparison with experiments, also the models itself can host interesting phenomena. An example of this is given in Chapter 5 where the confinement properties of these models with $d = 1$ and $D = 2, 3$ are investigated. The confinement on the Schwinger model is intuitively explained by the fact that the lower dimensional gauge fields generate linear potential between static charges. The results of this Chapter show that the situation is more subtle than that, as expanding the gauge fields to higher dimensions does not deconfine the system. This raises questions about the nature of confinenement, at least for one dimensional fermions, since this seems to be the key ingredient for this to happen. An interesting question consists into understanding how much can one increase the size of the system in the perpendicular dimensions before spoiling confinement. These results also highlight another advantage of the implementation of dimensional mismatch models in the context of quantum simulations of gauge theories: they provide very non-trivial model (with plaquette terms involved) where analytical non-perturbative computations are possible. This kind of situation is ideal to benchmark future quantum simulators.

The field of quantum simulations of gauge theories is still in an initial stage. In the future both experimental and theoretical developments are expected in order to achieve the long time goal of simulating QCD and other complicated theories. From the theoretical side, one should be able to find suitable toy models, characterize them (as much as one can) and identify mechanisms and suitable mappings between target and controllable degrees of freedom. If the final reward looks very appealing, one is also promised to find and learn a lot of interesting physics along the way.

Publications

During the period of this work, three publications were prepared. One published already in a peer-reviewed journal, one in arXiv and another in preparation which should be finished in the following weeks.

1. Joao C. Pinto Barros, Luca Lepori, and Andrea Trombettoni. Phase diagram and non-abelian symmetry locking for fermionic mixtures with unequal interactions. *Physical Review A*, 96(1), jul 2017.

2. Joao C Pinto Barros, Marcello Dalmonte, and Andrea Trombettoni. Long-range interactions from $U(1)$ gauge fields via dimensional mismatch. *arXiv preprint arXiv:1708.06585*, 2017.

3. Joao C. Pinto Barros, Marcello Dalmonte, and Andrea Trombettoni. Robustness of confinement properties of schwinger-thirring models. *To be submitted*, 2017.

Acknowledgements

I would like to express my gratitude and appreciation to Andrea Trombettoni for following me through these last three years. Apart from all physics I have learned with him, I would like to extend my thankfulness for his care and advisement. This extends beyond the realm of physics right to the domain of friendship. I also would like to thank Marcello Dalmonte with whom I started to work later on but whom I feel played a fundamental role during my PhD, either by his availability or by the enthusiastic way in which he discussed physics. I would like to thank Luca Lepori for his availability for long skype hours in order to finish the work and his care for detail.

I would like to express my gratitude to Uwe-Jens Wiese that readily received me in Bern. Despite being there for just two months, the time he spent teaching and discussing with me made me feel I learned much more than I would expect in 60 days. I also extend my gratitude to the whole group, which received me very well and with whom I also had the opportunity to discuss. I thank equally Constança Providencia and Silvia Chiacchiera for receiving me in Coimbra and for the availability on working together.

I am grateful to all the people I met and the nice stimulating environment that I found at SISSA. I should remark that nothing helps me clear my mind more than a good football match. Therefore, I specially thank all the people I shared the pitch in the SISSA football team.

I also have to thank all my familly for receiving me enthusiastically everytime I went back home. But a very special reference must be made to my parents. With my father I share the passion of for science and understanding. Since I was very young he was able to captivate me to the wonders of nature, which helped choose this path. Throughout my school years the support from my mother was omnipresent and and very important to me. I will probably never forget the image of her by my side, leaning over my desk while I was doing my first homeworks (and likelly my first calculations), while my brother was jumping on her back.

My greatest support during these four years was always from Joana. With her great times become better, hard times are not so bad. She is the reason why I never really had that much hard times during my PhD. Her advice, her support, her comprehension, I will allways hold most dear.

Bibliography

[1] Immanuel Bloch, Jean Dalibard, and Sylvain Nascimbene. Quantum simulations with ultracold quantum gases. *Nature Physics*, 8(4):267, 2012.

[2] Maciej Lewenstein, Anna Sanpera, and Verònica Ahufinger. *Ultracold Atoms in Optical Lattices: Simulating quantum many-body systems*. Oxford University Press, 2012.

[3] Richard P Feynman. Simulating physics with computers. *International journal of theoretical physics*, 21(6):467–488, 1982.

[4] Elliott H. Lieb. The hubbard model: Some rigorous results and open problems. In *NATO ASI Series*, pages 1–19. Springer US, 1995.

[5] Claudine Lacroix, Philippe Mendels, and Frédéric Mila. *Introduction to Frustrated Magnetism: Materials, Experiments, Theory*. Springer, 2013.

[6] Alexander W Glaetzle, Marcello Dalmonte, Rejish Nath, Ioannis Rousochatzakis, Roderich Moessner, and Peter Zoller. Quantum spin-ice and dimer models with rydberg atoms. *Physical Review X*, 4(4):041037, 2014.

[7] A Yu Kitaev. Fault-tolerant quantum computation by anyons. *Annals of Physics*, 303(1):2–30, 2003.

[8] Chetan Nayak, Steven H. Simon, Ady Stern, Michael Freedman, and Sankar Das Sarma. Non-abelian anyons and topological quantum computation. *Reviews of Modern Physics*, 80(3):1083–1159, sep 2008.

[9] Wilfried Buchmüller and Christoph Lüdeling. Field theory and standard model. *arXiv preprint hep-ph/0609174*, 2006.

[10] Michael Edward Peskin. *An introduction to quantum field theory*. Westview press, 1995.

[11] Michael Creutz. *Quarks, gluons and lattices*, volume 8. Cambridge University Press, 1983.

[12] Uwe-Jens Wiese. Towards quantum simulating qcd. *Nuclear Physics A*, 931:246–256, 2014.

[13] Julian Schwinger. Gauge invariance and mass. ii. *Phys. Rev.*, 128:2425–2429, Dec 1962.

[14] Yitzhak Frishman and Jacob Sonnenschein. *Non-Perturbative Field Theory*. Cambridge University Press, 2009.

[15] Esteban A Martinez, Christine A Muschik, Philipp Schindler, Daniel Nigg, Alexander Erhard, Markus Heyl, Philipp Hauke, Marcello Dalmonte, Thomas Monz, Peter Zoller, et al. Real-time dynamics of lattice gauge theories with a few-qubit quantum computer. *Nature*, 534(7608):516–519, 2016.

[16] Joao C. Pinto Barros, Luca Lepori, and Andrea Trombettoni. Phase diagram and non-abelian symmetry locking for fermionic mixtures with unequal interactions. *Physical Review A*, 96(1), jul 2017.

[17] Joao C Pinto Barros, Marcello Dalmonte, and Andrea Trombettoni. Long-range interactions from $u(1)$ gauge fields via dimensional mismatch. *arXiv preprint arXiv:1708.06585*, 2017.

[18] Joao C. Pinto Barros, Marcello Dalmonte, and Andrea Trombettoni. Robustness of confinement properties of schwinger-thirring models. *To be published*, 2017.

[19] N David Mermin and Herbert Wagner. Absence of ferromagnetism or antiferromagnetism in one-or two-dimensional isotropic heisenberg models. *Phys. Rev. Lett.*, 17(22):1133, 1966.

[20] PC Hohenberg. Existence of long-range order in one and two dimensions. *Phys. Rev.*, 158(2):383, 1967.

[21] Anna Vershynina and Elliott H Lieb. Lieb-robinson bounds. *Scholarpedia*, 8(9):31267, 2013.

[22] Philip W Anderson et al. More is different. *Science*, 177(4047):393–396, 1972.

[23] Reuven Y Rubinstein and Dirk P Kroese. *Simulation and the Monte Carlo method*, volume 10. John Wiley & Sons, 2016.

[24] Matthias Troyer and Uwe-Jens Wiese. Computational complexity and fundamental limitations to fermionic quantum monte carlo simulations. *Physical review letters*, 94(17):170201, 2005.

[25] Ulrich Schollwöck. The density-matrix renormalization group in the age of matrix product states. *Annals of Physics*, 326(1):96–192, 2011.

[26] J Ignacio Cirac and Frank Verstraete. Renormalization and tensor product states in spin chains and lattices. *Journal of Physics A: Mathematical and Theoretical*, 42(50):504004, 2009.

[27] R Augusiak, FM Cucchietti, and M Lewenstein. Many-body physics from a quantum information perspective. In *Modern Theories of Many-Particle Systems in Condensed Matter Physics*, pages 245–294. Springer, 2012.

[28] L. Tagliacozzo and G. Vidal. Entanglement renormalization and gauge symmetry. *Physical Review B*, 83(11), mar 2011.

[29] M.C. Banuls, K. Cichy, J.I. Cirac, and K. Jansen. The mass spectrum of the schwinger model with matrix product states. *Journal of High Energy Physics*, 2013(11), nov 2013.

[30] E Rico, T Pichler, M Dalmonte, P Zoller, and S Montangero. Tensor networks for lattice gauge theories and atomic quantum simulation. *Physical Review Letters*, 112(20):201601, 2014.

[31] L. Tagliacozzo, A. Celi, and M. Lewenstein. Tensor networks for lattice gauge theories with continuous groups. *Physical Review X*, 4(4), nov 2014.

[32] Boye Buyens, Jutho Haegeman, Karel Van Acoleyen, Henri Verschelde, and Frank Verstraete. Matrix product states for gauge field theories. *Physical Review Letters*, 113(9), aug 2014.

[33] Stefan Kühn, J. Ignacio Cirac, and Mari-Carmen Bañuls. Quantum simulation of the schwinger model: A study of feasibility. *Physical Review A*, 90(4), oct 2014.

[34] Pietro Silvi, Enrique Rico, Tommaso Calarco, and Simone Montangero. Lattice gauge tensor networks. *New Journal of Physics*, 16(10):103015, oct 2014.

[35] M. C. Banuls, K. Cichy, J. I. Cirac, K. Jansen, and H. Saito. Thermal evolution of the schwinger model with matrix product operators. *Physical Review D*, 92(3), aug 2015.

[36] Stefan Kühn, Erez Zohar, J. Ignacio Cirac, and Mari Carmen Bañuls. Non-abelian string breaking phenomena with matrix product states. *Journal of High Energy Physics*, 2015(7), jul 2015.

[37] Erez Zohar and Michele Burrello. Formulation of lattice gauge theories for quantum simulations. *Physical Review D*, 91(5), mar 2015.

[38] Erez Zohar, Michele Burrello, Thorsten B. Wahl, and J. Ignacio Cirac. Fermionic projected entangled pair states and local u(1) gauge theories. *Annals of Physics*, 363:385–439, dec 2015.

[39] Simone Notarnicola, Elisa Ercolessi, Paolo Facchi, Giuseppe Marmo, Saverio Pascazio, and Francesco V Pepe. Discrete abelian gauge theories for quantum simulations of qed. *Journal of Physics A: Mathematical and Theoretical*, 48(30):30FT01, 2015.

[40] T. Pichler, M. Dalmonte, E. Rico, P. Zoller, and S. Montangero. Real-time dynamics in u(1) lattice gauge theories with tensor networks. *Physical Review X*, 6(1), mar 2016.

[41] Erez Zohar and Michele Burrello. Building projected entangled pair states with a local gauge symmetry. *New Journal of Physics*, 18(4):043008, apr 2016.

[42] Pietro Silvi, Enrique Rico, Marcello Dalmonte, Ferdinand Tschirsich, and Simone Montangero. Finite-density phase diagram of a (1+ 1)-d non-abelian lattice gauge theory with tensor networks. *arXiv preprint arXiv:1606.05510*, 2016.

[43] Kai Zapp and Roman Orus. Tensor network simulation of qed on infinite lattices: learning from (1+ 1) d, and prospects for (2+ 1) d. *arXiv preprint arXiv:1704.03015*, 2017.

[44] Román Orús. A practical introduction to tensor networks: Matrix product states and projected entangled pair states. *Annals of Physics*, 349:117–158, 2014.

[45] M Dalmonte and S Montangero. Lattice gauge theory simulations in the quantum information era. *Contemporary Physics*, 57(3):388–412, 2016.

[46] Abner Shimony. Bell's theorem. In Edward N. Zalta, editor, *The Stanford Encyclopedia of Philosophy*. Metaphysics Research Lab, Stanford University, fall 2017 edition, 2017.

[47] J. Ignacio Cirac and Peter Zoller. Goals and opportunities in quantum simulation. *Nature Physics*, 8(4):264–266, apr 2012.

[48] Fabien Alet, Kedar Damle, and Sumiran Pujari. Sign-problem-free monte carlo simulation of certain frustrated quantum magnets. *Physical review letters*, 117(19):197203, 2016.

[49] M Alford, S Chandrasekharan, J Cox, and U-J Wiese. Solution of the complex action problem in the potts model for dense qcd. *Nuclear Physics B*, 602(1):61–86, 2001.

[50] Emilie Fulton Huffman and Shailesh Chandrasekharan. Solution to sign problems in half-filled spin-polarized electronic systems. *Physical Review B*, 89(11):111101, 2014.

[51] Michael L Wall. *Quantum Many-body Physics of Ultracold Molecules in Optical Lattices: Models and Simulation Methods*. Springer, 2015.

[52] Henk TC Stoof, Koos B Gubbels, and Dennis BM Dickerscheid. *Ultracold quantum fields*, volume 1. Springer, 2009.

[53] Immanuel Bloch, Jean Dalibard, and Wilhelm Zwerger. Many-body physics with ultracold gases. *Reviews of modern physics*, 80(3):885, 2008.

[54] Maciej Lewenstein, Anna Sanpera, Veronica Ahufinger, Bogdan Damski, Aditi Sen(De), and Ujjwal Sen. Ultracold atomic gases in optical lattices: mimicking condensed matter physics and beyond. *Advances in Physics*, 56(2):243–379, mar 2007.

[55] Giacomo Valtolina, Alessia Burchianti, Andrea Amico, Elettra Neri, Klejdja Xhani, Jorge Amin Seman, Andrea Trombettoni, Augusto Smerzi, Matteo Zaccanti, Massimo Inguscio, et al. Josephson effect in fermionic superfluids across the bec-bcs crossover. *Science*, 350(6267):1505–1508, 2015.

[56] Markus Greiner, Olaf Mandel, Tilman Esslinger, Theodor W Hänsch, and Immanuel Bloch. Quantum phase transition from a superfluid to a mott insulator in a gas of ultracold atoms. *nature*, 415(6867):39–44, 2002.

[57] Eugene Demler and Fei Zhou. Spinor bosonic atoms in optical lattices: Symmetry breaking and fractionalization. *Physical Review Letters*, 88(16), apr 2002.

[58] M. Lewenstein, L. Santos, M. A. Baranov, and H. Fehrmann. Atomic bose-fermi mixtures in an optical lattice. *Physical Review Letters*, 92(5), feb 2004.

[59] J. J. García-Ripoll, M. A. Martin-Delgado, and J. I. Cirac. Implementation of spin hamiltonians in optical lattices. *Physical Review Letters*, 93(25), dec 2004.

[60] Dieter Jaksch and Peter Zoller. Creation of effective magnetic fields in optical lattices: the hofstadter butterfly for cold neutral atoms. *New Journal of Physics*, 5(1):56, 2003.

[61] Anders S. Sørensen, Eugene Demler, and Mikhail D. Lukin. Fractional quantum hall states of atoms in optical lattices. *Physical Review Letters*, 94(8), mar 2005.

[62] J. Ruseckas, G. Juzeliūnas, P. Öhberg, and M. Fleischhauer. Non-abelian gauge potentials for ultracold atoms with degenerate dark states. *Physical Review Letters*, 95(1), jun 2005.

[63] Belén Paredes and Immanuel Bloch. Minimum instances of topological matter in an optical plaquette. *Physical Review A*, 77(2), feb 2008.

[64] L. J. Garay, J. R. Anglin, J. I. Cirac, and P. Zoller. Sonic black holes in dilute bose-einstein condensates. *Physical Review A*, 63(2), jan 2001.

[65] Carlos Barcelo, Stefano Liberati, and Matt Visser. Analogue gravity from bose-einstein condensates. *Classical and Quantum Gravity*, 18(6):1137, 2001.

[66] Uwe Fischer and Ralf Schützhold. Quantum simulation of cosmic inflation in two-component bose-einstein condensates. *Physical Review A*, 70(6), dec 2004.

[67] R. Gerritsma, G. Kirchmair, F. Zähringer, E. Solano, R. Blatt, and C. F. Roos. Quantum simulation of the dirac equation. *Nature*, 463(7277):68–71, jan 2010.

[68] L. Lepori, G. Mussardo, and A. Trombettoni. (3+1) massive dirac fermions with ultracold atoms in frustrated cubic optical lattices. *EPL (Europhysics Letters)*, 92(5):50003, dec 2010.

[69] Yue Yu and Kun Yang. Supersymmetry and the goldstino-like mode in bose-fermi mixtures. *Physical Review Letters*, 100(9), mar 2008.

[70] Yue Yu and Kun Yang. Simulating the wess-zumino supersymmetry model in optical lattices. *Physical Review Letters*, 105(15), oct 2010.

[71] T. Shi, Yue Yu, and C. P. Sun. Supersymmetric response of a bose-fermi mixture to photoassociation. *Physical Review A*, 81(1), jan 2010.

[72] O. Boada, A. Celi, J. I. Latorre, and M. Lewenstein. Quantum simulation of an extra dimension. *Physical Review Letters*, 108(13), mar 2012.

[73] Jun John Sakurai and Eugene D Commins. Modern quantum mechanics, revised edition, 1995.

[74] Kerson Huang and Chen Ning Yang. Quantum-mechanical many-body problem with hard-sphere interaction. *Physical review*, 105(3):767, 1957.

[75] C. J. Pethick and H. Smith. *Bose–Einstein Condensation in Dilute Gases*. Cambridge University Press, 2008.

[76] Dieter Jaksch and Peter Zoller. The cold atom hubbard toolbox. *Annals of physics*, 315(1):52–79, 2005.

[77] Neil W Ashcroft and N David Mermin. Solid state physics (holt, rinehart and winston, new york, 1976). *Google Scholar*, 403, 2005.

[78] Walter Kohn. Analytic properties of bloch waves and wannier functions. *Physical Review*, 115(4):809, 1959.

[79] AJ Moerdijk, BJ Verhaar, and A Axelsson. Resonances in ultracold collisions of li 6, li 7, and na 23. *Physical Review A*, 51(6):4852, 1995.

[80] Herman Feshbach. Unified theory of nuclear reactions. *Annals of Physics*, 5(4):357–390, 1958.

[81] Herman Feshbach. A unified theory of nuclear reactions. ii. *Annals of Physics*, 19(2):287–313, 1962.

[82] Ugo Fano. Effects of configuration interaction on intensities and phase shifts. *Physical Review*, 124(6):1866, 1961.

[83] Cheng Chin, Rudolf Grimm, Paul Julienne, and Eite Tiesinga. Feshbach resonances in ultracold gases. *Reviews of Modern Physics*, 82(2):1225, 2010.

[84] John Bardeen, Leon N Cooper, and John Robert Schrieffer. Theory of superconductivity. *Physical Review*, 108(5):1175, 1957.

[85] Mohit Randeria, W Zwerger, and M Zwierlein. The bcs–bec crossover and the unitary fermi gas. In *The BCS-BEC Crossover and the Unitary Fermi Gas*, pages 1–32. Springer, 2012.

[86] Qijin Chen, Jelena Stajic, Shina Tan, and Kathryn Levin. Bcs–bec crossover: From high temperature superconductors to ultracold superfluids. *Physics Reports*, 412(1):1–88, 2005.

[87] Sylvain Nascimbene, Nir Navon, Kaijun Jiang, Frédéric Chevy, and Christophe Salomon. Exploring the thermodynamics of a universal fermi gas. *arXiv preprint arXiv:0911.0747*, 2009.

[88] Kris Van Houcke, Félix Werner, Evgeny Kozik, Nikolay Prokofev, Boris Svistunov, MJH Ku, AT Sommer, LW Cheuk, Andre Schirotzek, and MW Zwierlein. Feynman diagrams versus fermi-gas feynman emulator. *arXiv preprint arXiv:1110.3747*, 2011.

[89] Matthew PA Fisher, Peter B Weichman, G Grinstein, and Daniel S Fisher. Boson localization and the superfluid-insulator transition. *Physical Review B*, 40(1):546, 1989.

[90] Dieter Jaksch, Ch Bruder, Juan Ignacio Cirac, Crispin W Gardiner, and Peter Zoller. Cold bosonic atoms in optical lattices. *Physical Review Letters*, 81(15):3108, 1998.

[91] MJ Mark, Elmar Haller, K Lauber, JG Danzl, AJ Daley, and H-C Nägerl. Precision measurements on a tunable mott insulator of ultracold atoms. *Physical review letters*, 107(17):175301, 2011.

[92] Jacob F Sherson, Christof Weitenberg, Manuel Endres, Marc Cheneau, Immanuel Bloch, and Stefan Kuhr. Single-atom resolved fluorescence imaging of an atomic mott insulator. *arXiv preprint arXiv:1006.3799*, 2010.

[93] Erez Berg, Emanuele G Dalla Torre, Thierry Giamarchi, and Ehud Altman. Rise and fall of hidden string order of lattice bosons. *Physical Review B*, 77(24):245119, 2008.

[94] Manuel Endres, Marc Cheneau, Takeshi Fukuhara, Christof Weitenberg, Peter Schauss, Christian Gross, Leonardo Mazza, Mari Carmen Banuls, L Pollet, Immanuel Bloch, et al. Observation of correlated particle-hole pairs and string order in low-dimensional mott insulators. *Science*, 334(6053):200–203, 2011.

[95] David J Gross and Frank Wilczek. Ultraviolet behavior of non-abelian gauge theories. *Physical Review Letters*, 30(26):1343, 1973.

[96] Harald Fritzsch, Murray Gell-Mann, and Heinrich Leutwyler. Advantages of the color octet gluon picture. *Physics Letters B*, 47(4):365–368, 1973.

[97] H David Politzer. Reliable perturbative results for strong interactions? *Physical Review Letters*, 30(26):1346, 1973.

[98] H.B. Nielsen and M. Ninomiya. A no-go theorem for regularizing chiral fermions. *Physics Letters B*, 105(2-3):219–223, oct 1981.

[99] H.B. Nielsen and M. Ninomiya. Absence of neutrinos on a lattice. *Nuclear Physics B*, 185(1):20–40, jul 1981.

[100] H.B. Nielsen and M. Ninomiya. Absence of neutrinos on a lattice. *Nuclear Physics B*, 193(1):173–194, dec 1981.

[101] D Horn. Finite matrix models with continuous local gauge invariance. *Physics Letters B*, 100(2):149–151, 1981.

[102] Peter Orland and Daniel Rohrlich. Lattice gauge magnets: Local isospin from spin. *Nuclear Physics B*, 338(3):647–672, 1990.

[103] Peter Orland. Exact solution of a quantum gauge magnet in 2+ 1 dimensions. *Nuclear Physics B*, 372(3):635–653, 1992.

[104] Shailesh Chandrasekharan and U-J Wiese. Quantum link models: A discrete approach to gauge theories. *Nuclear Physics B*, 492(1-2):455–471, 1997.

[105] R Brower, Shailesh Chandrasekharan, and U-J Wiese. Qcd as a quantum link model. *Physical Review D*, 60(9):094502, 1999.

[106] R Brower, S Chandrasekharan, S Riederer, and U-J Wiese. D-theory: field quantization by dimensional reduction of discrete variables. *Nuclear physics B*, 693(1):149–175, 2004.

[107] U-J Wiese. Ultracold quantum gases and lattice systems: quantum simulation of lattice gauge theories. *Annalen der Physik*, 525(10-11):777–796, 2013.

[108] Erez Zohar, J Ignacio Cirac, and Benni Reznik. Quantum simulations of lattice gauge theories using ultracold atoms in optical lattices. *Reports on Progress in Physics*, 79(1):014401, 2015.

[109] Jean Bellissard, Andreas van Elst, and Hermann Schulz-Baldes. The noncommutative geometry of the quantum hall effect. *Journal of Mathematical Physics*, 35(10):5373–5451, 1994.

[110] Daijiro Yoshioka. *The quantum Hall effect*, volume 133. Springer Science & Business Media, 2013.

[111] Jainendra K Jain. *Composite fermions*. Cambridge University Press, 2007.

[112] B Andrei Bernevig and Taylor L Hughes. *Topological insulators and topological superconductors*. Princeton University Press, 2013.

[113] Ching-Kai Chiu, Jeffrey CY Teo, Andreas P Schnyder, and Shinsei Ryu. Classification of topological quantum matter with symmetries. *Reviews of Modern Physics*, 88(3):035005, 2016.

[114] Emil Prodan and Hermann Schulz-Baldes. Bulk and boundary invariants for complex topological insulators. *arXiv preprint arXiv:1510.08744*, 2016.

[115] Douglas R Hofstadter. Energy levels and wave functions of bloch electrons in rational and irrational magnetic fields. *Physical review B*, 14(6):2239, 1976.

[116] DJ Thouless, Mahito Kohmoto, MP Nightingale, and M Den Nijs. Quantized hall conductance in a two-dimensional periodic potential. *Physical Review Letters*, 49(6):405, 1982.

[117] MC Geisler, JH Smet, V Umansky, K Von Klitzing, B Naundorf, R Ketzmerick, and H Schweizer. Detection of landau band coupling induced rearrangement of the hofstadter butterfly. *Physica E: Low-dimensional Systems and Nanostructures*, 25(2):227–232, 2004.

[118] Sorin Melinte, Mona Berciu, Chenggang Zhou, E Tutuc, SJ Papadakis, C Harrison, EP De Poortere, Mingshaw Wu, PM Chaikin, M Shayegan, et al. Laterally modulated 2d electron system in the extreme quantum limit. *Physical review letters*, 92(3):036802, 2004.

[119] Thomas Feil, K Vỳbornỳ, L Smrčka, Christian Gerl, and Werner Wegscheider. Vanishing cyclotron gaps in a two-dimensional electron system with a strong short-period modulation. *Physical Review B*, 75(7):075303, 2007.

[120] RV Gorbachev, GL Yu, DC Elias, R Jalil, AA Patel, A Mishchenko, AS Mayorov, CR Woods, JR Wallbank, M Mucha-Kruczynski, et al. Cloning of dirac fermions in graphene superlattices. *Nature*, 2013.

[121] Jean Dalibard, Fabrice Gerbier, Gediminas Juzeliūnas, and Patrik Öhberg. Colloquium: Artificial gauge potentials for neutral atoms. *Reviews of Modern Physics*, 83(4):1523, 2011.

[122] J Dalibard. Introduction to the physics of artificial gauge fields. *Quantum Matter at Ultralow Temperatures*, 2015.

[123] Michele Burrello, Luca Lepori, Simone Paganelli, and Andrea Trombettoni. Abelian gauge potentials on cubic lattices. *arXiv preprint arXiv:1706.02228*, 2017.

[124] Yakir Aharonov and David Bohm. Significance of electromagnetic potentials in the quantum theory. *Physical Review*, 115(3):485, 1959.

[125] Michael V Berry. Quantal phase factors accompanying adiabatic changes. In *Proceedings of the Royal Society of London A: Mathematical, Physical and Engineering Sciences*, volume 392, pages 45–57. The Royal Society, 1984.

[126] R Dum and M Olshanii. Gauge structures in atom-laser interaction: Bloch oscillations in a dark lattice. *Physical review letters*, 76(11):1788, 1996.

[127] PM Visser and G Nienhuis. Geometric potentials for subrecoil dynamics. *Physical Review A*, 57(6):4581, 1998.

[128] S. K. Dutta, B. K. Teo, and G. Raithel. Tunneling dynamics and gauge potentials in optical lattices. *Physical Review Letters*, 83(10):1934–1937, sep 1999.

[129] Y.-J. Lin, R. L. Compton, K. Jiménez-García, J. V. Porto, and I. B. Spielman. Synthetic magnetic fields for ultracold neutral atoms. *Nature*, 462(7273):628–632, dec 2009.

[130] N Goldman and J Dalibard. Periodically driven quantum systems: effective hamiltonians and engineered gauge fields. *Physical Review X*, 4(3):031027, 2014.

[131] J. Struck, C. Ölschläger, M. Weinberg, P. Hauke, J. Simonet, A. Eckardt, M. Lewenstein, K. Sengstock, and P. Windpassinger. Tunable gauge potential for neutral and spinless particles in driven optical lattices. *Physical Review Letters*, 108(22), may 2012.

[132] M. Aidelsburger, M. Atala, S. Nascimbène, S. Trotzky, Y.-A. Chen, and I. Bloch. Experimental realization of strong effective magnetic fields in an optical lattice. *Physical Review Letters*, 107(25), dec 2011.

[133] N. Goldman, J. Dalibard, M. Aidelsburger, and N. R. Cooper. Periodically driven quantum matter: The case of resonant modulations. *Physical Review A*, 91(3), mar 2015.

[134] M. Aidelsburger, M. Lohse, C. Schweizer, M. Atala, J. T. Barreiro, S. Nascimbène, N. R. Cooper, I. Bloch, and N. Goldman. Measuring the chern number of hofstadter bands with ultracold bosonic atoms. *Nature Physics*, 11(2):162–166, dec 2014.

[135] M. Aidelsburger, M. Atala, M. Lohse, J. T. Barreiro, B. Paredes, and I. Bloch. Realization of the hofstadter hamiltonian with ultracold atoms in optical lattices. *Physical Review Letters*, 111(18), oct 2013.

[136] Hirokazu Miyake, Georgios A. Siviloglou, Colin J. Kennedy, William Cody Burton, and Wolfgang Ketterle. Realizing the harper hamiltonian with laser-assisted tunneling in optical lattices. *Physical Review Letters*, 111(18), oct 2013.

[137] Hendrik Weimer, Markus Müller, Igor Lesanovsky, Peter Zoller, and Hans Peter Büchler. A rydberg quantum simulator. *Nature Physics*, 6(5):382–388, mar 2010.

[138] L Tagliacozzo, A Celi, A Zamora, and M Lewenstein. Optical abelian lattice gauge theories. *Annals of Physics*, 330:160–191, 2013.

[139] D. Banerjee, M. Dalmonte, M. Müller, E. Rico, P. Stebler, U.-J. Wiese, and P. Zoller. Atomic quantum simulation of dynamical gauge fields coupled to fermionic matter: From string breaking to evolution after a quench. *Physical Review Letters*, 109(17), oct 2012.

[140] V Kasper, Florian Hebenstreit, MK Oberthaler, and J Berges. Schwinger pair production with ultracold atoms. *Physics Letters B*, 760:742–746, 2016.

[141] Eliot Kapit and Erich Mueller. Optical-lattice hamiltonians for relativistic quantum electrodynamics. *Physical Review A*, 83(3):033625, 2011.

[142] Erez Zohar, J Ignacio Cirac, and Benni Reznik. Simulating (2+ 1)-dimensional lattice qed with dynamical matter using ultracold atoms. *Physical review letters*, 110(5):055302, 2013.

[143] Alexei Bazavov, Yannick Meurice, S-W Tsai, Judah Unmuth-Yockey, and Jin Zhang. Gauge-invariant implementation of the abelian-higgs model on optical lattices. *Physical Review D*, 92(7):076003, 2015.

[144] Erez Zohar, J. Ignacio Cirac, and Benni Reznik. Simulating compact quantum electrodynamics with ultracold atoms: Probing confinement and nonperturbative effects. *Physical Review Letters*, 109(12), sep 2012.

[145] Sumanta Tewari, VW Scarola, T Senthil, and S Das Sarma. Emergence of artificial photons in an optical lattice. *Physical review letters*, 97(20):200401, 2006.

[146] L Tagliacozzo, A Celi, P Orland, MW Mitchell, and M Lewenstein. Simulation of non-abelian gauge theories with optical lattices. *Nature communications*, 4:2615, 2013.

[147] Debasish Banerjee, Michael Bögli, M Dalmonte, E Rico, Pascal Stebler, U-J Wiese, and P Zoller. Atomic quantum simulation of u (n) and su (n) non-abelian lattice gauge theories. *Physical review letters*, 110(12):125303, 2013.

[148] K Stannigel, P Hauke, D Marcos, M Hafezi, S Diehl, M Dalmonte, and P Zoller. Constrained dynamics via the zeno effect in quantum simulation: Implementing non-abelian lattice gauge theories with cold atoms. *Physical review letters*, 112(12):120406, 2014.

[149] Erez Zohar, J. Ignacio Cirac, and Benni Reznik. Cold-atom quantum simulator for SU(2) yang-mills lattice gauge theory. *Physical Review Letters*, 110(12), mar 2013.

[150] Erez Zohar, J. Ignacio Cirac, and Benni Reznik. Quantum simulations of gauge theories with ultracold atoms: Local gauge invariance from angular-momentum conservation. *Physical Review A*, 88(2), aug 2013.

[151] Philipp Hauke, David Marcos, Marcello Dalmonte, and Peter Zoller. Quantum simulation of a lattice schwinger model in a chain of trapped ions. *Physical Review X*, 3(4):041018, 2013.

[152] D Marcos, P Rabl, E Rico, and P Zoller. Superconducting circuits for quantum simulation of dynamical gauge fields. *Physical review letters*, 111(11):110504, 2013.

[153] D Marcos, Philippe Widmer, E Rico, M Hafezi, P Rabl, U-J Wiese, and P Zoller. Two-dimensional lattice gauge theories with superconducting quantum circuits. *Annals of physics*, 351:634–654, 2014.

[154] A Mezzacapo, E Rico, C Sabín, IL Egusquiza, L Lamata, and E Solano. Non-abelian su (2) lattice gauge theories in superconducting circuits. *Physical review letters*, 115(24):240502, 2015.

[155] Benoit Doucot, Lev B Ioffe, and Julien Vidal. Discrete non-abelian gauge theories in two-dimensional lattices and their realizations in josephson-junction arrays. *arXiv preprint cond-mat/0302104*, 2003.

[156] Catherine Laflamme, Wynne Evans, Marcello Dalmonte, Urs Gerber, Héctor Mejía-Díaz, Wolfgang Bietenholz, Uwe-Jens Wiese, and Peter Zoller. Proposal for the quantum simulation of the cp (2) model on optical lattices. *arXiv preprint arXiv:1510.08492*, 2015.

[157] C Laflamme, Wynne Evans, M Dalmonte, Urs Gerber, H Mejía-Díaz, W Bietenholz, U-J Wiese, and P Zoller. Cp quantum field theories with alkaline-earth atoms in optical lattices. *Annals of physics*, 370:117–127, 2016.

[158] Erez Zohar, Alessandro Farace, Benni Reznik, and J. Ignacio Cirac. Digital quantum simulation of z2 lattice gauge theories with dynamical fermionic matter. *Physical Review Letters*, 118(7), feb 2017.

[159] Erez Zohar, Alessandro Farace, Benni Reznik, and J. Ignacio Cirac. Digital lattice gauge theories. *Physical Review A*, 95(2), feb 2017.

[160] G. K. Brennen, G. Pupillo, E. Rico, T. M. Stace, and D. Vodola. Loops and strings in a superconducting lattice gauge simulator. *Physical Review Letters*, 117(24), dec 2016.

[161] Amin Salami Dehkharghani, E Rico, NT Zinner, and A Negretti. Lattice gauge quantum simulation via state-dependent hopping. *arXiv preprint arXiv:1704.00664*, 2017.

[162] A d'Adda, M Lüscher, and P Di Vecchia. A 1n expandable series of non-linear σ models with instantons. *Nuclear Physics B*, 146(1):63–76, 1978.

[163] H Eichenherr. Su (n) invariant non-linear σ models. *Nuclear Physics B*, 146(1):215–223, 1978.

[164] Manu Mathur. Harmonic oscillator pre-potentials in su (2) lattice gauge theory. *Journal of Physics A: Mathematical and General*, 38(46):10015, 2005.

[165] Ramesh Anishetty, Manu Mathur, and Indrakshi Raychowdhury. Prepotential formulation of su (3) lattice gauge theory. *Journal of Physics A: Mathematical and Theoretical*, 43(3):035403, 2009.

[166] Yoshihito Kuno, Shinya Sakane, Kenichi Kasamatsu, Ikuo Ichinose, and Tetsuo Matsui. Atomic quantum simulation of a three-dimensional u(1) gauge-higgs model. *Physical Review A*, 94(6), dec 2016.

[167] Kenichi Kasamatsu, Ikuo Ichinose, and Tetsuo Matsui. Atomic quantum simulation of the lattice gauge-higgs model: Higgs couplings and emergence of exact local gauge symmetry. *Physical Review Letters*, 111(11), sep 2013.

[168] Yoshihito Kuno, Shinya Sakane, Kenichi Kasamatsu, Ikuo Ichinose, and Tetsuo Matsui. Quantum simulation of (1 + 1)-dimensional u(1) gauge-higgs model on a lattice by cold bose gases. *Physical Review D*, 95(9), may 2017.

[169] Daniel González-Cuadra, Erez Zohar, and J Ignacio Cirac. Quantum simulation of the abelian-higgs lattice gauge theory with ultracold atoms. *New Journal of Physics*, 19(6):063038, jun 2017.

[170] P Facchi and S Pascazio. Quantum zeno subspaces. *Physical review letters*, 89(8):080401, 2002.

[171] Seth Lloyd et al. Universal quantum simulators. *SCIENCE-NEW YORK THEN WASHINGTON-*, pages 1073–1077, 1996.

[172] Christine Muschik, Markus Heyl, Esteban A. Martinez, Thomas Monz, Philipp Schindler, Berit Vogell, Marcello Dalmonte, Philipp Hauke, Rainer Blatt, and Peter Zoller. U(1) wilson lattice gauge theories in digital quantum simulators. *New Journal of Physics*, sep 2017.

[173] Erez Zohar and Benni Reznik. Confinement and lattice quantum-electrodynamic electric flux tubes simulated with ultracold atoms. *Physical Review Letters*, 107(27), dec 2011.

[174] V Kasper, F Hebenstreit, F Jendrzejewski, M K Oberthaler, and J Berges. Implementing quantum electrodynamics with ultracold atomic systems. *New Journal of Physics*, 19(2):023030, feb 2017.

[175] T. Banks, Leonard Susskind, and John Kogut. Strong-coupling calculations of lattice gauge theories: (1 + 1)-dimensional exercises. *Physical Review D*, 13(4):1043–1053, feb 1976.

[176] P. Jordan and E. Wigner. uber das paulische aquivalenzverbot. *Zeitschrift f?r Physik*, 47(9-10):631–651, sep 1928.

[177] C. J. Hamer, Zheng Weihong, and J. Oitmaa. Series expansions for the massive schwinger model in hamiltonian lattice theory. *Physical Review D*, 56(1):55–67, jul 1997.

[178] Karl-Heinz Bennemann and John B. Ketterson, editors. *Novel Superfluids*. Oxford University Press, nov 2014.

[179] Mark G. Alford, Andreas Schmitt, Krishna Rajagopal, and Thomas Schäfer. Color superconductivity in dense quark matter. *Reviews of Modern Physics*, 80(4):1455–1515, nov 2008.

[180] Roberto Anglani, Roberto Casalbuoni, Marco Ciminale, Nicola Ippolito, Raoul Gatto, Massimo Mannarelli, and Marco Ruggieri. Crystalline color superconductors. *Reviews of Modern Physics*, 86(2):509–561, apr 2014.

[181] Roberto Auzzi, Stefano Bolognesi, Jarah Evslin, Kenichi Konishi, and Alexei Yung. Nonabelian superconductors: vortices and confinement in SQCD. *Nuclear Physics B*, 673(1-2):187–216, nov 2003.

[182] Amihay Hanany and David Tong. Vortices, instantons and branes. *Journal of High Energy Physics*, 2003(07):037–037, jul 2003.

[183] Roberto Auzzi, Stefano Bolognesi, Jarah Evslin, Kenichi Konishi, and Hitoshi Murayama. Non-abelian monopoles. *Nuclear Physics B*, 701(1-2):207–246, nov 2004.

[184] M. Shifman and A. Yung. Non-abelian string junctions as confined monopoles. *Physical Review D*, 70(4), aug 2004.

[185] Minoru Eto, Youichi Isozumi, Muneto Nitta, Keisuke Ohashi, and Norisuke Sakai. Moduli space of non-abelian vortices. *Physical Review Letters*, 96(16), apr 2006.

[186] Mark Alford, Krishna Rajagopal, and Frank Wilczek. Color-flavor locking and chiral symmetry breaking in high density QCD. *Nuclear Physics B*, 537(1-3):443–458, jan 1999.

[187] Luca Lepori, Andrea Trombettoni, and Walter Vinci. Simulation of two-flavor symmetry-locking phases in ultracold fermionic mixtures. *EPL (Europhysics Letters)*, 109(5):50002, mar 2015.

[188] Guido Pagano, Marco Mancini, Giacomo Cappellini, Pietro Lombardi, Florian Schäfer, Hui Hu, Xia-Ji Liu, Jacopo Catani, Carlo Sias, Massimo Inguscio, and Leonardo Fallani. A one-dimensional liquid of fermions with tunable spin. *Nature Physics*, 10(3):198–201, feb 2014.

[189] A. V. Gorshkov, M. Hermele, V. Gurarie, C. Xu, P. S. Julienne, J. Ye, P. Zoller, E. Demler, M. D. Lukin, and A. M. Rey. Two-orbital SU(n) magnetism with ultracold alkaline-earth atoms. *Nature Physics*, 6(4):289–295, feb 2010.

[190] Shintaro Taie, Yosuke Takasu, Seiji Sugawa, Rekishu Yamazaki, Takuya Tsujimoto, Ryo Murakami, and Yoshiro Takahashi. Realization of $SU(2)\times SU(6)$ system of fermions in a cold atomic gas. *Physical Review Letters*, 105(19), nov 2010.

[191] Eduardo Fradkin. *Field Theories of Condensed Matter Physics*. Cambridge University Press, 2013.

[192] S.-K. Yip. Theory of a fermionic superfluid with $SU(2)\times SU(6)$ symmetry. *Physical Review A*, 83(6), jun 2011.

[193] Massimo Mannarelli, Giuseppe Nardulli, and Marco Ruggieri. Evaluating the phase diagram of superconductors with asymmetric spin populations. *Physical Review A*, 74(3), sep 2006.

[194] G. Pagano, M. Mancini, G. Cappellini, L. Livi, C. Sias, J. Catani, M. Inguscio, and L. Fallani. Strongly interacting gas of two-electron fermions at an orbital feshbach resonance. *Physical Review Letters*, 115(26), dec 2015.

[195] M. Iazzi, S. Fantoni, and A. Trombettoni. Anisotropic ginzburg-landau and lawrence-doniach models for layered ultracold fermi gases. *EPL (Europhysics Letters)*, 100(3):36007, nov 2012.

[196] Wolfgang Ketterle and Martin W. Zwierlein. Making, probing and understanding ultracold fermi gases. *Proceedings of the International School of Physics "Enrico Fermi", Course CLXIV, Varenna, 20 - 30 June 2006, M. Inguscio, W. Ketterle, and C. Salomon eds. (Amsterdam, IOS Press, 2008)*, 2008.

[197] Anthony Zee. *Quantum field theory in a nutshell*. Princeton university press, 2010.

[198] Steven Weinberg. *Gravitation and cosmology: principles and applications of the general theory of relativity*, volume 1. Wiley New York, 1972.

[199] Rainer Blatt and Christian F Roos. Quantum simulations with trapped ions. *Nature Physics*, 8(4):277, 2012.

[200] T Lahaye, C Menotti, L Santos, M Lewenstein, and T Pfau. The physics of dipolar bosonic quantum gases. *Reports Prog. Phys.*, 71(12):126401, may 2009.

[201] M. Saffman, T. G. Walker, and K. Molmer. Quantum information with Rydberg atoms. *Rev. Mod. Phys.*, 82(3):2313–2363, sep 2009.

[202] Helmut Ritsch, Peter Domokos, Ferdinand Brennecke, and Tilman Esslinger. Cold atoms in cavity-generated dynamical optical potentials. *Rev. Mod. Phys.*, 85(2):553–601, apr 2013.

[203] Joseph W. Britton, Brian C. Sawyer, Adam C. Keith, C.-C. Joseph Wang, James K. Freericks, Hermann Uys, Michael J. Biercuk, and John J. Bollinger. Engineered two-dimensional Ising interactions in a trapped-ion quantum simulator with hundreds of spins. *Nature*, 484(7395):489–492, apr 2012.

[204] Peter Schauß, Marc Cheneau, Manuel Endres, Takeshi Fukuhara, Sebastian Hild, Ahmed Omran, Thomas Pohl, Christian Gross, Stefan Kuhr, and Immanuel Bloch. Observation of spatially ordered structures in a two-dimensional Rydberg gas. *Nature*, 491(7422):87–91, oct 2012.

[205] K. Aikawa, A. Frisch, M. Mark, S. Baier, A. Rietzler, R. Grimm, and F. Ferlaino. Bose-Einstein Condensation of Erbium. *Phys. Rev. Lett.*, 108(21):210401, may 2012.

[206] Mingwu Lu, Nathaniel Q. Burdick, and Benjamin L. Lev. Quantum Degenerate Dipolar Fermi Gas. *Phys. Rev. Lett.*, 108(21):215301, may 2012.

[207] Bo Yan, Steven A. Moses, Bryce Gadway, Jacob P. Covey, Kaden R. A. Hazzard, Ana Maria Rey, Deborah S. Jin, and Jun Ye. Observation of dipolar spin-exchange interactions with lattice-confined polar molecules. *Nature*, 501(7468):521–525, sep 2013.

[208] R Islam, C Senko, WC Campbell, S Korenblit, J Smith, A Lee, EE Edwards, C-CJ Wang, JK Freericks, and C Monroe. Emergence and Frustration of Magnetism with Variable-Range Interactions in a Quantum Simulator. *Science*, 340(6132):583–587, may 2013.

[209] Philip Richerme, Zhe-Xuan Gong, Aaron Lee, Crystal Senko, Jacob Smith, Michael Foss-Feig, Spyridon Michalakis, Alexey V. Gorshkov, and Christopher Monroe. Non-local propagation of correlations in quantum systems with long-range interactions. *Nature*, 511(7508):198–201, jan 2014.

[210] P. Jurcevic, B. P. Lanyon, P. Hauke, C. Hempel, P. Zoller, R. Blatt, and C. F. Roos. Quasiparticle engineering and entanglement propagation in a quantum many-body system. *Nature*, 511(7508):202–205, jul 2014.

[211] J. S. Douglas, H. Habibian, C.-L. Hung, A. V. Gorshkov, H. J. Kimble, and D. E. Chang. Quantum many-body models with cold atoms coupled to photonic crystals. *Nat. Photonics*, 9(5):326–331, apr 2015.

[212] H. Schempp, G. Günter, S. Wüster, M. Weidemüller, and S. Whitlock. Correlated Exciton Transport in Rydberg-Dressed-Atom Spin Chains. *Phys. Rev. Lett.*, 115(9):093002, apr 2015.

[213] Renate Landig, Ferdinand Brennecke, Rafael Mottl, Tobias Donner, and Tilman Esslinger. Measuring the dynamic structure factor of a quantum gas undergoing a structural phase transition. *Nat. Commun.*, 6(May):7046, mar 2015.

[214] Renate Landig, Lorenz Hruby, Nishant Dogra, Manuele Landini, Rafael Mottl, Tobias Donner, and Tilman Esslinger. Quantum phases from competing short- and long-range interactions in an optical lattice. *Nature*, 532(7600):476–479, oct 2016.

[215] Nicolas Laflorencie, Ian Affleck, and Mona Berciu. Critical phenomena and quantum phase transition in long range Heisenberg antiferromagnetic chains. *J. Stat. Mech. Theory Exp.*, 2005(12):P12001–P12001, 2005.

[216] Matthew B. Hastings and Tohru Koma. Spectral gap and exponential decay of correlations. *Commun. Math. Phys.*, 265(3):781–804, jul 2006.

[217] Thomas Koffel, M. Lewenstein, and Luca Tagliacozzo. Entanglement entropy for the long-range Ising chain in a transverse field. *Phys. Rev. Lett.*, 109(26):267203, dec 2012.

[218] J. Schachenmayer, B. P. Lanyon, C. F. Roos, and A. J. Daley. Entanglement Growth in Quench Dynamics with Variable Range Interactions. *Phys. Rev. X*, 3(3):031015, sep 2013.

[219] Jens Eisert, Mauritz van den Worm, Salvatore R. Manmana, and Michael Kastner. Breakdown of Quasilocality in Long-Range Quantum Lattice Models. *Phys. Rev. Lett.*, 111(26):260401, dec 2013.

[220] Zhe Xuan Gong, Michael Foss-Feig, Spyridon Michalakis, and Alexey V. Gorshkov. Persistence of locality in systems with power-law interactions. *Phys. Rev. Lett.*, 113(3), jan 2014.

[221] David Damanik, Marius Lemm, Milivoje Lukic, and William Yessen. New Anomalous Lieb-Robinson Bounds in Quasiperiodic X Y Chains. *Phys. Rev. Lett.*, 113(12):127202, sep 2014.

[222] Davide Vodola, Luca Lepori, Elisa Ercolessi, Alexey V. Gorshkov, and Guido Pupillo. Kitaev chains with long-range pairing. *Phys. Rev. Lett.*, 113(15), may 2014.

[223] Filiberto Ares, José G. Esteve, Fernando Falceto, and Amilcar R. De Queiroz. Entanglement in fermionic chains with finite-range coupling and broken symmetries. *Phys. Rev. A*, 92(4), 2015.

[224] Giacomo Gori, Simone Paganelli, Auditya Sharma, Pasquale Sodano, and Andrea Trombettoni. Explicit Hamiltonians inducing volume law for entanglement entropy in fermionic lattices. *Phys. Rev. B*, 91(24):245138, 2015.

[225] O. Viyuela, D. Vodola, G. Pupillo, and M. A. Martin-Delgado. Topological massive dirac edge modes and long-range superconducting hamiltonians. *Phys. Rev. B*, 94(12), nov 2016.

[226] Z.-X. Gong, Mohammad F. Maghrebi, Anzi Hu, Michael L. Wall, Michael Foss-Feig, and Alexey V. Gorshkov. Topological phases with long-range interactions. *Phys. Rev. B*, 93(4):041102, jan 2016.

[227] L. Lepori and L. Dell'Anna. Long-range topological insulators and weakened bulk-boundary correspondence. *New J. Phys.*, dec 2017.

[228] L. Lepori, A. Trombettoni, and D. Vodola. Singular dynamics and emergence of nonlocality in long-range quantum models. *J. Stat. Mech. Theory Exp.*, 3(3):1–19, mar 2016.

[229] Mohammad F. Maghrebi, Zhe-Xuan Gong, Michael Foss-Feig, and Alexey V. Gorshkov. Causality and quantum criticality in long-range lattice models. *Phys. Rev. B*, 93(12):125128, mar 2016.

[230] Lea F. Santos, Fausto Borgonovi, and Giuseppe Luca Celardo. Cooperative Shielding in Many-Body Systems with Long-Range Interaction. *Phys. Rev. Lett.*, 116(25):250402, jun 2016.

[231] Sebastian Fey and Kai Phillip Schmidt. Critical behavior of quantum magnets with long-range interactions in the thermodynamic limit. *Phys. Rev. B*, 94(7):075156, aug 2016.

[232] Z. X. Gong, Mohammad F. Maghrebi, Anzi Hu, Michael Foss-Feig, Phillip Richerme, Christopher Monroe, and Alexey V. Gorshkov. Kaleidoscope of quantum phases in a long-range interacting spin-1 chain. *Phys. Rev. B*, 93(20), oct 2016.

[233] István A. Kovács, Róbert Juhász, and Ferenc Iglói. Long-range random transverse-field Ising model in three dimensions. *Phys. Rev. B*, 93(18):184203, may 2016.

[234] Stephan Humeniuk. Quantum Monte Carlo study of long-range transverse-field Ising models on the triangular lattice. *Phys. Rev. B*, 93(10):104412, mar 2016.

[235] A. Bermudez, L. Tagliacozzo, G. Sierra, and P. Richerme. Long-range Heisenberg models in quasi-periodically driven crystals of trapped ions. *Phys. Rev. B*, 95(2):024431, jul 2016.

[236] Luca Lepori, Davide Vodola, Guido Pupillo, Giacomo Gori, and Andrea Trombettoni. Effective theory and breakdown of conformal symmetry in a long-range quantum chain. *Ann. Phys.*, 374:35–66, nov 2016.

[237] N. Defenu, A. Trombettoni, and S. Ruffo. Criticality and Phase Diagram of Quantum Long-Range Systems. *eprint arXiv:1704.00528*, apr 2017.

[238] Michael Foss-Feig, Zhe-Xuan Gong, Charles W. Clark, and Alexey V. Gorshkov. Nearly Linear Light Cones in Long-Range Interacting Quantum Systems. *Phys. Rev. Lett.*, 114(15):157201, apr 2015.

[239] M. A. Rajabpour and S. Sotiriadis. Quantum quench in long-range field theories. *Phys. Rev. B*, 91(4):045131, jan 2015.

[240] Lorenzo Cevolani, Giuseppe Carleo, and Laurent Sanchez-Palencia. Protected quasilocality in quantum systems with long-range interactions. *Phys. Rev. A*, 92(4):041603, oct 2015.

[241] Tomotaka Kuwahara. Asymptotic behavior of macroscopic observables in generic spin systems. *J. Stat. Mech. Theory Exp.*, 2016(5):053103, may 2016.

[242] Mathias Van Regemortel, Dries Sels, and Michiel Wouters. Information propagation and equilibration in long-range Kitaev chains. *Phys. Rev. A*, 93(3):032311, mar 2016.

[243] Anton S. Buyskikh, Maurizio Fagotti, Johannes Schachenmayer, Fabian Essler, and Andrew J. Daley. Entanglement growth and correlation spreading with variable-range interactions in spin and fermionic tunneling models. *Phys. Rev. A*, 93(5):053620, may 2016.

[244] Bruno Bertini, Fabian H L Essler, Stefan Groha, and Neil J Robinson. Prethermalization and Thermalization in Models with Weak Integrability Breaking. *Phys. Rev. Lett.*, 115(18):180601, oct 2015.

[245] E. Brezin, G. Parisi, and F. Ricci-Tersenghi. The Crossover Region Between Long-Range and Short-Range Interactions for the Critical Exponents. *J. Stat. Phys.*, 157(4-5):855–868, dec 2014.

[246] Maria Chiara Angelini, Giorgio Parisi, and Federico Ricci-Tersenghi. Relations between short-range and long-range Ising models. *Phys. Rev. E*, 89(6):062120, jun 2014.

[247] Nicoló Defenu, Andrea Trombettoni, and Alessandro Codello. Fixed-point structure and effective fractional dimensionality for O(N) models with long-range interactions. *Phys. Rev. E*, 92(5):052113, nov 2015.

[248] Connor Behan, Leonardo Rastelli, Slava Rychkov, and Bernardo Zan. A scaling theory for the long-range to short-range crossover and an infrared duality. *eprint arXiv:1703.05325*, 2017.

[249] Connor Behan, Leonardo Rastelli, Slava Rychkov, and Bernardo Zan. Long-range critical exponents near the short-range crossover. *Phys. Rev. Lett.*, 118(24):241601, 2017.

[250] G. E. Uhlenbeck, P. C. Hemmer, and M. Kac. On the van der Waals Theory of the Vapor-Liquid Equilibrium. I. Discussion of a One-Dimensional Model. *J. Math. Phys.*, 4(2):216, 1963.

[251] D. O'Dell, S. Giovanazzi, G. Kurizki, and V. M. Akulin. Bose-einstein condensates with $1/r$ interatomic attraction: Electromagnetically induced "gravity". *Phys. Rev. Lett.*, 84:5687–5690, Jun 2000.

[252] A. H. Castro Neto, F. Guinea, N. M. R. Peres, K. S. Novoselov, and A. K. Geim. The electronic properties of graphene. *Rev. Mod. Phys.*, 81:109–162, Jan 2009.

[253] EC Marino. Quantum electrodynamics of particles on a plane and the chern-simons theory. *Nucl. Phys. B*, 408(3):551–564, 1993.

[254] EC Marino, Leandro O Nascimento, Van Sérgio Alves, and C Morais Smith. Unitarity of theories containing fractional powers of the d'alembertian operator. *Phys. Rev. D*, 90(10):105003, 2014.

[255] A. V. Kotikov and S. Teber. Two-loop fermion self-energy in reduced quantum electrodynamics and application to the ultrarelativistic limit of graphene. *Phys. Rev. D*, 89:065038, Mar 2014.

[256] E. C. Marino, Leandro O. Nascimento, Van Sérgio Alves, and C. Morais Smith. Interaction induced quantum valley hall effect in graphene. *Phys. Rev. X*, 5:011040, Mar 2015.

[257] Leandro O. Nascimento, Van Sérgio Alves, Francisco Peña, C. Morais Smith, and E. C. Marino. Chiral-symmetry breaking in pseudoquantum electrodynamics at finite temperature. *Phys. Rev. D*, 92:025018, Jul 2015.

[258] Van Sérgio Alves, Reginaldo OC Junior, EC Marino, and Leandro O Nascimento. Dynamical mass generation in pseudoquantum electrodynamics with four-fermion interactions. *Phys. Rev. D*, 96(3):034005, 2017.

[259] N. Menezes, C. Morais Smith, and G. Palumbo. Excitonic gap generation in thin-film topological insulators . *eprint arXiv:1705.03482*, 2016.

[260] E. V. Gorbar, V. P. Gusynin, and V. A. Miransky. Dynamical chiral symmetry breaking on a brane in reduced qed. *Phys. Rev. D*, 64:105028, Oct 2001.

[261] N Menezes, Van Sergio Alves, EC Marino, L Nascimento, Leandro O Nascimento, and C Morais Smith. Valley-and spin-splitting due to interactions in graphene. *arXiv preprint arXiv:1601.07454*, 2016.

[262] L.D. Faddeev and V.N. Popov. Feynman diagrams for the yang-mills field. *Physics Letters B*, 25(1):29–30, jul 1967.

[263] John Cardy. *Scaling and renormalization in statistical physics*, volume 5. Cambridge university press, 1996.

[264] Walter E Thirring. A soluble relativistic field theory. *Annals of Physics*, 3(1):91–112, jan 1958.

[265] Jean Zinn-Justin. *Quantum Field Theory and Critical Phenomena*. Oxford University Press, jun 2002.

[266] Sidney Coleman. Quantum sine-gordon equation as the massive thirring model. *Phys. Rev. D*, 11(8):2088, 1975.

[267] M. V. Ostrogradsky. *Mem. Acad. St. Petersbourg*, 6:385, 1850.

[268] DG Barci and LE Oxman. Asymptotic states in nonlocal field theories. *Mod. Phys. Lett. A*, 12(07):493–500, 1997.

[269] RLPG Do Amaral and EC Marino. Canonical quantization of theories containing fractional powers of the d'alembertian operator. *J. Phys. A: Math. Gen.*, 25(19):5183, 1992.

[270] R Amorim and J Barcelos-Neto. Functional versus canonical quantization of a nonlocal massive vector-gauge theory. *J. Math. Phys.*, 40(2):585–600, 1999.

[271] Carsten Grosse Knetter. Effective lagrangians with higher derivatives and equations of motion. *Phys. Rev. D*, 49(12):6709, 1994.

[272] Christopher Arzt. Reduced effective lagrangians. *Phys. Lett. B*, 342(1):189–195, 1995.

[273] Bitan Roy, Vladimir Juričić, and Igor F. Herbut. Emergent lorentz symmetry near fermionic quantum critical points in two and three dimensions. *J. High Energy Phys.*, 2016(4):18, Apr 2016.

[274] X Deng, VE Kravtsov, GV Shlyapnikov, and L Santos. Algebraic localization in disordered one-dimensional systems with long-range hopping. *eprint arXiv:1706.04088*, 2017.

[275] Michael Pretko. Generalized electromagnetism of subdimensional particles: A spin liquid story. *Phys. Rev. B*, 96(3):035119, 2017.

[276] Patrick A. Lee, Naoto Nagaosa, and Xiao-Gang Wen. Doping a mott insulator: Physics of high-temperature superconductivity. *Rev. Mod. Phys.*, 78:17–85, Jan 2006.

[277] F. Wilczek. Qcd made simple. *Phys. Today*, 52:22, 2000.

[278] Alexander O Gogolin, Alexander A Nersesyan, and Alexei M Tsvelik. *Bosonization and strongly correlated systems*. Cambridge university press, 2004.

[279] Sidney Coleman, R Jackiw, and Leonard Susskind. Charge shielding and quark confinement in the massive schwinger model. *Ann. Phys.*, 93(1):267–275, 1975.

[280] Sidney Coleman. More about the massive schwinger model. *Annals of Physics*, 101(1):239–267, sep 1976.

[281] I. Nándori. On the renormalization of the bosonized multi-flavor schwinger model. *Physics Letters B*, 662(3):302 – 308, 2008.

[282] C. R. Hagen. New solutions of the thirring model. *Il Nuovo Cimento B (1965-1970)*, 51(1):169–186, Sep 1967.

[283] B. Klaiber. Thirring model. *pp 141-76 of Quantum Theory and Statistical Physics. Barut, Asim O. Brittin, Wesley E. (eds.). New York, Gordon and Breach, Science Publishers, 1968.*, Oct 1969.

[284] V. E. Korepin, N. M. Bogoliubov, and A. G. Izergin. Quantum inverse scattering method and correlation functions. pages xv–xx. Cambridge University Press.

[285] Alvaro de Souza Dutra, CP Natividade, H Boschi-Filho, RLPG Amaral, and LV Belvedere. Quartic fermion self-interactions in two-dimensional gauge theories. *Phys. Rev. D*, 55(8):4931, 1997.

[286] Dan M Stamper-Kurn and Masahito Ueda. Spinor bose gases: Symmetries, magnetism, and quantum dynamics. *Reviews of Modern Physics*, 85(3):1191, 2013.